

Dissertation

DESIGN OF NON-NATIVE PATHWAYS TO SYNTHESIZE POLYHYDROXYLATED COMPOUNDS

ausgeführt zum Zwecke der Erlangung des akademischen Grades eines
Doktors der technischen Wissenschaften unter der Leitung von

Prof. Dr. Marko D. Mihovilovic

Assistant Prof. Dr. Florian Rudroff

Institut für Angewandte Synthesechemie, E163

eingereicht an der Technischen Universität Wien

Fakultät für Technische Chemie

Von

Dipl.Ing. Thomas Wiesinger, BSc

Haspingergasse 1-3/1/5

1080 Wien

Wien, Februar 2018

LIFE IS LIKE RIDING A BICYCLE

TO KEEP YOUR BALANCE

YOU MUST KEEP MOVING

ALBERT EINSTEIN

Danksagung

Zu allererst möchte ich mich bei meiner Mama Christine bedanken vorallem für ihre endlose Unterstützung und dass sie mir im Leben alles ermöglicht hat.

Mein größter Dank jedoch gilt meiner **LISA**:

danke, dass es dich gibt und dass du immer für mich da bist!

Spezieller Dank gebührt Prof. Marko D. Mihovilovic für die Betreuung meiner Arbeit und vor allem für die lehrreiche Zeit, mit oft harten aber auch motivierenden Worten.

Bei Assistant Prof. Florian Rudroff möchte ich mich für die Möglichkeit bedanken, ein Teammitglied des FWF Projektes (P-24483-B20) gewesen zu sein, sowie für seine Unterstützung. Ganz besonders möchte ich meinen beiden weiteren Projektmitgliedern, Thomas Bayer und Sofia Milker, für ihre Hilfe im Labor sowie für die zahlreichen privaten Aktivitäten (v.a. Kochgruppe) danken.

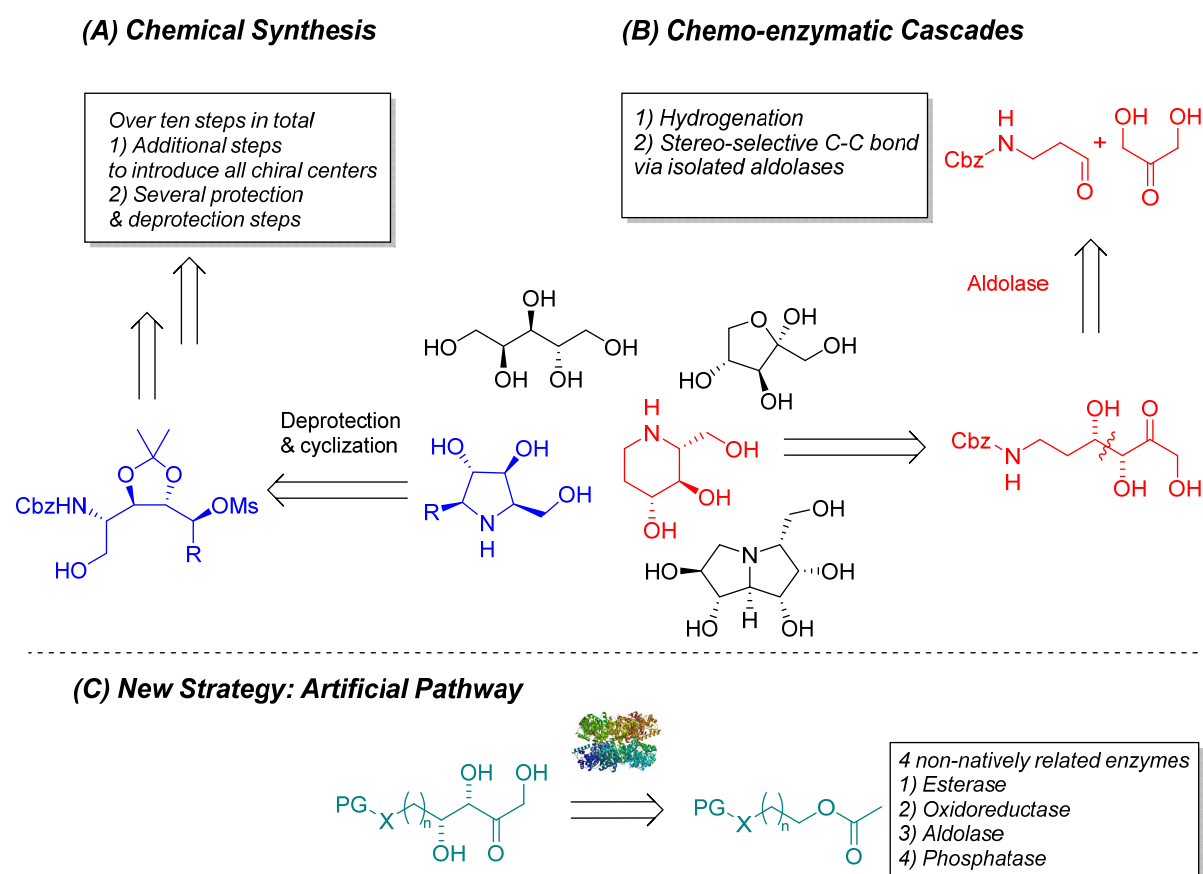
Vor allem möchte ich mich aber bei Christian Stanetty und Mathias Pickl bedanken, für deren Unterstützung bei wissenschaftlichen Fragenstellungen und für ihre motivierende Art, die mir den Abschluss dieser Arbeit erleichtert hat.

Mein weiterer Dank gilt der gesamten MDM Gruppe. Insbesondere möchte ich mich vor allem bei dem Review Team bedanken: Gerit Pototschnig, Patricia Schaaf und Michael Schnürch sowie bei allen anderen Gruppenmitgliedern, stellvertretend ganz besonders bei Leticia Goncalves, David Siebert, Dominik Dreier, Markus Draskovits, Laurin Wimmer, Max Haider, Anna Ressmann, Hamid Mansouri. Ebenfalls danksagen möchte ich Laszlo Czollner, Markus Schwarz und Stefan Kronister für deren Hilfe bei LC oder MPLC Problemstellungen.

Abschließend möchte ich noch meinen Freunden und meiner gesamten Familie danken, insbesondere meiner Cousine Birgit für das Vertrauen meiner Patenschaft für Vinzent.

Abstract

Over the past decade, enzyme mediated transformations in a cascade fashion have led to significant advances in asymmetric synthesis to generate important building block structures such as polyhydroxylated carbohydrates or heterocycles. These high value chiral molecules (e.g. *D*-fagomine, 1-deoxynojirimycin) were identified as essential substructures due to their activity against a wide range of diseases such as cancer and diabetes. Since these molecules represents attractive target products, different synthetic strategies **(A)** were applied over the years to synthesize them in a stereochemically pure fashion. Especially, dihydroxyacetone phosphate (DHAP) or dihydroxyacetone/hydroxyacetone (DHA/HA) dependent aldolases were investigated to control the orientation of the diol and were also implemented into chemo-enzymatic or *in vitro* cascade approaches **(B)**.

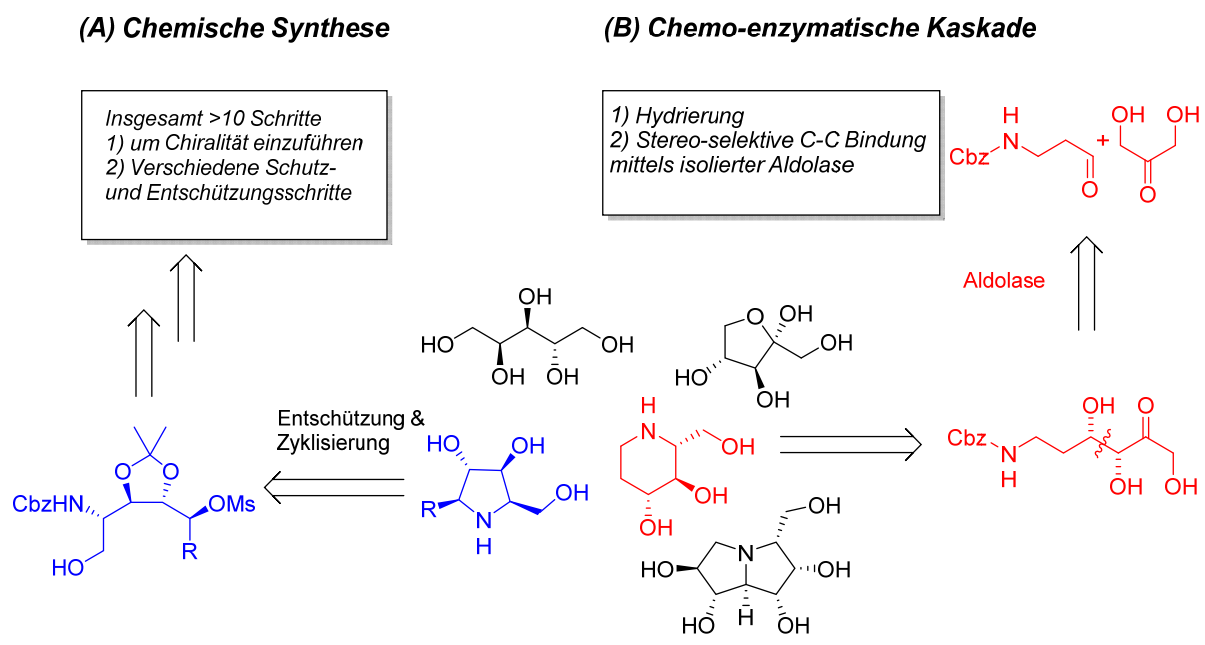


To overcome bottlenecks such as time consuming and atom inefficient protection/deprotection steps as well as elaborate intermediate purification of the described procedures **(A)** and **(B)**, two bio-inspired strategies (Pathway I and Pathway II) were established **(C)**. These developed whole cell biocatalysts will serve as a biocatalytic tool for the synthesis of the diastereomerically pure target molecules. Both pathways consist of several different enzymes, which were introduced to provide the central molecules, the aldol acceptor (aldehyde) and the related aldol product. The overall performance of

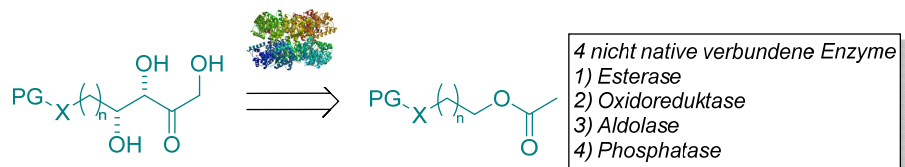
Pathway I was improved by different strategies on genetic (e.g. operon design) and process parameters (e.g. aldol donor concentration and cellular transport). The engineered *E. coli* strain combined with a refined solid-phase extraction (SPE) protocol, the diastereomerically pure target compounds were obtained in 3-fold higher isolated yields, compared to strategy (**B**). Results of Pathway II showed that under *in vitro* reaction conditions, DHAP dependent aldolase (FucA and RhuA) do not exclusively generate the related diastereomere, they always yielded in *syn/anti* mixtures. Additionally the isolation and characterization of the corresponding phosphorylated aldol adduct was achieved by a biocatalytic and chemical synthetic route. Especially, the observed NMR data were until now not presented in the literature.

Kurzfassung

In den letzten Jahren haben enzymvermittelte Kaskadenreaktionen zu bedeutenden Fortschritten in der asymmetrischen Synthese geführt, um u.a. wichtige Bausteine wie polyhydroxylierte Verbindungen zu erzeugen. Diese hochwertigen chiralen Moleküle (z.B. *D*-Fagomin, 1-Desoxynojirimycin) konnten aufgrund ihrer Aktivität gegen eine breite Palette von Krankheiten, wie Krebs und Diabetes identifiziert. Da diese Moleküle attraktive Produkte darstellen, wurden verschiedene Synthesestrategien **(A)** eingesetzt, um diese stereoselektiv zu synthetisieren. Insbesondere wurden Dihydroxyacetonphosphat- (DHAP) oder Dihydroxyaceton/Hydroxyaceton- (DHA/HA) abhängige Aldolasen untersucht, um die Orientierung des Diols zu steuern. Des Weiteren wurden Aldolasen auch in chemo-enzymatischen oder in *in vitro*-Kaskadenansätzen implementiert **(B)**.



(C) Neue Strategie: Bioinspirierte Route



Um zeitintensive und atomeffiziente Schutz- und Entschützungs-schritte, sowie eine aufwendige Intermediateaufreinigung der beschriebenen Verfahren **(A)** und **(B)** zu überwinden, wurden zwei bioinspirierte Strategien (Pathway I and Pathway II) etabliert **(C)**. Diese entwickelten Ganzzell-Biokatalysatoren werden als biokatalytisches Werkzeug für die asymmetrische Synthese der Zielmoleküle eingesetzt. Beide künstliche Stoffwechsel bestehen aus mehreren verschiedenen Enzymen, die eingeführt wurden, um die zentralen Moleküle, den Aldolakzeptor (Aldehyd) und das

verwandte Aldolprodukt, bereitzustellen. Die Gesamtleistung von Pathway I wurde durch verschiedene Strategien hinsichtlich genetischer Ebene (Operon-Design) und Prozessparameter (z. B. Aldol-Donor-Konzentration und zellulärer Transport) verbessert. Mittels dem gentechnisch veränderte *E. coli*-Stamm in Kombination mit einem verfeinerten Festphasenextraktionsprotokoll (SPE), konnten die diastereomer-reinen Zielverbindungen in einer 3fach höheren isolierten Ausbeuten erhalten werden, verglichen mit der Strategie (B). Die Ergebnisse von Pathway II zeigten, dass DHAP-abhängige Aldolasen (FucA und RhuA) unter *in vitro* Bedingungen nicht ausschließlich das verwandte Diastereomer erzeugen, sondern immer eine *syn/anti*-Mischung. Zusätzlich wurde die Isolierung und Charakterisierung des entsprechenden phosphorylierten Aldoladdukts auf biokatalytischem und chemischem Weg durchgeführt. Insbesondere waren die dafür erhaltenen NMR-Daten bis dato nicht Literatur bekannt.

Table of Contents

Danksagung	1
Abstract	2
Kurzfassung	4
Table of Contents	6
Synthetic Schemes.....	10
A I General Synthetic Schemes-Reference Synthesis	12
A I.1 Esterification of Carboxylic Acids.....	13
A I.2 Synthesis of Primary Alcohols.....	14
A I.3 Synthesis of Acetates.....	15
A I.4 Synthesis of Aldehydes	16
A I.5 Synthesis of Carboxylic Acids.....	17
A II Synthesis of Aldol Adducts by Pathway I.....	18
A III Synthesis of Aldol Adducts by Pathway I.....	19
A IV Synthesis of DHAP.....	20
A V Enzymatic and Chemical Strategies for the Synthesis of Phosphorylated Aldol Compounds	21
Introduction- Biotransformations in Organic Chemistry.....	22
A V.1 Cascade Type Reaction- <i>In Vitro</i> vs. <i>In Vivo</i> Setup.....	25
Enzymatic C-C Bond Formations in Organic Synthesis.....	30
Scope of the Thesis.....	39
A VI Requirements on the Designed Pathways.....	39
Results & Discussion.....	43
A VII Pathway I-Setup.....	43
A VIII Enzyme and Substrate Promiscuity	58
A VIII.1 Esterases-Acetate Hydrolysis.....	58
A VIII.2 Enzyme Mediated Oxidation Reactions.....	64
A VIII.3 Aldolases in Organic Synthesis-Stereoselective C-C Bond Formation.....	72
A VIII.4 DHA/HA-Dependent Fructose-6-phosphate Aldolase-Evaluation of <i>In vivo</i> Pathway I Settings	78
A IX Pathway I Assembly	82
A IX.1 Two Plasmid Approach-AlkJ/ Fsa1 A129S Co-expressed in <i>E. coli</i>	83
A IX.2 Optimization on Genetic Levels.....	84
A IX.3 Optimization on Process Parameters	87
A IX.4 Pathway I-Substrate Scope.....	91

A IX.5	Downstream Processing-Isolation and Purification of Polyhydroxylated Compounds	93
A IX.6	NMR Studies: Determination of Water Content in the Aldol Adduct	95
A X	Pathway I-Summary.....	99
A X.1	Pathway I-Application.....	100
A X.2	Chemo/enzymatic Cascade for the Synthesis of Polyhydroxylated Heterocycles	101
Scope of the Thesis: Pathway II.....		105
A XI	Introduction-DHAP Dependent Aldolases	106
A XI.1	Synthesis of DHAP.....	110
A I	DHAP dependent Aldolase: C-C Bond Forming Reactions in Asymmetric Synthesis.	113
A I.1	Photometric Activity Assay for Fructose-1,6-bisphosphate Aldolases.....	114
A I.2	Organic Solvent Studies for DHAP Aldolases.....	116
A II	C-C Bond Forming Reactions mediated by FucA, FruA and RhuA	122
A II.1	Preparative Scale Biotransformation Using Cell Free Extract of DHAP Dependent Aldolases	124
A III	Chemical Route to Phosphorylated Aldol Adducts.....	127
A III.1	Chemical Route I-Phosphorylated Aldol Compound	127
A III.2	Chemical Route II-Phosphorylated Aldol Compound	129
A IV	Phosphatases Mediated-Dephosphorylation	137
A IV.1	Phosphatase Phon-Sf: Dephosphorylation Activity.....	137
A V	Pathway II Assembly	141
A V.1	Solvent Studies for Two-Step <i>In Vitro</i> Transformation (FucA and Phon-Sf).....	143
A V.2	Optimization of <i>In Vitro</i> Assembled Pathway II.....	145
A VI	Isolation of Aldol Diastereomers	148
A VI.1	Pathway II- <i>In Vitro</i> Preparative Scale Experiments using FucA & Phon-Sf or RhuA & Phon-Sf	148
A VI.2	Identification of Aldol Diastereomers <i>via</i> ¹ H NMR	151
A VII	Pathway II- <i>In Vivo</i> Setting Evaluation	152
A VIII	Conclusion and Outlook of Pathway II.....	157
Experimental part.....		159
A IX	Materials and Methods–General & Chemical Synthesis	159
A X	Materials and Methods– Enzyme Production, SDS-PAGE Analysis, Biocatalyst Preparation and Characterization	161
A X.1	General Stock Solutions.....	161
A X.2	Standard Media Preparations.....	162
A XI	Bacterial Growth and Enzyme Production	165
A XII	General Protocol for Protein Expression & Cell Free Extract Preparation	168
A XII.1	Preparation of Permanent Cultures	168

A XII.2	Preparation of LB Agar Plates	168
A XII.3	Preparation of pre-cultures– LB medium	168
A XII.4	Preparation of Pre-cultures-LB-0.8G	168
A XII.5	Preparation of Growing Cells of Pfl or BS2	168
A XII.6	Preparation of Whole Cell Lyophilizates of <i>E. coli</i> BL21(DE3)/pET21b(+)_lk-adh	169
A XII.7	Preparation of Resting Cells of <i>E. coli</i> BL21(DE3)/pRR_rr-adh	169
A XII.8	Preparation of Whole Cell Lyophilizates of <i>E. coli</i> BL21(DE3)/pET22b(+)_adh-a	169
A XII.9	Preparation of Cell Free Extract of <i>E. coli</i> BL21(DE3)/pET26b(+)_adh-ht.....	170
A XII.10	Preparation of Resting Cells of <i>E. coli</i> BL21(DE3)/pKA1_alkJ	170
A XII.11	Preparation of Heat Shock-purified Fsa1 A129S Lyophilisates.....	170
A XII.12	Preparation of Resting Cells of <i>E. coli</i> BL21(DE3)	171
A XII.13	Preparation of Resting Cells of Fsa1 A129.....	171
A XII.14	Preparation of Pretreated Resting Cells of Fsa1 A129	171
A XII.15	Preparation of Resting Cells Co-expressing AlkJ and Fsa1 A129S from Two Plasmids....	172
A XII.16	Preparation of Resting Cells of the POP construct: AlkJ and Fsa1 A129S.....	172
A XII.17	Preparation of Cell Free Extract of DHAP Dependent Aldolases (FruA, FucA, RhuA)	173
A XII.18	Preparation of Cell Free Extract of Phon-Sf.....	174
A XII.19	Determination of Protein Concentration <i>via</i> Bradford	174
A XII.20	General Procedure for Expression Control-SDS PAGE.....	175
A XIII	General Biotransformation Conditions	176
A XIII.1	Pfe I & BS2 Biotransformation Conditions.....	176
A XIII.2	Alcohol Dehydrogenases-Sample Preparation for GC/FID	177
A XIII.3	Screening Conditions using a Two-Plasmid System of AlkJ and Fsa1 A129S.....	177
A XIII.4	Parameter Optimization by the pseudo-operon (POP) Construct with Different DHA Concentrations	178
A XIII.5	Procedure for Co-expressed Resting Cells (AlkJ + Fsa1 A129S)	178
A XIII.6	General Procedure of Preparative Biotransformation Using the POP Construct and DHA or HA	179
A XIV	Substrate Profile and Related Synthesis of Reference Material	180
A XIV.1	Esterification of Cbz-protected Amino Acids.....	180
A XIV.2	Reduction of the Aminoacid-methylesters to the Corresponding Alcohols.....	186
A XIV.3	Acetatylation of Primary Alcohols	190
A XIV.4	Aldehyde Synthesis.....	200
A XIV.5	Synthesis of Carboxylic Acids.....	205
A XIV.6	Synthesis of Aldol Adducts	209
A XIV.7	Synthesis of Acyclic Aldol Compounds with DHA and Co-expressed AlkJ and Fsa1 A129S 210	

A XIV.8	Synthesis of (3 <i>S</i> ,4 <i>S</i>)-1,3,4-Trihydroxy-5-phenylpentan-2-one (B _{5,FucA}) by FucA and Phon-Sf	215
A XIV.9	Synthesis of (3 <i>R</i> ,4 <i>S</i>)-1,3,4-Trihydroxy-5-phenylpentan-2-one (B _{5,RhuA}) by RhuA and Phon-Sf	217
A XIV.10	Synthesis of acyclic Aldol compounds with HA and co-expressed AlkJ and Fsa1 A129S	219
A XV	Hydrogenation of acyclic Aldol Compounds.....	224
A XV.1	Deprotection to the Cyclic Aldol Product	224
A XV.2	1-Deoxy- <i>D</i> -xylulose	225
A XV.3	(3 <i>S</i> ,4 <i>R</i>)-2-Methyltetrahydro-2 <i>H</i> -pyran-2,3,4-triol	226
A XVI	DHAP Synthesis.....	227
A XVII	Chemical Route to Phosphorylated Aldol Adduct	231
A XVII.1	Acetonide Protection to (B _{5,II}).....	231
A XVII.2	Phosphorylation using Dibenzyl- <i>N,N</i> -diisopropylphosphoramidite.....	232
A XVII.3	Dibenzyl-deprotection of HAP <i>via</i> Pd/C and H ₂ Balloon	234
A XVII.4	Deprotection to (3 <i>S</i> ,4 <i>R</i>)-1,3,4-Trihydroxy-5-phenylpentan-2-one (B _{6,chem})	236
A XVII.5	Biocatalytic route by RAMA to (3 <i>S</i> ,4 <i>R</i>)-1,3,4-Trihydroxy-5-phenylpentan-2-one (B ₆)	238
	Abbreviation List.....	240
	References.....	241
	Curriculum Vitae.....	245

Synthetic Schemes

All compounds prepared or used as starting materials in this thesis are labelled with letters and Arabic numerals, except aldol donor molecules, these are numbered with roman numerals. All other compounds that are depicted are numbered with Arabic numerals only. All compounds prepared or used in this thesis are numbered according to the depicted schemata (**Table 1 & Table 2, Figure 1**).

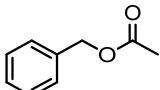
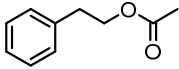
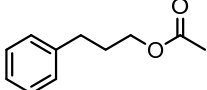
Table 1 Explanation of the compound numbering in this thesis.

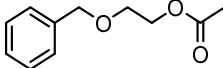
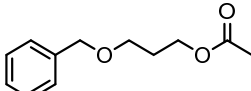
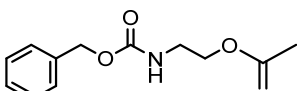
#	Compound
X _A	Methyl ester
X ₁	Acetate
X ₂	Primary alcohol
X ₃	Aldehyde
X ₄	Carboxylic acid
X ₅	Dephosphorylated aldol adduct
X ₆	Phosphorylated aldol adduct

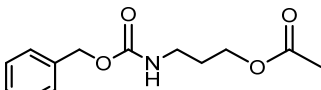
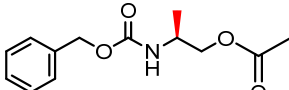
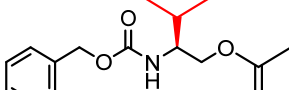
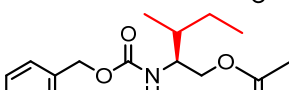
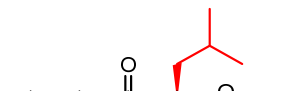
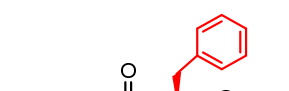
I	Hydroxyacetone
II	Dihydroxyacetone
III	Dihydroxyacetone phosphate

X differs for every compound series

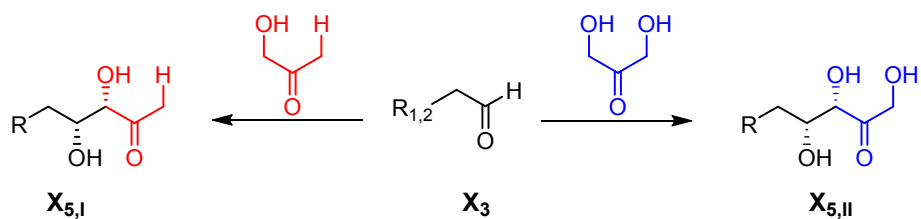
Table 2 Illustration of the compound numbering in this thesis.

Abbrev.	Acetate	Alcohol	Aldehyde	Acid
A ₁		A ₂	A ₃	A ₄
B ₁		B ₂	B ₃	B ₄
C ₁		C ₂	C ₃	C ₄

D ₁		D ₂	D ₃	D ₄
E ₁		E ₂	E ₃	E ₄
F ₁		F ₂	F ₃	F ₄

G ₁		G ₂	G ₃	G ₄
H ₁		H ₂	H ₃	H ₄
I ₁		I ₂	I ₃	I ₄
J ₁		J ₂	J ₃	J ₄
K ₁		K ₂	K ₃	K ₄
L ₁		L ₂	L ₃	L ₄

In general, substrates and synthesized reference material were numbered according to Table 2. Aldol adducts were numbered with X_{5,I} for the HA related compound and X_{5,II} for the DHA adduct.



A I General Synthetic Schemes-Reference Synthesis

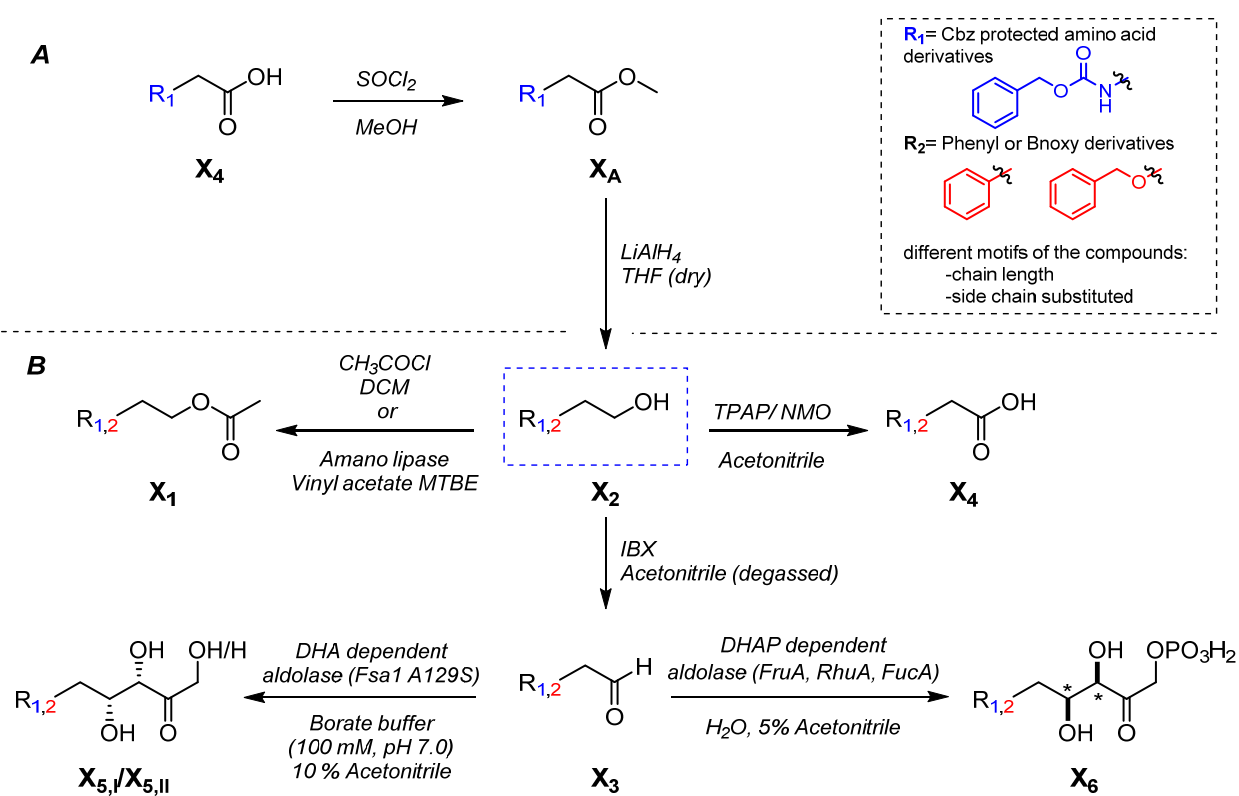


Figure 1 General synthetic schemes for the synthesis of reference material.

A I.1 Esterification of Carboxylic Acids

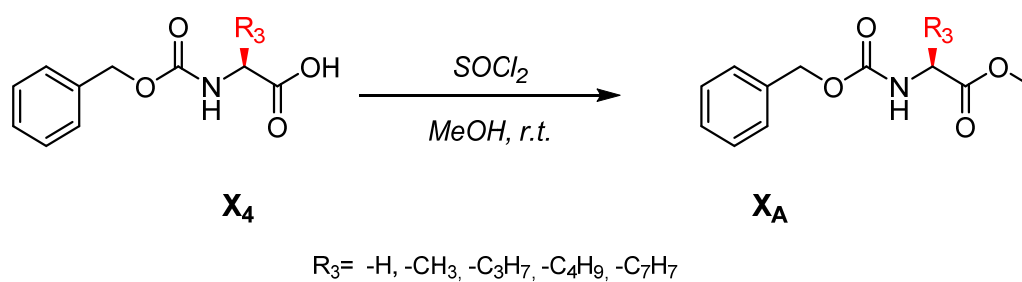


Table 3 Yields of various methyl esters.

	Ester	Yield [%]
F_A		99
H_A		97
I_A		99
J_A		91
K_A		93
L_A		99

A 1.2 Synthesis of Primary Alcohols

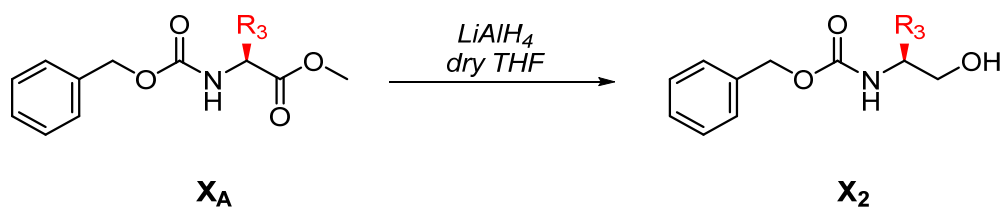
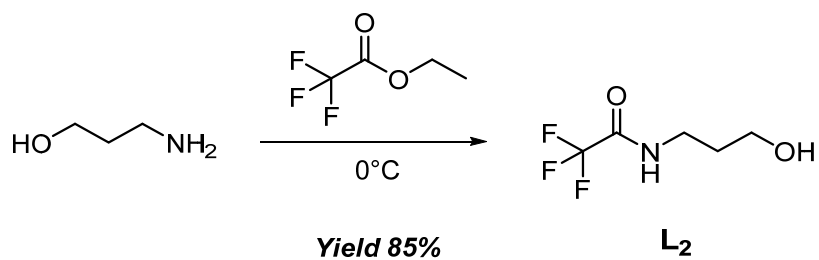


Table 4 Yields of Cbz-protected amino alcohols (R_3 in red).

	Product	Yield (%)
H ₂		70
I ₂		84
J ₂		71



A 1.3 Synthesis of Acetates

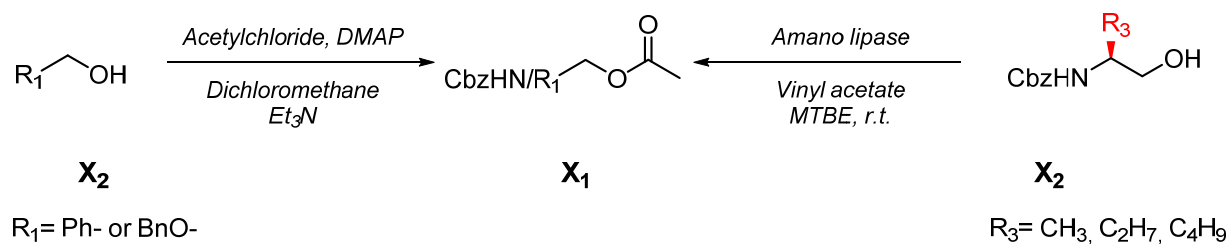


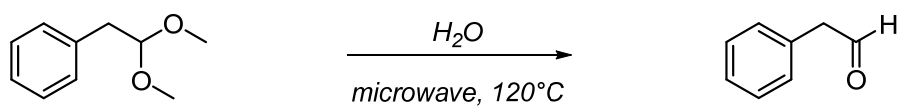
Table 5 Yields for synthesized acetates using acetylchloride.

#	Acetate	Yield [%]
A ₁		79
B ₁		30
C ₁		39
D ₁		75
E ₁		70
F ₁		70
G ₁		80

Table 6 Yields for synthesized acetates using an Amano lipase (R₁ in red).

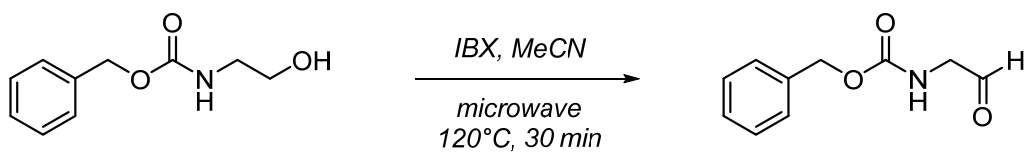
#	Acetate	Yield [%]
H ₁		86
I ₁		99
J ₁		99

A 1.4 Synthesis of Aldehydes



Yield 77 %

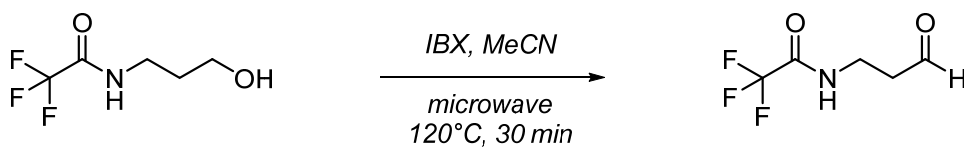
B₃



F₂

Yield 70 %

F₃

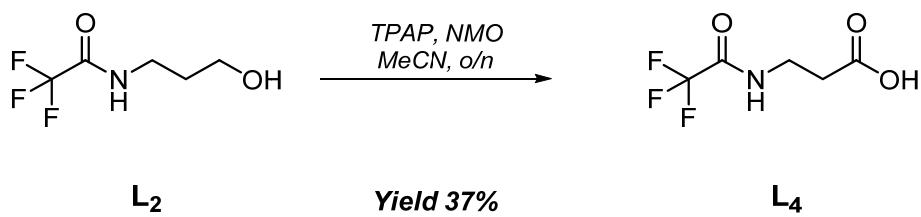
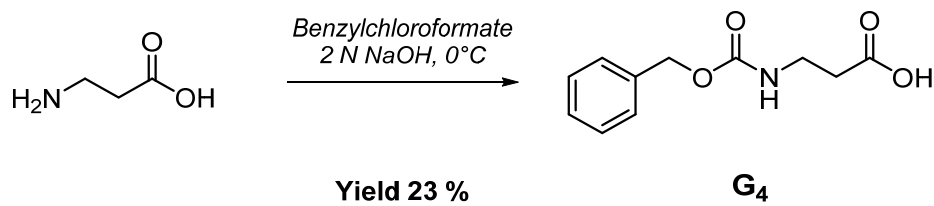
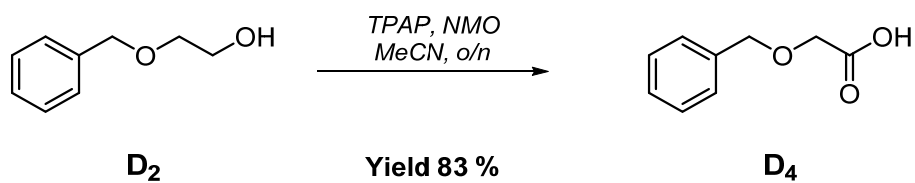


L₂

Yield 78%

L₃

A 1.5 Synthesis of Carboxylic Acids



A II Synthesis of Aldol Adducts by Pathway I

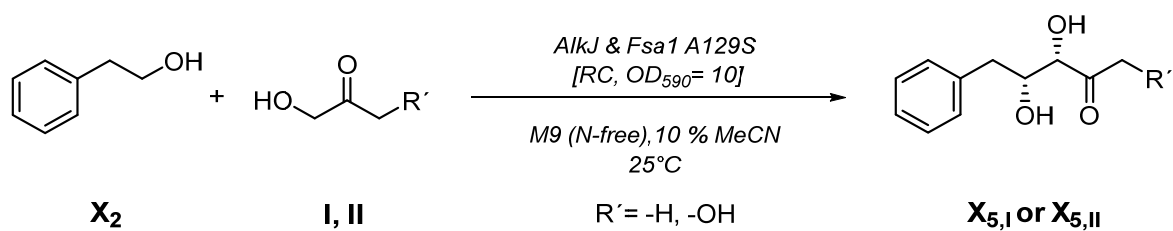


Table 7 Yields for dephosphorylated aldol adducts mediated by the POP construct (co-expressed AlkJ & Fsa1 A129S).

		Isolated Yields [%]			
	Acceptor	Donor	[A]	[B]	[C]
B _{5,I}		HA	40	-	70
B _{5,II}		DHA	-	28	78
D _{5,I}		HA	22	42	89
D _{5,II}		DHA	-	37	60
E _{5,I}		HA	20	21	61
E _{5,II}		DHA	-	18	64
G _{5,I}		HA	-	32	82
G _{5,II}		DHA	-	35	90

Different work up and isolations strategies were applied: **[A]** Extraction with organic solvent; **[B]** RP-HPLC; **[C]** SPE purified

A III Synthesis of Aldol Adducts by Pathway I

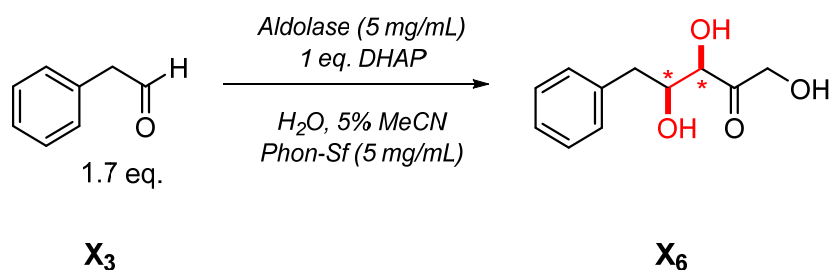
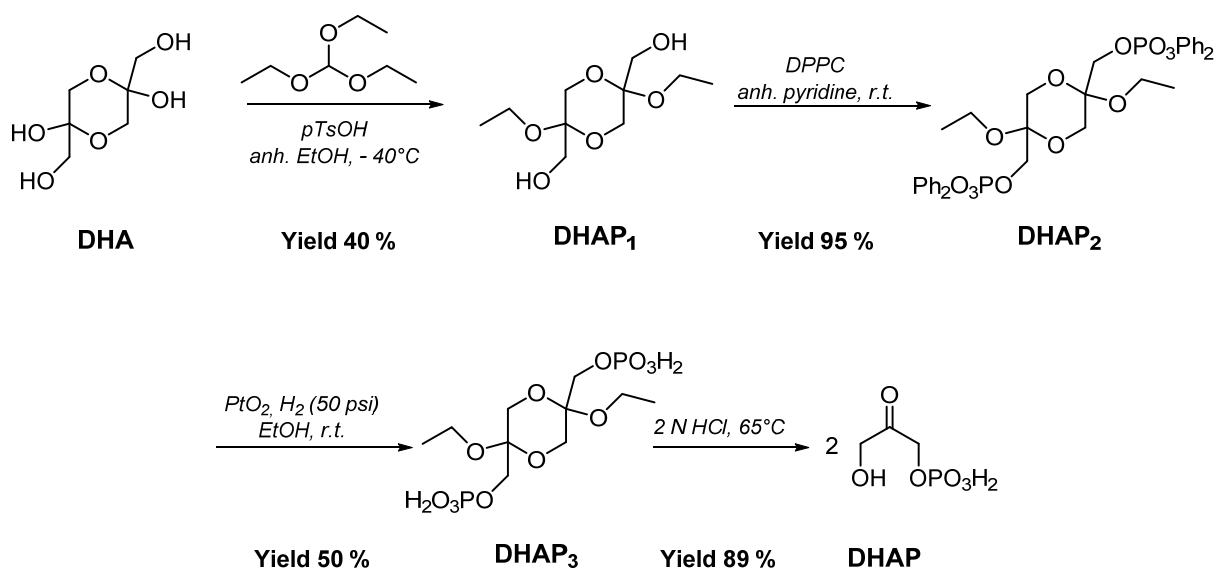


Table 8 Yields for dephosphorylated aldol adducts by preparative *in vitro* biotransformations using a DHAP dependent aldolase and an acidic phosphatase.

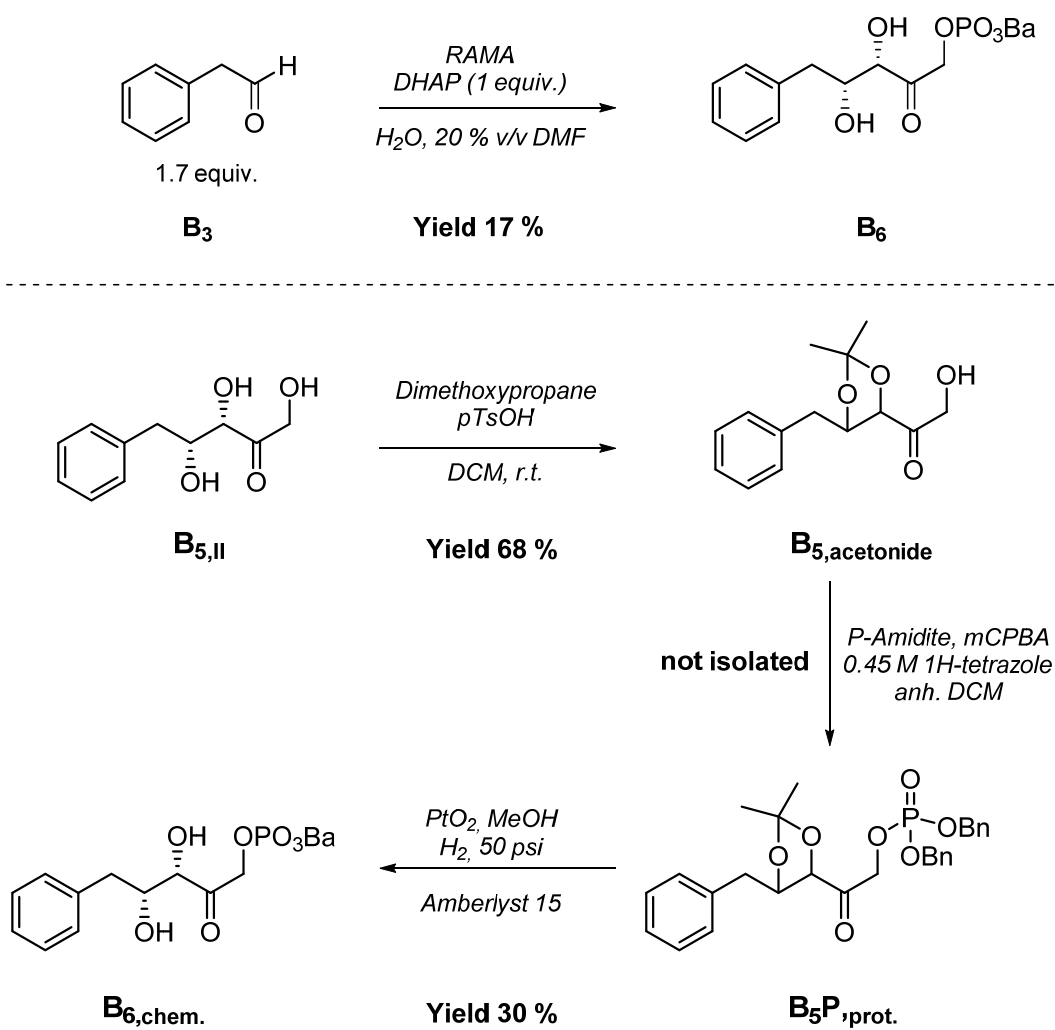
#	Substrate	Aldolase	Yield [%]	Stereoselectivity (<i>syn/anti</i>)
B _{6,FucA}		RhuA	15%	80/20
B _{6,RhuA}		RhuA	29%	60/40
D _{6,FucA}		FucA	10 %	[A]
E _{6,FucA}		FucA	n.a. [B]	-
G _{6,FucA}		FucA	10 %	[A]
L _{6,FucA}		FucA	n.a. [B]	-

[A]: *syn/anti* mixtures, mainly biotransformation impurities (4-2 ppm); [B]: according to LC/MS no product in the collected fractions after SPE.

A IV Synthesis of DHAP



A V Enzymatic and Chemical Strategies for the Synthesis of Phosphorylated Aldol Compounds



Introduction- Biotransformations in Organic Chemistry

Since decades, enzyme mediated transformations are omni-present in our daily life, for example (i) food production (fermentation products: cheese, beer etc.), (ii) additives for detergents, and (iii) more and more in chemical synthesis for important building blocks of fine chemicals (pharmaceuticals, flavors and fragrances) (**Table 9**).^{1,2,3,4}

From an environmental and economical point-of-view, biocatalysis represents an attractive alternative to conventional chemical transformations due to high chemo-, regio- and stereoselective transformations under mild reaction conditions (e.g. water as solvent, pH, low reaction temperature). Furthermore, enzymes are (i) compatible with each other (ii) not restricted to their natural substrates (iii) can catalyze a broad range of different transformations (e.g. hydrolysis, oxidation, reduction, halogenation etc.). Enzymes are efficient catalyst with high turnover rates, which are relatively simple and cheap to prepare.⁵

However, biocatalytic processes have several disadvantages such as highly diluted aqueous substrate solutions and on an industrial scale, waste water treatment.⁶ Additionally, limitations including biocatalyst preparation, recyclability and especially the required enzymes accessibility in large quantities for practical applications have to be considered.⁷

Table 9 The journey of biocatalysis over the last decades.^{6,7}

Time	Catalytic efficiency and selectivity
1980s	Crude enzyme preparation
1990s	Whole wild-type microbial cell
2000s	Isolated & overexpressed enzyme
2010s	Optimized enzyme mutants/artificial cascades

¹ M. T. Reetz, *JACS* **2013**, *135*, 12480-12496.

² T. Hudlicky, *Chem. Rev.* **2011**, *111*, 3995-3997.

³ T. Hudlicky, J. W. Reed, *Chem. Soc. Rev.* **2009**, *38*, 3117-3132.

⁴ C. M. Clouthier, J. N. Pelletier, *Chem. Soc. Rev.* **2012**, *41*, 1585-1605.

⁵ K. Faber, *Biotransformations in organic chemistry*, Springer-Verlag, **2011**.

⁶ Y. Ni, D. Holtmann, F. Hollmann, *ChemCatChem* **2014**, *6*, 930-943.

⁷ M. T. Reetz, *Chem. Rec.* **2016**, 2449-2459.

In the early 1980s, the first biocatalytic processes, which were utilizing cell extracts or whole microbes on industrial scale were established. These were applied to convert non-native substrates into pharmaceutical intermediates or fine chemicals.⁸

For these transformations, most commonly used enzyme classes were lipases, ketoreductases, proteases, aldolases, and hydroxynitrile lyases.⁹ New microbiology techniques, such as recombinant DNA technology, opened doors to enhance the portfolio of enzyme mediated reactions in organic synthesis.¹⁰ Especially, one of the major limitations, the lack of available biocatalysts, was solved by these improvements.¹¹

In addition to the discovery of novel enzymes to overcome limitations including a narrow substrate scope, poor selectivity, and low stability under reaction conditions, protein engineering has emerged as a very powerful strategy to develop new biocatalyst, with tailor-made properties (e.g. selectivity, stability, solvent tolerance, pH, temperature, etc.).¹² Besides, computational techniques and side-directed mutagenesis, directed evolution has expanded the toolbox of enzyme mediated reactions drastically. Moreover, the design of enzyme-variants give access to a new set of enzyme mediated reactions that were limited or simply not possible without that technologies.^{13,14,15}

Recently, directed evolution of various heme proteins from *Rhodothermus marinus* was successfully applied to generate unknown enzymatic activity for selective carbon-silicon coupling reactions (**Figure 2**). In nature, no organosilicon compounds nor metabolic pathways to create them are described, what makes this constructed artificial activity even more impressive.¹⁶

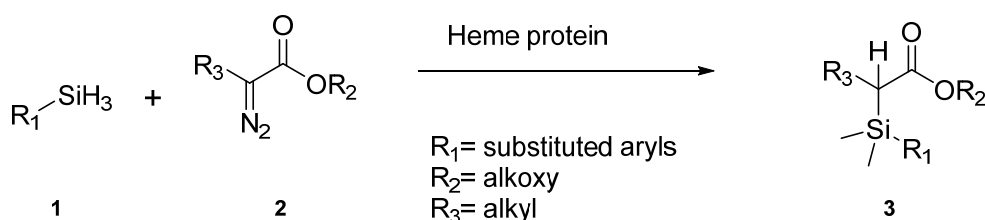


Figure 2 Enzyme mediated C-Si coupling by optimized heme proteins.

In general, a set of three Cytochrome c variants were capable of catalyzing the insertion of ethyl 2-diazopropanoate (**2**) into the Si-H bond of dimethyl(phenyl)silane (**1**) and derivatives. In total, 22 aryl

⁸ U. T. Bornscheuer, G. W. Huisman, R. J. Kazlauskas, S. Lutz, J. C. Moore, K. Robins, *Nature* **2012**, *485*, 185-194.

⁹ U. T. Bornscheuer, *Angew. Chem., Int. Ed.* **2016**, *55*, 4372-4373.

¹⁰ B. M. Nestl, S. C. Hammer, B. A. Nebel, B. Hauer, *Angew. Chem., Int. Ed.* **2014**, *53*, 3070-3095.

¹¹ G. A. Strohmeier, H. Pichler, O. May, M. Gruber-Khadjawi, *Chem. Rev.* **2011**, *111*, 4141-4164.

¹² R. O. M. A. de Souza, L. S. M. Miranda, U. T. Bornscheuer, *Chem. Eur. J.* **2017**, *23*, 12040-12063.

¹³ M. T. Reetz, *Angew. Chem., Int. Ed.* **2011**, *50*, 138-174.

¹⁴ K. A. Powell, S. W. Ramer, S. B. del Cardayré, W. P. C. Stemmer, M. B. Tobin, P. F. Longchamp, G. W. Huisman, *Angew. Chem., Int. Ed.* **2001**, *40*, 3948-3959.

¹⁵ M. T. Reetz, J. D. Carballeira, *Nat. Protocols* **2007**, *2*, 891-903.

¹⁶ S. B. J. Kan, R. D. Lewis, K. Chen, F. H. Arnold, *Science* **2016**, *354*, 1048-1051.

or alkyl substituted substrates were investigated and the newly formed C-Si bond (**3**) was observed with perfect enantioselectivity (ee) and high isolated yields (>70 %).

With focus to new transformations, which are limited or even not assessable by chemical protocol, a showcase example, the trifluoromethylation of unprotected phenol (**5**), was achieved by an enzyme mediated C-CF₃ bond formation (**Figure 3**). The target molecules (**6**) were observed with high regioselectivity by the recombination of radicals generated *via* two different pathways: (i) laccase from *Agaricus bisporus* for the formation of the phenol radical; (ii) *in situ* formation of electrophilic CF₃-radical (**4**) from either Langlois' reagent (NaSO₂CF₃) or Baran's zinc sulfinate (Zn(SO₂CF₃)₂=TFMS).¹⁷

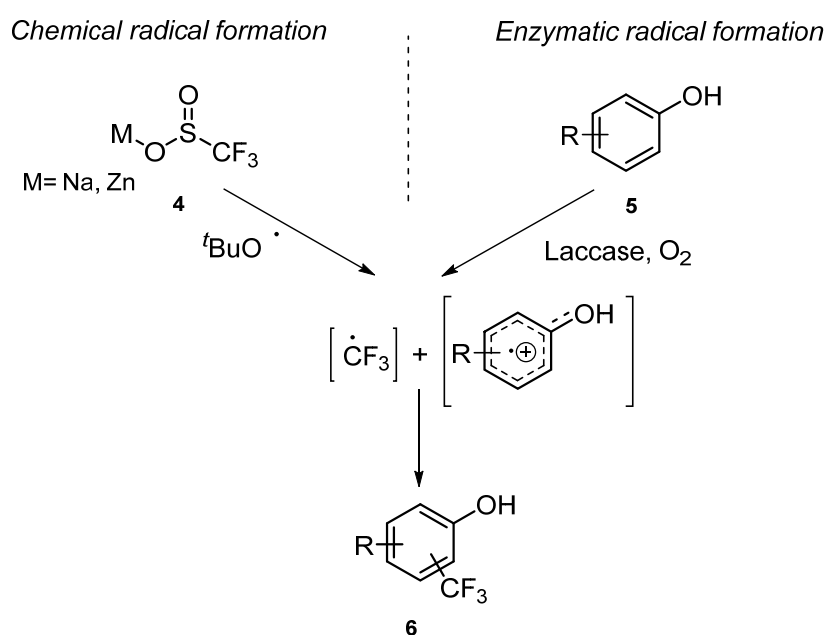


Figure 3 Chemo-enzymatic cascade for the regioselective trifluoromethylation of unprotected phenols.

In addition to the improvements of single step transformations towards novel enzyme mediated reactions, the combination of enzymes in a cascade fashion further expand the repertoire of organic reactions. Nature creates complex structures very efficiently from simple, readily-available, inexpensive starting materials with low waste production and without intermediate purification through metabolic pathways. However, nature is not able to produce everything we want, or in quantities we need, therefore artificial pathways (*in vitro* and *in vivo*) of natively non-related enzymes as well as artificial metallo-enzymes (incorporation of an organometallic moiety within a protein host) display attractive alternatives.¹⁸

¹⁷ R. C. Simon, E. Busto, N. Richter, V. Resch, K. N. Houk, W. Kroutil, *Nature Commun.* **2016**, *7*, 13323.

¹⁸ V. Kohler, Y. M. Wilson, M. Durrenberger, D. Ghislieri, E. Churakova, T. Quinto, L. Knorr, D. Haussinger, F. Hollmann, N. J. Turner, T. R. Ward, *Nat. Chem.* **2013**, *5*, 93-99.

A V.1 Cascade Type Reaction-*In Vitro* vs. *In Vivo* Setup

In general, an enzymatic cascade reaction describes a multi-step process that consists of two or more reaction steps catalyzed by enzymes without recovery of the intermediates. This concept is inspired by metabolic pathways, in which enzymes are linked to convert all kinds of substrates over several steps to demanded products. Due to the low concentrations of all reaction partners, byproduct formation is hindered and selectivities are enhanced. Biocatalytic cascade reactions are classified into four basic designs, namely, linear, parallel, orthogonal, and cyclic cascades (**Figure 4 & 5**). The most common linear system converts a substrate into a single product *via* one or more independent enzyme mediated reactions (**Figure 5**).¹⁹

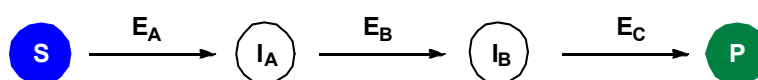


Figure 4 Illustration of a linear cascade setup in a sequential (Enzymes E_A , E_B , and E_C are added after completion of every single step) or concurrent fashion (all enzymes are added at the beginning).

This type of transformations can be performed in (i) a sequential mode (**Figure 4**, after the first step $S \rightarrow I_A$ is completed by enzyme E_A , the next enzyme E_B is added) or (ii) in a concurrent fashion (**Figure 4**, all enzymes (E_A , E_B , E_C) are added simultaneous with the substrate). The combination of several enzyme mediated transformations in a one-pot fashion offers advantages such as (i) shorter process time and lower costs, because no intermediate isolation or purification (ii) reversible reactions can be driven to completion, and (iii) the concentrations of toxic or unstable intermediates is reduced. In the case of multi-enzymatic cascades, performed in a linear one-pot fashion, the compatibility of the single enzymes has to be considered.^{20,21} Consequently, well balanced multistep biocatalytic routes can overcome thermodynamic hurdles and minimize the formation of byproducts.

The second regularly used setup are parallel cascades, which are closely related to orthogonal cascades and both are common designs in the field of redox biocatalysis (**Figure 5, A & B**). These coupled, simultaneously occurring processes are typically used for cofactor recycling systems in order to make their use more efficient.²² In an orthogonal cascade setting, a co-substrate (S_2) leads to an intermediate (**I**) that is converted *in situ* to the co-product (P_2) and this design is for example investigated to shift the reaction towards the primary product (P_1) by a driving force of side-product (P_2). Another cascade setup is the so called cyclic concept, which is typically used for stereoinversion processes (**Figure 5, C**).

¹⁹ R. C. Simon, N. Richter, E. Busto, W. Kroutil, *ACS Catal.* **2013**, *4*, 129-143.

²⁰ A. Bruggink, R. Schoevaart, T. Kieboom, *Org. Process Res. Dev.* **2003**, *7*, 622-640.

²¹ J. H. Schrittwieser, S. Velikogne, M. Hall, W. Kroutil, *Chem. Rev.* **2017**.

²² J. H. Schrittwieser, J. Sattler, V. Resch, F. G. Mutti, W. Kroutil, *Curr. Opin. Biotechnol.* **2011**, *15*.

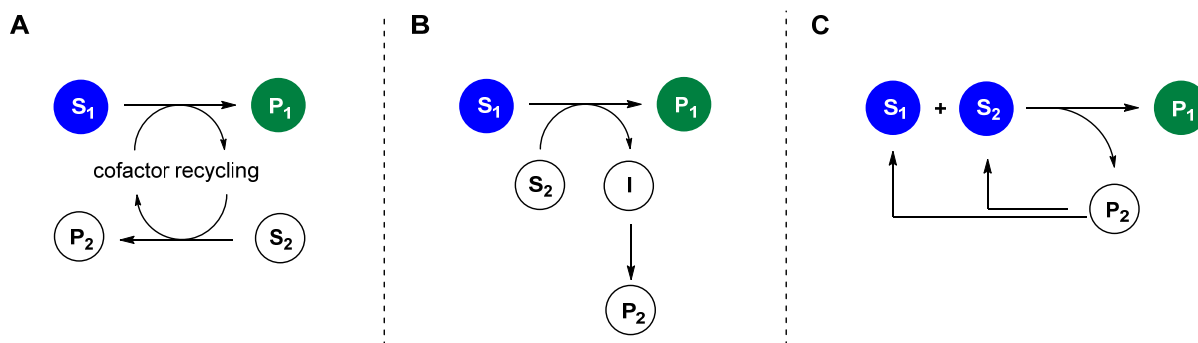


Figure 5 Illustration of a (A) parallel, (B) orthogonal, and (C) cyclic cascade setup.

In general, two starting materials (e.g. two enantiomers) are converted into the desired product (P_1) and the additionally generated coproduct (P_2) is transformed back and serve again as starting material.

Besides the classification concerning the cascade design, enzyme cascades can be divided due to the biocatalysts conditions into cell-free systems (*in vitro*) and whole cell transformations (*in vivo*) (Figure 6). Typically, the selection of the system depends on different factors, like the availability of gene sequences and heterologous enzymes, cofactor requirements, substrate uptake or product release, as well as the metabolic stability of substrates and product.

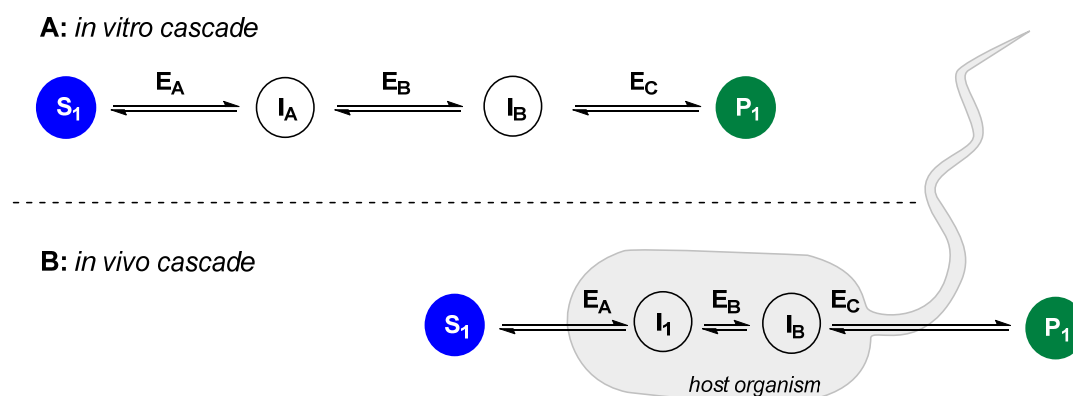


Figure 6 Comparison of *in vitro* and *in vivo* cascade setups.

The term “systems biocatalysis” has been used by Fessner to describe *in vitro* cascades, based on enzymatic and chemo-enzymatic reactions.²³ Isolated enzymes in a cascade fashion are often used to generate difficult or even not synthetically producible compounds in perfect chemo-, regio-, or stereoselectivity. In principle, *in vitro* cascades are performed by a combination of a set of selected enzymes. A fine balanced cascade concerning biocatalyst quantities, cofactor recycling and reaction conditions can avoid side product formation and enhances the substrate flux towards the target molecule. Additionally, competitive activities of an enzyme towards or by another cascade intermediate can be easily reduced by a sequential reaction setup.

²³ W.-D. Fessner, *N. Biotechnol.* **2015**, *32*, 658-664.

However, some drawbacks have to be discussed. In case of *in vitro* approaches, often time-consuming and elaborate enzyme purification as well as expensive, external cofactor supply are major drawbacks of such processes.^{24,25,26} When a multistep enzymatic cascade is designed *in vivo*, substrate uptake, product release and intrinsic host activity might be major challenges. *E. coli*, the most commonly used host organism is protected by the outer membrane, a lipophilic bilayer, which acts as a barrier for hydrophilic small molecules although it has stabilization effects on the expressed proteins. In general, substrate and product transport occur *via* diffusion processes, since active transporters are most likely not available for non-natural substrates.²⁷ Once the substrate has entered the cell, intrinsic activity of the host organism can metabolize such compounds, similar to the intrinsic activity of *E. coli* towards cytotoxic aldehydes.²⁸

To improve the overall performance of microbial cell factories different strategies can be proceeded: (i) fine tuning of cellular properties such as genetics (e.g. gene knock out) and/or physiology (e.g. membrane permeability and substrate uptake), (ii) process engineering (e.g. buffer, temperature, pH, use of biphasic systems), and (iii) catalyst design (e.g. protein engineering).^{29,30}

In Table 10, some advantages and disadvantages of cell free to whole cell biocatalysts are summarized.³¹

Table 10 Advantages and disadvantages of biocatalyst applications

	Cell-free systems	Whole cells
Pathway design	(+) tolerates harsher conditions (-) decreased stability and activity (-) membrane proteins can be used	(+) membrane proteins can be used (+) more stable (natural conditions) (-) cell wall: selective barrier: substrate uptake vs. product excretion (-) non-natural substrate can be cytotoxic
Process control	(+) easier process manipulation (+) direct substrate addition (+) defined enzyme stoichiometry	(+) cofactor recycling by the host organism (-) endogenous regulation is difficult (e.g. amount of enzyme to background) (±) heterologous activity can generate by-products
Costs	(+) simple storage and transfer (+) simple apparatus (-) cofactor addition & recycling (-) enzyme isolation and purification	(+) precursors from cheap medium substrates in case of metabolic engineering (-) upscaling: expensive apparatus

²⁴ M. Schrewe, N. Ladkau, B. Bühler, A. Schmid, *Adv. Synth. Catal.* **2013**, *355*, 1693-1697.

²⁵ B. Lin, Y. Tao, *Microb. Cell. Fact.* **2017**, *16*, 106.

²⁶ J. Wachtmeister, D. Rother, *Curr. Opin. Biotechnol.* **2016**, *42*, 169-177.

²⁷ S. Boyarskiy, D. Tullman-Ercek, *Curr. Opin. Chem. Biol.* **2015**, *28*, 15-19.

²⁸ T. Bayer, S. Milker, T. Wiesinger, M. Winkler, M. D. Mihovilovic, F. Rudroff, *ChemCatChem* **2017**, 2919–2923.

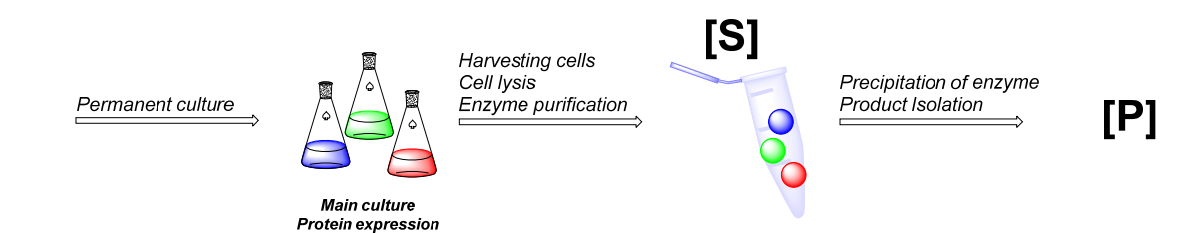
²⁹ A. M. Weeks, M. C. Chang, *Biochem.* **2011**, *50*, 5404-5418.

³⁰ T. Bayer, S. Milker, T. Wiesinger, F. Rudroff, M. D. Mihovilovic, *Advanced Synthesis & Catalysis* **2015**, *357*, 1587-1618.

³¹ Q. M. Dudley, A. S. Karim, M. C. Jewett, *Biotechnol. J.* **2015**, *10*, 69-82.

In Figure 7, the general work flow for the preparation and application of *in vitro* cascades and *in vivo* systems are depicted. Both strategies start with inoculation of an overnight culture in a growth media followed by protein expression, which is induced by for example with isopropyl- β -D-thiogalactopyranoside (IPTG) in an appropriate media, depending on the enzyme. The biocatalyst preparation for *in vitro* transformations requires additional working steps, (i) harvesting of main culture, (ii) cell lysis and (iii) enzyme purification, which is only mandatory if the cell free extract interferes with the desired reaction (**Figure 7, A**). Whole cell biocatalyzed reaction can be subdivided into two sections (i) resting and (ii) growing cells (**Figure 7, B**). In both cases, the organism is cultivated in a nutrient-rich medium and the substrate is added after the biomass production has reached a substantial level. In contrast to growing cells, where the substrate is added after a defined period of growth, resting cells are cultivated until the biomass production has reached a plateau. Additionally, the cells may be harvested, washed and resuspended in a nitrogen-free buffer, which contains all important ingredients to maintain the host metabolism. Whole cell biocatalysts are beneficial due to (i) simple and easy catalyst preparation, (ii) fast catalyst removal by centrifugation or filtration and (iii) no need of addition of expensive and instable cofactors.

A) Work flow for *in vitro* pathway setup



B) Work flow for *in vivo* pathway setup

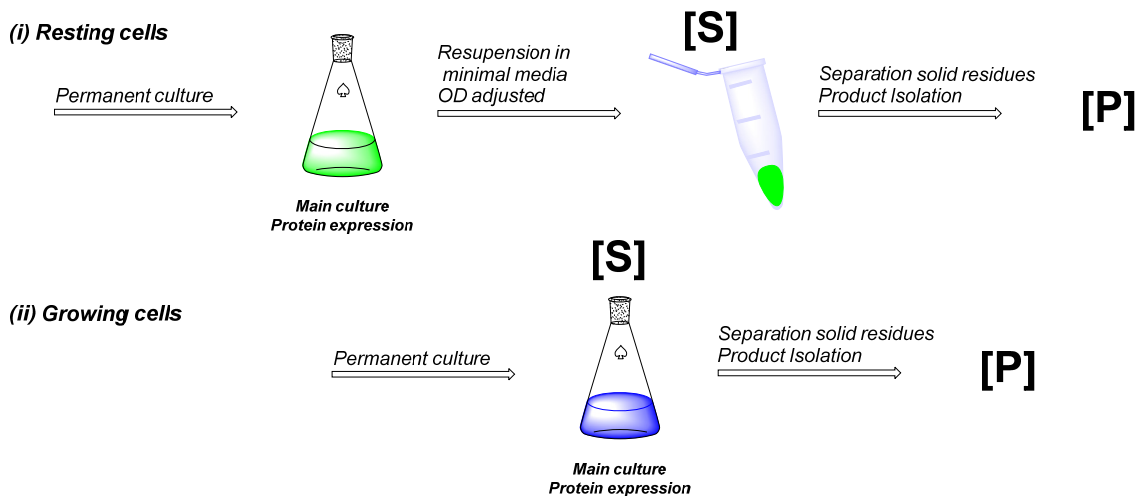


Figure 7 General work flow for synthetic applications of different biocatalyst preparations.

The major disadvantages are competing reactions, which lead to the production of byproducts. This drawback can be circumvented by the use of isolated enzymes, which enables a more easily controlled

biocatalytic system. However, this biocatalyst preparation has to deal with decreased catalyst stability, elaborate and time-consuming enzyme purification (e.g. chromatography) and the need of expensive cofactors (e.g. NAD(P)H). In case of whole cells, the main culture itself can serve as active biocatalyst, which is known as growing cells (**Figure 7**, (ii)). Resting cells, on the other hand, are cells which were harvested and used after resuspension in a resting cell medium which lacks for the growth essential nitrogen (**Figure 7**, (i)). A minimal medium contains ingredients such as glucose, which are required to maintain all intracellular pathways of the whole cell biocatalyst but no additional cell growth is supported. To establish this so called “microbial cell factories”, detailed know-how of molecular biology techniques are required for the (i) co-expression of several enzymes into a host organism, (ii) expression stability and quantity of all utilized enzymes as well as (iii) determination of growth behavior.³²

³² T. Bayer, S. Milker, T. Wiesinger, F. Rudroff, M. D. Mihovilovic, *Adv. Synth. Catal.* **2015**, 357, 1587-1618.

Enzymatic C-C Bond Formations in Organic Synthesis

The skeleton of many organic molecules is based of carbon-carbon bonds and their construction is one of the simplest methodologies to increase structural complexity with respect to chirality and the introduction of new functional groups. In a single transformation step, two fragments are connected to form a new C-C bond as well as two new stereogenic centers. The resulting products are important motifs for countless of bioactive agents.^{33,34} In both areas, biocatalysis as well as chemo-catalysis, investigations for efficient C-C bond formations, such as aldol reactions, cyanohydrin formation, acyloin synthesis were conducted and summarized in several reviews (**Figure 8**).^{35,36} These developments of novel synthetic methods, regardless of their nature (enzyme or chemo mediated), enable opportunities for the planning of new targeted synthetic routes.

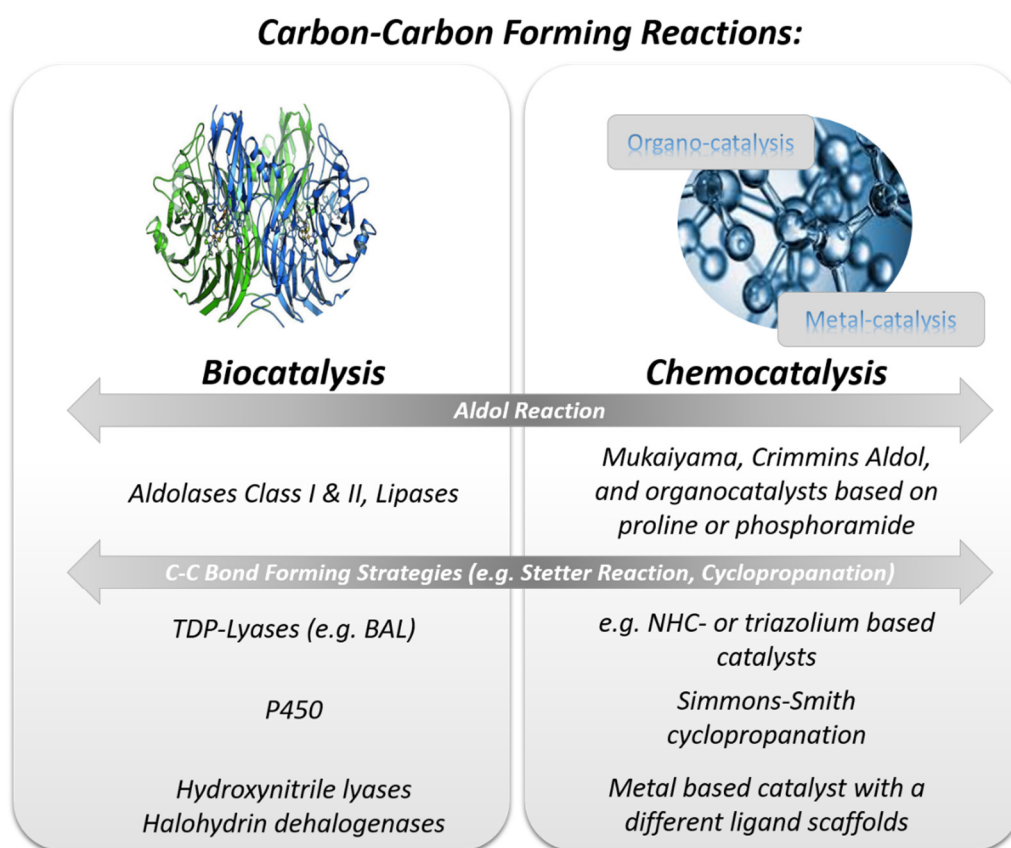


Figure 8 Comparison of C-C bond forming reactions in the fields of biocatalysis and chemocatalysis.

³³ M. Brovetto, D. Gamenara, P. Saenz Méndez, G. A. Seoane, *Chem. Rev.* **2011**, *111*, 4346-4403.

³⁴ N. G. Schmidt, E. Eger, W. Kroutil, *ACS Catal.* **2016**, *6*, 4286-4311.

³⁵ M. Hömig, P. Sonderrmann, N. J. Turner, E. M. Carreira, *Angew. Chem., Int. Ed.* **2017**, *56*, 8942-8973.

³⁶ R. O. M. A. de Souza, L. S. M. Miranda, U. T. Bornscheuer, *Chem. Eur. J.* **2017**, *23*, 12040-12063.

As depicted in Figure 8, a diverse toolbox for C-C bond formation reactions is available that contains enzyme mediated reactions as well as the related chemical counterpart reactions (e.g. Aldol reaction, Stetter type addition, etc.). But there are also prominent examples of chemical transformations, such as coupling reactions (e.g. Heck, Suzuki), metathesis or C-H activation, which have especially with focus to substrate scope and flexibility nearly no enzymatic counterpart reactions.^{37,38,39,40}

Enzyme catalyzed C-C bond formations, which focus on selectivity (stereo-, regio-, and chemo) are difficult to mimic by conventional synthetic approaches. Additionally, the increased tolerance of enzymes for unnatural substrates and “harsher” reaction conditions (e.g. amount of organic solvent, temperature, etc.) explains the increasing implementation of biocatalyzed synthetic routes of non-natural products.

For the design of enzymatic pathways, the idea of “biocatalytic” retrosynthesis is often investigated, which is based on the concept of targeted disconnections of complex to smaller molecules (**7**).⁴¹ In the mid-1960s, first retrosynthetic approaches for the design of new synthetic routes were established and the essential principles of retrosynthesis were proposed by E. J. Corey (**Figure 9**).⁴²

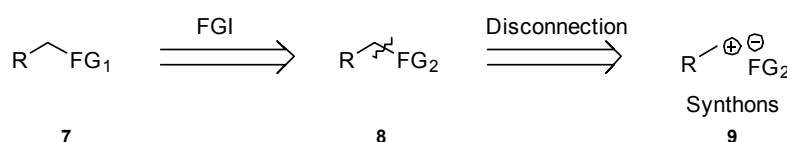


Figure 9 Retrosynthetic key steps for the design of a multi-enzymatic cascade.

Functional group interconversions (FGI) and targeted bond disconnections are the basis of retrosynthesis and require a toolbox of different transformations (**8**, **9**). For transformations, which are critical due to selectivity (stereo-, regio-, and chemo-), enzyme mediated reactions are increasingly considered and are applied several times to multiple-enzyme cascade processes (*in vitro* or *in vivo*).^{43,44,45,46,47,48}

Consequently, the next step was to combine enzymes and chemo-catalysts in so called “chemo-enzymatic” cascade reactions. Chemo-enzymatic processes in a one-pot fashion are of great interest for the selective synthesis of chiral building blocks, but are still limited due to compatibility issues, and

³⁷ C. C. Johansson-Seechurn, M. O. Kitching, T. J. Colacot, V. Snieckus, *Angew. Chem., Int. Ed.* **2012**, *51*, 5062-5085.

³⁸ A. H. Hoveyda, A. R. Zhugralin, *Nature* **2007**, *450*, 243-251.

³⁹ T. Gensch, M. N. Hopkinson, F. Glorius, J. Wencel-Delord, *Chem. Soc. Rev.* **2016**, *45*, 2900-2936.

⁴⁰ H. M. L. Davies, D. Morton, *J. Org. Chem.* **2016**, *81*, 343-350.

⁴¹ N. J. Turner, E. O'Reilly, *Nat. Chem. Biol.* **2013**, *9*, 285-288.

⁴² E. J. Corey, *Chem. Soc. Rev.* **1988**, *17*, 111-133.

⁴³ P. Both, H. Busch, P. P. Kelly, F. G. Mutti, N. J. Turner, S. L. Flitsch, *Angew. Chem., Int. Ed.* **2016**, *55*, 1511-1513.

⁴⁴ J. Muschiol, C. Peters, N. Oberleitner, M. D. Mihovilovic, U. T. Bornscheuer, F. Rudroff, *Chem. Commun.* **2015**, *51*, 5798-5811.

⁴⁵ N. Ladkau, A. Schmid, B. Bühler, *Curr. Opin. Biotechnol.* **2014**, *30*, 178-189.

⁴⁶ M. Schrewe, M. K. Julsing, B. Bühler, A. Schmid, *Chem. Soc. Rev.* **2013**, *42*, 6346-6377.

⁴⁷ E.-M. Fischereeder, D. Pressnitz, W. Kroutil, *ACS Catal.* **2016**, *6*, 23-30.

⁴⁸ M. Mifsud, S. Gargiulo, S. Iborra, I. W. Arends, F. Hollmann, A. Corma, *Nat. Commun.* **2014**, *5*, 3145.

thereby, most of these processes are performed in a sequential mode or with an additional enzyme protection system (e.g. biphasic setup, polymer membrane).^{49,50,51}

Besides the combination of a biocatalyst with a metal catalyst,^{52,53,54,55} organocatalysts were also investigated, but mainly in a sequential fashion due to biocatalyst/organocatalyst inhibition under the applied reaction conditions (**Figure 10**).⁵⁶

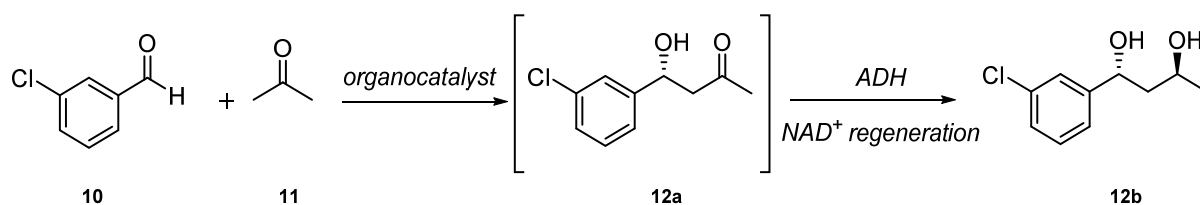


Figure 10 Organocatalyzed C-C coupling reaction combined with an ADH mediated ketone reduction.

An often-limiting factor for enzymatic C-C bond forming reactions is the very restricted donor or acceptor promiscuity of the enzymes (**10**, **11**). Therefore, organocatalyzed reactions (e.g. Aldol,⁵⁷ Mannich⁵⁸) combined with stereoselective enzymatic transformation (**12a**, **12b**) present an attractive alternative in respect to asymmetric synthesis. Obviously, both reaction classes, biocatalyzed as well as chemo-catalyzed, combined or alone, are powerful tools and are fast growing research fields, which should be equally taken into account for the planning of new synthetic routes. Due to the low environmental impact, perfect selectivity and the ability to combine enzymes in a cascade fashion, biocatalysis represents more than an alternative to conventional chemical transformations, which requires, for example, stoichiometric amounts of often also toxic reagents. Additionally, a major benefit of enzyme mediated reactions is their identical working conditions that enables the design of artificial enzyme pathways.

Within the next sections, selected case studies for cascade reactions, which especially involve a C-C bond forming transformation will be discussed.

⁴⁹ P. Schaaf, PhD Thesis, **2017**.

⁵⁰ H. Gröger, W. Hummel, *Curr. Opin. Chem. Biol.* **2014**, *19*, 171-179.

⁵¹ E. García-Junceda, I. Lavandera, D. Rother, J. H. Schrittwieser, *J. Mol. Catal. B: Enzym.* **2015**, *114*, 1-6.

⁵² H. Sato, W. Hummel, H. Gröger, *Angew. Chem., Int. Ed.* **2015**, *54*, 4488-4492.

⁵³ J. Latham, J.-M. Henry, H. H. Sharif, B. R. K. Menon, S. A. Shepherd, M. F. Greaney, J. Micklefield, *Nature Commun.* **2016**, *7*.

⁵⁴ Á. Gómez Baraibar, D. Reichert, C. Mügge, S. Seger, H. Gröger, R. Kourist, *Angew. Chem., Int. Ed.* **2016**, *55*, 14823-14827.

⁵⁵ N. Ríos-Lombardía, C. Vidal, E. Liardo, F. Morís, J. García-Álvarez, J. González-Sabín, *Angew. Chem., Int. Ed.* **2016**, *55*, 8691-8695.

⁵⁶ E. Liardo, N. Ríos-Lombardía, F. Morís, F. Rebolledo, J. González-Sabín, *ACS Catal.* **2017**, 4768-4774.

⁵⁷ M. Heidlindemann, G. Rulli, A. Berkessel, W. Hummel, H. Gröger, *ACS Catal.* **2014**, *4*, 1099-1103.

⁵⁸ R. C. Simon, E. Busto, J. H. Schrittwieser, J. H. Sattler, J. Pietruszka, K. Faber, W. Kroutil, *Chem. Commun.* **2014**, *50*, 15669-15672.

A V.1.1 Showcase Examples of *In Vitro* and *In Vivo* Cascades Approaches

As introduced before, C-C coupling reactions are one of the key transformations in chemical synthesis. In order to enable the formation of the desired product in an economically friendly as well as in a chemo-, regio-, and stereoselective manner, enzyme mediated reactions were established. The most prominent biocatalytic carbonylation reactions are based on the use of lyases, such as aldolases (EC 4.1.2.13), hydroxynitrile lyase (EC 4.1.2.47), benzaldehyde lyase (EC 4.2.1.38) and pyruvate decarboxylase (Figure 11).^{59,60,61}

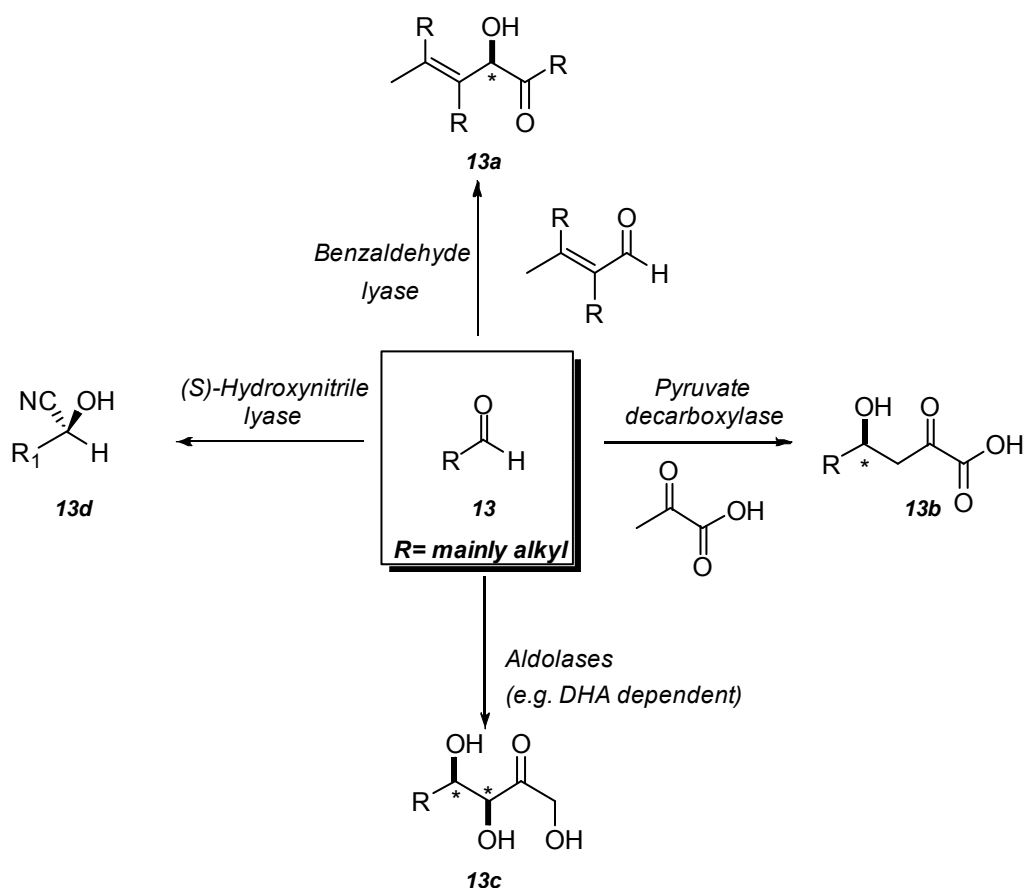


Figure 11 Overview of frequently used enzyme mediated C-C bond forming reactions

The following examples will involve (i) *in vitro* enzyme cascades as well as (ii) *in vivo* cascades, which are focused on enzyme mediated bond formations. An illustrative example for a stereoselective multi-enzymatic *in vitro* cascades with an efficient recycling strategy to provide pyruvate for a carbonylation reaction with benzaldehyde was published in 2013 (Figure 11).^{62,63}

⁵⁹ M. Brovotto, D. Gamenara, P. Saenz Méndez, G. A. Seoane, *Chem. Rev.* **2011**, *111*, 4346-4403.

⁶⁰ N. G. Schmidt, E. Eger, W. Kroutil, *ACS Catal.* **2016**, *6*, 4286-4311.

⁶¹ M. Müller, G. A. Sprenger, M. Pohl, *Curr. Opin. Chem. Biol.* **2013**, *17*, 261-270.

⁶² T. Sehl, H. C. Hailes, J. M. Ward, U. Menyes, M. Pohl, D. Rother, *Green Chem.* **2014**, *16*, 3341-3348.

⁶³ T. Sehl, H. C. Hailes, J. M. Ward, R. Wardenga, E. von Lieres, H. Offermann, R. Westphal, M. Pohl, D. Rother, *Angew. Chem., Int. Ed.* **2013**, *52*, 6772-6775.

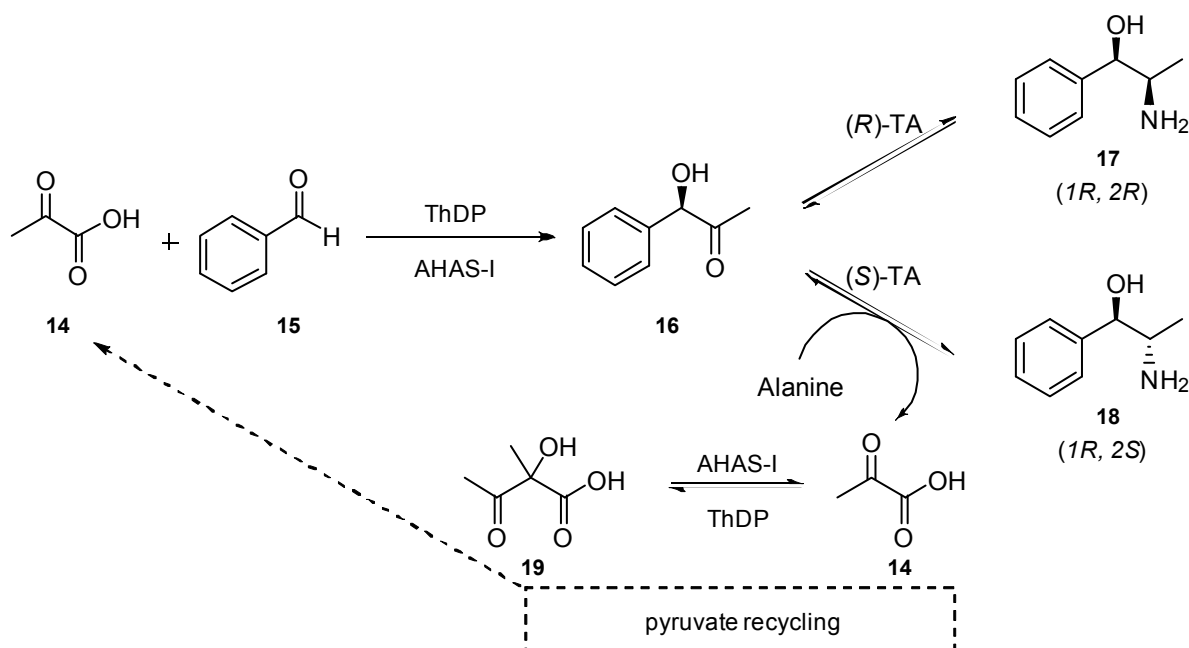


Figure 12 Two step *in vitro* cascade for the formation of (1*R*,2*R*)-norpseudoephedrine and (1*R*,2*S*)-norephedrine starting from benzaldehyde and pyruvate with a regeneration system for pyruvate from alanine (amine donor).

This biocatalytic route provided enantiomerically pure (*ee*>98%) (1*R*,2*R*)-norpseudoephedrine (**17**), or (1*R*,2*S*)-norephedrine (**18**) in excellent yields after applying an optimized recycling strategy for the pyruvate, which is acting as a nucleophile during the first cascade step. First, decarboxylation of pyruvate (**19**, **14**) was performed *via* thiamine diphosphate (ThDP)-dependent acetoxyacid synthase I from *E. coli* (AHAS-I) and an *in situ* C-C bond formation with benzaldehyde (**15**) as acceptor affording the intermediate (*R*)-phenylacetylcarbinol (**16**). Subsequently, (*R*)- or (*S*)-selective transaminases from different organisms (e.g. *Chromobacterium violaceum*) using alanine as amine donor were implemented into the cascade and afford the enantiomerically pure products in excellent yields (**17**, **18**). Moreover, the formed pyruvate byproduct generated by the stereoselective amination from alanine was redirected or “recycled” into the cascade and served again as substrate. Since benzaldehyde was also converted by the transaminases to the corresponding amine, best results were obtained in a sequential reaction setup, adding the TA after full consumption of the electrophile (>96% conversion; high *de* & *ee* >98%).

With focus on asymmetric synthesis of challenging heterocyclic compounds, a multi-enzymatic cascade approach to provide benzylisoquinoline alkaloids in stereoselective fashion was published by Lichman *et al.* (**Figure 13**).⁶⁴ First, substituted benzylamine derivatives (**20**) were transformed *via* a transaminase (ω -TA) from *Chromobacterium violaceum* or *P. putida*, both showed similar activity towards the model substrate, using pyruvate as the amine acceptor to the corresponding aldehyde (**21**). Subsequently, the asymmetric Pictet-Spengler reaction was mediated by the plant enzyme norcoclaurine synthase (NCS) between the formed aldehyde (**21**) and added primary amine (**20**).

⁶⁴ B. R. Lichman, E. D. Lamming, T. Pesnot, J. M. Smith, H. C. Hailles, J. M. Ward, *Green Chem.* **2015**, *17*, 852-855.

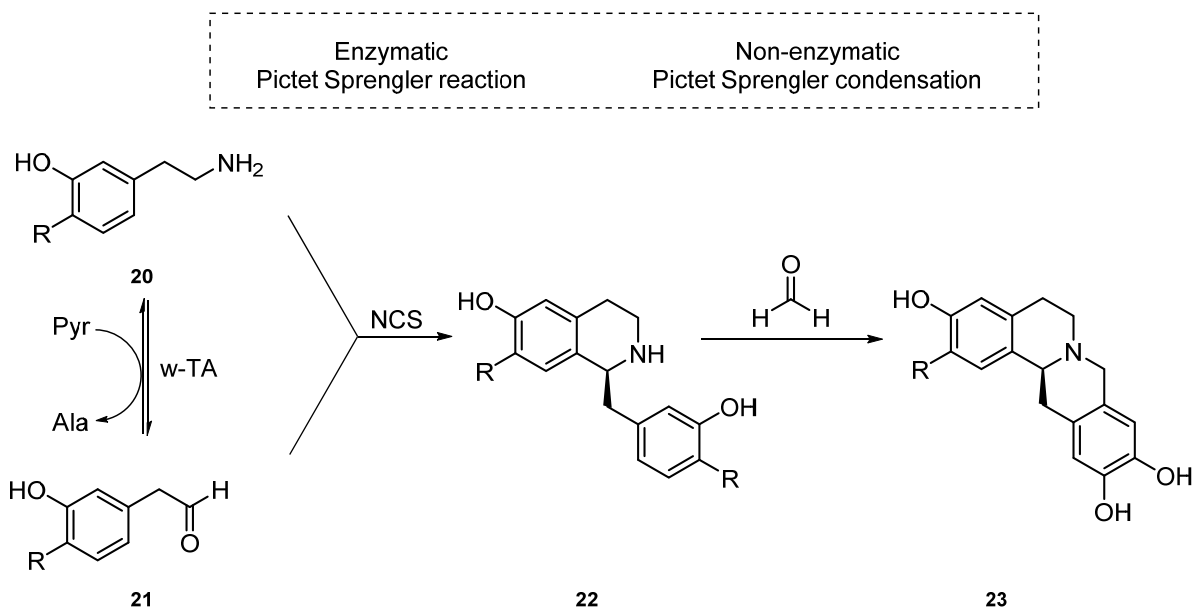


Figure 13 *In vitro* Cascade in a triangular configuration for the synthesis of benzylisoquinoline alkaloids consisting of a transaminase (w-TA) and a norcoclaurine synthase (NCS).

The stoichiometry of the coupling reagents was controlled by the equivalents of added pyruvate. Also, this cascade approach deals with undesirable side reactions. A racemization of the product occurred due to a non-enzymatic Pictet-Sprengler reaction in buffer of the formed aldehyde intermediate. To circumvent aldehyde accumulation, the reactions rates of both applied enzymes were balanced by the amount of added biocatalysts and under optimized reaction conditions, the corresponding Pictet-Sprengler adduct (**22**) was isolated in 62% yield. Furthermore, the addition of formaldehyde initiated a non-enzymatic Pictet-Sprengler condensation to afford tetrahydroprotoberberine (**23**). To demonstrate the usefulness of that reaction setup, a preparative scale experiment using lysate of TA and NCS afford the final product in 42% isolated yield with an enantiomeric excess of >95%.

During the last years, lyases such as phenylalanine ammonia lyase (PAL) from *Anabaena variabilis* or tyrosine phenol lyase (TPL) from *Citrobacter freundii* were recognized as powerful tools for regioselective functionalization of phenol derivatives (**25**, **26**).^{65,66,67} A regioselective C-C coupling of substituted phenols and pyruvate in the presence of ammonia displays the key cascade step for several linear processes (**Figure 14**).

⁶⁵ S. T. Ahmed, F. Parmeggiani, N. J. Weise, S. L. Flitsch, N. J. Turner, *Org. Lett.* **2016**, *18*, 5468-5471.

⁶⁶ A. Dennig, E. Busto, W. Kroutil, K. Faber, *ACS Catal.* **2015**, *5*, 7503-7506.

⁶⁷ E. Busto, M. Gerstmann, F. Tobola, E. Dittmann, B. Wilschi, W. Kroutil, *Catal. Sci. Technol.* **2016**.

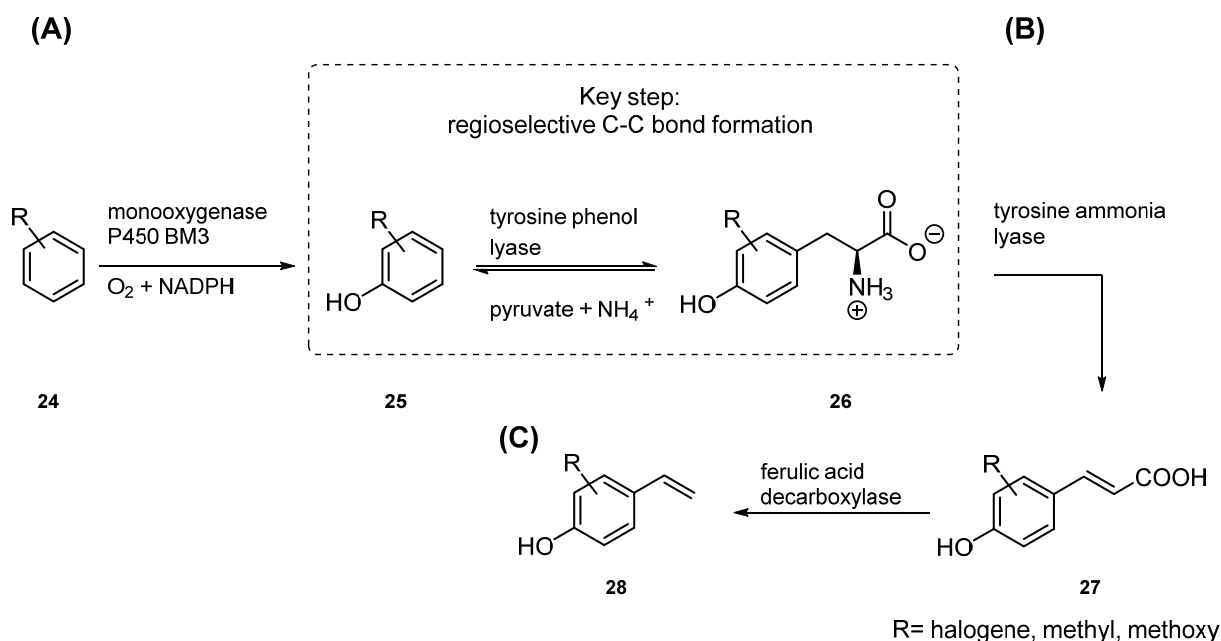


Figure 14 Summary of different *in vitro* cascades, which contains a regioselective C-C coupling catalyzed by the tyrosine phenol lyases.

This transformation was implemented into different biocatalytic systems (A) combined with the monooxygenase P450 BM3 for a regioselective hydroxylation (24) in *o*-position of mono-substituted arenes (B) followed by deamination (tyrosine ammonia lyase from *Citrobacter freundii* to afford *p*-coumaric acid derivatives (27) (C) additional decarboxylation by the ferulic acid decarboxylase from *Enterobacter sp.* yielded with a high regioselectivity exclusively at desired para vinylated product (28).⁶⁸

These multi-enzymatic cascades, based on tyrosine phenol lyases, emphasizes the compatibility of enzymes under optimized reactions conditions and an even more modular cascade concept, by designing a whole cell biocatalyst, was reported by the group of Li.

Three different artificial pathways consisting of four to eight non-natively related enzymes for the synthesis of chiral α -hydroxyacids, 1,2-amino alcohols, and α -amino acids from terminal alkenes were designed (Figure 15).^{69,70} Each module was located on a single plasmid and co-expressed in *E. coli*. Different combinations of the expression constructs were investigated to reduce the metabolic burden and enzymes were selected to avoid the formation of byproducts or unreactive intermediates. In particular, each following enzyme had a higher activity than the previous one to pull the reactions equilibrium towards product side.

⁶⁸ E. Busto, R. C. Simon, W. Kroutil, *Angew. Chem., Int. Ed.* **2015**, *54*, 10899-10902.

⁶⁹ Y. Zhou, S. Wu, Z. Li, *Angew. Chem., Int. Ed.* **2016**, *55*, 11647-11650.

⁷⁰ S. Wu, Y. Zhou, T. Wang, H.-P. Too, D. I. C. Wang, Z. Li, *Nat. Commun.* **2016**, *7*.

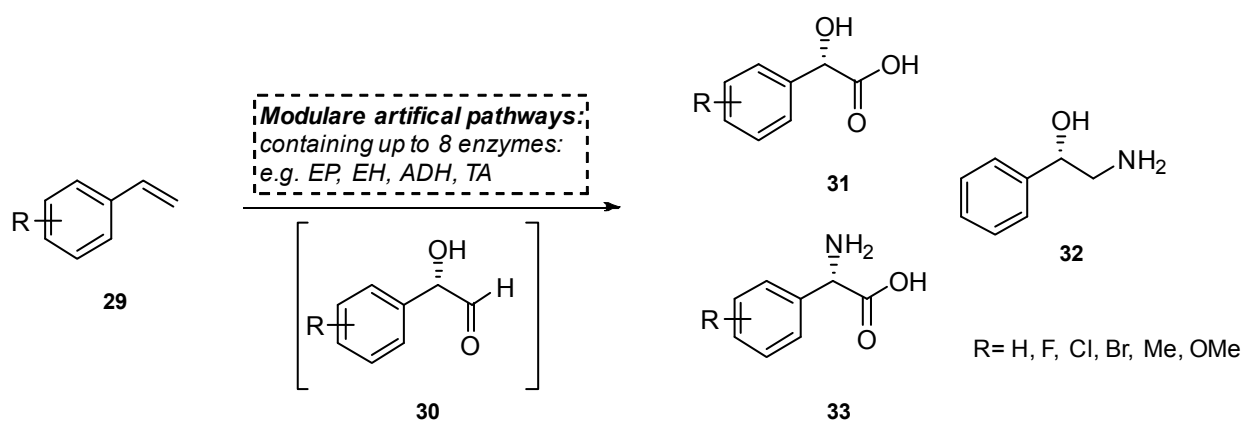


Figure 15 Modular pathway design for functionalization of substituted alkenes.

In all pathways, module 1 was installed, consisting of an epoxidase (EP) from *Spingomonas sp.* and epoxide hydrolase (EH) from *P. putida* for the production of 1,2-diol from a series of substituted alkenes (**29**). During a selective oxidation via AlkJ from *P. putida*., the intracellular formed aldehyde (**30**) was *in situ* converted by a ω -transaminase from *E. coli* to the amine or with an additional ADH from *B. subtilis* to the corresponding carboxylic acid in isolated yields up to 72% and 98% ee (**31-33**). To enhance the overall productivity of artificial pathways, different strategies of reaction and catalyst engineering were applied for the functionalization of the terminal non-activated C-H bonds of fatty acid methyl esters (FAMEs) by the group of Schmid and Bühler (**Figure 16**).^{71,72} Two different pathways were designed, both contain the alkane monooxygenase AlkBGT from *P. putida*, which is capable to oxidize alkanes (DAME) to the corresponding carboxylic acid (DDAME). Due to limited substrate uptake and substrate flux through the cascade, AlkBGT was co-expressed with the outer membrane protein *alkL*, and AlkJ, all from *P. putida*.

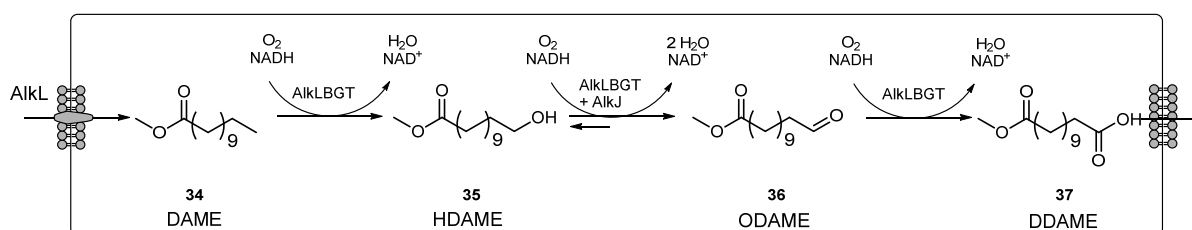


Figure 16 Illustration of an optimized artificial pathway. (34) DAME: dodecanedioic acid methyl ester; (35) HDAME: 12-hydroxydodecanoic acid methyl ester; (36) ODAME: 12-oxododecanoic acid methyl ester; (37) DDAME: dodecanedioic acid monomethyl ester.

The introduction of an additional ADH, namely AlkJ was necessary to shift the reaction equilibrium towards the thermodynamically disfavored aldehyde moiety (**36**). Finally, DDAME (**37**) is generated by AlkLBGT, transported through the cell membrane and isolated on industrial scale quantities. In addition to optimization strategies on process levels, an artificial pathway with an enhanced substrate flux was established in an engineered *E. coli* strain by Prather and coworkers. A targeted gene deletion

⁷¹ M. Schrewe, M. K. Julsing, K. Lange, E. Czarnotta, A. Schmid, B. Bühler, *Biotechnology and Bioengineering* **2014**, *111*, 1820-1830.

⁷² M. Schrewe, N. Ladkau, B. Bühler, A. Schmid, *Adv. Synth. Catal.* **2013**, *355*, 1693-1697.

approach was performed to minimize intrinsic aromatic aldehyde reductase activity and the established “RARE” strain was used for the production of vanillin from vanillate by CAR from *N. iowensis*.⁷³

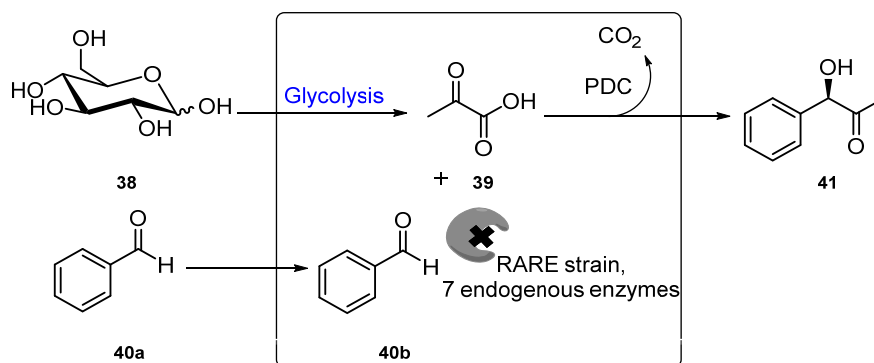


Figure 17 *In vivo* cascade for the synthesis of *L*-phenylacetyl carbinol by over-expressed PDC in the optimized RARE strain. Moreover, a concurrent C-C bond formation of the reactive aldehyde intermediate and the glycolytic product pyruvate (**39**) by recombinant pyruvate decarboxylase (PDC) mutant from *Zymomonas mobilis* was described (**Figure 17**). Within 24 h, 5 mM benzaldehyde (**40a,b**) was exclusively transformed to the chiral pharmaceutical intermediate *L*-phenylacetyl carbinol (**41**).

This result underlines our project proposal (**Figure 18**), to establish a whole cell biocatalyst for the synthesis polyhydroxylated compounds (e.g. **B₅**) by utilizing the glycolytic intermediated DHAP, provided by the host organism.

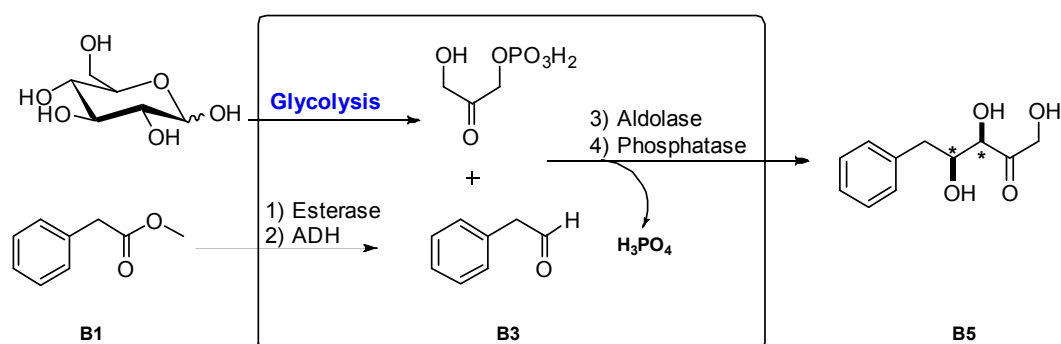


Figure 18 *In vivo* cascade for the synthesis of *L*-phenylacetyl carbinol by over-expressed PDC in the optimized RARE strain. As shown in Figure 18, the glycolysis of the host organism is used for the supply the aldol nucleophile DHAP, which subsequently undergoes a C-C bond forming reaction followed by a dephosphorylation step to enable a sufficient product secretion.

⁷³ A. M. Kunjapur, K. L. J. Prather, *Environ. Microbiol. Rep* **2015**, *81*, 1892-1901.

Scope of the Thesis

A VI Requirements on the Designed Pathways

In the past years significant improvements of stereoselective aldolase mediated reactions for the preparation of carbohydrates and derivatives were reported. However, these approaches mainly deal with isolated enzymes (*in vitro*) by a single transformation setup that is utilizing the instable aldol acceptor aldehyde. Therefore, two different artificial pathways were established in the host organism *E. coli* and these have served as a biocatalytic tool for the synthesis of polyhydroxylated compounds, which are important building blocks for fine chemicals and pharmaceuticals (**Figure 19**).⁷⁴

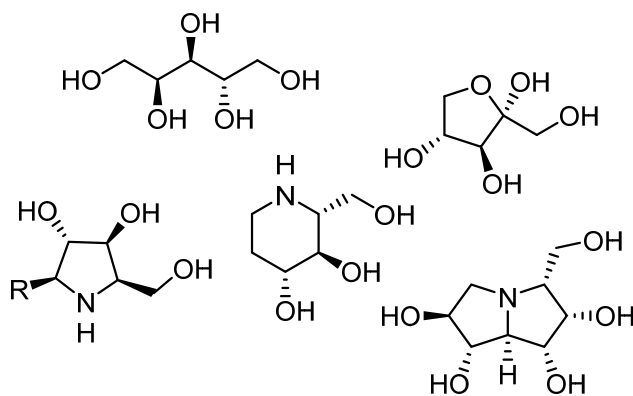


Figure 19 Target products of the designed pathways.

For example, aldose carbohydrates, *O*-phosphorylated sugars (e.g. 1-deoxy-*D*-fructose-6-phosphate, 1-deoxy-*D*-xylose-5-phosphate, *D*-arabinose-5-phosphate, etc.), and the nitrogen containing azasugars are therapeutically important frameworks with biological activities including inhibition of glycosidases, glycotransferases, or hexoaminidases.⁷⁵

In general, both *de novo* pathways are designed for the synthesis of carbohydrate derivatives but they mainly differ by the type of aldolase, which is utilized for the stereoselective C-C bond forming reaction. The initial pathway steps, an esterase mediated hydrolysis followed by an *in situ* oxidation of the generated primary alcohol were implemented, to design an efficient synthetic route to provide the required aldehyde (aldol acceptor molecule) in sufficient quantities (**Figure 20**).

Pathway I was linked by a redox biotransformation (oxidation using an ADH) to the energy balance of the host organism and the aldol donor molecule, in this case DHA or HA, was added to the

⁷⁴ N. J. Turner, E. O'Reilly, *Nat. Chem. Biol.* **2013**, *9*, 285-288.

⁷⁵ F. Moris-Varas, X.-H. Qian, C.-H. Wong, *JACS* **1996**, *118*, 7647-7652.

biotransformation mixture (**Figure 20, left**). In comparison, Pathway II, which is additionally linked to the central carbon metabolism by utilizing the glycolytic intermediate DHAP as an aldol nucleophile for the stereoselective C-C forming reaction, catalyzed by an DHAP dependent aldolase (**Figure 20, right**). Moreover, Pathway I as well as Pathway II has included some features due to the nature of the C-C bond forming aldolases. In case of Pathway I, the highly stereoselective Fsa1 A129S aldolase is implemented, which displays a broad range of donor-substrate combinations. In contrast, Pathway II is restricted to the phosphorylated aldol donor molecule DHAP. With focus on the generated stereogenic centers, the choice of the appropriate aldolase (FruA, FucA, RhuA, and TagA) gives access to all four possible diastereomers.

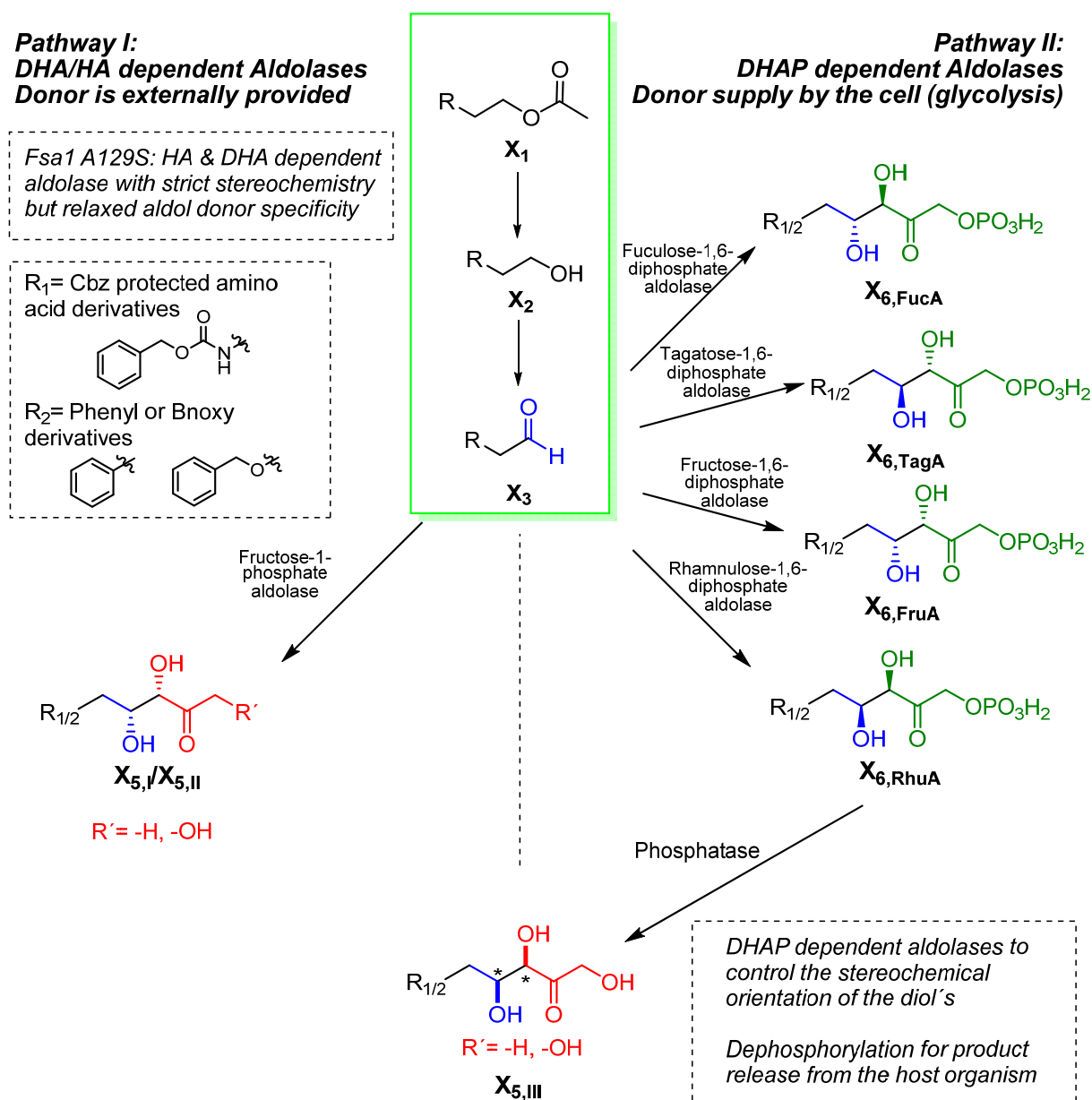


Figure 20 Pathway setup to control stereoselectivity of aldol adduct and extended aldol donor promiscuity.

As mentioned above, the key step of the designed pathways was a stereoselective aldolase mediated C-C coupling reaction between an aldol donor (e.g. DHAP, DHA, or HA) and different aldehyde acceptor

molecules (X_5). These highly reactive but also cytotoxic aldol electrophiles were provided after a functional group interconversion (FGI) of a primary alcohol by an oxidoreductase (X_3). To pay attention to an efficient substrate uptake, lipophilic acetates will serve as starting materials due to their ability to pass the cell membrane by passive diffusion. The initial transformation of the designed pathways will be an esterase mediated hydrolysis of the acetates (X_1) to the corresponding alcohol (X_2).

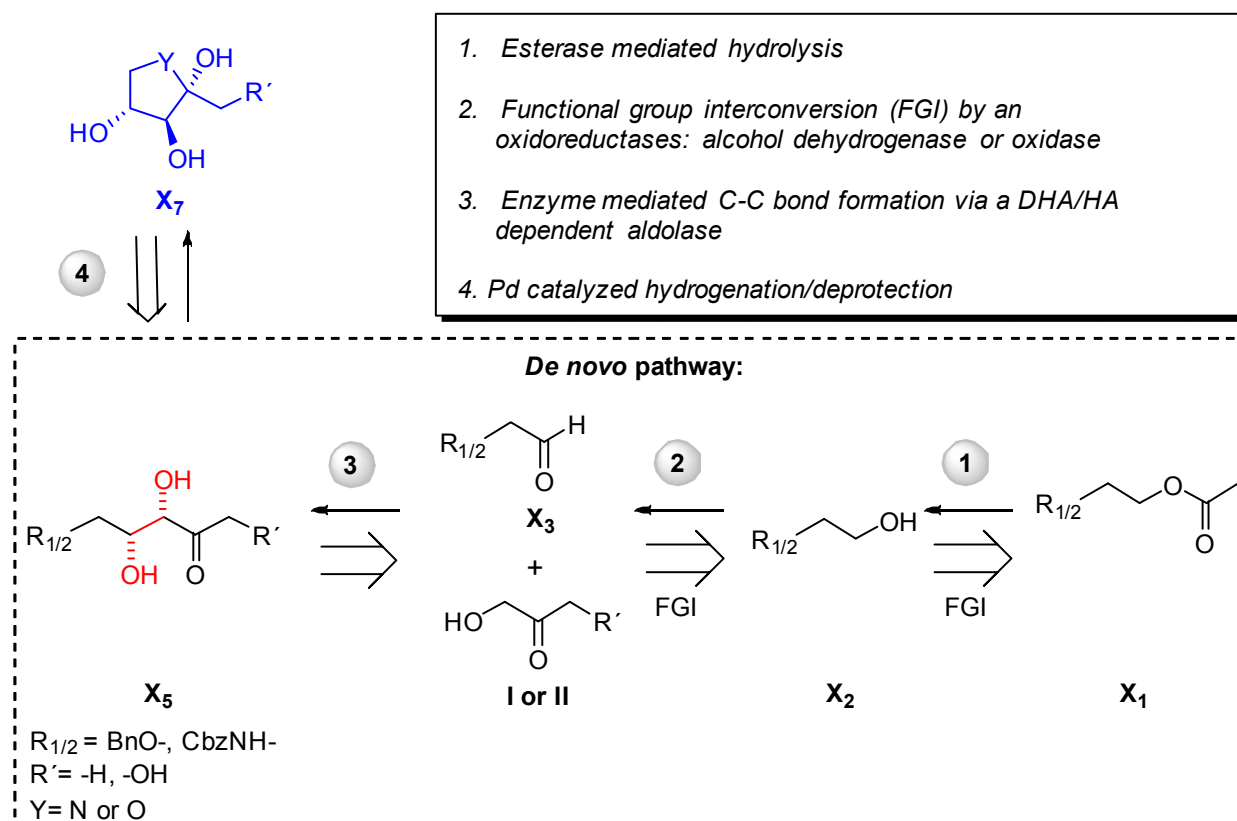
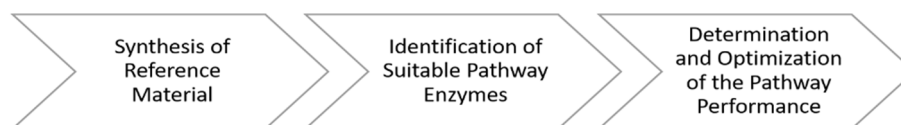


Figure 21 Illustration of pathway I: [1] aldolase; [2] ADH or oxidase; [3] esterase for the synthesis of polyhydroxylated compounds. (R= Ph-, BnO-, Cbz-; X= -H, -OH, -OPO₃H₂)

In Pathway I, the DHA/HA dependent fructose-6-phosphate variant (Fsa1 A129S) is implemented (3), because this enzyme is featured by a relaxed aldol donor scope and its perfect stereoselectivity towards the synthesis of related (3*R*,4*S*) diastereomers (X_5). In contrast, Pathway II was designed to increase the stereochemical diversity of our target molecules by use of DHAP dependent aldolases.

The experimental work of this thesis can be divided in three main parts:



After the synthesis and characterization of all required reference compounds, preliminary screenings were performed to identify suitable enzymes for the conversion of our selected starting materials to

the corresponding aldol adducts (**Figure 21, steps 1-3**). Since the isolation and purification of polyhydroxylated compounds is a known yield determine issue, we developed a SPE purification protocol and in combination with improvements on genetic and process levels, the overall performance of Pathway I was improved significantly.

Results & Discussion

A VII Pathway I-Setup

Over the last years, stereochemically controlled C-C bond formation reactions promoted by the fructose-6-phosphate aldolase variant (Fsa1 A129S from *Escherichia coli* (*E. coli*)) have been intensively studied to provide biologically relevant molecules.^{76,77} The designed Pathway I is consisting of an esterase mediated acetate hydrolysis (**X₁**), followed by an alcohol dehydrogenase (ADH) for oxidation of a primary alcohols (**X₂**) to the corresponding aldehydes (**X₃**), which are *in situ* converted by the DHA or HA dependent Fsa1 A129S to the diastereomerically pure target aldol adducts (**Figure 22, X₅**).

The initial esterase mediated hydrolysis was implemented due to the lack of active transporters for non-natural substrates, which were expected to pass the lipophilic cell membrane by diffusion more readily than the more polar corresponding alcohols. With respect to that, lipophilic acetates (**X₁**) will serve as starting materials for Pathway I. The following pathway steps are designed by coupling enzymes according to their functional group transformations for each individual substrate (**Figure 22, X₁, X₂, X₃**). Especially, an *in vivo* biocatalyst utilizing *E. coli* resting cells with a co-expressed oxidoreductase and aldolase can solve some major bottlenecks like (i) accumulation of cytotoxic aldehydes or (ii) elimination of over-oxidation activity to the carboxylic acid by the concurrent C-C bond formation.

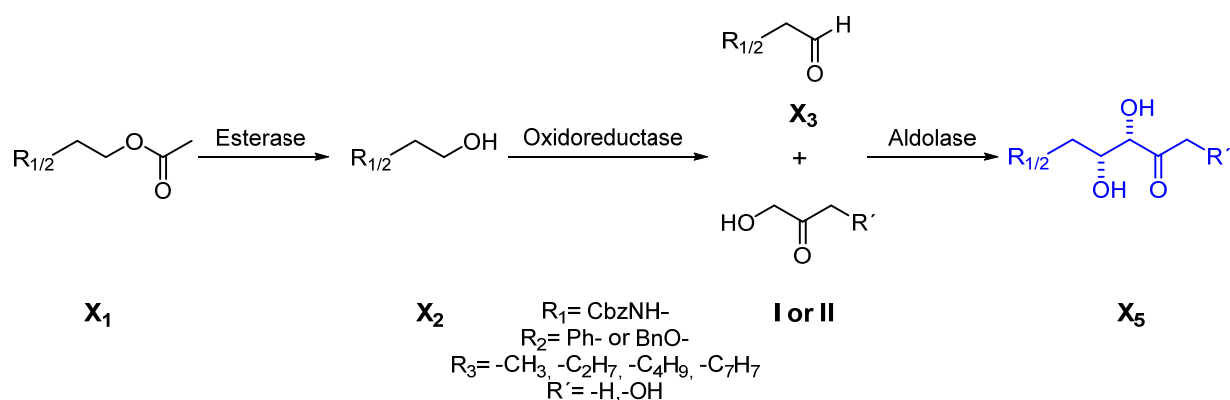


Figure 22 Illustration of Pathway I: [1] Fsa1 S129A (DHA dependent aldolase); [2] ADH or oxidase; [3] esterase for the synthesis of polyhydroxylated compounds.

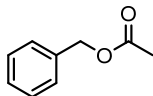
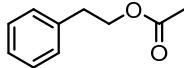
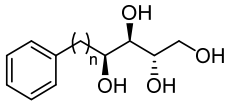
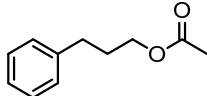
In general, structurally diverse substrates containing different functional groups and residues were investigated.

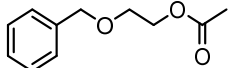
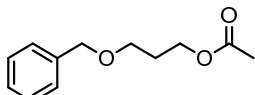
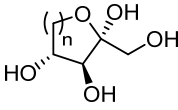
⁷⁶ D. Güçlü, A. Szekrenyi, X. Garrabou, M. Kickstein, S. Junker, P. Clapés, W.-D. Fessner, *ACS Catal.* **2016**, *6*, 1848-1852.

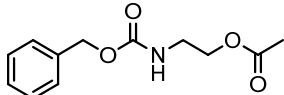
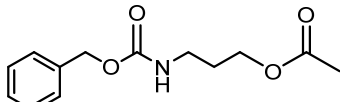
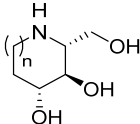
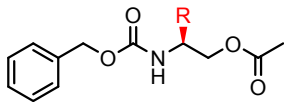
⁷⁷ A. L. Concia, L. Gomez, J. Bujons, T. Parella, C. Vilaplana, P. J. Cardona, J. Joglar, P. Clapes, *Org. Biomol. Chem.* **2013**, *11*, 2005-2021.

Several synthetic applications using aldolases or aldolase type biocatalysts with the common donor molecules DHAP or DHA were reported in the literature. Since the enzyme catalyzed C-C coupling step depicts the key step of Pathway I, a substrate library was built up around known aldolase substrate motifs (**Table 11**).^{78,79} These selected compounds containing lipophilic residues, such as phenyl moieties or benzyl and Cbz protecting groups, were chosen to facilitate the isolation of the highly polar pathway products from aqueous buffer solutions. Furthermore, the length of the alkyl linker chain ($n=1-3$) and substitutions in the linker were systematically investigated.

Table 11 Substrate library and their applications.

Abbrev.	Acetate (Pathway I & II substrates)	Target products
A ₁		Polyols
B ₁		 $n = 1, 2, 3$
C ₁		

D ₁		Deoxy-sugars
E ₁		 $n = 1, 2$

F ₁		Aza-sugars
G ₁		 $n = 1, 2$
H ₁ -L ₁		

As previously mentioned, three non-natively related enzymes were connected to establish Pathway I. The identification of suitable enzymes and their reactivity/selectivity towards a selected substrate library was investigated by single biotransformations for each individual step.

⁷⁸ S. M. Dean, W. A. Greenberg, C.-H. Wong, *Adv. Synth. Catal.* **2007**, *349*, 1308-1320.

⁷⁹ A. L. Concia, C. Lozano, J. A. Castillo, T. Parella, J. Joglar, P. Clapes, *Chem. Eur. J.* **2009**, *15*, 3808-3816.

A VII.1.1 Synthesis of Starting & Reference Material

With focus on the identification of suitable enzymes, the development of synthetic strategies to obtain reference material was the first major goal of this thesis. Since different general structures, (e.g. phenyl, benzyloxy or Cbz protected amines) with similar functional groups were envisioned, it would be advantageous if all required intermediates could be prepared by broadly applicable synthetic procedures. All performed reactions and results are discussed in the upcoming section.

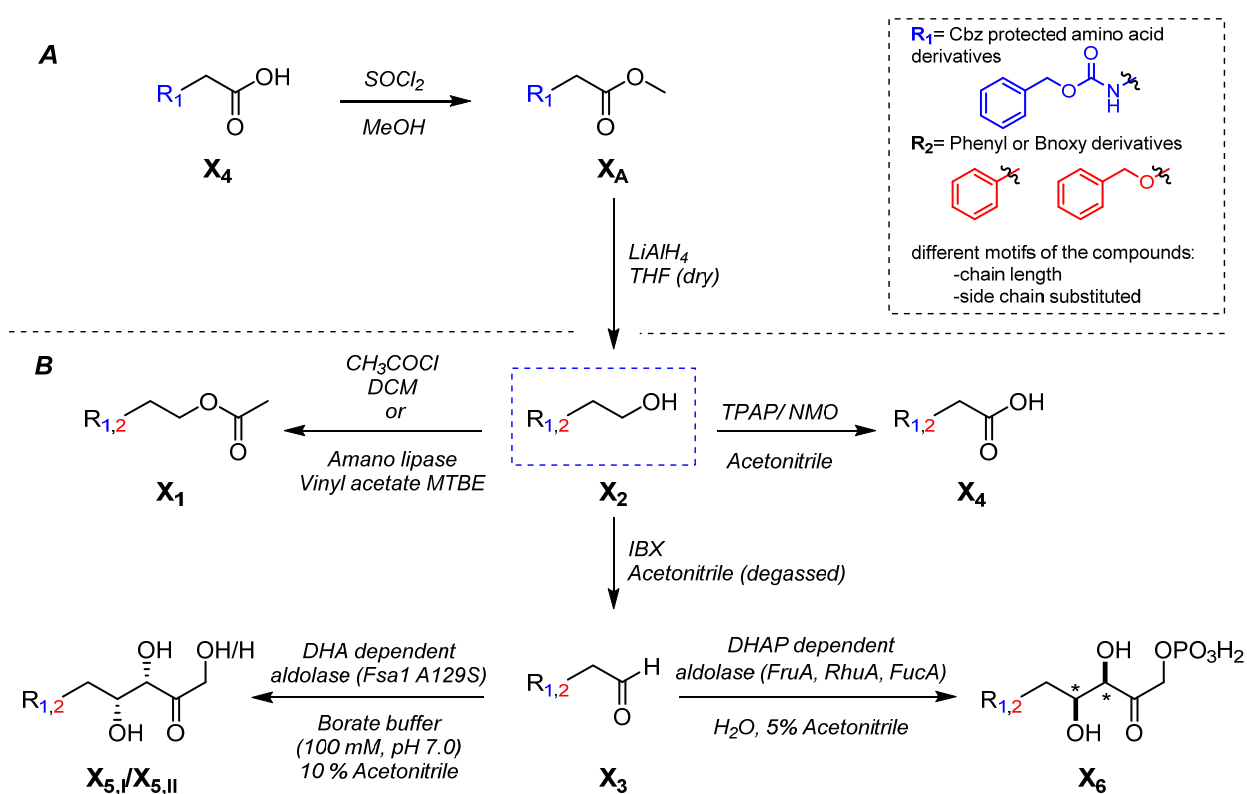


Figure 23 Overview of applied synthetic methods to generate all required reference compounds for Pathway I & II.

In the case of Cbz-protected material (R_1), commercially available protected amino acids were used as starting material for the preparation of all required compounds. First, the carboxylic acid (X_4) was converted to the corresponding methyl ester (X_A), which gave the primary alcohol (X_2) upon reduction by LiAlH_4 . This served as starting material for all further transformations (**Figure 23**), especially for the commercially available phenylic-structures or benzyloxy-protected primary alcohols (X_2).

A VII.1.2 Esterification of Cbz-protected Aminoalcohols

Commercially available Cbz-protected amino acids were esterified to the corresponding methyl ester using thionyl chloride according to an established procedure.⁸⁰ Due to the higher reduction reactivity towards primary alcohols, the esterification of Cbz-protected amino acids was performed. This organo-aluminum compound can be used for the synthesis of primary alcohols as well as the corresponding aldehydes. Both are required reference compounds for our designed pathways and therefore DIBAL-H displays an efficient route for the synthesis of them.

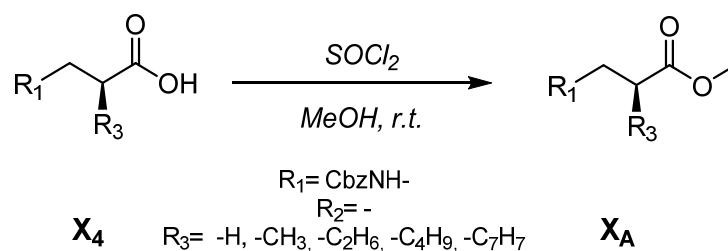


Figure 24 Esterification of Cbz-protected amino acids.

The esterification was performed in reaction vials equipped with an argon balloon in dry methanol and the pure product was obtained without further purification steps in excellent yields (**Figure 24**, **Table 12**).

Table 12 Yield of the methyl esters.

	Ester	Yield [%]
F_A	Glycine, <i>N</i> -[(phenylmethoxy)carbonyl]-, methyl ester	99
G_A	<i>L</i> -Alanine, <i>N</i> -[(phenylmethoxy)carbonyl]-, methyl ester	97
H_A	<i>L</i> -Valine, <i>N</i> -[(phenylmethoxy)carbonyl]-, methyl ester	99
I_A	<i>L</i> -Isoleucine, <i>N</i> -[(phenylmethoxy)carbonyl]-, methyl ester	91
J_A	<i>L</i> -Leucine, <i>N</i> -[(phenylmethoxy)carbonyl]-, methyl ester	93
K_A	<i>L</i> -Phenylalanine, <i>N</i> -[(phenylmethoxy)carbonyl]-, methyl ester	99

⁸⁰ T. Linder, PhD Thesis, 2016.

A VII.1.3 Reduction of Cbz-protected Amino-methylesters using DIBAL-H

Methyl esters (X_A), obtained previously by the esterification of the corresponding acids, were used for the synthesis of the required primary alcohols (X_2).

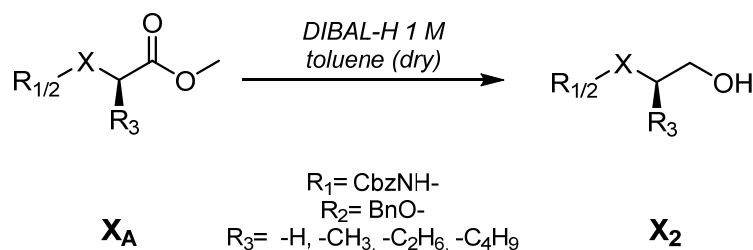


Figure 25 Reduction of Cbz-protected amino methyl esters by DIBAL-H.

In order to avoid side reaction activity, the reaction mixture was cooled to -80°C before DIBAL-H (2 equiv.) was added dropwise and after additional two hours of stirring, the temperature was gradually raised to room temperature in order to drive the reaction to completion (**Figure 25**). TLC as well as GC/MS indicated that the reduction of 3-phenyl propionic acid methyl ester was complete after 2 hours without side product formation (**Table 13, C₂**).

For the reduction of *N*-Cbz-glycine or *N*-Cbz-valine methyl esters, additional DIBAL-H had to be added and the mixture was stirred over night until full starting material consumption was monitored *via* TLC. The reduction of *N*-Cbz-glycine methyl ester was quenched with methanol and 2 N HCl and after extractive work-up a brown oil was obtained in 40% crude yield. In contrast, the *N*-Cbz-valine methyl ester reduction was quenching with potassium sodium tartrate, instead of 2 N HCl, in ethyl acetate and gave a mixture of side products in low yield (26%) (**Table 13, 2 & 3**). Based on the results obtained for the DIBAL-H reduction, *N*-Cbz protected alcohols were targeted *via* classical NaBH_4 or LiAlH_4 protocols (**Figure 26**).

A VII.1.4 Reduction of Cbz-protected Amino-methylesters using NaBH_4 or LiAlH_4

First, treatment of *N*-Cbz-alanine methyl ester dissolved in THF with NaBH_4 (5 equiv.) in the presence of catalytic amounts of methanol gave full consumption of starting material within two hours.⁸¹ Besides the primary alcohol, the corresponding aldehyde was indicated by TLC. Even when additional NaBH_4 and methanol were added to the reactions solution and stirred under reflux conditions for several hours, complete reduction could not be obtained.

⁸¹ R. S. B. Gonçalves, A. C. Pinheiro, E. T. da Silva, J. C. S. da Costa, C. R. Kaiser, M. V. N. de Souza, *Synth. Commun.* **2011**, *41*, 1276-1281.

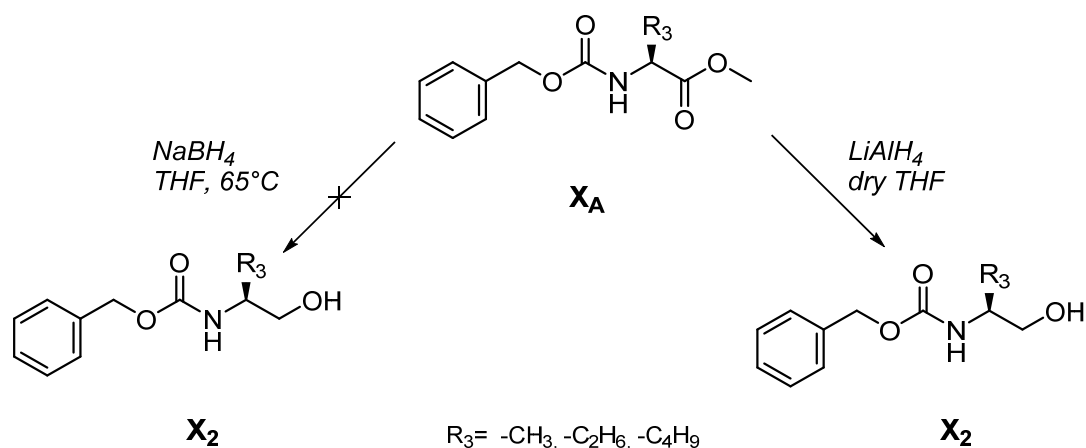


Figure 26 Reduction to the of Cbz-amino methyl esters $NaBH_4$ and $LiAlH_4$

Alternatively, the reduction was performed by lithium aluminum hydride ($LiAlH_4$).⁸² In preliminary test reactions, $LiAlH_4$ showed promising alcohol formation and the pure target compounds was afforded after column chromatography in good yields (**Table 13, 6-8**).

Table 13 Summary of all performed reductions using the corresponding methylesters of different carboxylic acids.

#	Methyl ester	Reducing agent	Equiv. (in total)	Solvent	Yield [%]	Product
C ₂	3-phenyl propionic acid	DIBAL-H	2	toluene (dry) ^[a]	-	alcohol
F ₂	N-Cbz-glycine	DIBAL-H	3	toluene (dry) ^[a]	40	mixture
H ₂	N-Cbz-valine	DIBAL-H	3.5	toluene (dry) ^[a]	26	mixture
G ₂	N-Cbz-alanine	$NaBH_4$	5	THF /MeOH (3/2)	-	-
G ₂	N-Cbz-alanine	$NaBH_4$	7.5	THF /MeOH (3/2)	10	mixture
H ₂	N-Cbz-valine	$LiAlH_4$	1.2	THF (dry)	70	alcohol
H ₂	N-Cbz-alanine	$LiAlH_4$	1.3	THF (dry)	84	alcohol
I ₂	N-Cbz-isoleucine	$LiAlH_4$	1.3	THF (dry)	71	alcohol

^[a] dried over NaH for 14 h

⁸² K. Schwetlick, *Organikum*, Wiley, 2009.

A VII.1.5 Acetylation of the Primary Alcohol

In order to obtain the acetylated substrates for Pathway I, two distinct approaches were conducted, either with the classic esterification by using acetyl chloride (**Figure 27, left**) or a biocatalytic approach by utilizing lipase in order to avoid undesirable side chain racemization in the case of the Cbz-protected amino acids (**Figure 27, right**).^{83,84}

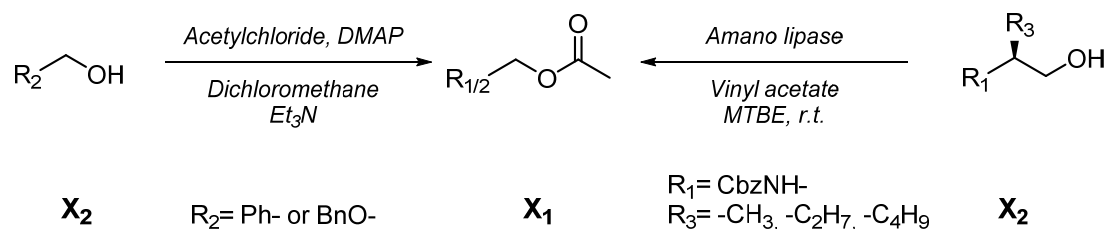


Figure 27 Acetate synthesis by two different strategies. (left) Steglich esterification ($\text{R}_2 = \text{Ph- or BnO-}$) or a lipase mediated acetylation with vinyl acetate ($\text{R}_1 = \text{CbzNH-}$).

A VII.1.5.1 Acetylation with Acetylchloride/DMAP

Acetylation of primary alcohols was performed and gave the desired acetates in moderate to good isolated yields after column chromatography (**Table 14, A₁-G₁**).

Table 14 Yields for acetylation using acetylchloride.

#	Acetate	Yield [%]
A ₁		79
B ₁		30
C ₁		39
D ₁		75
E ₁		70
F ₁		70
G ₁		80

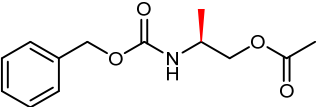
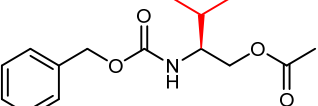
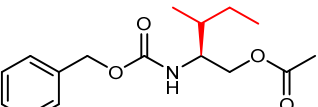
⁸³ M.J. Fink, PhD Thesis, **2014**.

⁸⁴ L. Rycek, PhD Thesis, **2015**.

A VII.1.5.2 Acetylation with Amano lipase

In contrast to the chemical acetylation, lipase mediated esterification of the α -substituted *N*-Cbz-alcohols by using vinyl acetate in MTBE at room temperature was completed within four hours without any additional purification step (**Table 15**).⁸⁵

Table 15 Acetylation *via* Amano lipase

#	Acetate	Yield [%]
H ₁		86
I ₁		99
J ₁		99

A VII.1.6 Aldehyde Synthesis

A VII.1.6.1 Synthesis of Phenylacetaldehyde by Acetate Deprotection

The first synthetic step to synthesize phenylacetaldehyde (**B₂**) was an easy dimethyl acetate deprotection according to Procopio *et al.* (**Figure 28**).⁸⁶

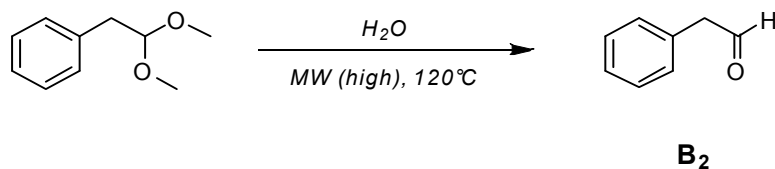


Figure 28 Dimethyl-acetate deprotection under MW conditions in water.

Phenylacetaldehyde dimethyl acetal was dissolved in H₂O (HPLC grade) and heated to 120°C for 40 minutes under MW irradiation. After extractive work up, the pure product was afforded in 77% yield, confirmed by NMR analysis.

⁸⁵ L. Rycek, PhD Thesis, **2015**.

⁸⁶ A. Procopio, M. Gaspari, M. Nardi, M. Oliverio, A. Tagarelli, G. Sindona, *Tetrahedron Lett.* **2007**, *48*, 8623-8627.

A VII.1.6.2 Aldehyde Synthesis by Different Oxidation or Reduction Reagents

In the literature, several methods (DIBAL-H, Dess Martin, PCC, IBX, etc.) are described to synthesize aldehydes by selective oxidation of the corresponding primary alcohol (**Figure 29**).

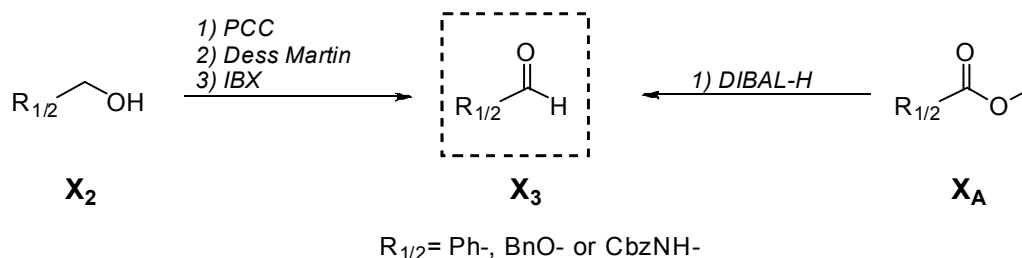


Figure 29 Oxidation and reduction strategies for the selective aldehyde synthesis.

As mentioned above, Cbz-protected amino methyl esters were synthesized and can serve as starting materials for the synthesis of primary alcohols as well as for the selective reduction *via* DIBAL-H to the aldehyde moiety. In order to synthesize the required substrates (aldehyde and primary alcohol), in an easy and efficient way, a synthetic route using DIBAL-H was selected. With this reducing agent, both compounds can be generated by starting from the corresponding ester (**Figure 30**).

In contrast to the protocol for primary alcohols, low temperatures and stoichiometric amounts of DIBAL-H are required to avoid over-reduction to the primary alcohol (**C₂**).

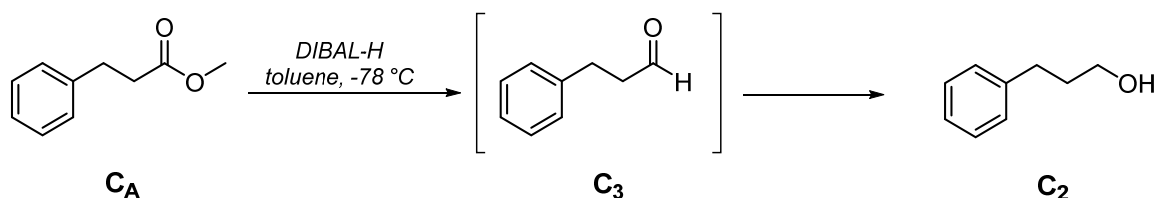


Figure 30 Aldehyde synthesis by DIBAL-H reduction of the corresponding methyl ester.

The NMR data of the crude material showed that mainly the alcohol and not the aldehyde (**C₃**) was formed. In order to suppress this side reaction, DIBAL-H was added slowly (temperature control) and the dry solvent was degassed prior to use, but after work-up, mainly the undesired alcohol (**C₂**) was observed.

A VII.1.6.3 Aldehyde Synthesis-PCC or Dess Martin

Alternatively, the synthesis of required aldehydes was performed according to standard oxidation protocols using pyridinium chlorochromate (PCC) or the Dess Martin reagent (**Figure 31**).^{87,88}

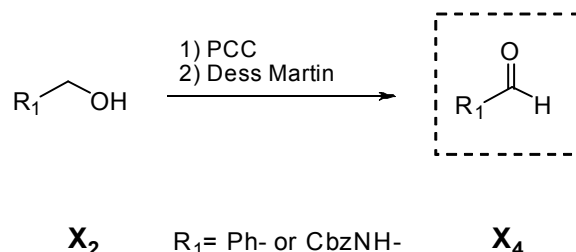
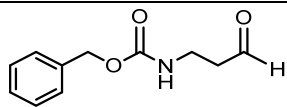
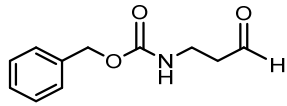
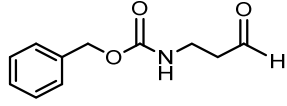
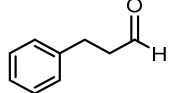


Figure 31 Oxidation of primary alcohol to the corresponding aldehyde.

Several attempts using these reagents as well as optimizations of the work-up procedure were conducted, but all of them were very unselective towards aldehyde formation and gave a mixture of alcohol/aldehyde/carboxylic acid (**Table 16**).

Table 16 Summary of different approaches for the synthesis of aldehydes.

#	Aldehyde	Reagent	Yield [%]	Problem
1		Dess Martin periodinane	25	>40 % byproduct (mainly the corresponding acid)
2		PCC	<10%	Recrystallization according to the literature ⁸⁹
3		PCC	35%	Extractive work up (2 times) and recrystallization
4		DIBAL-H	-	Only alcohol formation → Commercially available

A VII.1.6.4 Oxidation of Primary Alcohol with IBX

Since several synthetic protocols (**Table 16, 1-3**) for the synthesis of benzyl (3-oxopropyl)carbamate (**F₃**) failed, 2-iodoxybenzoic acid (IBX) was selected. The major benefit of this oxidation agent is the decreased over-oxidation capacity to the corresponding carboxylic acid in comparison to the Dess Martin reagent.

In contrast to the paper by More *et al.* (reflux over hours), the reaction was performed in the microwave due to shorter reaction times of around 20 min (**Figure 32**).⁹⁰ Under reflux conditions, reaction times of around 7 h for aromatic primary alcohols are described.

⁸⁷ M.J. Fink, PhD Thesis, **2014**.

⁸⁸ G. Pototschnig, PhD Thesis, **2016**.

⁸⁹ M. Kakudo, *Acta. Crysta.* **1961**

⁹⁰ J. D. More, N. S. Finney, *Org. Lett.* **2002**, *4*, 3001-3003.

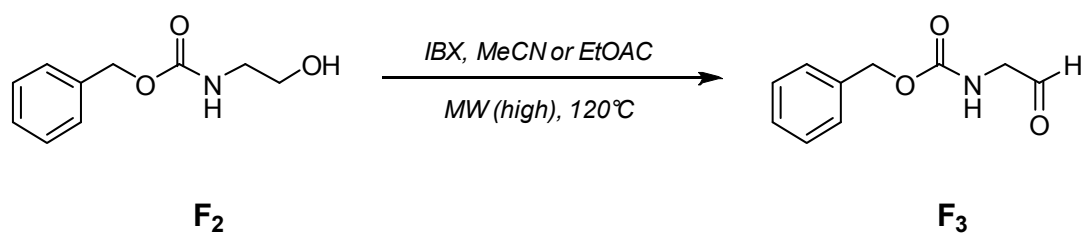


Figure 32 Selective oxidation of a primary alcohol to the corresponding aldehyde by IBX(self-synthesized)

N-Cbz-ethanolamine (**F₂**) and IBX (purchased, 45 wt%) were mixed in ethyl acetate and heated in the microwave at 120°C for altogether 45 minutes. After TLC indicated full conversion and a yellow-white solid was obtained. ¹H-NMR showed various side products, especially the over-oxidation product, the corresponding carboxylic acid (**F₄**).

Since it was not clear what other additives were part of the purchased IBX (45 wt%) mixture and whether they affected the reaction, for the second attempt self-prepared IBX was used.⁹¹

The oxidation was once carried out in acetonitrile and once in ethyl acetate, to determine the solvent effects on reaction time and side product formation.

The reaction was somewhat slower in acetonitrile (half an hour compared to 20 minutes in ethyl acetate), but no side products were formed. After filtration through celite, no further purification steps were required and the pure product was obtained in 70% yield.

⁹¹ M. Frigerio, M. Santagostino, S. Sputore, *J. Org. Chem.* **1999**, *64*, 4537-4538.

A VII.1.7 Oxidation Methods for Carboxylic Acids

For the synthesis of commercially not available benzyloxy-protected carboxylic acids different strategies (Jones, TEMPO/BAIB and NMO/TPAP) have been accomplished. Since the isolation and purification of benzyloxy-protected carboxylic acids was limited due to the formation of benzoic acid, several oxidation strategies were applied to identify of the most selective protocol (**Figure 33**).

A VII.1.8 Synthesis of 2-(benzyloxy)acetic acid

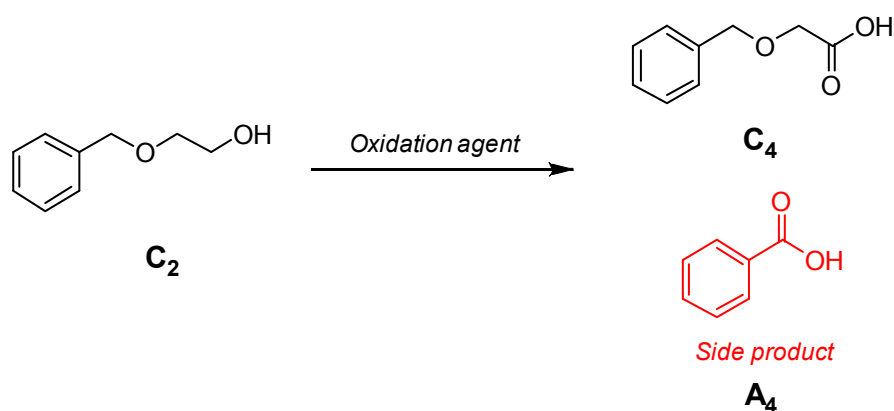


Figure 33 Oxidation of 2-(benzyloxy)-acetic acid.

The synthesis of 2-(benzyloxy)acetic acid is often performed by using 2-bromo-acetic acid and benzyl alcohol and posed a bigger challenge under oxidative conditions than expected.⁹² Therefore, several experiments (**Table 17**) were required, to avoid the undesirable carbon chain cleavage of a difficult to separate mixture of benzoic acid and the target product. Finally, the desired acid was synthesized according the Ley-oxidation protocol using tetrapropylammonium perruthenate (TPAP) and *N*-methylmorpholine *N*-oxide (NMO) without the addition of a molecular sieve. After extractive work-up with 2 N HCl and EtOAc, pure 2-(benzyloxy)acetic acid was obtained and confirmed *via* ¹H and ¹³C-NMR spectroscopy.

Table 17 Oxidation methods for synthesis of 2-(benzyloxy)acetic acid

#	Oxidation method	
1	TEMPO/ BAIB	no product formation ^[a]
2	Jones (CrO ₃)	mixture of A₄ / C₄
3	KMnO ₄	no product formation ^[a]
4	Ley (TPAP/ NMO/ H ₂ O)	83%

^[a] according to ¹H-NMR and GC/MS

⁹² L. C. Dias, E. C. Polo, *J. Org. Chem.* **2017**, *82*, 4072-4112.

The oxidation with NMO catalyzed by TPAP (Ley oxidation) provides an easy and fast synthetic method to obtain exclusively 2-(benzyloxy)acetic acid (**C₄**) without the formation of benzoic acid (**A₄**). After purification by column chromatography the pure product was isolated in 83% yield.

A VII.1.9 Synthesis of 3-(((benzyloxy)carbonyl)amino)propanoic acid

The synthesis of the Cbz-protected β -amino acid was accomplished by the reaction of β -alanine and benzylchloroformate under basic conditions at 0°C (**Figure 34**).⁹³

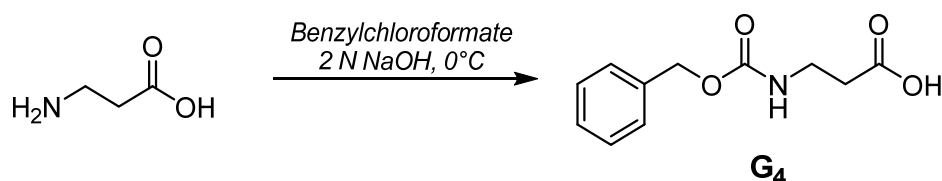


Figure 34 Cbz-protection of β -alanine by benzylchloroformate.

The pure product was obtained in 27% isolated yield after recrystallization in water with drops of ethanol and 2 N HCl. In the literature protocol, the pure Cbz-protected acid was obtained in 84 % after extractive work up and concentration at high vacuo without any further purification.⁹³ In our case, an additional purification/recrystallization step was necessary to observe the pure product, according to NMR analysis. The low isolated yield and low recovery was mainly attributed to recrystallization issues in water with drops of ethanol.

⁹³ A. K. Mallik, H. Qiu, Y. Kuwahara, M. Takafuji, H. Ihara, *Chem. Commun.* **2015**, 51, 14243-14246.

A VII.1.10 Enzyme Mediated Reference Synthesis of Acyclic Aldol Compounds-Employing DHA/HA Donors

The stereoselective C-C bond formation by DHA/HA dependent aldolases was studied in detail. The aldol addition of DHA or HA to our model substrates (**B₃-G₃**) was catalyzed by the fructose-6-phosphate aldolase variant Fsa1 A129S to furnish (**B_{5,I}/B_{5,II}- G_{5,I}/G_{5,II}**). The most valuable feature of Fsa1 A129S is the perfect stereochemistry to generated exclusively the (3*S*,4*R*)-diastereomer as well as the high thermostability, which enables a simple and easy to apply heat shock purification protocol after cell lysis of the recombinant expression host. Thus, the synthesis of required aldol reference material was accomplished in a single-step enzyme transformation by Fsa1 A129S lyophilizates at 25-30°C and shaking (200 rpm) overnight (**Figure 35**). Typically, 1.5 mg of lyophilized Fsa1 A129S cell powder per mg_[substrate] were resuspended in a 100 mM borate buffer (pH 7.0) and the reaction was started by the addition of the aldol donor (1.5 equiv.).^{94,95}

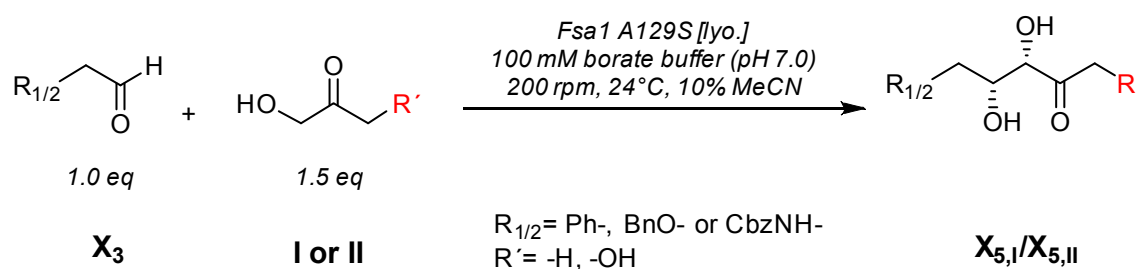


Figure 35 Reagents and conditions of aldol synthesis catalyzed by FSA A129S lyophilizates

Although full conversion of the aldehydes was observed, indicated by GC/FID and RP-TLC (acetonitrile/H₂O 3:1, R_f = 0.7) to the corresponding aldol products (**B_{5,I}/B_{5,II}- G_{5,I}/G_{5,II}**), massive loss of material upon purification of these polar molecules was encountered *via* reversed phase (RP) chromatography (**Table 18**).^{96,97,98} These isolation issues and the optimization strategies, which were applied to improve the isolated yields for polyhydroxylated compounds is discussed in section A. IX.5. Since Fsa1 A129S is highly selective for the formation of the (3*S*,4*R*)-diastereoisomer, for all aldehydes exclusively the predicted *syn* conformers were obtained, confirmed by NMR data and optical rotation values.

⁹⁴ A. L. Concia, C. Lozano, J. A. Castillo, T. Parella, J. Joglar, P. Clapes, *Chem. Eur. J.* **2009**, *15*, 3808-3816.

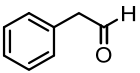
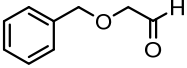
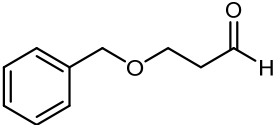
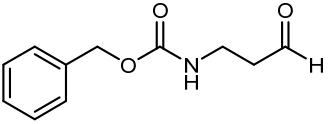
⁹⁵ M. Sudar, Z. Findrik, D. Vasic-Racki, P. Clapes, C. Lozano, *Enzyme Microb. Technol.* **2013**, *53*, 38-45.

⁹⁶ A. L. Concia, C. Lozano, J. A. Castillo, T. Parella, J. Joglar, P. Clapes, *Chem. Eur. J.* **2009**, *15*, 3808-3816.

⁹⁷ A. L. Concia, L. Gomez, J. Bujons, T. Parella, C. Vilaplana, P. J. Cardona, J. Joglar, P. Clapes, *Org. Biomol. Chem.* **2013**, *11*, 2005-2021.

⁹⁸ M. Wei, Z. Li, T. Li, B. Wu, Y. Liu, J. Qu, X. Li, L. Li, L. Cai, P. G. Wang, *ACS Catal.* **2015**, *5*, 4060-4065.

Table 18 Conversion and isolated yields for Fsa1 A129S (purified lyophilizates) mediated aldol reactions with DHA/HA.

Substrate	Product	Conversion/Yield [%]	
		R' = OH	R' = H
	B₅	>99/35	>99/40
	D₅	>99/37	>99/42
	E₅	>99/18	>99/21
	G₅	>99/35	>99/32

A VIII Enzyme and Substrate Promiscuity

A VIII.1 Esterases-Acetate Hydrolysis

Hydrolases can be divided into different subclasses (e.g. esterase, lipases, proteases) and together they form the enzyme class 3 (EC 3).⁹⁹ From a synthetic point of view, hydrolases are widely used because of their broad substrate scope and they do not require additional cofactors. Furthermore, hydrolases tolerate high amounts of organic solvents and show high enantioselectivity, which makes them highly potent and robust biocatalysts.¹⁰⁰ Esterases are enzymes which can catalyze the hydrolytic cleavage of acetates to the corresponding primary alcohol. Esterases are widely used for example in the synthesis of optically pure building blocks as well as in the degradation of natural materials and industrial waste. Depending on the solvent, the formation of an ester (organic solvent) or under aqueous conditions the hydrolysis is preferred transformation.¹⁰¹

Mechanistically, the substrate is transformed in the active site by a catalytic triade.¹⁰² First, a nucleophilic attack by the serine hydroxyl group occurs and forms a stabilized (by histidine and aspartate) tetrahedral intermediate followed by the release of the alcohol and the formation of an acyl enzyme complex (**Figure 36**).

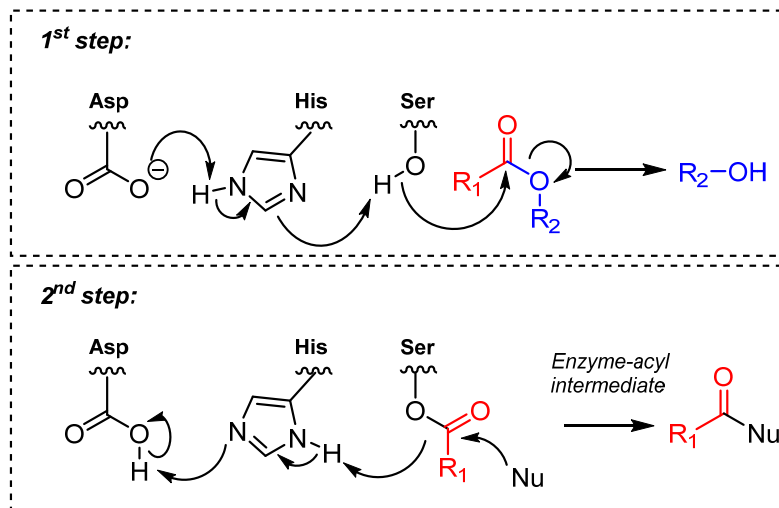


Figure 36 Mechanism “catalytic triade” of an esterase mediated hydrolysis.

Next, water is acting as nucleophile and generates another tetrahedral intermediate, which leads to the desired product after the cleavage of the acyl-enzyme bond.

In 1990, the aryl esterase *Pseudomonas fluorescens* (Pfe I) was described the first time and showed promising catalytic activity for ester hydrolysis for a broad range of different acetates. Pfe I was cloned

⁹⁹ U. T. Bornscheuer, R. J. Kazlauskas, in *Hydrolases in Organic Synthesis*, Wiley-VCH Verlag GmbH & Co. KGaA, **2006**, pp. 61-140.

¹⁰⁰ M. Breuer, K. Ditrich, T. Habicher, B. Hauer, M. Keßeler, R. Stürmer, T. Zelinski, *Angew. Chem., Int. Ed.* **2004**, *43*, 788-824.

¹⁰¹ T. Panda, B. S. Gowrishankar, *Appl. Microbiol. Biotechnol.* **2005**, *67*, 160-169.

¹⁰² K. Faber, *Biotransformations in organic chemistry*, Springer-Verlag, **2011**.

and expressed by Pelletier and Altenbucher and the crystal structure was solved by Cheeseman, which showed also the typical catalytic triad (Ser94-His251-Asp222). Over the last years, investigations towards substrate scope, preferred acyl chains of C2-C4 as well as good enantioselectivity for phenylethan-2-ol was identified. Optimization studies to improve the overall performance of Pfe I boosted the catalytic activity at high temperatures (up 70°C) and between a pH range of 5 to 10. Another esterase from *Bacillus subtilis* (BS2) was selected for the acetate hydrolysis due to the broad substrate promiscuity and good overexpression in *E. coli*. In general, BS2 showed activity towards several esters and acetates (methyl, benzyl, or *tert*-butyl) and was identified as one of the most active and consequently widely used biocatalyst for synthetic purposes.^{103,104}

A VIII.1.1 Activity Assay-Hydrolysis of *p*-Nitrophenylacetate

The hydrolysis activities of Pfe I and BS 2 were determined by a photometric activity assay using *p*-nitrophenylacetate (**42**), which is almost colorless in aqueous solution (**Figure 37**).¹⁰⁵



Figure 37 Photometric activity assay using *p*-nitrophenylacetate.

After enzyme mediated hydrolysis under slightly basic buffer conditions (50 mM Tris HCl, pH 7.25), *p*-nitrophenol (**43**) is released and the solution turns yellow. The increase of the extinction related to the ester cleavage was monitored at 405 nm.

The activity assay was carried out with two different CCE concentrations: 0.01 and 0.05 mg/ml, determined *via* a Bradford protein assay. In general, the assay was performed in 24 well plates, started by the addition of CFE to a solution of substrate and buffer, and monitored over 10 min. In addition to reaction triplicates, the blank reaction (without enzyme, self hydrolysis) as well as a negative control (BL 21(DE3), same expression protocol like in case of recombinant expression hosts for Pfe I or BS2) were performed and depicted in **Figure 38**.

¹⁰³ M. Schmidt, E. Henke, B. Heinze, R. Kourist, A. Hidalgo, U. T. Bornscheuer, *Biotechnol. J.* **2007**, *2*, 249-253.

¹⁰⁴ M. Schmidt, E. Barbayianni, I. Fotakopoulou, M. Höhne, V. Constantinou-Kokotou, U. T. Bornscheuer, G. Kokotos, *J. Org. Chem.* **2005**, *70*, 3737-3740.

¹⁰⁵https://www.sigmaaldrich.com/content/dam/sigma-aldrich/docs/Sigma/Product_Information_Sheet/2/n8130pis.pdf

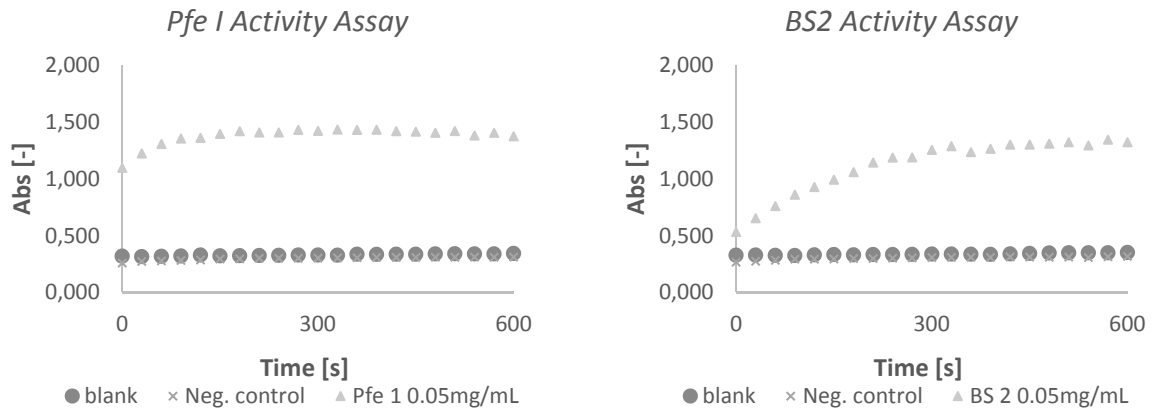


Figure 38 Esterase activity assay, hydrolysis of *p*-nitrophenylphosphate monitored at 405 nm in 50 mM Tris HCl (pH 7.25) using CFE of Pfe I and BS2.

Alternatively, this setting was also applied to determine hydrolysis activity of Pfe I and BS 2 growing cells. After induction by IPTG, the cell cultures containing overexpressed Pfe I or BS2 were shaken for an additional 90 min according to the expression protocol. Subsequently, the hydrolysis activity was again monitored at 405 nm (**Figure 39**).

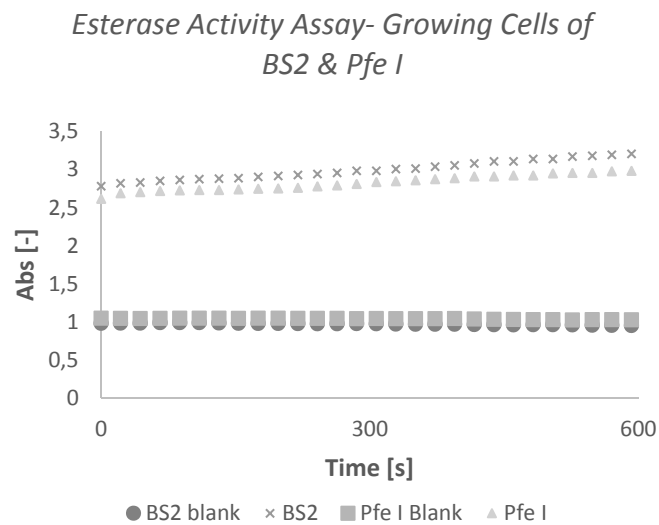


Figure 39 Esterase activity assay, hydrolysis of *p*-nitrophenylphosphate monitored at 405 nm in 50 mM Tris HCl (pH 7.25) using growing cells [90 min after induction with IPTG] of Pfe I and BS2.

Both esterases, Pfe I and BS2 showed high activity towards acetate hydrolysis and were applied to initial *in vivo* substrate studies.

A VIII.1.2 Hydrolysis Mediated by Growing Cells Expressing Pfe I and BS 2

Both enzymes are known for their broad and flexible substrate scope and were tested with all synthesized acetates (**Figure 40, Table 19**). These compounds served as starting materials and the conversion to the primary alcohol was monitored by HPLC.

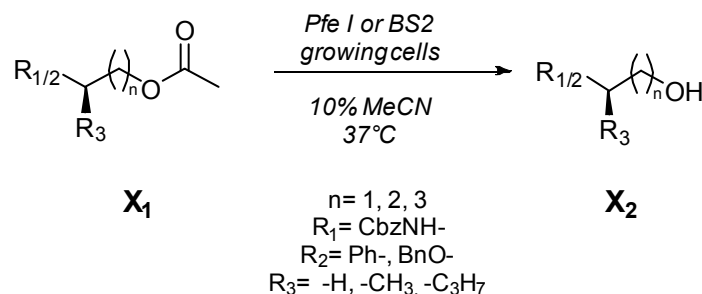


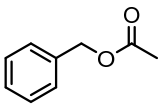
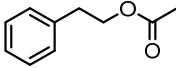
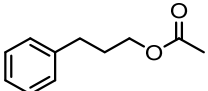
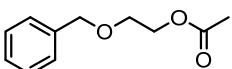
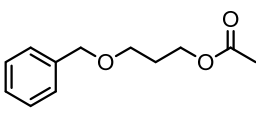
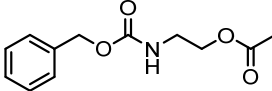
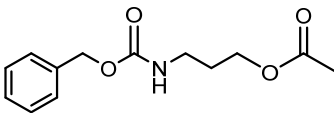
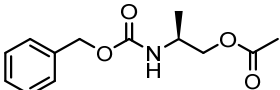
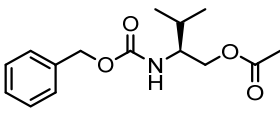
Figure 40 Esterase mediated acetate hydrolysis.

Table 19 General settings for Esterase mediated growing cell experiments

	μL	Final conc.
V_r	1000	-
Growing cells	950	-
Substrate (100 mM Stock)	50	5 mM

To determine substrate and enzyme promiscuity for both esterases, growing cells were prepared in TB medium and 1 h after induction by IPTG, the substrate was added (final concentration of 5 mM 5% v/v acetonitrile). Biotransformations were performed in 24 well plates, equipped with an oxygen transparent foil at 37°C, 250 rpm, and samples were taken after 0, 1 and 24 h. 100 μL of the reaction mixture were diluted with 200 μL acetonitrile including the internal standard caffeine (1 mM). The solid residues were separated by centrifugation and after filtration through a syringe filter, the samples were analyzed by LC/MS. Table 20 summarize the results for esterase mediated hydrolysis by growing cells expressing Pfe I or BS2. Within this study, both esterases showed moderated to excellent conversion of all substrates. In the case of Pfe I, all acetates were transformed to the corresponding alcohols (4-73%) within one hour but with decreased activity towards substrates containing heteroatoms or substituents in the carbon chain. However, lower activity and moderate conversion within 20 hours of around 60-70% was observed for Cbz-protected amino alcohols. Acetates bearing an aromatic moiety (**A₁-E₁**) were converted to the corresponding alcohol (>99%) after 20 h (**Table 20**).

Table 20 Rel. conversion of the esterase mediated hydrolysis of acetates to the corresponding primary alcohol.

#	Substrate	Pfel [%] [1 h/20 h]	BS2 [%] [1 h/20 h]
A ₁		29/99	99/99
B ₁		4/99	99/99
C ₁		73/99	99/99
D ₁		23/99	99/99
E ₁		11/99	99/99
F ₁		4/49	62/99
G ₁		4/60	99/99
H ₁		16/75	99/99
I ₁		10/70	99/99

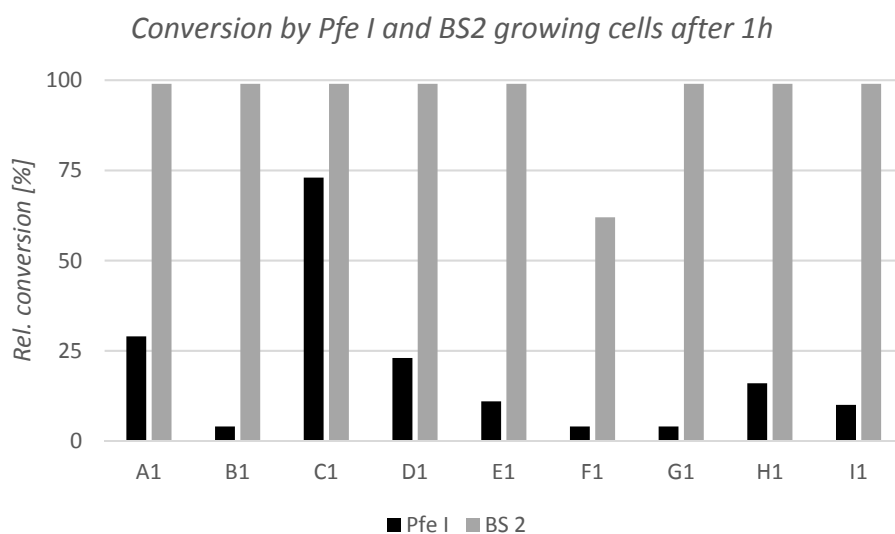


Figure 41 Comparison of esterase mediated hydrolysis after one hour for all library substrates.

In contrast, growing cells of BS 2 gave complete consumption of all substrates (**A₁-I₁**) within one hour (>99%), except **F₁** (62%), which requires additional reaction time to give exclusively amino alcohol (**F₁-I₁**) (**Figure 41**).

Because of these results, BS 2 was selected as suitable biocatalyst for the first pathway step, the hydrolysis to the primary alcohol.

A VIII.2 Enzyme Mediated Oxidation Reactions

The resulting primary alcohols of the esterase mediated hydrolysis were oxidized in the next cascade step to the corresponding aldehyde by using an oxidoreductase. Biocatalytic alternatives for the selective oxidation of primary alcohols to the corresponding aldehyde can be divided into two main enzyme classes (i) alcohol dehydrogenases (ADH) and (ii) alcohol oxidases. ADHs can be isolated from nearly every organism and are therefore the most popular biocatalyst for redox reactions.^{106,107} In the case of thermodynamically disfavored oxidation reactions, an efficient cofactor recycling system is required to shift the equilibrium (**Figure 42**). This enzyme class catalyzes the interconversion of alcohols (**44**) to aldehydes (**45**) or ketones by the consumption of stoichiometric amounts of the nicotinamide adenine dinucleotide cofactor (NAD⁺) or its phosphorylated analog NADP⁺. Besides mild reactions conditions, an important feature of redox enzymes is their stereo- and chemo-selectivity, controlled by the three-dimensional framework of a protein. The identification of a versatile oxidation system, which is for example not limited to primary or secondary alcohols, would depict a major improvement for ADH mediated transformations.¹⁰⁸

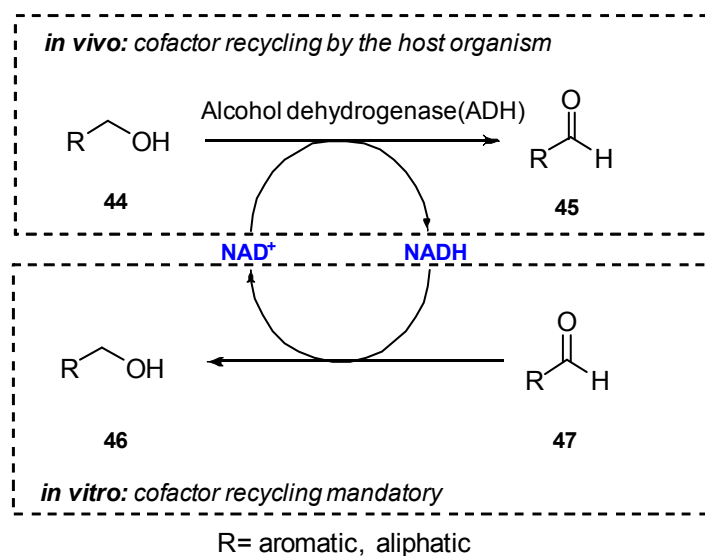


Figure 42 General settings for alcohol dehydrogenase under *in vivo* or *in vitro* conditions.

In contrast to hydrolases, ADHs are not so simple to handle for synthetic applications, because of a rather narrow substrate scope and these enzymes requires an efficient, external cofactor recycling system (**46, 47**) under *in vitro* reaction conditions (**Figure 42**).¹⁰⁹ This bottleneck can be circumvented by the use of whole cells, which will manage the cofactor supply and regeneration throughout the

¹⁰⁶ F. Hollmann, I. W. C. E. Arends, K. Buehler, A. Schallmeyer, B. Bühler, *Green Chem.* **2011**, *13*, 226.

¹⁰⁷ W. Kroutil, H. Mang, K. Edegger, K. Faber, *Curr. Opin. Biotechnol.* **2004**, *8*, 120-126.

¹⁰⁸ J. Liu, S. Wu, Z. Li, *Curr Opin Chem Biol* **2018**, *43*, 77-86.

¹⁰⁹ J. H. Sattler, M. Fuchs, K. Tauber, F. G. Mutti, K. Faber, J. Pfeffer, T. Haas, W. Kroutil, *Angew. Chem., Int. Ed.* **2012**, *51*, 9156-9159.

reaction.¹¹⁰ In the review of Bühler *et al.*, a comprehensive overview of enzyme mediated oxidation or reductions with applications in organic synthesis was summarized.¹¹¹

Horse liver was the source for one of first ADHs described in several synthetic applications (HLADH), because of the broad substrate tolerance towards primary and secondary alcohols, the perfect (S)- stereoselectivity, and high reactivity in water-saturated organic solvents.¹¹²

The oxidation or reduction activity under *in vitro* process conditions is mainly controlled by the addition of co-substrates. Due to the thermodynamically disfavored formation of aldehyde, a significant molar excess of the co-substrate has to be applied to shift the reaction equilibrium.¹¹³ Co-substrates are non-protein molecules that maintain and accelerate an enzyme mediated reaction. In case of ADH's, often high quantities of the co-substrate (e.g. 20 equiv. of acetaldehyde) is required, especially for the thermodynamically disfavored oxidation.¹¹⁴

This requirement was also considered during the substrate promiscuity studies for the identification of a suitable ADH for our designed pathways.

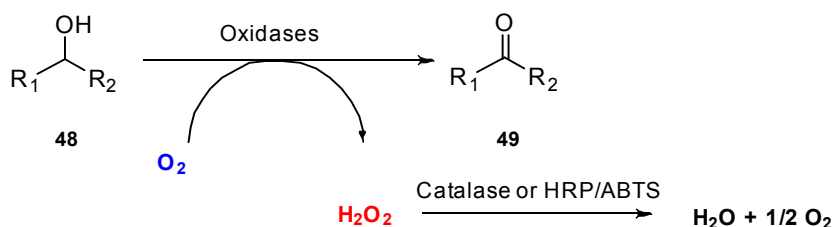


Figure 43 Biocatalytic oxidation by an oxidase with the required degradation of hydroxyl peroxide using a catalase.

Besides alcohol dehydrogenases, FAD- and copper-containing oxidases are frequently used oxidoreductases, which utilize oxygen as electron acceptor (**Table 21**). During the reaction, cytotoxic hydrogen peroxide (H₂O₂) is generated, which is a known enzyme inhibitor and displays a major disadvantage to integrate oxidases in *in vivo* pathways (**Figure 43**). In order to avoid enzyme deactivation, a catalase is usually applied to decompose the generated hydrogen peroxide to water and oxygen.¹¹⁵

¹¹⁰ N. Oberleitner, C. Peters, J. Muschiol, M. Kadow, S. Saß, T. Bayer, P. Schaaf, N. Iqbal, F. Rudroff, M. D. Mihovilovic, U. T. Bornscheuer, *ChemCatChem* **2013**, *5*, 3524-3528.

¹¹¹ F. Hollmann, I. W. C. E. Arends, K. Buehler, A. Schallmey, B. Bühler, *Green Chem.* **2011**, *13*, 226.

¹¹² J. H. Schrittwieser, S. Velikogne, M. Hall, W. Kroutil, *Chem. Rev.* **2017**.

¹¹³ J. H. Schrittwieser, J. Sattler, V. Resch, F. G. Mutti, W. Kroutil, *Curr. Opin. Biotechnol.* **2011**, *15*.

¹¹⁴ J. H. Sattler, M. Fuchs, K. Tauber, F. G. Mutti, K. Faber, J. Pfeffer, T. Haas, W. Kroutil, *Angew. Chem., Int. Ed.* **2012**, *51*, 9156-9159.

¹¹⁵ M. Pickl, M. Fuchs, S. M. Glueck, K. Faber, *Appl. Microbiol. Biotechnol.* **2015**, *99*, 6617-6642.

Table 21 Advantages and disadvantages of ADHs and oxidases due to *in vivo* and *in vitro* applications.

ADH	Oxidases
<ul style="list-style-type: none">• ADHs are cofactor (NAD(P)⁺) dependent and an efficient cofactor recycling system is required, because of the thermodynamically disfavored oxidation step.• Advantages for whole cell biocatalysts: cofactor/ cofactor recycling provided by the host organism	<ul style="list-style-type: none">• Alcohol oxidases utilizing molecular oxygen as electron donor• Major drawbacks for whole cell biocatalysts: cell toxic hydrogen peroxide• Most of them are membrane associated proteins and have a narrow substrate scope

A VIII.2.1 Substrate & Enzyme (ADH) Promiscuity

In an initial study, a subset of five ADHs from different bacterial strains for the selective oxidation of primary alcohols to the corresponding aldehyde were screened. Additionally, the selected enzyme should give no over-oxidation to the related carboxylic acid. Consequently, the selected LK-ADH from *Lactobacillus kefir*¹¹⁶ and RR-ADH from *Rhodococcus ruber* (*R. ruber*)¹¹⁷ as well as ADH-ht from *Bacillus stearothermophilus*¹¹⁸ were employed but did not show any conversion of the provided primary alcohols (**B₂-G₂**) to the corresponding aldehydes (**Table 22**). The thermostable ADH-ht from *Bacillus stearothermophilus*, an ADH with oxidation activity towards primary alcohols,¹¹⁹ exclusively accepted the Cbz-protected amino alcohol (**G₂**) consuming 27% of the alcohol in 2 h according to GC/FID. Furthermore, ADH-a from *R. ruber*,¹²⁰ which is reported for secondary alcohols with few exceptions such as 2-phenylethanol (**B₂**) showed no activity towards our model substrates. In biotransformations employing AlkJ, an ADH from *P. putida* known for the oxidation of aliphatic alcohols, the alcohols **B₂-G₂** were fully consumed within 2 h reaction time but also over-oxidation to the carboxylic acid was observed (15-20%). Because of its properties, AlkJ, a membrane associated NAD(P)⁺-independent ADH, can improve the substrate uptake and promotes the thermodynamically disfavored alcohol oxidation by taking advantage from the irreversibility of O₂ reduction in the electron transport chain.^{121,122,123}

¹¹⁶ A. Weckbecker, W. Hummel, *Biocatalysis and Biotransformation* **2006**, *24*, 380-389.

¹¹⁷ W. Stampfer, B. Kosjek, C. Moitzi, W. Kroutil, K. Faber, *Angewandte Chemie* **2002**, *41*, 1014-1017.

¹¹⁸ R. Cannio, M. Rossi, S. Bartolucci, *Eur. J. Biochem.* **1994**, *222*, 345-352.

¹¹⁹ J. H. Sattler, M. Fuchs, K. Tauber, F. G. Mutti, K. Faber, J. Pfeffer, T. Haas, W. Kroutil, *Angew. Chem., Int. Ed.* **2012**, *51*, 9156-9159.

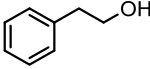
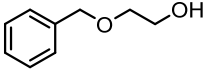
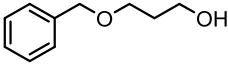
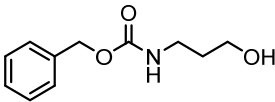
¹²⁰ C. Wuensch, H. Lechner, S. M. Glueck, K. Zangger, M. Hall, K. Faber, *ChemCatChem* **2013**, *5*, 1744-1748.

¹²¹ T. Bayer, S. Milker, T. Wiesinger, F. Rudroff, M. D. Mihovilovic, *Advanced Synthesis & Catalysis* **2015**, *357*, 1587-1618.

¹²² M. Schrewe, M. K. Julsing, K. Lange, E. Czarnotta, A. Schmid, B. Bühler, *Biotechnology and Bioengineering* **2014**, *111*, 1820-1830.

¹²³ S. Wu, Y. Zhou, T. Wang, H.-P. Too, D. I. C. Wang, Z. Li, *Nat. Commun.* **2016**, *7*.

Table 22 ADH promiscuity toward selected substrate profile with 2 h.

#	Substrate	LK-ADH	RR-ADH	ADH-ht	ADH-a	AlkJ ^[a]
1	 B₂	n.c.	n.c.	n.c.	n.c.	>99
2	 D₂	n.c.	n.c.	n.c.	n.c.	>99
3	 E₂	n.c.	n.c.	n.c.	n.c.	>99
4	 F₂	n.c.	n.c.	27	n.c.	>99

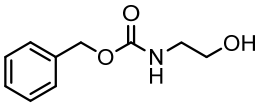
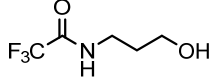
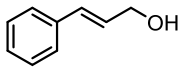
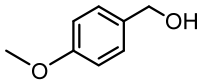
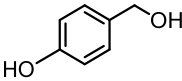
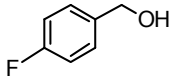
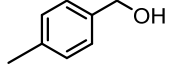

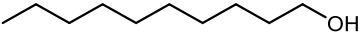
After AlkJ was identified as a suitable ADH for known aldolase acceptor molecules, further investigations towards an extended substrate scope containing aliphatic, aromatic as well as to CF₃- or Cbz- protected amino alcohols were carried out.

A VIII.2.2 Substrate Profile of AlkJ

To identify the promiscuity of AlkJ for non-natural substrates, whole cells were tested with substituted aromatic, aliphatic, and protected amino alcohols. Activity was measured by detecting the oxidation of the starting material over time. For the production of active AlkJ whole cells, an optimized expression protocol was followed. After harvesting and resuspension in resting cell media (OD₅₉₀= 20), activity was determined by the transformation of our model substrate (**B₂**) and cells were stored at 4°C prior to use for not more than 24 h.

After 24 h, an equilibrium between alcohol and carboxylic acid was established, without detectable amounts of aldehyde (**Table 23**). During the recorded time course (0, 1, and 5 h), aldehyde concentrations of around 20% were quantified by GC/FID.

Table 23 Summary of obtained relative conversion [%] after 24 h for the AlkJ substrate scope screenings.

#	Substrate		Alcohol [%]	Carboxylic acid [%]
1		G₂	50	28
2		L₂	n.d.	>95
3		M₂	n.d.	97
4		N₂	70	30
5		O₂	n.d.	>95
6		P₂	n.d.	>95
7		Q₂	n.d.	>95
8		R₂	n.d.	>95
9		S₂	5	92

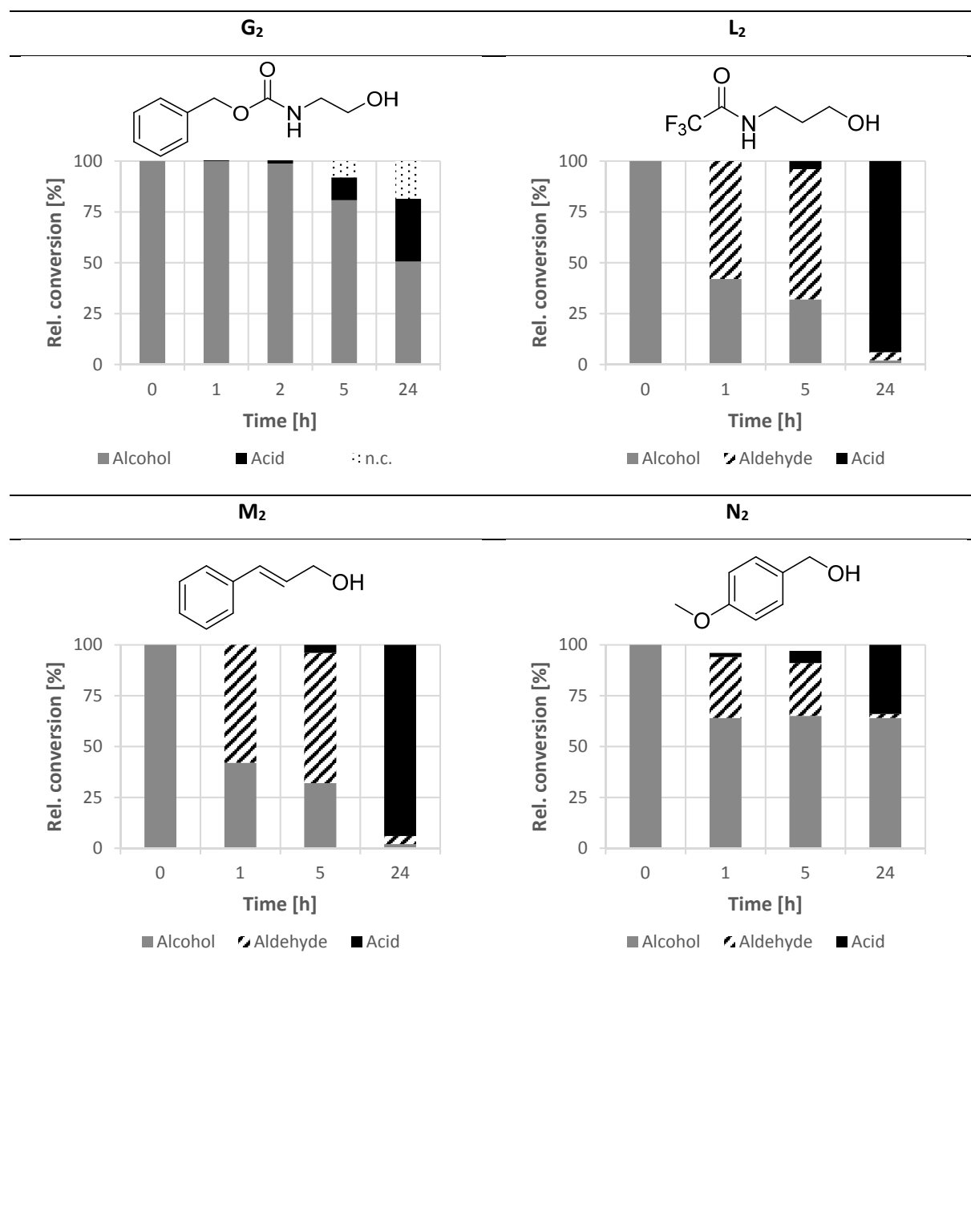
n.d. not detected

In comparison to our model substrates, benzyl (3-hydroxypropyl)carbamate (**F₂**) (**Table 22, 4**), selective oxidation by AlkJ was limited for the Cbz-protected amino alcohol (**G₂**) (**Table 23, 1**). A reduced chain length of one carbon led to around 30% acid formation after 24 h without detection of the corresponding aldehyde. Protected amino propanol (**F₂, L₂**) (e.g. Cbz- or CF₃-) gave good substrate consumptions (>70%) within 2 h, which is most probably related to the additional CH₂ compared to Cbz-protected amino ethanol (**G₂**) (**Table 23, 1**). Alternatively, cinnamyl alcohol (**M₂**), which contains an unsaturated side chain was tested and afforded similar results (60% after 1 h) compared to the protected amino propanol (**F₂, L₂**) (**Table 23, 3**). Besides investigations concerning chain length effects, substituted benzylalcohols (**N₂-Q₂**) were tested. In general, all of them were converted within 24 h to the corresponding acid, except the para-methoxy substituted one, which resulted in 30% over-oxidation product (**Table 23, 4**). AlkJ is known as highly active towards aliphatic substrates,¹²⁴ such as octanol, dodecanol and the oxidation of these substrates gave the

¹²⁴ M. Schrewe, M. K. Julsing, K. Lange, E. Czarnotta, A. Schmid, B. Bühler, *Biotechnol. Bioeng.* **2014**, *111*, 1820-1830.

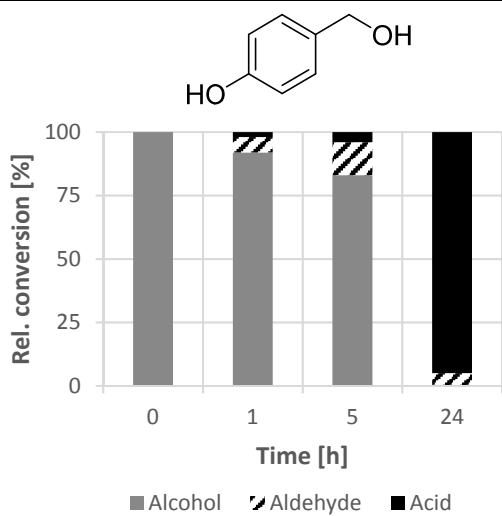
expected fast starting material consumption of 65% within 1 h (Table 24, R₂ & S₂).¹²⁵ For additional information of the oxidation process of all applied substrates, a comprehensive summary of the AlkJ substrate scope screening is depicted in Table 24.

Table 24 Summary of the AlkJ substrate scope screening over time.

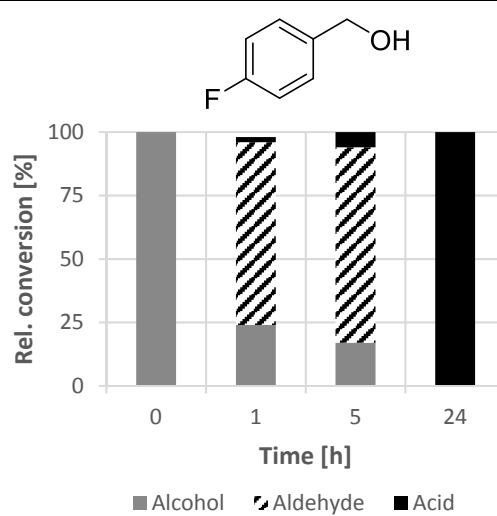


¹²⁵ M. Schrewe, N. Ladkau, B. Bühler, A. Schmid, *Adv. Synth. Catal.* **2013**, 355, 1693-1697.

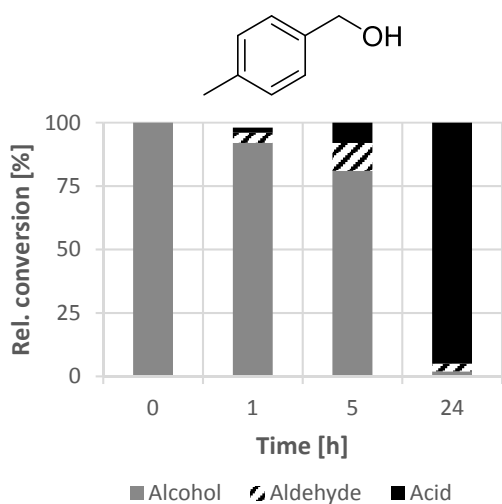
O₂



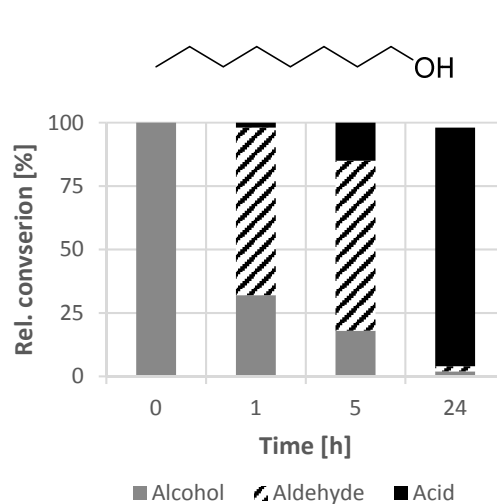
P₂



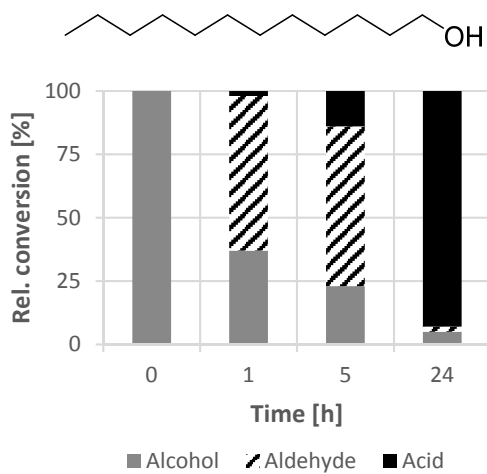
Q₂



R₂



S₂



As summarized in Tables 22-24, the oxidation of primary alcohols to the corresponding aldehyde often deals with undesirable, but thermodynamically favored over-oxidation to the carboxylic acid. With focus to C-C bond forming reactions (e.g. aldol reaction) under *in vivo* reaction conditions, the formation of a carboxylic acid represents dead-end due to missing endogenous carboxylate reducing activity. A biocatalytic method, to re-route the substrate-flux back to the aldehyde, represents CAR_{Ni}, a carboxylic acid reductase from *N. iowensis*.^{126,127} Besides that, different elegant solutions were reported, like biphasic systems,¹²⁸ gene knock outs (KOs),¹²⁹ or multi-enzymatic cascades^{125,130} to eliminate undesired over-oxidation activity. A xylene monooxygenase from *Pseudomonas putida* was applied for selective oxidation of pseudocumene to 3,4-dimethyl benzaldehyde by an *in situ* removal of the reactive aldehyde intermediate from the organic layer. For this concept, dioctylphthalate was used as second organic phase to prevent over oxidation and under optimized process conditions, the product was obtained in high product titers of 0.22 M with 70% isolated yield. Another efficient strategy, an *in situ* intermediate transformation, is utilized in several multi-enzymatic cascade setups by applying different enzymes (e.g. transaminases).¹³¹

¹²⁶ K. Napora-Wijata, K. Robins, A. Osorio-Lozada, M. Winkler, *ChemCatChem* **2014**, *6*, 1089-1095.

¹²⁷ M. K. Akhtar, N. J. Turner, P. R. Jones, *Proc. Natl. Acad. Sci. U.S.A.* **2013**, *110*, 87-92.

¹²⁸ F. Hollmann, I. W. C. E. Arends, K. Buehler, A. Schallmey, B. Bühler, *Green Chem.* **2011**, *13*, 226.

¹²⁹ N. Oberleitner, C. Peters, J. Muschiol, M. Kadow, S. Saß, T. Bayer, P. Schaaf, N. Iqbal, F. Rudroff, M. D. Mihovilovic, U. T. Bornscheuer, *ChemCatChem* **2013**, *5*, 3524-3528.

¹³⁰ T. Bayer, S. Milker, T. Wiesinger, F. Rudroff, M. D. Mihovilovic, *Adv. Synth. Catal.* **2015**, *357*, 1587-1618.

¹³¹ R. C. Simon, N. Richter, E. Busto, W. Kroutil, *ACS Catal.* **2014**, *4*, 129-143.

A VIII.3 Aldolases in Organic Synthesis-Stereoselective C-C Bond Formation

In the final transformation step of Pathway I, the resulting aldehyde (aldol acceptor) will undergo an aldol reaction with an aldol donor (nucleophile) to form a new C-C bond and two new chiral centers are introduced simultaneously.

In nature, aldolases are mainly used for the bond cleavage of complex carbohydrate motifs into metabolic intermediates (e.g. glycolysis). For synthetic applications, the reaction equilibrium is inverted by adding an excess of aldol donor nucleophile. Aldol adducts contain an α - β dihydroxy-carbonyl moiety with specific stereochemistry and are found in many natural and synthetic important molecules (e.g. polyketides, carbohydrates, etc.). Since the newly formed stereogenic centers influences biological and chemical properties of the aldol product, the main challenge for synthetic protocols is to gain complete control over the diol orientation.

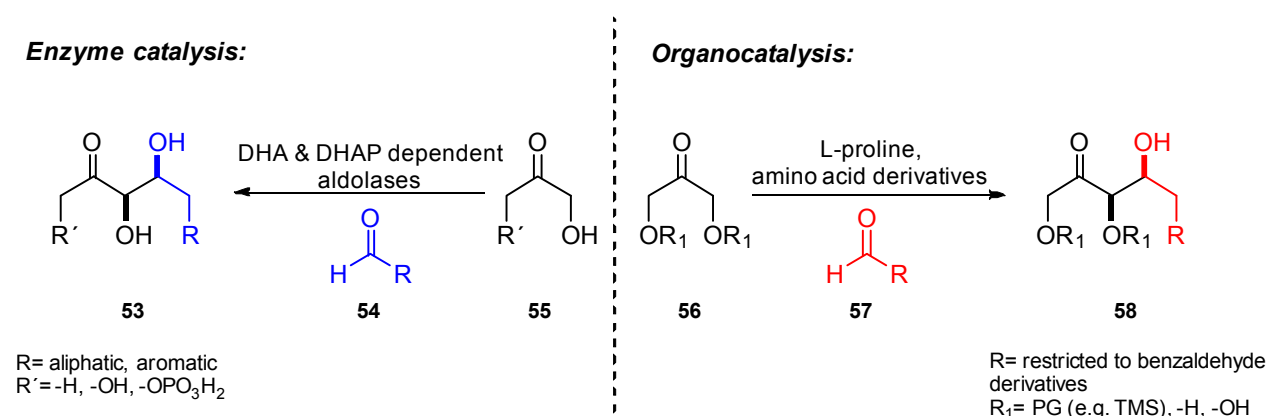


Figure 44 Comparison of enzyme or organocatalyzed aldol reactions.

Due to limitation of aldolases (e.g. aldol acceptor specificity, temperature, buffer, etc.) organocatalysts like proline derivatives were designed to mimic these enzyme class (Figure 44).^{132,133,134}

¹³² J. Kofoed, T. Darbre, J. L. Reymond, *Chem. Commun.* **2006**, 1482-1484.

¹³³ N. Mase, C. F. Barbas, 3rd, *Org. Biomol. Chem.* **2010**, *8*, 4043-4050.

¹³⁴ D. Enders, C. Grondal, *Angew. Chem., Int. Ed.* **2005**, *44*, 1210-1212.

A VIII.3.1 Organocatalyzed Aldol Reactions- Testreactions to Improve the Isolation & Purification of Aldol Adducts

Developments for chemical asymmetric aldol synthesis are inspired by nature and focused on organocatalyzed e.g. threonine- and proline-catalyzed transformations.^{135,136,137} A major bottleneck, in order to obtain stereochemically pure products often protecting groups are installed to avoid side product formation.¹³⁸

In contrast to aldolases, which are operating in aqueous buffer solutions, reactions mediated by an organocatalyst are performed in polar, organic solvents, such as DMSO, DMF or chloroform. Contradictory to native aldolases, the presence of bulk water can result in low yields and poor stereoselectivity for organocatalyzed reactions.¹³⁹ Aldolases form a hydrophobic protecting pocket at their active side to exclude bulk water. Due to the limitation of organocatalysts for the generation of such protecting mechanisms different strategies were applied (e.g. chiral catalysts, additives, solvent) to improve stereoselectivity and yield for these transformations. In general, organocatalyzed aldol reactions require relatively high catalyst loadings up to 30%. This bottleneck is mainly attributed to required water content, which is necessary to avoid catalyst inhibition but also has a negative effect on the enamine formation during the initial step of these kind of transformation.^{140,141}

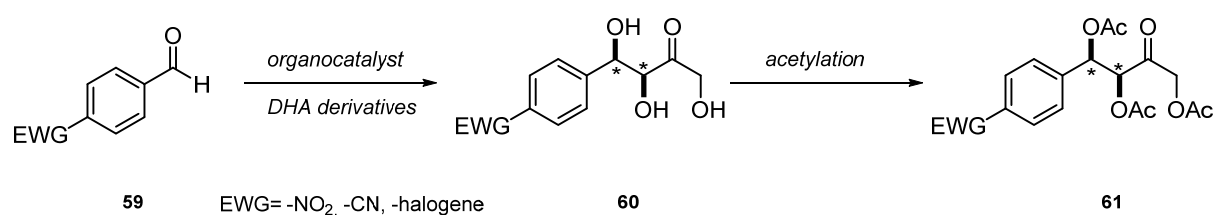


Figure 45 Exemplary work flow of organocatalyzed aldol reactions to isolate polyhydroxylated compounds.

Organocatalyzed aldol reactions are often limited to protected dihydroxyacetone derivatives (**61**) and also very restricted to the acceptor aldehyde (**59**) scope (**Figure 45**). In particular, organocatalyzed aldol reactions are limited to aromatic aldehydes that bearing electron-withdrawing substituents to enhance the electrophilicity of the carbonyl group.¹⁴² For the identification of the stereoselectivities and especially for the isolation of aldol adducts, the triol product is routinely per-acetylated and analyzed *via* HPLC.

¹³⁵ B. List, R. A. Lerner, C. F. Barbas, *JACS* **2000**, *122*, 2395-2396.

¹³⁶ S. S. V. Ramasastry, K. Albertshofer, N. Utsumi, C. F. Barbas, *Org. Lett.* **2008**, *10*, 1621-1624.

¹³⁷ N. Utsumi, M. Imai, F. Tanaka, S. S. V. Ramasastry, C. F. Barbas, *Org. Lett.* **2007**, *9*, 3445-3448.

¹³⁸ J. T. Suri, D. B. Ramachary, C. F. Barbas, *Org. Lett.* **2005**, *7*, 1383-1385.

¹³⁹ M. Markert, R. Mahrwald, *Chem. Eur. J.* **2008**, *14*, 40-48.

¹⁴⁰ J. Huang, X. Zhang, D. W. Armstrong, *Angew. Chem., Int. Ed.* **2007**, *46*, 9073-9077.

¹⁴¹ S. S. V. Ramasastry, K. Albertshofer, N. Utsumi, F. Tanaka, C. F. Barbas, *Angew. Chem., Int. Ed.* **2007**, *46*, 5572-5575.

¹⁴² C. Wu, X. Fu, X. Ma, S. Li, *Tetrahedron: Asymmetry* **2010**, *21*, 2465-2470.

Since the isolation of unprotected aldol derivatives is a challenging task, organocatalytic model reactions were carried out in order to obtain unprotected aldol molecules. For the synthesis of benzaldehyde based aldol product (**A₅**), the commercially available threonine based catalyst (*O*-^tBu-L-Thr; **Figure 46**) was selected due to stereoselectivity and applicability of unprotected dihydroxyacetone (**Figure 46**)¹⁴³

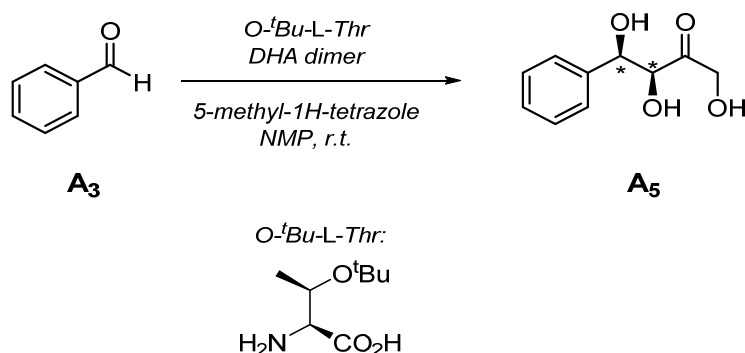


Figure 46 Organocatalyzed aldol reaction of benzaldehyde and DHA.

The reaction was performed with freshly distilled benzaldehyde and the homogenous solution was stirred at room temperature until full conversion of the starting material, monitored *via* TLC (DCM: Isopropanol 10:1). The reaction mixture was filtered through Celite, concentrated and purified by preparative RP-HPLC. Since NMP, which was still present after lyophilization overnight, and the desired product showed pretty similar behavior on RP material, two times preparative HPLC and concentration at high vacuum over night was required to afford the pure product in low yields (<10%). The main limitation of threonine based organocatalysts is that they cannot be used for a C-C bond forming reaction between donor (**II**) and acceptor molecules (**B₃**), which contains both acidic protons next to the carbonyl functionality (**Figure 47**). In this case, the direct aldol reaction catalyzed ^tBu-threonine led to an inseparable mixture of several byproducts without isolation of the desire aldol adduct (**B₅**) (**Figure 46**). This unselective reaction behavior was also not possible to control by adaptations of the protocol like adding the aldehyde in small portions or performing the reaction at lower temperatures.

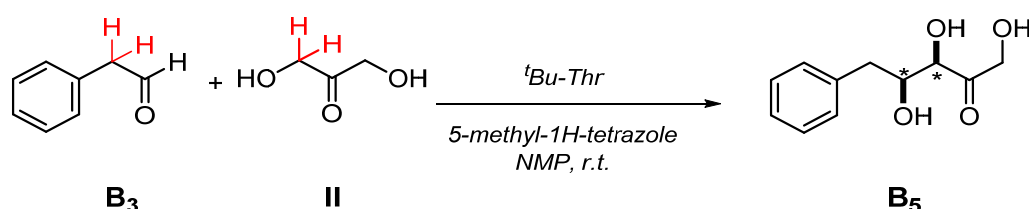


Figure 47 Organocatalyzed aldol reaction of phenylacetaldehyde and DHA.

¹⁴³ S. S. V. Ramasastry, K. Albertshofer, N. Utsumi, F. Tanaka, C. F. Barbas, *Angew. Chem., Int. Ed.* **2007**, *46*, 5572-5575.

This main limitation of chemical approaches can be effectively overcome by enzymatic transformations using DHAP- or DHA- dependent aldolases and illustrate an powerful enzymatic transformation without a chemical counterpart reaction (**A VIII.4**).

A VIII.3.2 Aldolase in Asymmetric Synthesis

In general, aldolases (EC 4.1.x.x) are classified as lyases, and more specifically sub-grouped according to their donor specificity into (i) pyruvate/oxaloacetate/2-oxobutyrate dependent enzymes, (ii) DHAP dependent enzymes, (iii) DHA dependent enzymes, and enzyme variants that accepting other non-phosphorylated derivatives (**Table 25, Figure 51**).¹⁴⁴ Generally, aldolases tolerate a broad range of aldol acceptor structures but they are very strict towards the donor molecules (e.g. DHAP, DHA, HA, etc.). DHAP and DHA dependent aldolases are the best studied class thus far and offer a protecting group free and “green” alternative for asymmetric synthesis of polyhydroxylated compounds. Aldolases are classified based on the mechanism of donor substrate activation. Class I aldolases activate substrates through an iminium ion formation step followed by enamine formation, whereas class II aldolases activate substrates by forming a zinc enolate. Mechanistically, a nucleophilic attack of the aldol donor, which typically is a ketone enolate or transiently formed enamine to an aldehyde (aldol acceptor) is conducted to generated aldol adducts containing two new stereogenic centres (**Figure 48**).¹⁴⁵

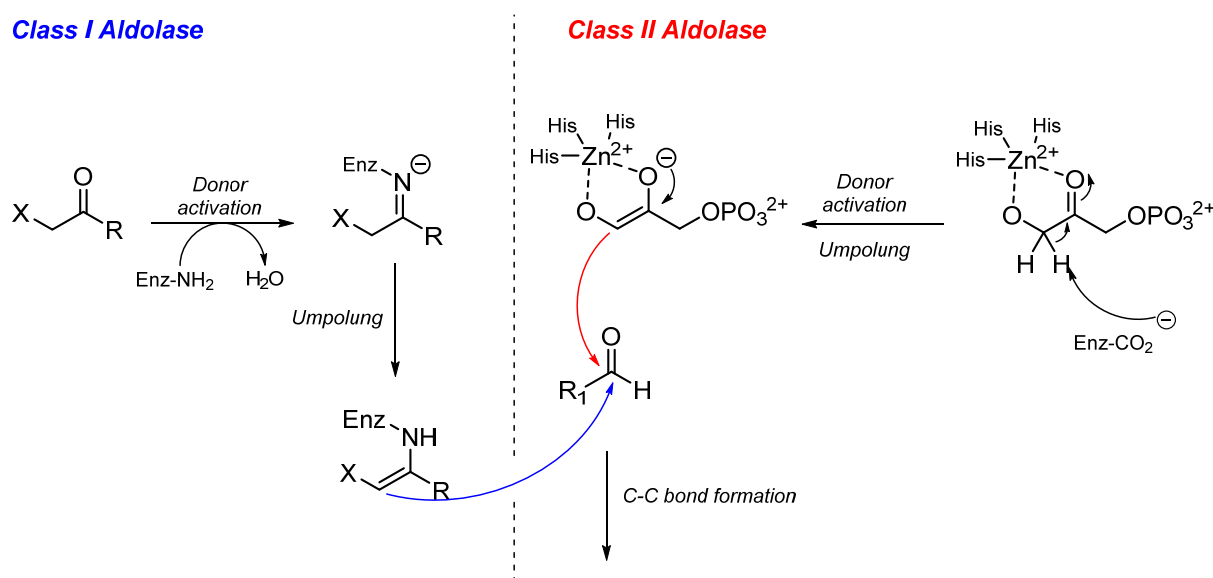
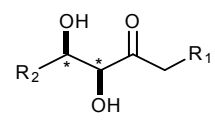
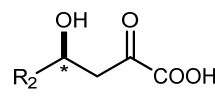
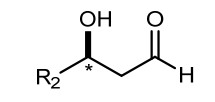
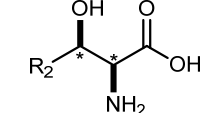


Figure 48 DHAP dependent aldolases- mechanism of class I and class II.

¹⁴⁴ P. Clapés, X. Garrabou, *Adv. Synth. Catal.* **2011**, 353, 2263-2283.

¹⁴⁵ M. Brovotto, D. Gaménara, P. Saenz Méndez, G. A. Seoane, *Chem. Rev.* **2011**, 111, 4346-4403.

Table 25 Types of aldolases listed according to their donor specificity (R₂= aromatic, aliphatic)

Donor	Product
DHAP or DHA/HA $\text{HO}-\text{CH}_2-\overset{\text{O}}{\parallel}{\text{C}}-\text{CH}_2-\text{R}_1$ $\text{R}_1 = -\text{OPO}_3^{2-}, -\text{OH}, -\text{H}$	
Pyruvate or phosphoenolpyruvate $\text{CH}_3-\overset{\text{O}}{\parallel}{\text{C}}-\text{COOH}$ or $\text{CH}_2=\overset{\text{O}}{\parallel}{\text{C}}-\text{COOH}$	
Acetaldehyde $\text{CH}_3-\overset{\text{O}}{\parallel}{\text{C}}-\text{H}$	
Glycine $\text{H}_2\text{N}-\text{CH}_2-\text{COOH}$	

Other subgroups that can catalyze C-C bond formation are for example transketolases or thiamine diphosphate-dependent enzymes for acyloin condensation such as pyruvate decarboxylases (**Figure 49**).^{146,147}

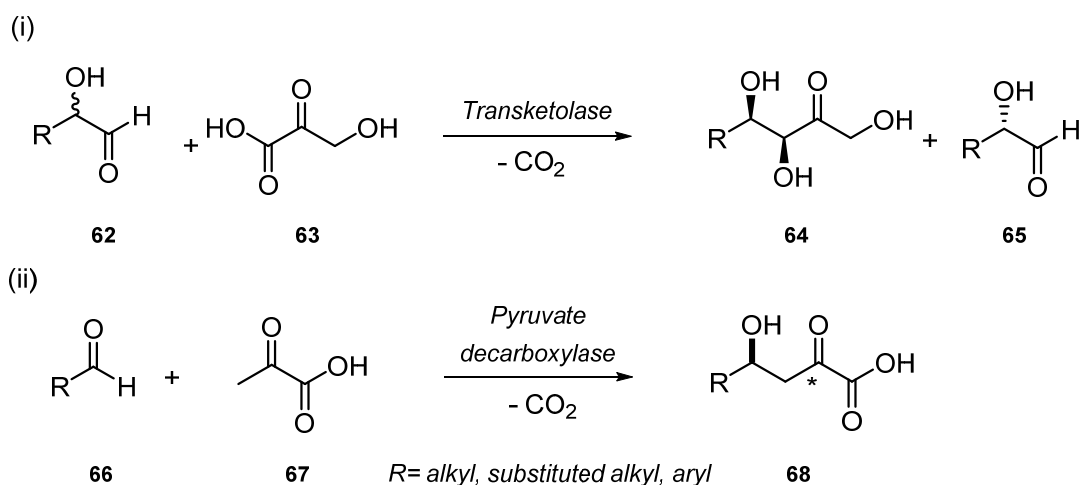


Figure 49 Illustration of enzyme mediated C-C bond forming reactions (i) Kinetic resolution by a transketolase, and (ii) acyloin condensation by a pyruvate decarboxylase.

First contribution to aldolase catalyzed condensation reactions was published by the group of Whitesides using RAMA (rabbit muscle aldolase, E.C.4.1.2.13) on a preparative scale.^{148,149} One of the first *in vitro* cascade containing an aldolase mediated step was reported by Fessner and co-workers for the synthesis of branched-chain saccharide.¹⁵⁰ Initially, DHAP was generated from renewable resources

¹⁴⁶ T. Saravanan, M.-L. Reif, D. Yi, M. Lorilliere, F. Charmantray, L. Hecquet, W.-D. Fessner, *Green Chem.* **2017**.

¹⁴⁷ N. G. Schmidt, E. Eger, W. Kroutil, *ACS Catal.* **2016**, *6*, 4286-4311.

¹⁴⁸ C. H. Wong, G. M. Whitesides, *J. Org. Chem.* **1983**, *48*, 3199-3205.

¹⁴⁹ M. D. Bednarski, E. S. Simon, N. Bischofberger, W. D. Fessner, M. J. Kim, W. Lees, T. Saito, H. Waldmann, G. M. Whitesides, *JACS* **1989**, *111*, 627-635.

¹⁵⁰ W.-D. Fessner, C. Walter, *Angew. Chem., Int. Ed.* **1992**, *31*, 614-616.

(e.g. glucose, fructose, and sucrose) followed by a diastereoselective carbonylation with different aldehydes to afford a series of rare carbohydrates. In 2003, the synthesis of *L*-fructose by a four enzyme one-pot cascade approach was reported, containing a RhuA mediated C-C coupling step. Initially, a galactose oxidase (GOase from *Dactylium dendroides*) mediated oxidation of glycerol (**69**) to *L*-glyceraldehyde (**70a**) was performed followed by a stereoselective aldol reaction and dephosphorylation to accomplish the desired product (**71**) in 55% isolated yield (**Figure 50**).¹⁵¹

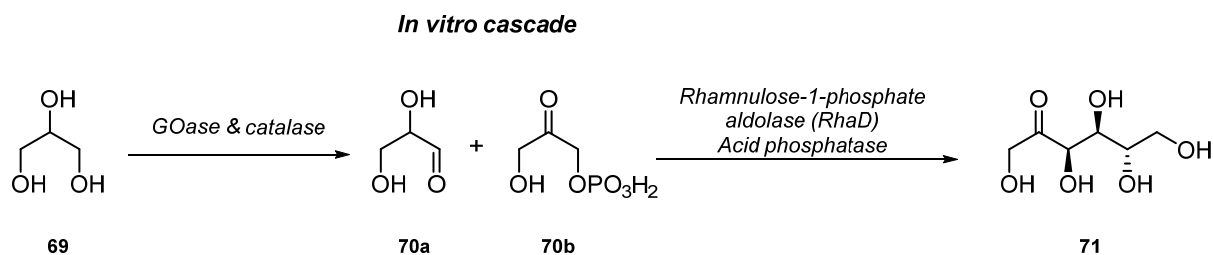


Figure 50 *In vitro* cascade for the synthesis of polyhydroxylated compounds.

Due to the hydrogen peroxide production during the initial oxidation of glycerol (**62**) by GOase (degradation *via* catalase), the introduction of oxidases into artificial whole cell cascades are often avoided. Nevertheless, engineered oxidases (e.g. galactose oxidase (GOase)) are presented for *in vitro* tandem oxidation reactions.^{152,153}

The groups of Clapes and Fessner reported during the last years several synthetic applications using aldolases and their variants with the common donor molecules DHAP or DHA.^{154,155,156,157} The most prominent drawback of DHAP dependent aldolases, is the strict selectivity towards the unstable and expensive donor molecule (DHAP), what is also a limitation towards industrial applications. Structural variations in the donor molecule can lead to decreased C-C bond forming activity, which reflects the strong mechanistic influence of steric and electronic factors of the phosphate moiety.

¹⁵¹ D. Franke, T. Machajewski, C. C. Hsu, C. H. Wong, *J. Org. Chem.* **2003**, *68*, 6828-6831.

¹⁵² B. Bechi, S. Herter, S. McKenna, C. Riley, S. Leimkuhler, N. J. Turner, A. J. Carnell, *Green Chem.* **2014**, *16*, 4524-4529.

¹⁵³ S. Herter, S. M. McKenna, A. R. Frazer, S. Leimkuhler, A. J. Carnell, N. J. Turner, *ChemCatChem* **2015**, *7*, 2313-2317.

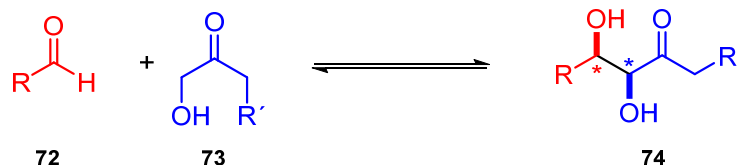
¹⁵⁴ A. L. Concia, L. Gómez, T. Parella, J. Joglar, P. Clapés, *J. Org. Chem.* **2014**, *79*, 5386-5389.

¹⁵⁵ I. Oroz-Guinea, K. Hernández, F. Camps Bres, C. Guérard-Hélaine, M. Lemaire, P. Clapés, E. García-Junceda, *Adv. Synth. Catal.* **2015**, *357*, 1951-1960.

¹⁵⁶ W.-D. Fessner, D. Heyl, M. Rale, *Catal. Sci. Technol.* **2012**, *2*, 1596-1601.

¹⁵⁷ M. Rale, S. Schneider, G. A. Sprenger, A. K. Samland, W. D. Fessner, *Chem. Eur. J.* **2011**, *17*, 2623-2632.

Acceptors: R= aromatic, aliphatic



Donors:

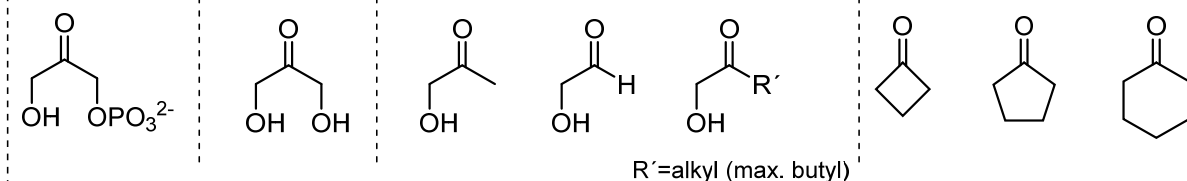


Figure 51 Summary of suitable aldol acceptor and donor molecules for stereoselective aldol reaction mediated by DHAP dependent aldolases or variants.

Protein engineering and *de novo* enzyme design have all been applied to overcome bottlenecks like stability, substrate specificity and stereoselectivity.¹⁵⁸ Recently, transformations of non-natural substrates by engineered Fsa variants were reported, which shows how effective genetic mutations of aldolases can be towards a broader aldol acceptor or donor portfolio (**Figure 51**). These strategies will open doors to new synthetic tools for the generation of (non)-carbohydrate chiral building block structures.^{159,160,161,162}

For our proof of concept study, the well studied and robust DHA/HA-dependent Fsa A129S was selected as a catalyst for the crucial C-C bond formation.

A VIII.4 DHA/HA-Dependent Fructose-6-phosphate Aldolase-Evaluation of *In vivo* Pathway I Settings

Fructose-6-phosphate aldolase (FSA) from *E. coli* is a member of class 1 aldolases, which accepts a wide range of aldol acceptors substrates. Moreover, it has a high affinity towards non-phosphorylated dihydroxyacetone phosphate derivatives such as dihydroxyacetone (DHA), hydroxyacetone (HA), glycolaldehyde (GA), and 1-hydroxy-2-butanone (HB).^{163,164,165} Subsuming, Fsa *wt* and variants are very attractive biocatalysts for the asymmetric synthesis of polyhydroxylated compounds, by exclusively generating the (3*S*,4*R*) diastereomer. The potential of FSA as a catalyst in organic synthesis can be

¹⁵⁸ C. L. Windle, M. Muller, A. Nelson, A. Berry, *Curr. Opin. Chem. Biol.* **2014**, *19*, 25-33.

¹⁵⁹ D. Güclü, A. Szekrenyi, X. Garrabou, M. Kickstein, S. Junker, P. Clapés, W.-D. Fessner, *ACS Catal.* **2016**, *6*, 1848-1852.

¹⁶⁰ A. Szekrenyi, X. Garrabou, T. Parella, J. Joglar, J. Bujons, P. Clapés, *Nat. Chem.* **2015**, *7*, 724-729.

¹⁶¹ R. Roldán, I. Sanchez-Moreno, T. Scheidt, V. Hélaïne, M. Lemaire, T. Parella, P. Clapés, W.-D. Fessner, C. Guérard-Hélaïne, *Chem. Eur. J.* **2017**, *5005*–5009.

¹⁶² R. Obexer, A. Godina, X. Garrabou, P. R. E. Mittl, D. Baker, A. D. Griffiths, D. Hilvert, *Nat. Chem.* **2016**.

¹⁶³ A. Soler, M. L. Gutiérrez, J. Bujons, T. Parella, C. Minguillon, J. Joglar, P. Clapés, *Adv. Synth. Catal.* **2015**, *357*, 1787-1807.

¹⁶⁴ J. A. Castillo, C. Guérard-Hélaïne, M. Gutiérrez, X. Garrabou, M. Sancelme, M. Schürmann, T. Inoue, V. Hélaïne, F. Charmantray, T. Gefflaut, L. Hecquet, J. Joglar, P. Clapés, G. A. Sprenger, M. Lemaire, *Adv. Synth. Catal.* **2010**, *352*, 1039-1046.

¹⁶⁵ M. Sugiyama, Z. Hong, P. H. Liang, S. M. Dean, L. J. Whalen, W. A. Greenberg, C. H. Wong, *JACS* **2007**, *129*, 14811-14817.

underlined by (i) high temperature stability at 75°C (half lifetime of 16 h), (ii) simple enzyme purification by a heat shock protocol to eliminate *E. coli* background activity, (iii) broad pH range (5.5-11.0), (iv) high tolerance towards organic co-solvents such as DMSO, DMF, and acetonitrile, and (v) storage in lyophilized form without loss of activity over months.^{166,167,168}

Within this work, a variant of FSA *wt*, Fsa1 A129S was investigated. This mutant was constituted by a single amino acid substitution by replacing alanine by serine at position 129. In comparison to the wild type, Fsa1 A129S is highly active towards the donor molecule DHA and this feature is of great interest for the synthesis of polyhydroxylated reference material in a stereoselective fashion.

A VIII.4.1 Efficient DHA Uptake & Product Secretion

After the transport of the primary alcohol through the cell membrane was indicated by *in vivo* esterase or AlkJ experiments, the uptake ability of the hydrophilic aldol donor molecules (DHA and HA) was investigated. DHA used as carbon source for an efficient cell growth as well as the DHA production under shake-flask conditions by the oxidation of glycerol using *E. coli* whole cells underlines the ability of DHA to pass the cell membrane.^{169,170,171} Until now, the exact mechanism of the DHA transport is not known.¹⁷²

Since AlkJ was identified as a suitable ADH, but also with over-oxidation activity, DHA uptake rate can limit the subsequent aldol reaction and consequently avoid the over-oxidation of the aldehyde intermediate to the unwanted carboxylic acid side product. A simple but non-specific treatment method for bacterial cells is the addition of solvents or detergents such as toluene or EDTA.¹⁷³ This procedure can also negatively affect the cell metabolism, but it is one of the easiest ways to improve cell wall permeability and the substrate uptake rate.

To identify the uptake process of DHA, two different types of resting cells were prepared and compared due to the aldol product formation over time. Pretreatment of FSA A129S resting cells was performed by adding 1% toluene and 5mM EDTA and the mixture was incubated at 30°C. After 30 min incubation time, pretreated resting cells were harvested and resuspended in minimal media (M9 N-free). Fsa1A129S containing resting cells without treatment served as control material and were also resuspended in M9 N-free media.

The reaction was performed in baffled flasks using 4 equiv. DHA and 1 equiv. benzoyethanal (**D₃**), which was the best performing substrate during all preliminary studies (**Figure 52**).

¹⁶⁶ A. L. Concia, C. Lozano, J. A. Castillo, T. Parella, J. Joglar, P. Clapes, *Chemistry* **2009**, *15*, 3808-3816.

¹⁶⁷ M. Sudar, Z. Findrik, D. Vasic-Racki, P. Clapes, C. Lozano, *Enzyme Microb. Technol.* **2013**, *53*, 38-45.

¹⁶⁸ M. Schurmann, G. A. Sprenger, *J Biol Chem* **2001**, *276*, 11055-11061.

¹⁶⁹ R. Z. Jin, E. C. C. Lin, *Microbiology* **1984**, *130*, 83-88.

¹⁷⁰ Y. J. Zhou, W. Yang, L. Wang, Z. Zhu, S. Zhang, Z. K. Zhao, *Microb. Cell. Fact.* **2013**, *12*, 103-103.

¹⁷¹ Z.-C. Hu, Y.-G. Zheng, Y.-C. Shen, *Bioresour. Technol.* **2011**, *102*, 7177-7182.

¹⁷² S. Milker, PhD Thesis, **2017**.

¹⁷³ H. J. Park, J. Jung, H. Choi, K. N. Uhm, H. K. Kim, *J. Microbiol. Biotechnol.* **2010**, *20*, 1300-1306.

The reaction progress was monitored *via* HPLC and after 2.5 h around 50% product formation was indicated for both pretreated or non-treated resting cells.

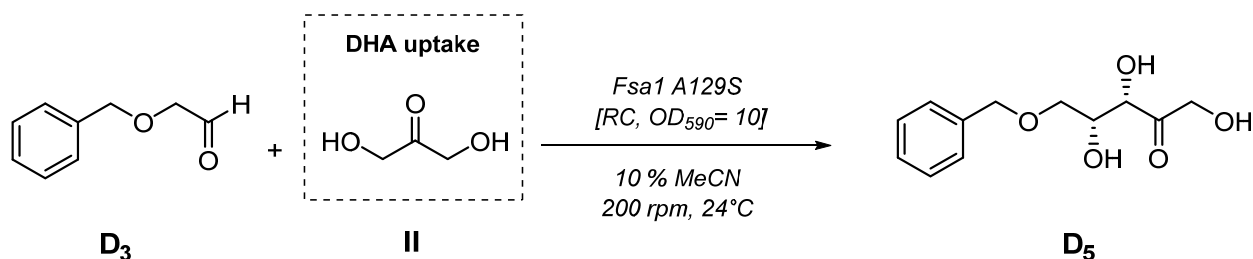


Figure 52 DHA uptake rate of *E. coli* (Fsa 1 A129S) resting cells.

After 24 h, the starting material (**D₃**) was fully converted but without any improvement of the product formation, exclusively the carboxylic acid (**D₄**) was observed as side product. It is noteworthy that the pretreatment for increased membrane permeability do not lead to better conversions like non-treated cells (Figure 53).

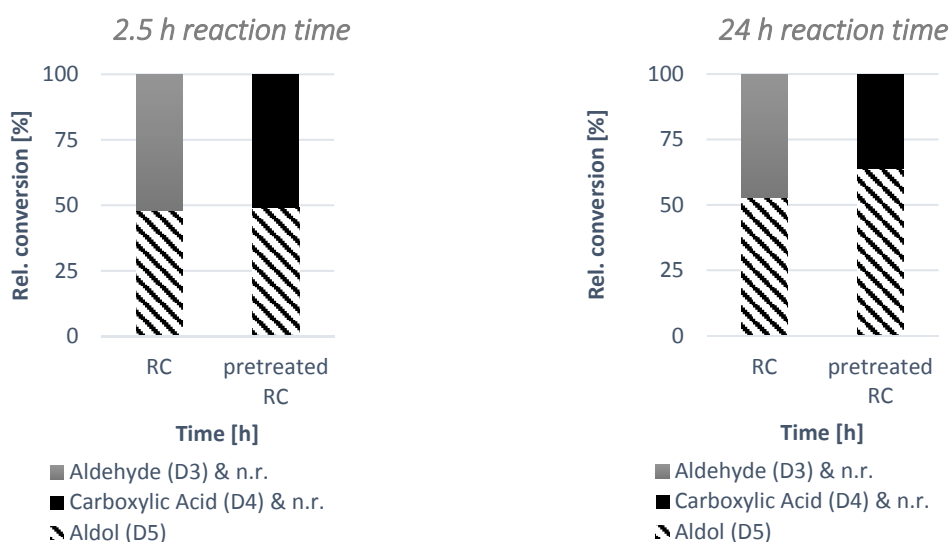


Figure 53 Comparison of DHA uptake rate using pretreated and non-treated *E. coli* (Fsa 1 A129S) resting cells.

These results were a major breakthrough for the design of Pathway I, because they clearly showed the uptake of donor molecule (DHA, **II**) as well as the diffusion of the dephosphorylated product (**X_s**) through the cell membrane was confirmed.

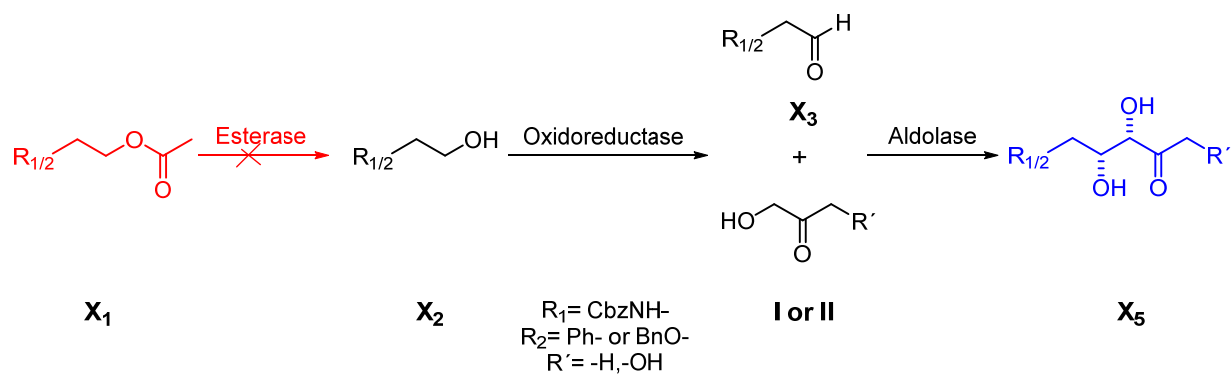


Figure 54 Summary of experimental Pathway I results.

Furthermore, the initial hydrolysis step by an esterase can be neglected due to satisfactory uptake of primary alcohols, evaluated during the AlkJ substrate studies (**Figure 54**). This finding additionally simplified the design concept for Pathway I.

A IX Pathway I Assembly

The group of Clapes investigated two strategies, a chemo-enzymatic approach using TEMPO/laccase or an *in vitro* cascade consisting of HLADH and a NADH oxidase (NOX from *Lactococcus lactis*) for the oxidation of amino alcohols (**75**).^{174,175} HLADH requires an efficient cofactor recycling system, namely NOX to shift the reaction equilibrium towards the thermodynamically disfavored aldehyde. Both strategies have to deal with the low selectivity due to the over-oxidation (up to 50%) to the corresponding acid (**77**) and the rather narrow substrate scope, limited to amino alcohols (**75**).

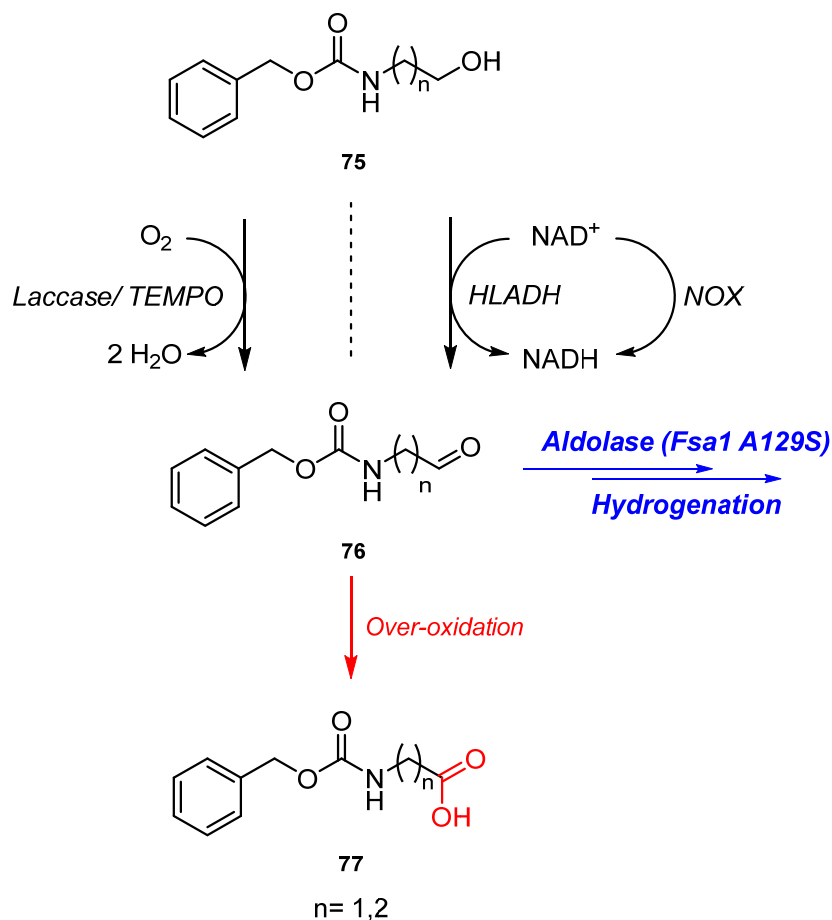


Figure 55 *In vitro* cascade approaches consisting of an enzyme mediated oxidation and a concurrent aldol reaction.

In contrast to these *in vitro* protocols (**Figure 55**), which are performed in a sequential fashion or require an additional cofactor recycling system, a whole cell biocatalyst that co-expresses both enzymes of interest would be significant improvement for the synthesis of aldol adducts. Under optimized fermentation conditions, the identified ADH (AlkJ) combined with the DHA dependent aldolase variant Fsa1 A129S will circumvent bottlenecks such as (i) elaborate isolation of the reactive aldehyde intermediate, (ii) the accumulation of cytotoxic aldehydes, and (iii) unselective over-oxidation to the corresponding carboxylic acid.

¹⁷⁴ M. Mifsud, A. Szekrényi, J. Joglar, P. Clapés, *J. Mol. Catal. B: Enzym.* **2012**, *84*, 102-107.

¹⁷⁵ M. Sudar, Z. Findrik, D. Vasic-Racki, A. Soler, P. Clapes, *RSC Adv.* **2015**, *5*, 69819-69828.

A IX.1 Two Plasmid Approach-AlkJ/ Fsa1 A129S Co-expressed in *E. coli*

First, a two-plasmid approach with co-expressed pKA1/alkJ + pET16b/fsa1A129S in *E. coli* was performed (**Figure 56**). Resting cells (RC) were prepared and resuspended in M9 media (N-free) and applied with our model substrates (**B₂**, **D₂**, **E₂**) and 4 equiv. of DHA (**Table 26**). The reaction mixture was prepared in 8 mL vials with screw cap as follows:

Table 26 Resting cell screening using two plasmid system of AlkJ and Fsa1 A129S.

Reaction mixture		Final concentration
2.607 mL	RCs (OD ₅₉₀ = 12.5)	OD ₅₉₀ = 10.0
0.060 mL	DHA monomer (1 M)	20 mM (4 eq.)
0.333 mL	substrate (50 mM in MeCN)	5 mM (10% (v/v) MeCN)

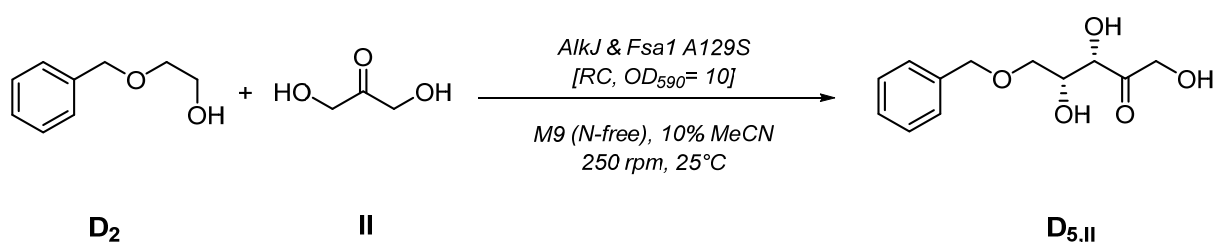


Figure 56 Two plasmid approach (pKA1/alkJ + pET16b/fsa1 A129S) with 2-(benzyloxy)ethan-1-ol and 4.0 eq. of DHA monomer.

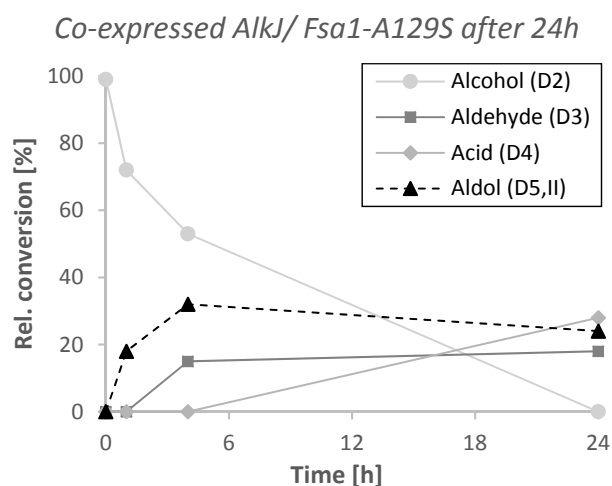


Figure 57 Aldol adduct formation by the two plasmid approach (pKA1/alkJ + pET16b/fsa1 A129S) with 2-(benzyloxy)ethan-1-ol and 4.0 eq. of DHA monomer.

Following the reaction over time for **D₅** revealed that after four hours a plateau of product formation (35%) was achieved, whereby 53% of the primary alcohol was still remaining (**Figure 57**). As indicated

in Figure 57, nearly full starting material consumption after 24 h was obtained, but besides the formation of around 35% acyclic aldol adducts, also 40% of the over-oxidation product, the carboxylic acid was generated.

Furthermore, phenylethanol (**B**₂) and 3-benzyloxypropan-1-ol (**E**₂) were transformed to the corresponding aldol adduct, but within similar results of 30% product formation within 24 h and around 20% carboxylic acid (**Figure 58**).

Taken together, these experiments indicated the principal feasibility of Pathway I design; however, the need for further optimization also became apparent.

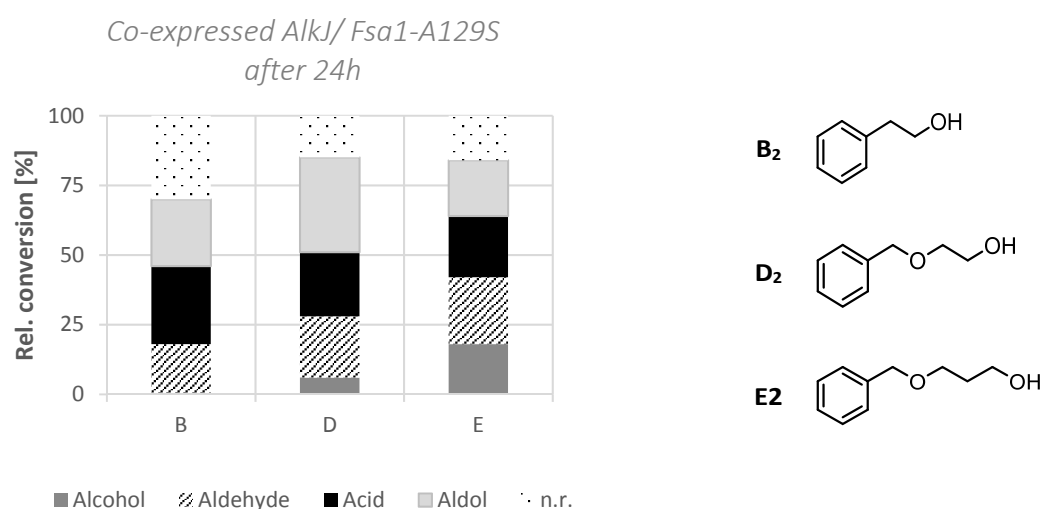


Figure 58 Two plasmid approach (pKA1/alkJ + pET16b/fsa1 A129S) with 5 mM **B**₂, **D**₂, **E**₂ and 4.0 eq. of DHA monomer.

After these promising results of the first *in vivo* experiments using co-expressed AlkJ and Fsa1 A129S, optimization strategies on genetic (e.g. operon design, regulatory elements, etc.) and process parameters (e.g. aldol donor concentration, reaction time) have to be applied to improve the overall performance of Pathway I.

A IX.2 Optimization on Genetic Levels

The optimization on genetic levels was conducted by Thomas Bayer and discussed in detail in his PhD thesis.¹⁷⁶ Herein, a short summary of his work is given and these published data serves as template for the upcoming sections.¹⁷⁷

The introduction of an artificial pathway into a living organism can increase the metabolic burden (e.g. growth rate, expression stability, etc.) and can decrease the overall performance of the whole cell catalyst. To tackle this obstacle, three different constructions of a single vector containing AlkJ and Fsa1 A129S were designed and therefore, the pKA1/alkJ vector served as plasmid backbone to

¹⁷⁶ T. Bayer, PhD Thesis, **2017**.

¹⁷⁷ T. Wiesinger, T. Bayer, S. Milker, M. D. Mihovilovic, F. Rudroff, *ChemBiochem* **2017**.

assemble the genes of *alkJ* and *fsa1 A129S* in three different genetic architectures (i) operon (OPE), (ii) pseudo-operon (POP), and (iii) monocistronic configuration (MON) (**Figure 59**).¹⁷⁸

The single vectors containing *AlkJ* and *Fsa1 A129S* were assembled by two different methods: FastCloning (FC)¹⁷⁹ and the application of a seamless ligation cloning extract (SLiCE).¹⁸⁰

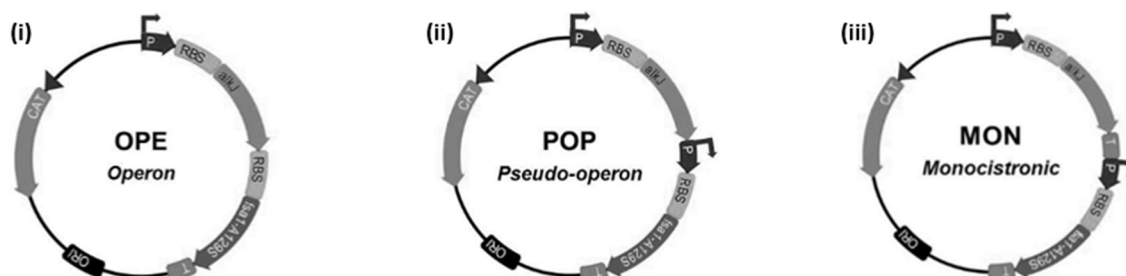


Figure 59 Illustration of genetic architectures of *AlkJ* and *Fsa1 A129S* on single plasmids. (i) Operon: one promoter (P) & terminator (T). (ii) Pseudo-operon: two Ps and one T. (iii) Monocistronic configuration: two Ps and two Ts; ORI: origin of replication; RBS: ribosome binding site; CAT: chloramphenicol acetyltransferase

In contrast to operons, where the expression of *alkJ* and *fsa1 A129S* is controlled by one T7 promoter (PT7) in front of the *alkJ* gene and one T7 terminator (TT7) downstream of the aldolase-coding region, the POP as well as the MON plasmid contains an additional promoter.

Furthermore, the MON construct contains an additional terminator sequence, which is located between the *alkJ* stop codon and the PT7 of the aldolase-coding region. In order to compare the growth behavior of the one plasmid constructs to the two-plasmid construct (pKA1/*alkJ* + pET16b/*fsa1 A129S*) or the empty host control *E. coli* BL21 (DE3), the bacterial growth in rich medium (LB medium, **Figure 60**) and in minimal medium (M9 resting cell media, **Figure 60**) was monitored. In LB medium nearly no differences regarding growth behavior was observed for the *E. coli* BL21 (DE3) control and the transformants. In contrast, growth curves in M9 medium showed shorter initial lag phases ($t_{(\text{growth max})}$ after 7.6 h) for the unburdened *E. coli* BL21 (DE3), followed by the POP plasmid construct (**Figure 61, Table 27**)

¹⁷⁸ T. Bayer, S. Milker, T. Wiesinger, F. Rudroff, M. D. Mihovilovic, *Adv. Synth. Catal.* **2015**, 357, 1587-1618.

¹⁷⁹ C. Li, A. Wen, B. Shen, J. Lu, Y. Huang, Y. Chang, *BMC Biotechnol.* **2011**, 11, 92.

¹⁸⁰ Y. Zhang, U. Werling, W. Edelmann, *Nucleic Acids Res.* **2012**, 40, e55.

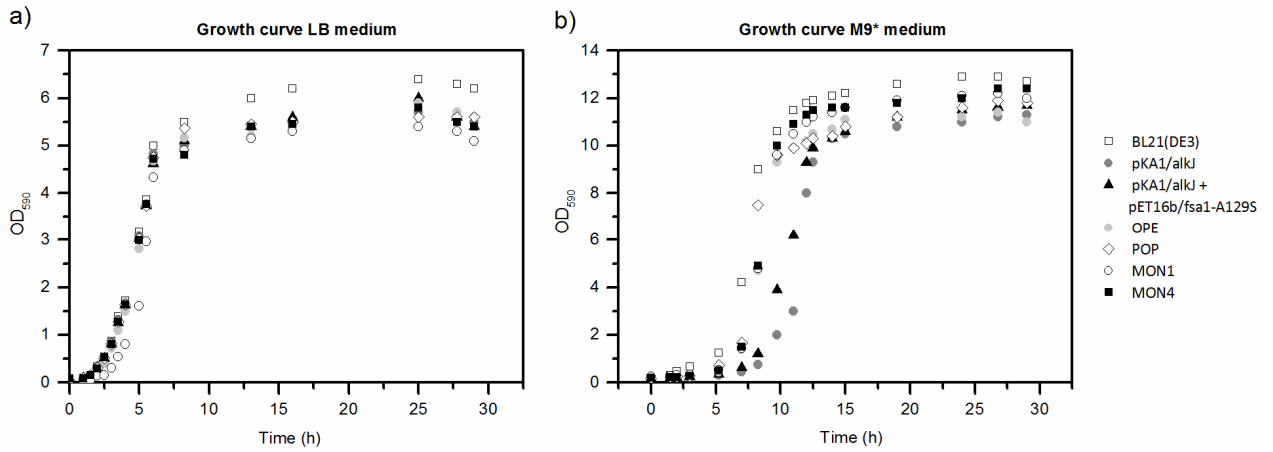


Figure 60 Growth monitoring of wild type *E. coli* BL21(DE3), single plasmid systems (pKA1/alkJ), two plasmid (pKA1/alkJ + pET16b/fsa1 A129S) and co-transformants a) in LBmedium at 37°C with shaking; b) in M9-N* medium at 37°C.

To determine the time of maximal growth ($t_{\text{growth,max}}$) of all designed constructs, dOD_{590}/dt was plotted versus the growth time in Figure 61 (Matlab R2012b).

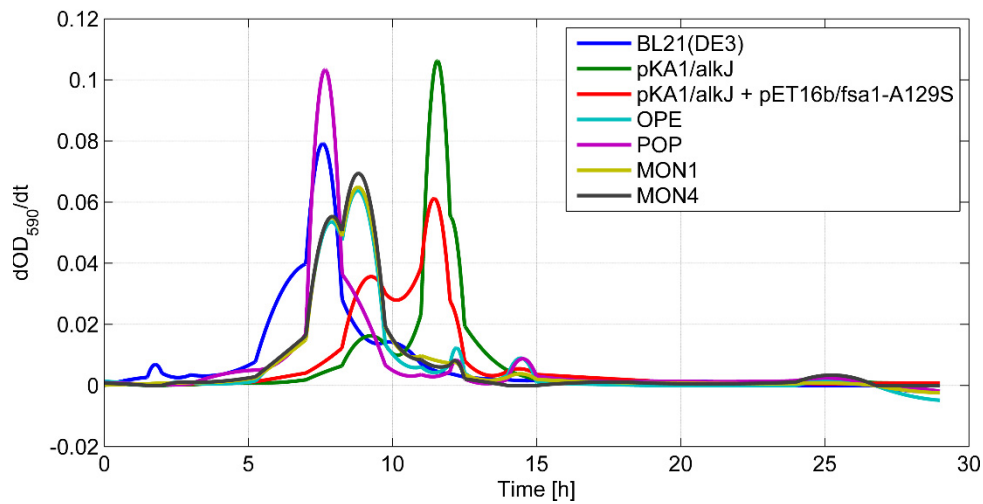


Figure 61 Determination of maximal growth ($t_{\text{growth,max}}$) in M9 media for all prepared constructs: POP after 7.6 h; all other one plasmid constructs after 8.8 h.

The POP construct and the empty host organism grew faster than all other configurations, which is depicted by the maximal growth rate and shorter lag phases (**Table 27**).

Table 27 Growth behavior and Fsa1 A129S expression of wild type and different transformants.

Vector	Growth Rate [h ⁻¹]	t _(growth max) [h]	Fold-increase of soluble Fsa1 129S ^[a]
Empty host [BL21 (DE3)]	0.66	7.6	-
pKA1/alkJ	0.56	11.6	-
pKA1/alkJ pET16b/fsa1 A129S	0.55	11.5	1
OPE	0.70	8.8	0.50 ± 0.32
POP	0.76	7.7	1.02 ± 0.12
MON1	0.66	8.8	0.94 ± 0.29
MON4	0.69	8.8	1.12 ± 0.24

^[a] Bradford assay was performed with Fsa1 A129S after purification by heat shock (HS). Normalization: [g] cell pellet.

For further characterization, expression studies of all constructs were performed under the optimized conditions and the enzyme production was monitored over time (0–19 h) by SDS-PAGE analysis. Due to the stable production of soluble Fsa1 A129S and the beneficial growth behavior (**Table 25**), POP transformants of *E. coli* BL21 (DE3) were used for Pathway I optimization studies on process parameters.

A IX.3 Optimization on Process Parameters

After pathway construction and successful optimization on a genetic level providing the best performing construct with regards to growth rate and enzyme expression levels, the pseudo-operon configuration (POP) was introduced to optimization studies on process parameters (**Figure 62**).

Consequently, careful studies to different aldol donor quantities were conducted over time to circumvent byproduct formation. Therefore, three different aldol donor concentrations (0, 5, 20 equiv. DHA or HA monomer) were applied and the product formation was monitored *via* GC/FID and LC/MS.

A IX.3.1 Donor Concentration-DHA

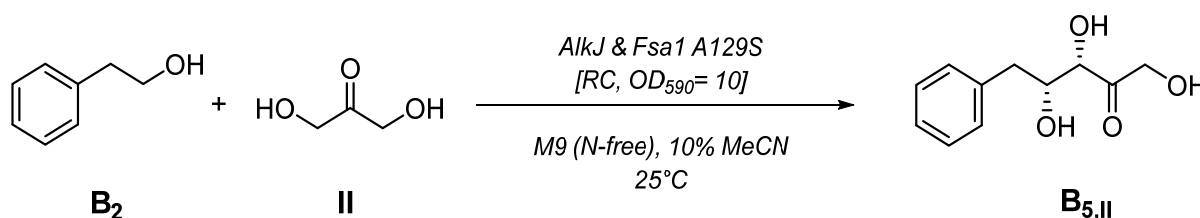


Figure 62 Optimization of process parameter, different donor concentration DHA (0, 5, 20 equiv.) with 5 mM phenylethanol (B₂) and the POP construct.

In the absence of DHA, 75% consumption of starting material (**B**₂) was obtained within 3 h and mainly the cytotoxic aldehyde (**B**₃) was detected (60%). After 6 h, **B**₃ was further oxidized by AlkJ and after 24 h exclusively the corresponding carboxylic acid (**B**₄) was generated (**Figure 63**).

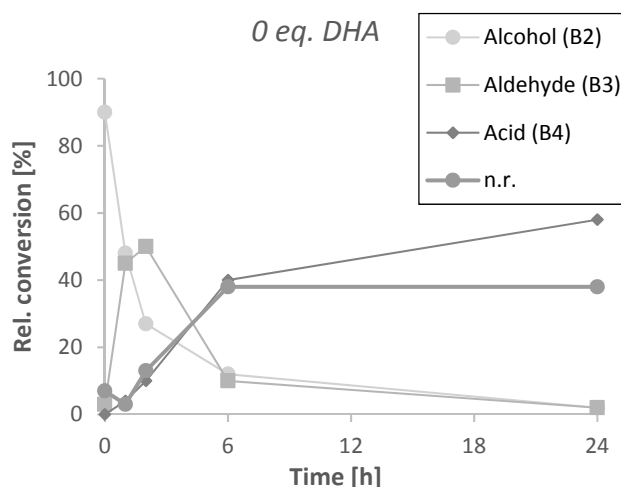


Figure 63 Aldol formation using 0 equiv. DHA, 5 mM **B**₂ and the POP construct. (n.r. not recovered)

In contrast, the addition of 5 equiv. DHA led to efficient carboligation (**B**_{5,II}) between the aldehyde (**B**₃) and the supplied donor molecule (**II**) within 2 h. Unfortunately, longer reaction times led to the retro aldol reaction and accumulation of the aldehyde, which ultimately resulted in the unwanted carboxylic acid side product (**B**₄) after 24 h (**Figure 64**). The formation of the corresponding carboxylic acid represents a pathway sink and is limiting the aldol adduct generation at all.

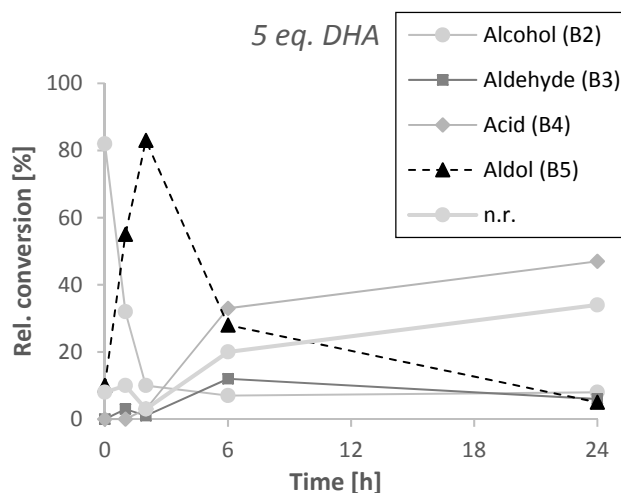


Figure 64 Aldol formation using 5 equiv. DHA, 5 mM **B**₂ and the POP construct. (n.r. not recovered)

The effect of increased aldol donor quantity (20 equiv. of DHA) to drive the reaction to completion and avoid retro aldol activity is depicted in Figure 64. In contrast to 5 equiv. DHA, the reached plateau of aldol product formation after 2 h (>85%) was not affected by any side reaction (over-oxidation) or intrinsic activity over hours (**Figure 65**).

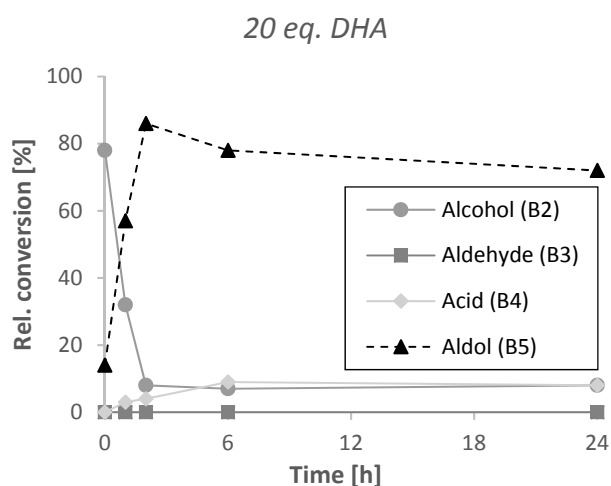


Figure 65 Aldol formation using 20 equiv. DHA, 5 mM B₂ and the POP construct.

A IX.3.2 Donor Concentration-HA

Besides studies on the effects of the DHA concentration studies using HA (II) were also conducted for the identification of the best working biotransformation conditions due to starting material consumption and hindered side reaction activity. In general, same reaction settings as described with DHA were used, such as 0, 5, and 20 equiv. of HA, 5 mM substrate and *E. coli* resting cells of the pseudo-operon construct in M9 (N-free) medium (Figure 66).

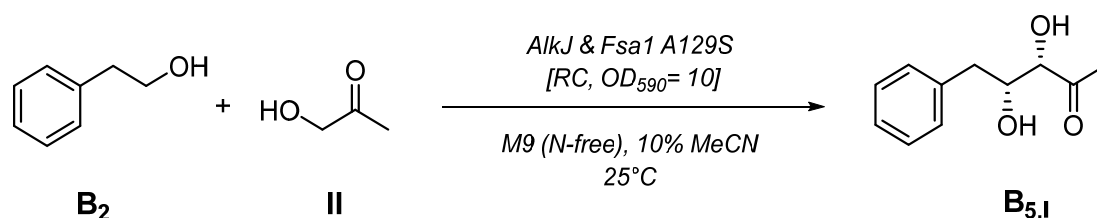


Figure 66 Optimization of process parameter, different donor concentration HA (0, 5, 20 equiv.) with 5 mM phenylethanol (B₂) and the POP construct.

Switching the aldol donor from DHA to HA led to similar results due to suppressed byproduct formation using donor concentrations up to 20 equivalents, however increased reaction times were necessary to obtain full starting material consumption. These results also correlate well with reported activity of FSA wt and Fsa1 A129S towards DHA and HA (Table 28).¹⁸¹

Table 28 Activity of Fsa wt to Fsa1 A129S mutant for the aldol donor molecules DHA and HA.

Substrate	K _M [mM]	FSA wt		Fsa1 A129S		
		k _{cat} [s ⁻¹]	k _{cat} /k _M [s ⁻¹ mM ⁻¹]	K _M [mM]	k _{cat} [s ⁻¹]	k _{cat} /k _M [s ⁻¹ mM ⁻¹]
DHA	32±2	116	4	11±1	760	69
HA	17.4±0.5	2527	145	22±3	899	41

¹⁸¹ J. A. Castillo, C. Guérard-Hélaine, M. Gutiérrez, X. Garrabou, M. Sancelme, M. Schürmann, T. Inoue, V. Hélaine, F. Charmantray, T. Gefflaut, L. Hecquet, J. Joglar, P. Clapés, G. A. Sprenger, M. Lemaire, *Adv. Synth. Catal.* **2010**, 352, 1039-1046.

The catalytic efficiency of Fsa1 A129S in the presence of the donor DHA is 7-fold higher than for the wild type enzyme. In contrast, the affinity of HA is for both enzymes in the same mM range but the activity for the FSA wt is 3-fold higher. Besides the formation of 50% aldol adduct, a significant amount of the carboxylic acid (25%) is also generated by the use of 5 equiv. HA (**Figure 67**).

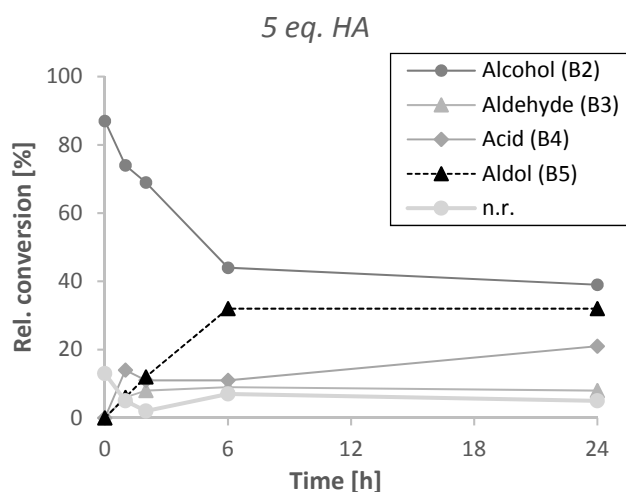


Figure 67 Aldol formation using 5 equiv. HA, 5 mM B₂ and the POP construct.

However, byproduct formation was completely avoided with a high excess of HA (20 equiv.) and yielded in almost 60% of the desired product within 24 h (**Figure 68**).

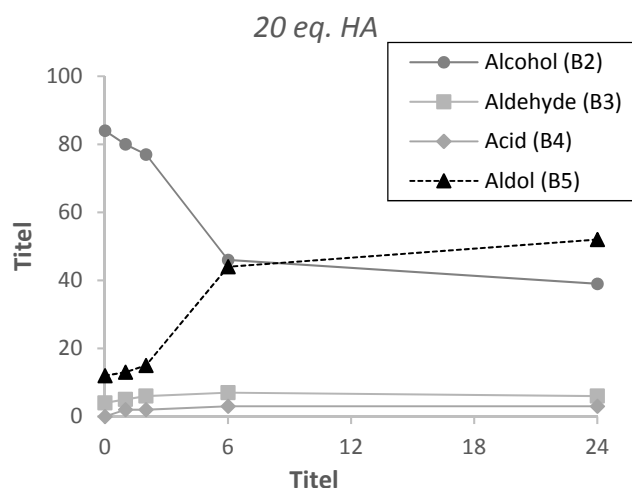


Figure 68 Aldol formation using 20 equiv. HA, 5 mM B₂ and the POP construct.

Due to the lower activity of Fsa1 A129S to the aldol donor HA, full substrate conversion was achieved between 24 to 48 h, depending on the activity of the POP resting cells. This fact has to be considered during preparative scale biotransformations by a close monitoring *via* RP-TLC and GC/FID until full consumption of the starting material is indicated. In general, the POP construct showed increased activity by using permanent cultures for the cultivation of resting cells instead of single colonies. The

activity of POP resting cells was determined by the reaction of phenylacetaldehyde (**B₃**) and DHA (20 equiv.). Active resting cells, which were applied for further studies gave at least 50% substrate consumption within 2 h, monitored *via* GC/FID

A IX.4 Pathway I-Substrate Scope

To study the substrate promiscuity of the designed pathway, α -substituted *N*-Cbz-protected aminoalcohols (**F_{2,II}**- **J₂**) were tested on analytical scale experiments. These class of substrates combined with the POP construct can give access to substituted imino-sugar derivatives.¹⁸² When the reaction was carried out under the optimized conditions (POP construct, 20 equiv. DHA) low conversions of the primary alcohols to the over-oxidation product was observed (**Figure 69**).

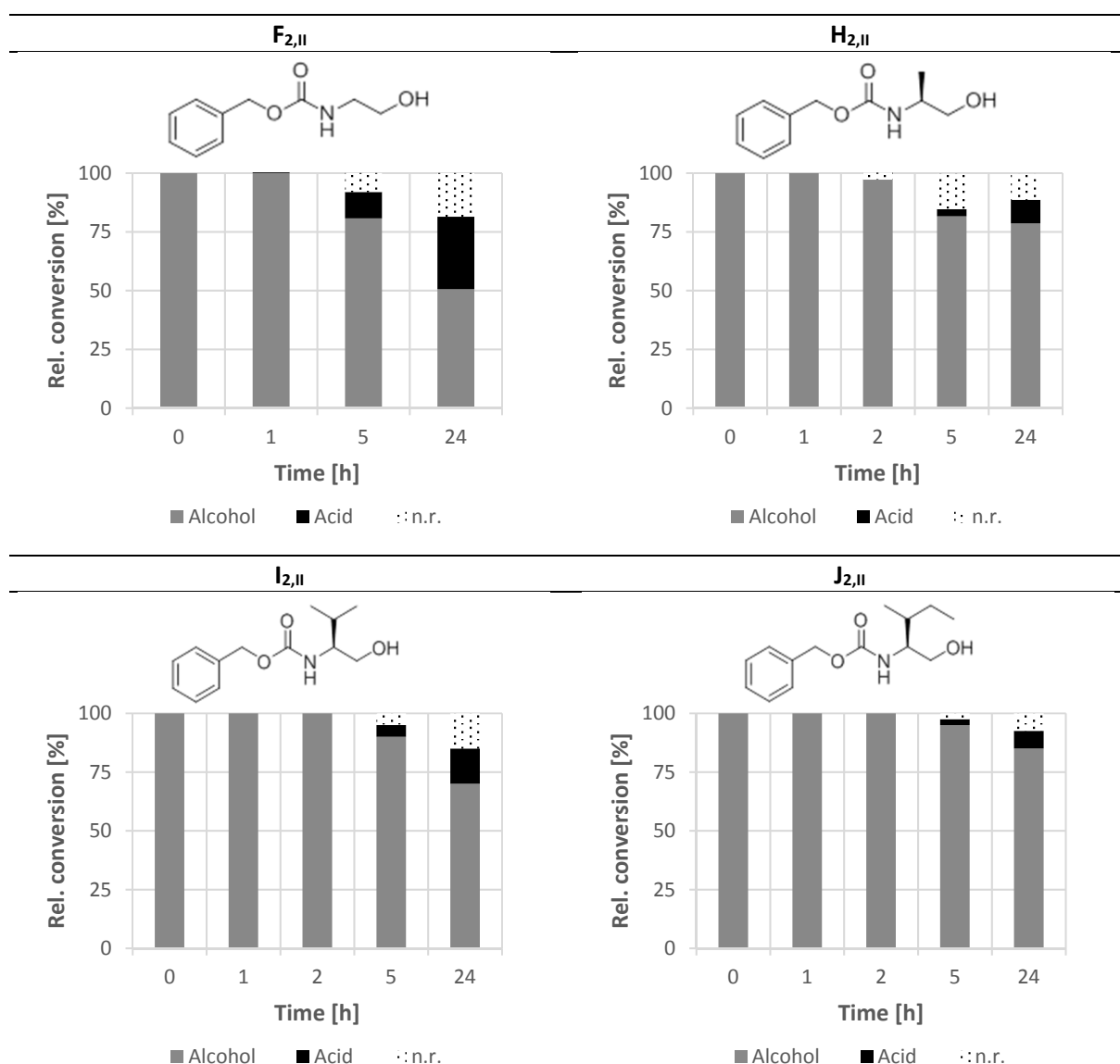


Figure 69 Substrate conversions using POP construct, 20 equiv. of DHA, and different α -substituted *N*-Cbz-protected amino-alcohols. (n.r. not recovered)

¹⁸² J. A. Castillo, J. Calveras, J. Casas, M. Mitjans, M. P. Vinardell, T. Parella, T. Inoue, G. A. Sprenger, J. Joglar, P. Clapes, *Org. Lett.* **2006**, *8*, 6067-6070.

As displayed in Figure 69, no product formation at all was detected by LC/MS after 24 h. Within this recorded time course around 10% of the corresponding acid was generated. These observed results are in accordance with the literature.¹⁸³ To increase the activity of Fsa1 A129S towards α -substituted *N*-Cbz-protected amino-alcohols, double to triple mutation for example FSA A129S/ A165G for methyl substituted amino-aldehyde have to be applied.

Furthermore, analytical experiments to enlarge the aldol donor scope towards fluorinated molecules were conducted. Fsa1 A129S activity towards the commercially available, but highly toxic difluoroacetone (DFA), was tested in combination with our model aldol acceptor (**B₂**) and the well-established POP resting cells conditions (**Figure 70**).

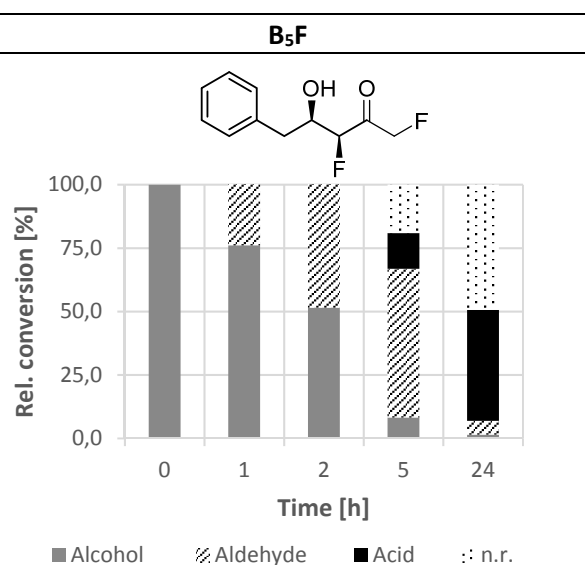


Figure 70 Substrate consumption using POP construct, 20 equiv. of DFA, and different α -substituted *N*-Cbz-protected amino-alcohols. (n.r. not recovered)

The alcohol consumption and mainly carboxylic acid formation was monitored by GC/FID, unfortunately no product formation of the corresponding aldol adduct (**B₅F**) was observed by LC/MS. Various attempts by LC/MS, using different columns (C18 or PFP) and solvent gradients (H₂O + 0.1% formic acid/acetonitrile + 0.1% formic acid) to identify the desired products were unsuccessful. According to GC-FID, LC/MS, and RP-TLC the identification of a side product was not possible, no prominent peak was observed with the different applied analytical methods. After these results, no further studies were conducted on fluorinated aldol nucleophiles.

¹⁸³ M. Gutierrez, T. Parella, J. Joglar, J. Bujons, P. Clapes, *Chem. Commun.* **2011**, 47, 5762-5764.

A IX.5 Downstream Processing-Isolation and Purification of Polyhydroxylated Compounds

Since genetic (POP construct) and process parameter studies (20 eq. DHA or HA) led to increased overall performance and eliminated side reaction activity, preparative scale biotransformations were performed. The reaction progress was monitored *via* GC/FID, until full consumption of starting material was observed and the aqueous mixture was then applied to different purification strategies.

As previously mentioned and also described in the literature, the isolation of polyhydroxylated compounds from an aqueous solution is a major bottleneck of aldolase mediated C-C bond forming reactions.¹⁸⁴¹⁸⁵¹⁸⁶ To purify such compounds, several strategies were reported (**Figure 71**), like (A) extraction with organic solvents (e.g. ethyl acetate or dichloromethane) or (C) by reversed phase (RP) preparative HPLC. It turned out that the extraction protocol (A) was limited to corresponding HA aldol products, since the DHA compound was distributed in both layers (organic/aqueous) after at least more than 10 extractions steps monitored *via* RP-TLC.

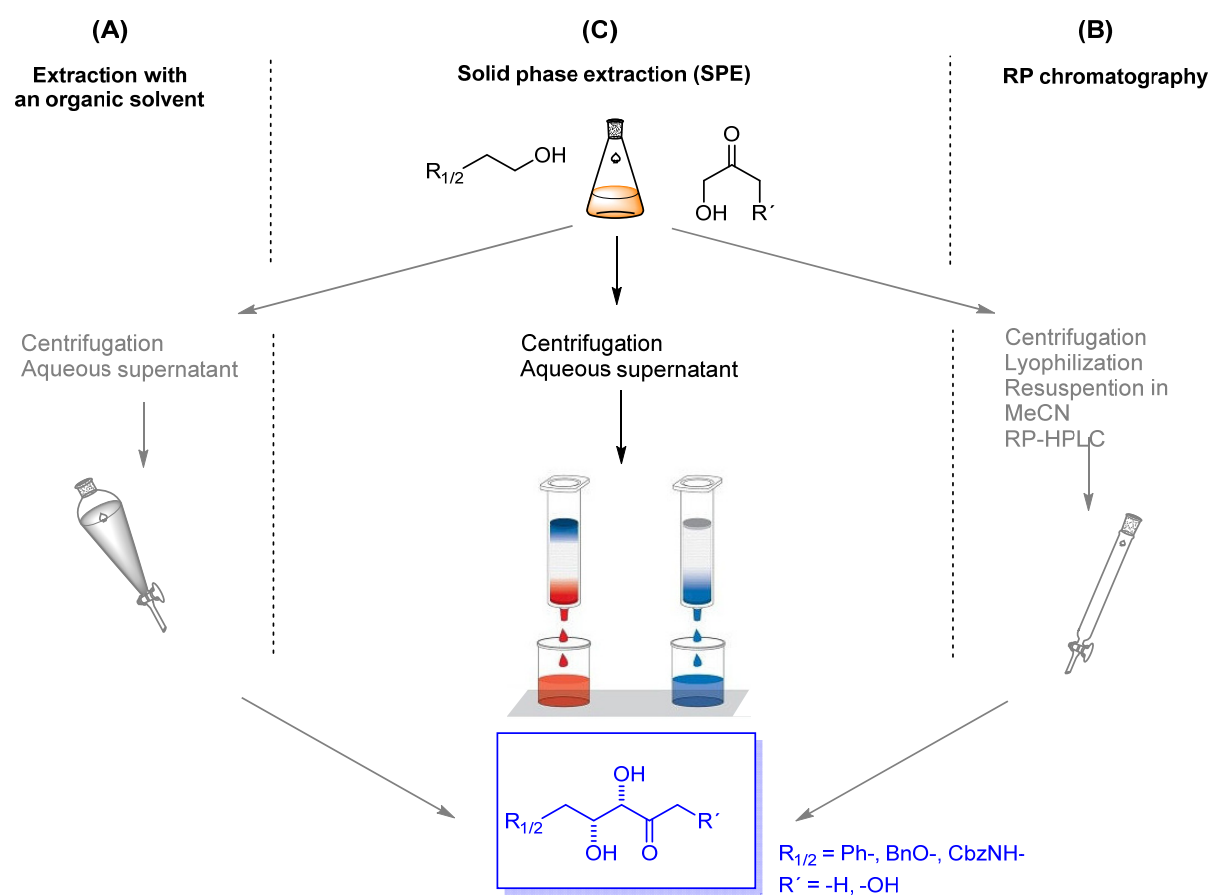


Figure 71 Purification strategies and the work flow for the isolation of acyclic aldol adducts.

¹⁸⁴ M. Wei, Z. Li, T. Li, B. Wu, Y. Liu, J. Qu, X. Li, L. Li, L. Cai, P. G. Wang, *ACS Catal.* **2015**, *5*, 4060-4065.

¹⁸⁵ A. L. Concia, C. Lozano, J. A. Castillo, T. Parella, J. Joglar, P. Clapes, *Chem. Eur. J.* **2009**, *15*, 3808-3816.

¹⁸⁶ A. L. Concia, L. Gomez, J. Bujons, T. Parella, C. Vilaplana, P. J. Cardona, J. Joglar, P. Clapes, *Org. Biomol. Chem.* **2013**, *11*, 2005-2021.

As an alternative for the solvent extraction, an RP-HPLC purification protocol was applied (C). But also this strategy showed some bottlenecks, especially the sample preparation. After full consumption of the acceptor aldehyde according to RP-TLC, the solid biotransformation material was centrifuged and the aqueous layer was lyophilized overnight. The obtained powder was dissolved several times in methanol or acetonitrile until no aldol adduct was remaining, monitored by RP-TLC and concentrated again. This sample preparation was mainly responsible for massive loss in yield (isolated yields of approx. 40%) due to the low product solubility in acetonitrile or methanol in presence of all biotransformation residues (e.g. buffer salts, DHA excess) (Table 32).

As mentioned above, the challenging purification of the target molecules from an aqueous solution is mainly responsible for low isolated yields. To overcome such limitations, we established a solid phase extraction (SPE) purification protocol for aldol adducts (Figure 71, B).

This SPE protocol does not require elaborate sample preparation and therefore represents an attractive tool for the elaborate purification of polyhydroxylated compounds. A single centrifugation step to separate solid biotransformation material from the aqueous layer has to be performed and the obtained supernatant is then continuously transferred onto a C18-reversed phase silica gel packed column and separated by applying a solvent gradient. Finally, the product fraction is collected, concentrated which afforded the pure target molecule without further purification steps.

A IX.5.1 SPE Purification-Optimization Cartridge Size

Preparative scale experiments were typically performed in 200 mL baffled Erlenmeyer flask (approx. 1 mg/mL product concentration). To identify best separation performance, different sizes of C18 packed cartridges were tested. In some cases, the capacity of the C18 material was overloaded or decreased purity of the aldol adduct was obtained (Table 29).

Table 29 SPE optimization studies: C18 material to biotransformation volume.

#	C18 material [g]	mL	Isolation issues
1	5	100	Product elution with 95% H ₂ O, solid phase capacity was overloaded
2	12	100	
3	12	200 ^[b]	Mixture of byproducts and product according to ¹ H NMR
4	25	200	
5	25	400	Product elution with 95% H ₂ O, solid phase capacity was overloaded

Best separation results, based on product purity (NMR analysis) and yield, were obtained for a ratio of C18 material (g) to biotransformation medium (mL) of 1:8 (25g/ 200mL) in presence of 200 mg aldol adduct (Table 29, 4). Figure 72 depicts a typical SPE run, which gave the pure target products after 30

minutes, monitored by a PDA detector at 200 and 210 nm (blue, pink) and an electron light scattering detector (ELSD) (green).

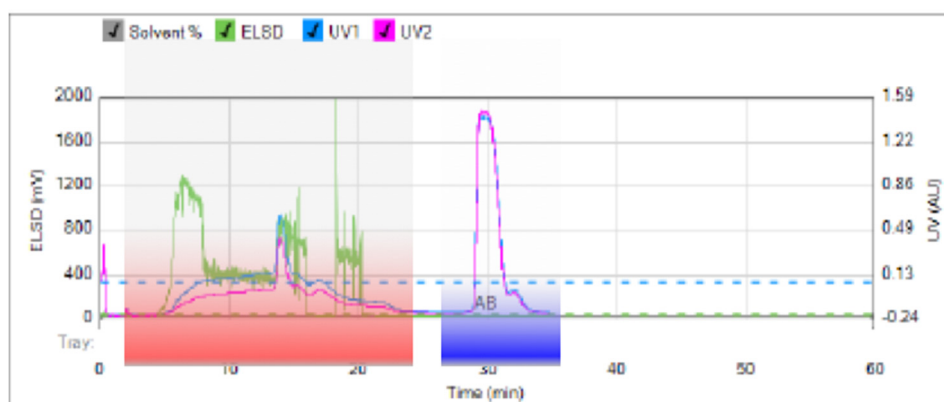


Figure 72 Illustration of an SPE run. (red) Biotransformation residues and byproducts (buffer salts, DHA, etc.); (blue) Pure target compound.

After the elution of all byproducts (buffer salts, DHA, etc.) using 95% H₂O and 5% methanol for 25 min, the mobile phase composition was changed subsequently to exclusively methanol (>95%) to flash the diastereomerically pure product (de > 99) from the column.

The entire SPE purification was performed in less than 1 h in good to excellent yields (up to 90%) and the product purity was confirmed, after concentration at high vacuum and 30°C, by NMR and LC/MS (**Figure 72**). The use of methanol as solvent is also beneficial for the subsequent transformation towards *D*-fagomine, since it is one of the most prominent solvents applied in catalytic hydrogenations. The eluent of the SPE purification can be used directly without any further treatment (see **A X.1**). Since the concentrations of aldol adducts in the biotransformation mixture differed from the expected concentrations, the prepared analytical standards used for the calibration were analyzed. Therefore, several ¹H and ³¹P NMR experiments were performed, especially to validate the water content or inorganic phosphor amounts after concentration of the product fraction. ¹H NMR experiments in methanol-*d*₄, DMSO-*d*₆ resulted in an average water content of 10%, which fits to a monohydrate form of the acyclic compound. This resolved the inconsistency between the calibration and the concentrations in the biotransformation mixture (see **A IX.6**). Additionally, ³¹P NMR measurements gave no signals for inorganic phosphor compounds and the efficiency of the established SPE purification protocol has been confirmed.

A IX.6 NMR Studies: Determination of Water Content in the Aldol Adduct

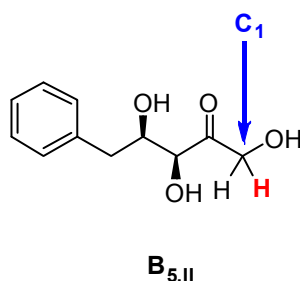
Reference compounds for analytical scale experiments were prepared on preparative scale and product purity was confirmed by NMR (¹H and ¹³C NMR) and LC/MS. The pure compounds were used for HPLC standard calibration.

We performed our optimization studies on analytical scale and reaction progress was monitored *via* GC/FID and HPLC analysis. Due to the polarity of the aldol product (**B_{5,I}**/**B_{5,II}**), GC/FID measurements were limited to compounds (**B₂₋₄**). The conversion of the primary alcohol (**B₂**) to the corresponding aldehyde (**B₃**) as well as the over-oxidation activity to the carboxylic acid (**B₄**) was detected by both systems (HPLC and GC/FID). Proper quantification of the aldol adduct was only possible *via* HPLC analysis.

Within this orthogonal analysis we found deviations between our starting concentration of alcohol (**B₂**) and the final aldol product (**B_{5,II}**). Values of approximately 110% theoretical yield were obtained. First the purity of our intermediates and products was checked and confirmed again by NMR and MS analysis. Standard calibration curves were reinvestigated, but the experimental results did not change even after several repetitions. Finally, we hypothesized, that the only “impurities” in the aldol product, which would affect our analysis are water and/or inorganic salts from the reaction medium.

The ability of ketoses to form hydrates in aqueous solution was suggested to be a reasonable explanation, which effects the calibration on HPLC. Therefore, ¹H NMR experiments in methanol-*d*₄ and DMSO-*d*₆ were performed to determine the molecular water content after concentration of the product fractions on high *vacuum* over more than 24h. For these measurements, a solvent blank (800 μL) as well as 4 mg of the product, dissolved in the same amount of solvent were analyzed.

For proper calculations, the water and solvent peaks were referenced to the proton at the C1 position, next to the primary alcohol.



A IX.6.1 NMR Study in Methanol-*d*₄ and DMSO-*d*₆

Table 30 Calculation of molecular water content in the aldol adduct by ¹H NMR measured in methanol-*d*₄

	Product [C1-H] [Integral]	DMSO- <i>d</i> ₆ [Integral]	H ₂ O [Integral]
Blank	-	2.98	5.21
Product	1	2.98	9.76

$$\text{Fold amount of H}_2\text{O related to } ^1\text{H NMR integral: } \frac{H_2O(p) - H_2O(blank)}{2} = \frac{9.76 - 5.21}{2} = 2.275$$

$$\text{Molar mass of the containing H}_2\text{O: } M(\text{H}_2\text{O}) = 2.275 * 18 = 40.95 \text{ g mol}^{-1}$$

$$\frac{M(\text{product})}{M(\text{product}) + M(\text{H}_2\text{O})} = \frac{210.09}{251.04} = 0.84$$

$$\% \text{ H}_2\text{O in the sample: } [\%] = 100 - 84 = \underline{16\%}$$

Table 31 Calculation of molecular water content in the aldol adduct by ¹H NMR measured in DMSO-d6

	Product [C1-H] [Integral]	DMSO-d6 [Integral]	H ₂ O [Integral]
Blank	-	24.67	59.95
Product	1	24.67	62.58

Fold amount of H₂O related to ¹H NMR integral: $\frac{H_2O(p)-H_2O(blank)}{2} = \frac{62.58-59.95}{2} = 1.32$

Molar mass of the containing H₂O: $M(H_2O) = 1.32 * 18 = 23.67 \text{ g mol}^{-1}$

$$\frac{M(product)}{M(product)+n(H_2O)} = \frac{210.09}{233.76} = 0.90$$

% H₂O of the sample: $[%] = 100-90 = 10\%$

In summary we confirmed our hypothesis, that the isolated aldol adducts typically contain one mol-equivalent (like a monohydrate) of water which is difficult or even impossible to remove completely. This issue in the biocatalytic synthesis of polyhydroxylated compounds, which affects the overall performance/outcome of the reaction, was so far neglected or underrepresented in the literature.

A IX.6.2 NMR Studies: Determination of Inorganic Components

After determination and quantification of the water content of the aldol adduct (**B₅**) we wanted to exclude other impurities like inorganic salts. Within our developed SPE purification protocol all hydrophilic compounds (e.g. DHA, buffer components, etc.) were eluted by washing the C18 material with approximately 20 column volumes of 95% water/5% MeOH.

In general, the nitrogen free resting cell media consist mainly of phosphates, which should be eluted as all other buffer components within the first minutes of the SPE purification (**Figure 72**). Due to the low but known solubility of inorganic phosphates in methanol, additional ³¹P NMR measurements were performed. We compared ³¹P NMRs of three aldol products with the ³¹P NMR of KH₂PO₄ (e.g. buffer salts (KH₂PO₄= 0 ppm) dissolved in methanol. As depicted in the following ³¹P NMR, no inorganic P-containing impurity could be detected (**Figure 73**).



Figure 73 ^{31}P NMR of different aldol adducts compared to KH_2PO_4 .

Based on the ^1H and ^{31}P NMR results, the efficiency of the SPE purification method was confirmed and compared it to previously reported literature values (**Table 32, D**). Especially, the obtained values of the SPE protocol (up to 91% isolated yield after two steps) of the corresponding aldol adducts compared to single step transformations using isolated Fsa1 A129S.

A X Pathway I-Summary

The combination of AlkJ and the Fsa1 A129S in pseudo-operon configuration with 20 equiv. DHA or HA and the optimized solid phase extraction method (SPE) afforded diastereomerically pure products (**B**_{5,I}/**B**_{5,II}-**G**_{5,I}/**G**_{5,II}) in very good yields (**Table 32, C**), compared to published literature values for single Fsa1 A129S mediated reactions (**Figure 74, Table 32, D**).

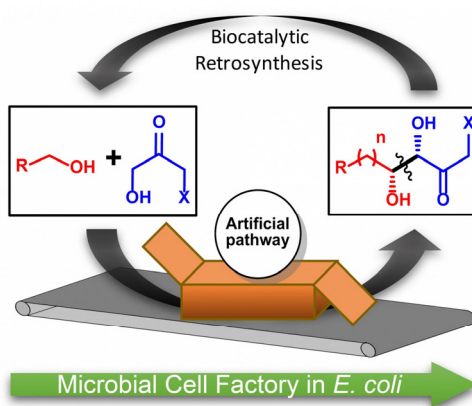
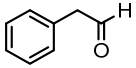
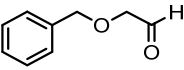
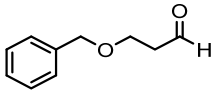
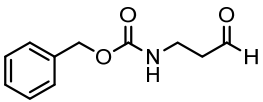


Figure 74 Illustration of the optimized Pathway I.

Table 32 Summary of isolated yields for acyclic aldol adducts, observed by all applied purification strategies.

Acceptor	Donor	Isolated Yields [%]			
		A	B	C	D (Lit. ¹⁸⁷)
 B ₃	HA	40	-	70	48
	DHA	-	28	78	46
 D ₃	HA	22	42	89	71
	DHA	-	37	60	28
 E ₃	HA	20	21	61	n.a.
	DHA	-	18	64	n.a.
 G ₃	HA	-	32	82	n.a.
	DHA	-	35	90	79

A: Extraction with an organic solvent (e.g. EtOAc); **B:** RP-HPLC; **C:** SPE protocol

¹⁸⁷ A. L. Concia, C. Lozano, J. A. Castillo, T. Parella, J. Joglar, P. Clapes, *Chem. Eur. J.* **2009**, *15*, 3808-3816.

A X.1 Pathway I-Application

Based on the Pathway I results (**A VIII.2.1** & **A IX**), a so-called “Hidden Reservoir” approach for cytotoxic aldehydes was established.¹⁸⁸ During the optimization of Pathway I, the over-oxidation of the aldehyde intermediate to the corresponding carboxylic acid was addressed as the major yield determining step for upcoming C-C bond forming reaction. In general, cytotoxic aldehydes can increase the metabolic burden of a living cell, which lead to unwanted side reactions and decreased productivity. The “Hidden Reservoir” approach was introduced to control the redox equilibrium between alcohols (**78a**), aldehydes (**79**) and carboxylic acids (**78b**) (**Figure 75**). In particular, a redox system involving two enzymes, namely an alcohol dehydrogenase (AlkJ) and carboxylic acid reductase (CAR from *Nocardia iowensis*), which is dependent on the activity of an *E. coli* phosphopantetheinyl transferase (PPTase),¹⁸⁹ were combined to protect the host organism from high, non-viable aldehyde concentrations. Moreover, the flexibility to start with either the alcohol (**78a**) or the acid (**78b**) can be beneficial concerning substrate availability.

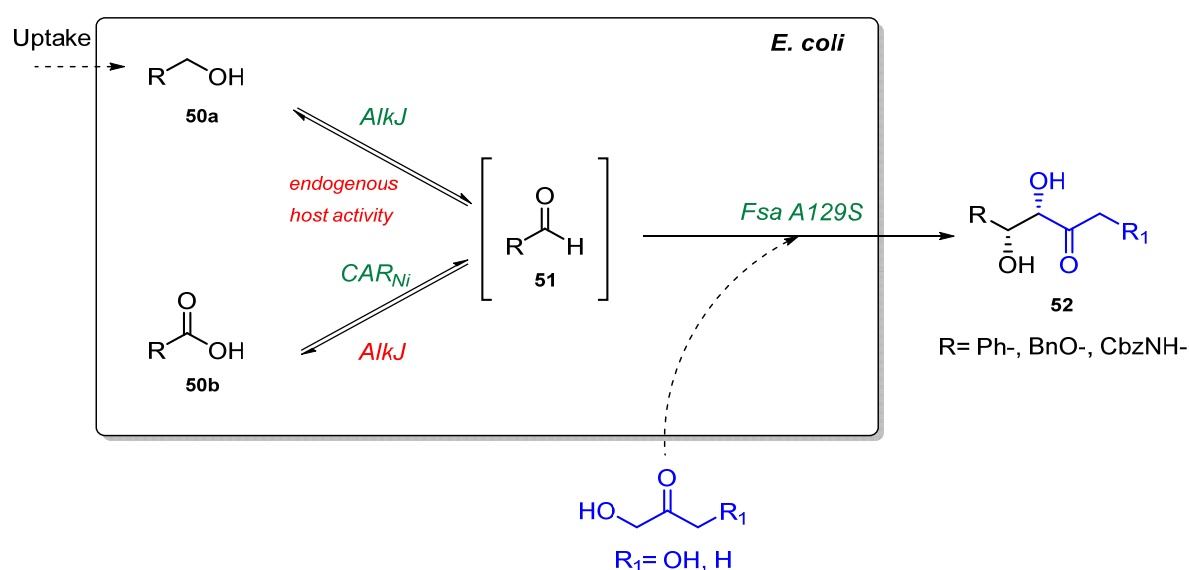


Figure 75 "Hidden Reservoir" approach for a steady, non-viable aldehyde formation in *E. coli*.

To underline the benefits of the continuous aldehyde formation, an aldolase mediated carbon-carbon bond formation in the presence of dihydroxyacetone/hydroxyacetone was performed to afford diastereomerically pure aldol adducts (**80**) in 70% yield. In contrast to Pathway I (20 equiv. donor DHA/HA), this approach gave similar results by utilizing only 5 equiv. of DHA/HA.

¹⁸⁸ T. Bayer, S. Milker, T. Wiesinger, M. Winkler, M. D. Mihovilovic, F. Rudroff, *ChemCatChem* **2017**, 2919–2923.

¹⁸⁹ K. Napora-Wijata, K. Robins, A. Osorio-Lozada, M. Winkler, *ChemCatChem* **2014**, 6, 1089-1095.

A X.2 Chemo/enzymatic Cascade for the Synthesis of Polyhydroxylated Heterocycles

Since the isolation of acyclic aldol adducts showed some issues, a “one-pot” chemo-enzymatic process was established, which is utilized with an artificial mini-pathway (**Figure 76, 1**) and a heterogeneous palladium catalyst (**Figure 76, 2**).^{190,191}

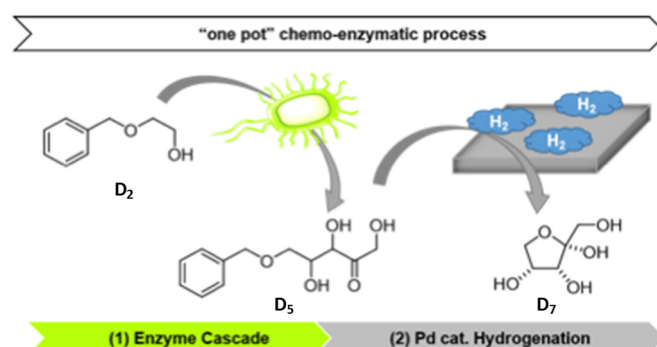


Figure 76 Illustration of a chemo-enzymatic cascade for the synthesis of polyhydroxylated heterocycles.

By coupling a single whole cell catalyst with co-expressed enzymes (AlkJ and Fsa1 S129A) and an intramolecular cyclization mediated by a metal catalyst, polyhydroxylated heterocycles can be synthesized without elaborate intermediate isolation.

The hydrogenation in minimal media was shown to be feasible by the group of Balskus, in 2014.¹⁹² The described sequence consists of a whole cell catalyst for hydrogen generation followed by a Pt catalyzed (Royer catalyst) hydrogenation without external hydrogen supply (**Figure 77**).

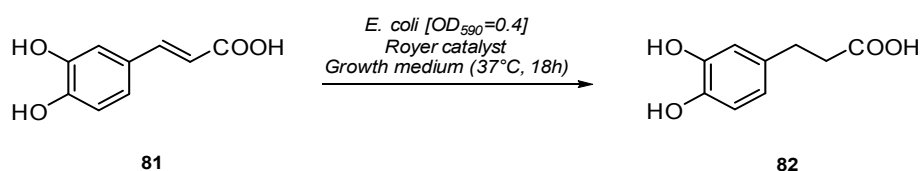


Figure 77 Hydrogenation by an optimized *E. coli* strain in minimal media.

Despite being independent of external hydrogen supply, the optimized protocol gave excellent isolated yields of 80% for their model substrates.

A X.2.1 Heterogeneous Catalyst Selection

To identify a suitable hydrogenation catalyst that leads to the cyclization of acyclic aldol compounds in an aqueous solution, different Pd catalysts (e.g. Pd/C, Pd(OH)₂/C) or PtO₂ catalyst were tested. Furthermore, this kind of metal assisted deprotection approach under different hydrogenation conditions (e.g. solvents, H₂ pressure) was performed to obtain optimized reaction parameters in

¹⁹⁰ J. Muschiol, C. Peters, N. Oberleitner, M. D. Mihovilovic, U. T. Bornscheuer, F. Rudroff, *Chem. Commun.* **2015**, 51, 5798-5811.

¹⁹¹ M. J. Fink, M. Schön, F. Rudroff, M. Schnürch, M. D. Mihovilovic, *ChemCatChem* **2013**, 5, 724-727.

¹⁹² G. Sirasani, L. Tong, E. P. Balskus, *Angew. Chem., Int. Ed.* **2014**, 53, 7785-7788.

resting cell media (M9 N-free). Because of the elaborate synthesis of acyclic aldol molecules, two model substrates 2-(benzyloxy)ethan-1-ol (**D**₂) and (benzyloxy)carbonyl)glycine (**F**₂) were used for the optimization studies. To follow the reaction progress, TLC with different staining agents were conducted, the free amino acid was visualized selectively *via* ninhydrin and for the diol detection a cerium molybdate stain was used.

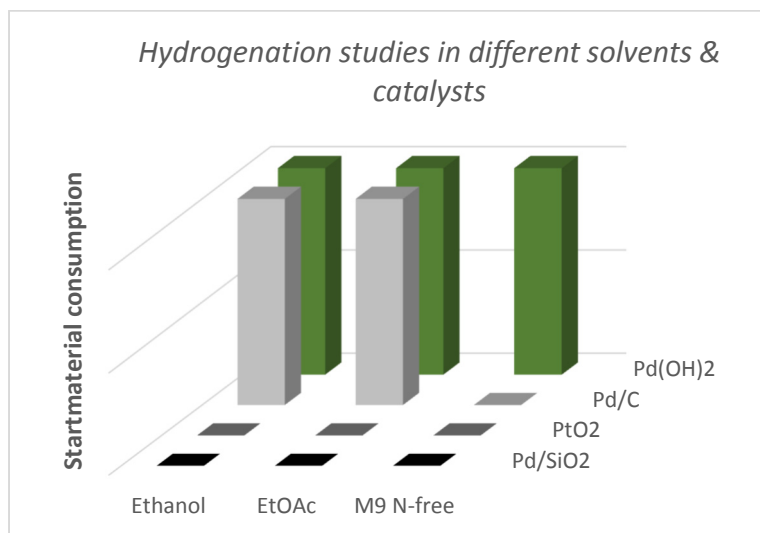


Figure 78 Summary of heterogeneous catalyst

Out of four different catalytic species (approx. 10 w% resp. substrate), the best performing catalyst Pd(OH)₂ yielded in quantitative conversion of the model substrate in organic solvents as well as in M9 media at 1 bar (H₂ balloon) (Figure 77).

We tested organic solvents and aqueous reaction media (e.g. EtOH, EtOAc, minimal media), however no remarkable influence on the reaction process was observed. Consequently, we used aqueous M9 (N-free) medium for the reduction.

The optimized hydrogenation conditions (Pd(OH)₂, M9 media, and 1 bar H₂) were applied to synthesize the cyclic target molecules starting from the corresponding acyclic aldol adducts.

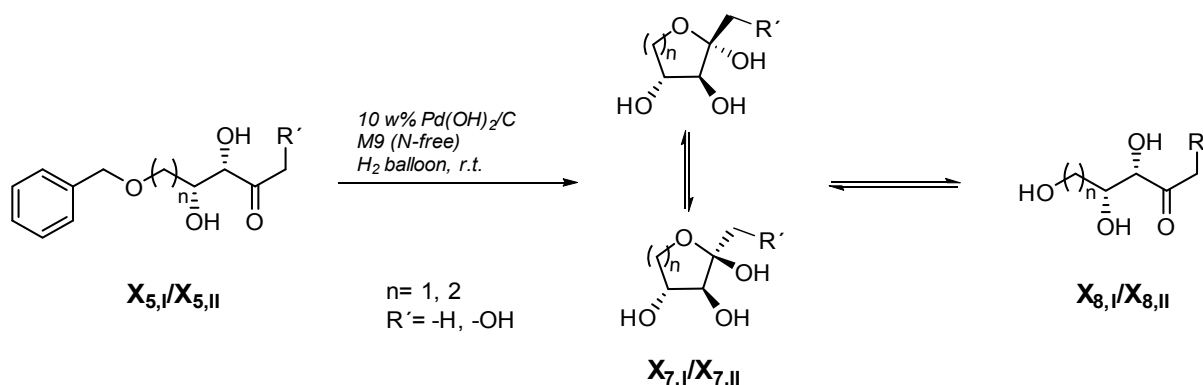


Figure 79 Pd(OH)₂/C deprotection under optimized hydrogenation conditions in M9 media.

The crude biotransformation solution, which contains mainly the acyclic aldol adducts ($X_{5,I}$ or $X_{5,II}$) were directly used for the Pd catalyzed deprotection. Therefore, the solid material was separated *via* centrifugation and the supernatant was transferred to a glass vial equipped with a H₂ balloon. The reaction progress was monitored *via* TLC and by LC/MS and after full consumption of the acyclic aldol adduct, the reaction mixture was flash filtrated through RP silica C18 with MeOH/H₂O (2:1) and gave the final product in quantitative yield, confirmed by LC/MS and NMR analysis

The interpretation of recorded spectra, however, is limited, since product exists as a mixture of three isomers (α , β and acyclic deprotected moiety). After deprotection of the benzylic group, a mixture of two cyclic isomers (α and β) and acyclic ketose product was obtained, which are in equilibrium with each other (**Figure 79**).¹⁹³

The resulting ¹H-NMR spectrum is in accordance to the literature reported shifts in the range of 3.0-4.5 ppm (3.21 & 4.77 NMR solvent), which are related to the protons of the carbon skeleton (**Figure 80**). A singlet for the CH₃ end group at 2.24 ppm is explicit to see and proves the existence of the acyclic form in the mixture. Furthermore, the lack of characteristic ¹H and ¹³C NMR signals for aromatic protons underlines the successful deprotection in an aqueous buffer. In particular, the ¹³C NMR measurement confirms the formation of the acyclic adduct, because of the significant carbonyl shift at 213.1 ppm. Similar results were observed for the deprotection of the corresponding DHA aldol product.

¹⁹³ A. L. Concia, C. Lozano, J. A. Castillo, T. Parella, J. Joglar, P. Clapes, *Chem. Eur. J.* **2009**, *15*, 3808-3816.

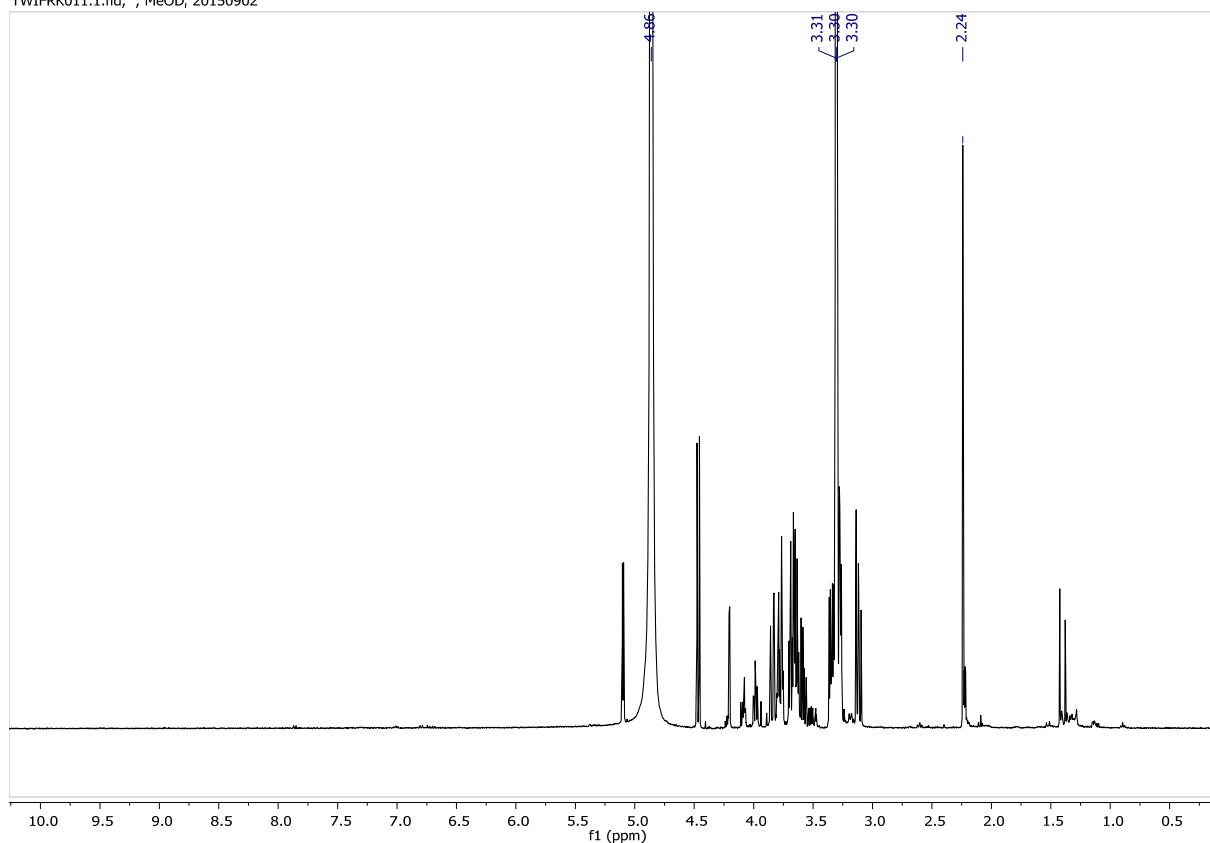


Figure 80 ^1H NMR after Pd catalyzed deprotection to (**X_{7,II}**).

Shortly after we had established the optimized reaction conditions, the group of Wang presented in their publication the *in situ* hydrogenation to the final target molecules besides the *in vivo* aldolase approach, as well.¹⁹⁴ They also showed $\text{Pd}(\text{OH})_2/\text{C}$ as a suitable catalyst for hydrogenation reactions in aqueous solutions and because of these published results, no further investigations were conducted towards the synthesis of the cyclized aldol products by a chemo-enzymatic cascade.

¹⁹⁴ M. Wei, Z. Li, T. Li, B. Wu, Y. Liu, J. Qu, X. Li, L. Li, L. Cai, P. G. Wang, *ACS Catal.* **2015**, *5*, 4060-4065.

Scope of the Thesis: Pathway II

During the second main part of this thesis, an artificial pathway was established that is directly connected to the central carbon metabolism of the host organism *E. coli*. Since AlkJ was shown as a suitable enzyme for the oxidation of primary alcohols (X_2) to the corresponding aldol acceptor aldehydes (X_3) in Pathway I, this enzyme was again implemented. Subsequently, the intercellular formed aldehyde and the glycolytic intermediate DHAP (**Figure 81**, green part) are linked in an enzyme mediated asymmetric aldol reaction to synthesize three of the four possible diastereoisomerically pure diol intermediates (X_6) (**Figure 81**).

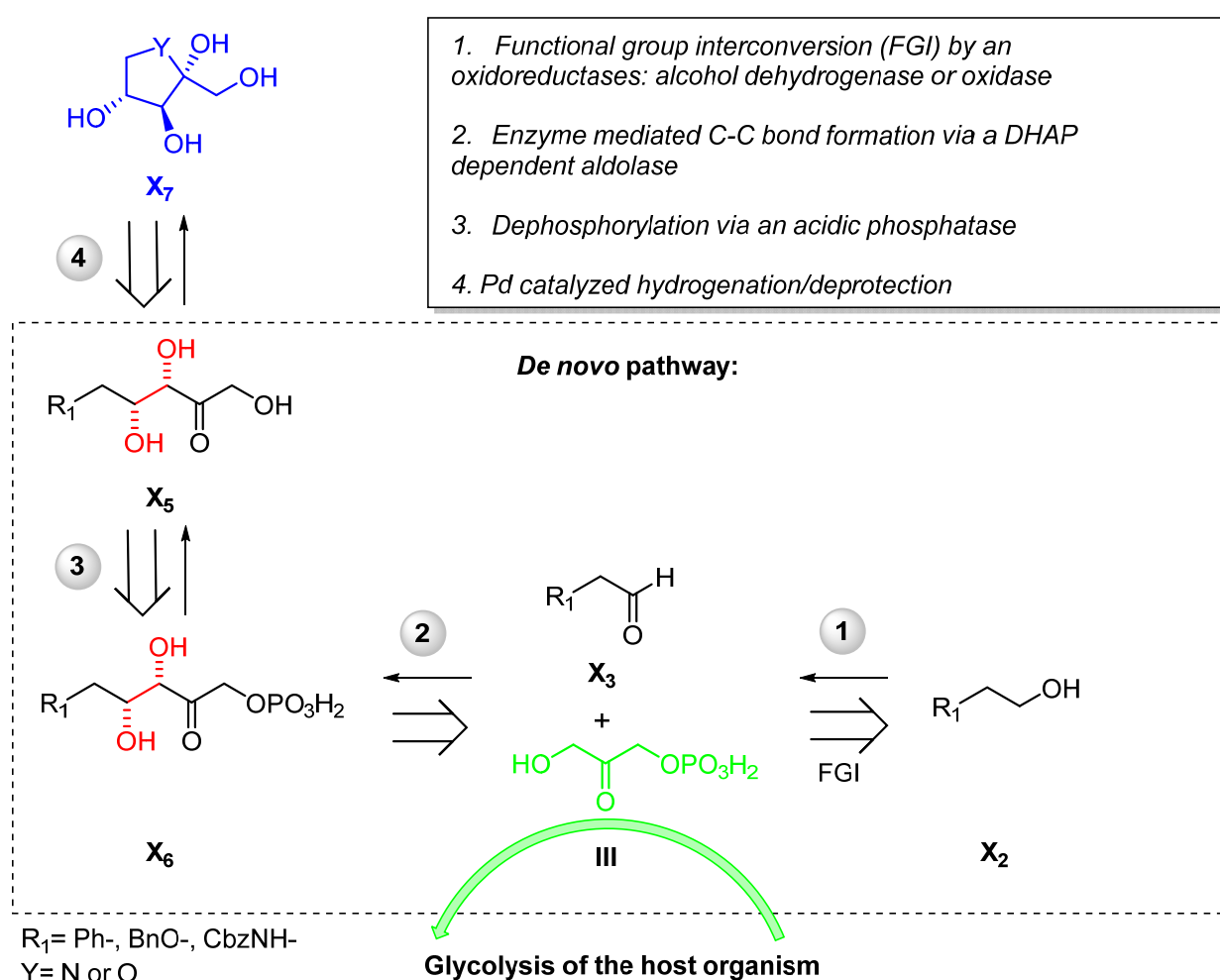


Figure 81 Overview of the biocatalytic retrosynthesis of Pathway II.

In general, charged molecules are not able to pass the lipophilic cell membrane, the cascade is completed by the cleavage of the phosphate group *via* an acidic phosphatase (X_5), which additionally shifts the reaction equilibrium towards the desired product. In contrast to Pathway I, which was focused on the donor promiscuity, the stereoselective C-C coupling *via* DHAP depending aldolases

(FucA, FruA, and RhuA, TagA was not available for this studies) constitutes the key step of Pathway II (**Figure 82**, blue marked structures). To control the stereochemical properties of the aldol adducts (**83-86**), in detail the orientation of the 1,2-diol motif, the choice of the appropriate enzyme is the key to access the different stereoisomers (**Figure 82**).

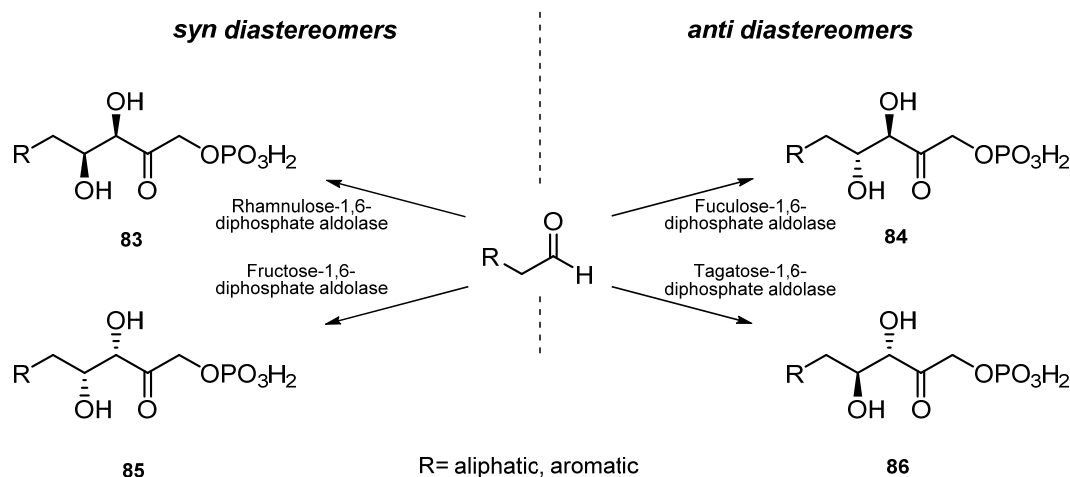


Figure 82 Four DHAP dependent aldolases and stereochemical properties.

In contrast to fructose-1,6-diphosphate and rhamnulose-1,6-diphosphate, which exclusively provide the *syn* diastereomer, tagatose-1,6-diphosphate and fucose-1,6-diphosphate aldolase gave the corresponding *anti*-orientated 1,2-diols.

A XI Introduction-DHAP Dependent Aldolases

In nature, aldolases are involved in metabolic and catabolic transformations of carbohydrates such as the C-C bond cleavage at the 1,2-diol junction that link the aldol donor (**III**) and acceptor (**88**) (**Figure 83**).

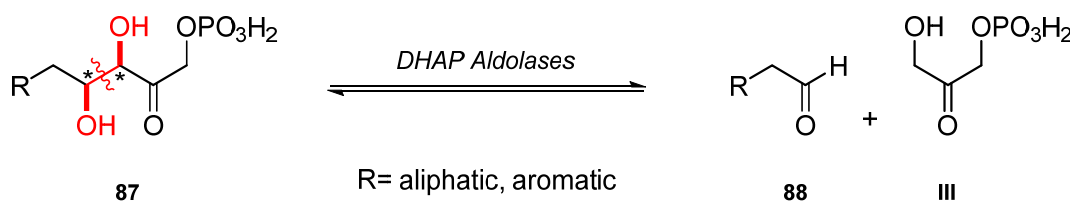


Figure 83 C-C bond formation or cleavage by DHAP dependent aldolase.

A prominent example is the metabolic breakdown of glucose, the formed fructose-1,6-bisphosphate (**89**) is irreversibly cleaved by fructose-1,6-bisphosphate aldolase into two triose phosphate moieties, namely glyceraldehyde (GAP, **90**) and DHAP (**III**) (**Figure 84**). Metabolic pathways are enzyme-mediated biochemical reactions that lead to biosynthesis (anabolism) or breakdown (catabolism) of natural product to small molecules within a cell. The glycolysis and Krebs cycle metabolic pathways, in aerobic respiration, produce precursors of various important cellular molecules such as the primary metabolite

ATP. Additionally, during the glycolysis, pyruvate (**91**), the end product, as well as the intermediate DHAP are potential donor molecules for C-C bond forming reactions and would be provided by the host organism under optimized *in vivo* conditions.¹⁹⁵

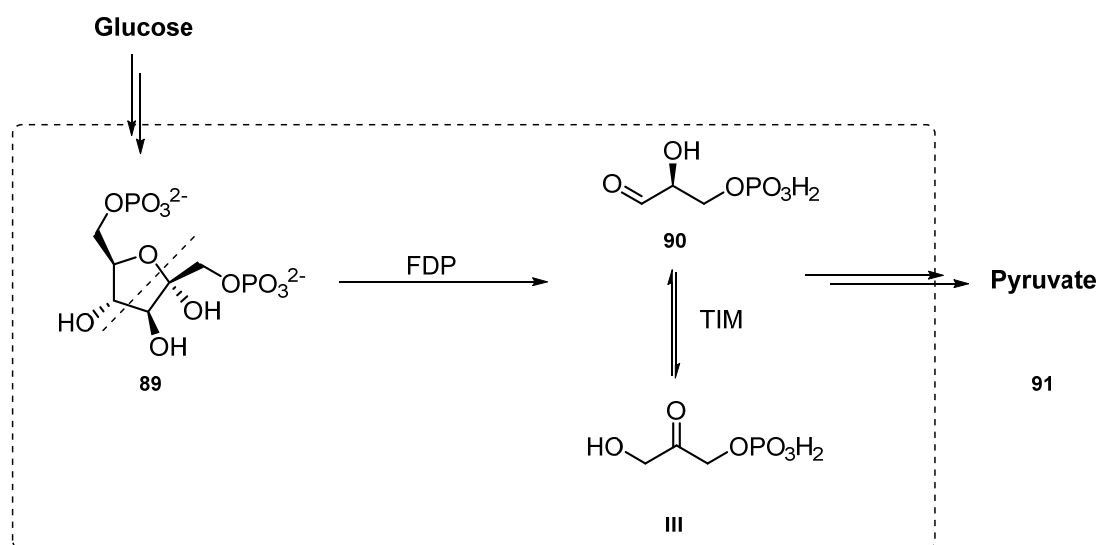


Figure 84 Shortcut of the glycolysis. GAP and DHAP generation by Fructose-1,6-bisphosphate aldolase (FDP) and triose phosphate isomerase (TIM).

Until now, artificial pathways were often designed because of the beneficial cofactor supply and efficient cofactor recycling by the host organism, in addition to facile production of all required biocatalysts in their native environment within the cell. Next step for such cell factories was the connection of a heterologous pathway with a metabolic pathway tapping into the carbon-balance of the cell.¹⁹⁶

This strategy will be an alternative to known synthetic or *in vitro* enzymatic procedures (e.g. DHAP dependent aldolases) due to the generation of DHAP by simply feeding glucose to the engineered organism. An easier downstream processing of such an *in vivo* pathway can be advantageous compared to the *in vitro* cascade, starting from bulk chemical glycerol.

Over the last decades, several groups investigated DHAP dependent aldolases to synthesize stereochemically pure rare sugar molecules. In asymmetric synthesis DHAP dependent aldolases are very interesting because of the high level of stereocontrol at positions C3 and C4, but a major drawback are the required large quantities of DHAP (aldol nucleophile) to shift the reaction equilibrium towards the formation of a new C-C bond.^{197,198,199} This natural donor molecule, DHAP, is in isolated form (Mg, Na salt) expensive and instable in aqueous solutions ($t \sim 20\text{h}$ at pH 7).²⁰⁰ Typically, aldolases are very

¹⁹⁵ A. M. Kunjapur, Y. Tarasova, K. L. J. Prather, *JACS* **2014**, *136*, 11644-11654.

¹⁹⁶ M. H. Wei, Z. J. Li, T. H. Li, B. L. Wu, Y. P. Liu, J. Y. Qu, X. Li, L. Li, L. Cai, P. G. Wang, *ACS Catal.* **2015**, *5*, 4060-4065.

¹⁹⁷ K. Fesko, M. Gruber-Khadjawi, *ChemCatChem* **2013**, *5*, 1248-1272.

¹⁹⁸ N. G. Schmidt, E. Eger, W. Kroutil, *ACS Catal.* **2016**, *6*, 4286-4311.

¹⁹⁹ T. Bayer, S. Milker, T. Wiesinger, M. Winkler, M. D. Mihovilovic, F. Rudroff, *ChemCatChem* **2017**, 2919-2923.

²⁰⁰ K. Faber, *Biotransformations in organic chemistry*, Springer-Verlag, **2011**.

specific to the donor molecules (DHAP/DHA) but operate with a broad range of acceptors (unhindered aliphatic and protected alkoxy or amino aldehydes (Bn, Cbz, CF₃, etc.)).²⁰¹

Alternative strategies to eliminate the requirement of DHAP were established: (i) by engineering enzymes with a broad donor scope (e.g. DHA/HA dependent aldolases)²⁰² or (ii) by development of synthetic DHAP protocols.²⁰³ Synthetic protocols are mainly struggling with the low stability of intermediates and consequently these routes are focused to prepare storable precursor molecules. Many of these precursors consist of protected DHAP dimers, which were generated during multistep synthetic routes. The most common methodology was presented by Jung *et al.* and is described in detail in section A XI.2. Chemical phosphorylation of protected-dihydroxyacetone, a stable (long-term storage at -20°C) precursor molecule, provides DHAP in large quantities.

In order to avoid time consuming and atom inefficient protecting and deprotecting steps, and elaborate purification of labile intermediates, enzymatic protocols for the generation of DHAP (III) were developed (Figure 85).

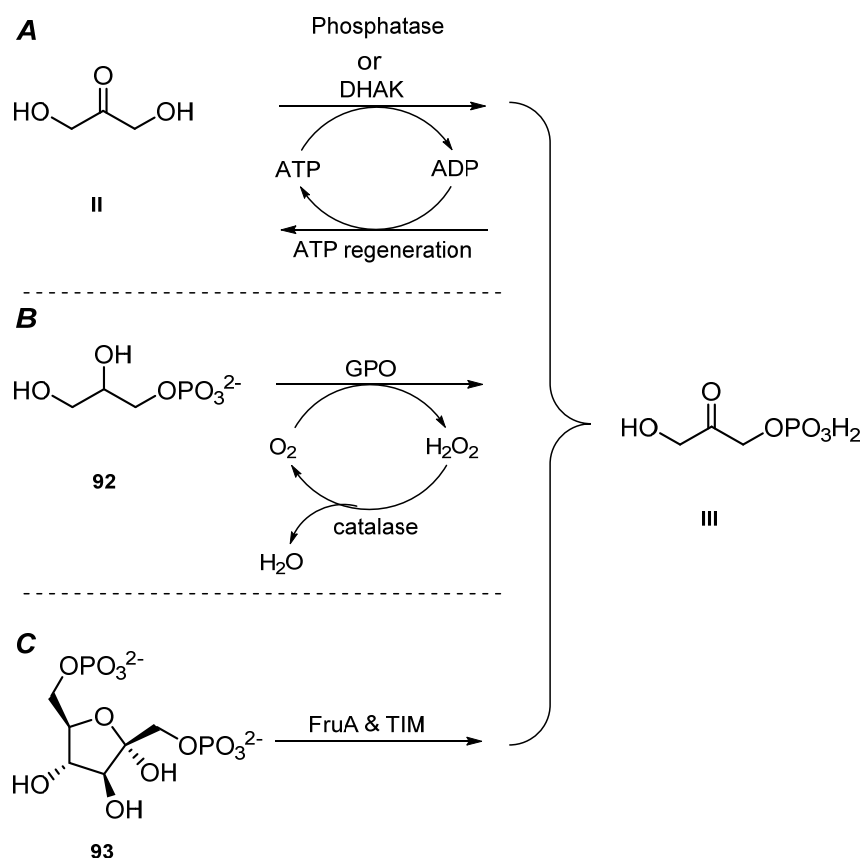


Figure 85 Enzyme mediated strategies for the synthesis of DHAP.

In Figure 85, three enzyme mediated strategies are displayed: (A) phosphorylation of DHA by a phosphatase or dihydroxyacetone kinase (DHAK, ATP dependent); (B) oxidation of glycerol-3-

²⁰¹ M. D. Bednarski, E. S. Simon, N. Bischofberger, W. D. Fessner, M. J. Kim, W. Lees, T. Saito, H. Waldmann, G. M. Whitesides, *JACS* **1989**, *111*, 627-635.

²⁰² D. Güclü, A. Szekrenyi, X. Garrabou, M. Kickstein, S. Junker, P. Clapés, W.-D. Fessner, *ACS Catal.* **2016**, *6*, 1848-1852.

²⁰³ S.-H. Jung, J.-H. Jeong, P. Miller, C.-H. Wong, *J. Org. Chem.* **1994**, *59*, 7182-7184.

phosphate (**92**) and (**C**) cleavage and isomerization of fructose-1,6-bisphosphate (FDP) *via* FDP aldolase and triose phosphate isomerase (TIM) (**Figure 85**).

In a four enzyme cascade approach, the strategies (**A**) and (**B**) were combined to provide DHAP from glycerol, followed by a *in situ* aldol reaction *via* a Fructose-1,6-bisphosphate aldolase from rabbit muscle aldolase (RAMA) and dephosphorylation by the same phosphatase (Phon-Sf from *Shigella flexneri*), which is used in the first step for the phosphorylation of the aldol donor molecule (**Figure 86**).²⁰⁴

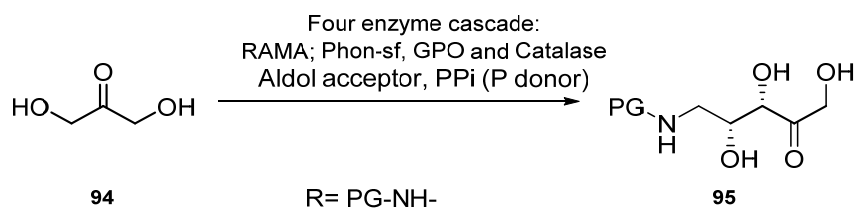


Figure 86 *In vitro* cascade consisting of a phosphorylation and dephosphorylation step, catalyzed by Phon-Sf.

The presented enzymes as well as reaction conditions we have selected as template for our Pathway II design and all observed results will be discussed in the upcoming sections.

²⁰⁴ L. Babich, L. J. C. van Hemert, A. Bury, A. F. Hartog, P. Falcicchio, J. van der Oost, T. van Herk, R. Wever, F. P. J. T. Rutjes, *Green Chem.* **2011**, *13*, 2895-2900.

A XI.1 Synthesis of DHAP

In order to synthesize DHAP (**III**), different strategies were available, which are mainly using the DHA dimer for all required transformations (**Figure 87**). The development of synthetic protocols was used for the generation of larger amounts of DHAP (**III**), which was mandatory for *in vitro* optimization as well as preparative scale biotransformations utilizing DHAP dependent aldolases.²⁰⁵

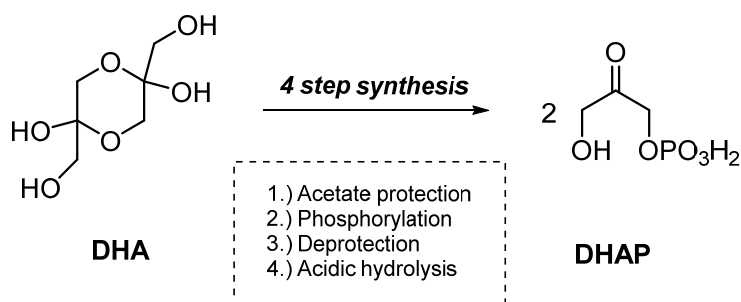


Figure 87 Synthetic strategy for the synthesis of DHAP starting from DHA dimer.

A well working synthesis towards dihydroxyacetone phosphate (DHAP) was established by Jung *et al.*²⁰⁶ This four-step synthesis is starting from the commercially available dihydroxyacetone dimer (DHA). After acetal protection, phosphorylation of the free primary alcohol afforded fully protected phosphorylated **DHAP₂** dimer. Subsequently, a PtO₂ catalyzed phenyl-deprotection under hydrogenation conditions is applied. Finally, acidic hydrolysis afforded the final product **DHAP** monomer in an aqueous stock solution.

A XI.1.1 Protection of the Acetate Position of DHA Dimer

At first, the protection of dihydroxyacetone dimer (**DHA**) to the corresponding diethyl acetal (**DHAP₁**) *via* triethyl orthoformate in presence of *p*TsOH in anhydrous EtOH proceeded slowly.²⁰⁷ The major challenge was to avoid the cleavage of the DHA dimer during the synthetic procedure due to low DHA dimer stability in water. To minimize side reaction activity (e.g. monomerization), the reaction was carried out at low temperatures (0°C) under argon atmosphere and in anhydrous EtOH (**Figure 88**).

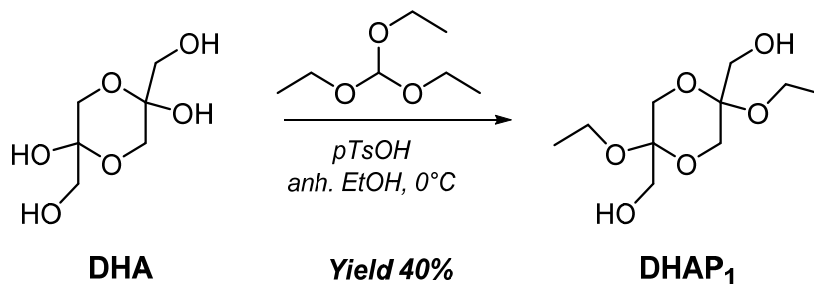


Figure 88 Acetal protection of DHA dimer using triethyl-orthoformate under acidic conditions.

²⁰⁵ S.-H. Jung, J.-H. Jeong, P. Miller, C.-H. Wong, *J. Org. Chem.* **1994**, *59*, 7182-7184.

²⁰⁶ S.-H. Jung, J.-H. Jeong, P. Miller, C.-H. Wong, *J. Org. Chem.* **1994**, *59*, 7182-7184.

²⁰⁷ A. N. Zelikin, D. Putnam, *Macromolecules* **2005**, *38*, 5532-5537.

Full consumption of starting material was observed after reaction times of around 48 h and **DHAP₁** was isolated in 40% yield after trituration (EtOAc and heptane) and recrystallization in EtOAc. Noteworthy, recrystallization proceeded with almost full recovery in moderate yield of 75 % (Lit. 74 %).²⁰²

A XI.1.2 Phosphorylation of the Primary Alcohol of Protected DHA Dimer

In order to introduce phosphorus groups at the free primary alcohols of **DHAP₁**, diphenyl phosphoryl chloride was added slowly to a mixture of **DHAP₁** dissolved in anhydrous pyridine under ice bath cooling (**Figure 89**).

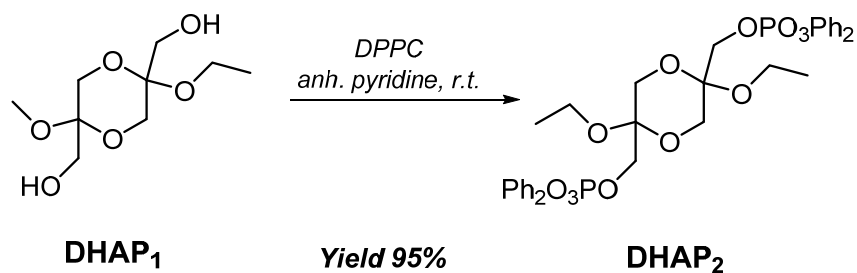


Figure 89 Phosphorylation of acetal protected DHA dimer.

Diphenyl-phosphorylation of 1,3-dihydroxyacetone diethyl acetal (**DHAP₂**) proceeded without the formation of byproducts, according to TLC (PE:EtOAc 1:5; $R_f=0.87$) in excellent yields (>95%; Lit: 96%).²⁰⁸ However, complete removal of pyridine proved to be a tedious task, requiring extensive washing with 2 N HCl and *n*-heptane followed by extended freeze-drying and lyophilization overnight. The extraction protocol was repeated until ¹H NMR showed no residual pyridine. According to NMR analysis, the isolated colorless powder **DHAP₂** exists as a mixture of *syn* and *anti* isomers.

A XI.1.3 Phenyl-deprotection of Phosphorylated DHA Dimer

The third reaction step, a Pt catalyzed hydrogenation was performed in the high-pressure PARR apparatus (**Figure 90**).

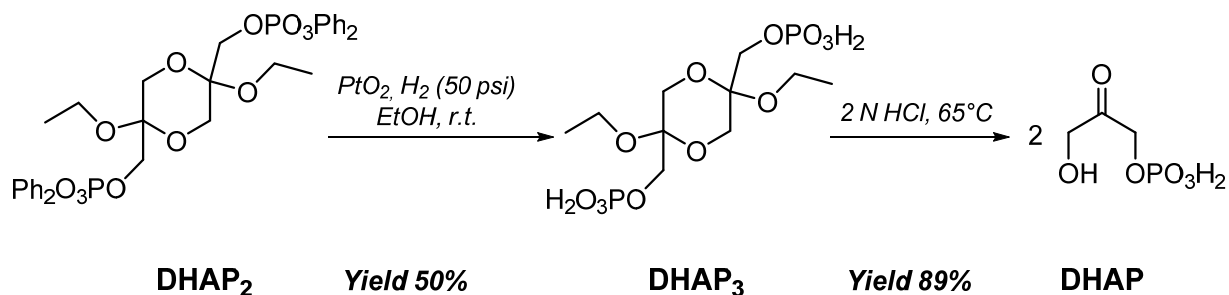


Figure 90 Phenyl-deprotection by PtO₂ catalyzed hydrogenation and acidic hydrolysis for the generation of a DHAP stock solution.

²⁰⁸ S.-H. Jung, J.-H. Jeong, P. Miller, C.-H. Wong, *J. Org. Chem.* **1994**, *59*, 7182-7184.

Therefore, **DHAP**₂ was dissolved in anhydrous EtOH and PtO₂ (10 w%) was added in a high pressure flask equipped with an additional stirring bar. Hydrogenation was performed at 50 psi H₂ pressure and room temperature overnight. After full conversion monitored by TLC (CH₂Cl₂/MeOH/DIPE/AcOH 4:1:1:0.3) and ¹H NMR (aliquot was concentrated and dissolved in CDCl₃), the catalyst was removed *via* flash filtration through Celite and the organic solvent was removed under high vacuum to isolate pure **DHAP**₃ in 50% yield (Lit: not isolated, *in situ* dimer cleavage).²⁰⁹

It was particularly important that pyridine, a known catalyst poison for heterogeneous catalysis, from the phosphorylation step, was removed by acidic extraction as well as trituration with *n*-heptane as described for **DHAP**₂. Low impurities of **DHAP**₂ led to inefficient phenyl deprotection and the reaction had to be performed a second time by first filtration and then addition of new PtO₂.

A XI.1.4 Acidic Hydrolysis of DHAP Dimer

Finally, **DHAP**₃ was dissolved in water and acidified by 2 N HCl to pH 1 (**Figure 90**). The acidic hydrolysis was accomplished in a closed 8 mL reaction vial at 65°C for 5 h. After RP-TLC (MeOH: H₂O 3:1; R_f= 0.95) indicates full starting material consumption, the obtained brownish solution was cooled to room temperature, pH was adjusted to 4 and the obtained DHAP stock solution was stored at -20°C. The final concentration of the DHAP stock solution was determined *via* LC-MS/MS and yielded in a 0.42 M solution (89%).

²⁰⁹ S.-H. Jung, J.-H. Jeong, P. Miller, C.-H. Wong, *J. Org. Chem.* **1994**, *59*, 7182-7184.

A I DHAP dependent Aldolase: C-C Bond Forming Reactions in Asymmetric Synthesis

Already in 1989, pioneering work for DHAP dependent aldolases in asymmetric synthesis was published by the group of Whitesides.²¹⁰ In this landmark contribution, the first highly efficient and stereoselective C-C formation catalyzed by Fructose-1,6-bisphosphate aldolase from rabbit muscle aldolase (RAMA) was reported for a broad range of aldol acceptor molecules (up to 30 aldehydes). Since stereoselectivity and activity of these enzymes can differ, particularly by the use of non-natural substrates, studies to evaluate the effect of the reaction conditions and substrates were reported.^{211,212,213}

In general, the stability of DHAP is a known issue, because under reactions conditions, DHAP, can undergo oxidative dephosphorylation rendering inorganic phosphate and methylglyoxal, both are strong inhibitors of DHAP dependent aldolases. Sometimes the aldolase itself is responsible for the DHAP degradation. General aspects and experiential key issues of DHAP dependent aldolase for synthetic applications are summarized (**Table 33**).²¹⁴

Table 33 Summary of important experiential parameters of DHAP dependent aldolases, especially RAMA.

DHAP stability	<ul style="list-style-type: none">• Decomposition in water, limiting reagent (1.7 equiv.)
Buffer	<ul style="list-style-type: none">• Mixed water/organic solvent solutions to circumvent DHAP degradation
Organic solvents	<ul style="list-style-type: none">• 20% v/v cosolvent (DMF, DMSO), to ensure solubility of aldol acceptor
Yield/ Stereoselectivity	<ul style="list-style-type: none">• Low temperature enhances yield/selectivity (<i>dr</i>) [%]• Enzyme purity is crucial
Purification	Take advantage of the charged phosphate group: <ul style="list-style-type: none">• Precipitation (e.g. barium salt)• Ion-exchange chromatography

For initial studies to identify optimal reaction conditions, purchased RAMA cell powder was used for the C-C bond formation of DHAP and phenylacetaldehyde (**B₃**). In general, the isolation and purification of phosphorylated aldol adducts is completely underrepresented, especially with respect to NMR

²¹⁰ M. D. Bednarski, E. S. Simon, N. Bischofberger, W. D. Fessner, M. J. Kim, W. Lees, T. Saito, H. Waldmann, G. M. Whitesides, *JACS* **1989**, *111*, 627-635.

²¹¹ T. Suau, G. Álvaro, M. D. Benaiges, J. López-Santín, *Biotechnol. Bioeng.* **2006**, *93*, 48-55.

²¹² R. Schoevaart, F. van Rantwijk, R. A. Sheldon, *Biotechnol. Bioeng.* **2000**, *70*, 349-352.

²¹³ G. Labbe, S. de Groot, T. Rasmusson, G. Milojevic, G. I. Dmitrienko, J. G. Guillemette, *Protein expression and purification* **2011**, *80*, 224-233.

²¹⁴ M. D. Bednarski, E. S. Simon, N. Bischofberger, W. D. Fessner, M. J. Kim, W. Lees, T. Saito, H. Waldmann, G. M. Whitesides, *JACS* **1989**, *111*, 627-635.

analysis. With regards to that, purified RAMA lyophilizates were used for the synthesis of the corresponding target compounds according to literature known and well-established reaction conditions.²¹⁵ Initially, the RAMA activity was determined by a photometric assay utilizing the natural substrate Fructose 1,6-bisphosphate (F-1,6-BP) as well as several preliminary solvents studies were performed due to the low aldehyde solubility in water, which depicts a fundamental problem for enzyme mediated aldol reactions.

A 1.1 Photometric Activity Assay for Fructose-1,6-bisphosphate Aldolases

In the case of fructose-1,6-bisphosphate aldolases (FruA) and purified RAMA cell powder, an easy to apply activity assay was performed according to a literature known procedure (**Figure 91**). During this coupled photometric assay, the NADH consumption for the reduction of DHAP to the corresponding 1,2-diol was monitored at 340 nm. All stock solutions were prepared as described (**Table 34**).²¹⁶

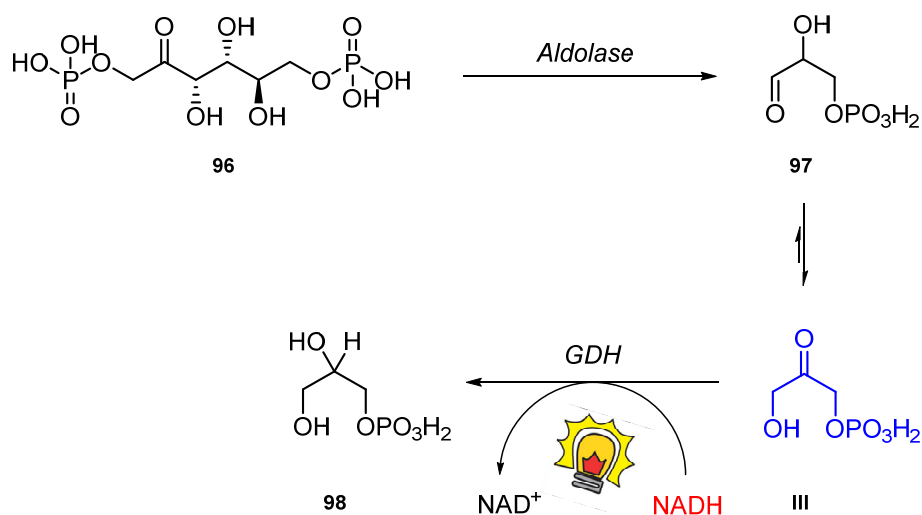


Figure 91 Photometric activity assay for Fructose-1,6-bisphosphate aldolases by determination of NADH consumption.

Table 34 Activity assay setup for Fructose-1,6-bisphosphate aldolase

Conditions
T= 25°C, pH= 7.4, A 340 nm, Light path= 1 cm
Solution A
100 mM Tris HCl Buffer, pH 7.4. (Prepare 250 μL in dionized water (dH ₂ O) using Trizma Base adjust to pH 7.4 with 1 N HCl.)
Solution B
58 mM Fructose 1,6-Diphosphate Solution (Prepare 1 mL in dH ₂ O using D-Fructose-1,6-diphosphate, Tetra(cyclohexylammonium) salt)
Solution C
4.0 mM β-Nicotinamide adenine dinucleotide, reduced Form Solution (β-NADH) (Prepare 2 mL in cold dH ₂ O β-Nicotinamide adenine dinucleotide, reduced Form, disodium salt).
Solution D

²¹⁵ M. D. Bednarski, E. S. Simon, N. Bischofberger, W. D. Fessner, M. J. Kim, W. Lees, T. Saito, H. Waldmann, G. M. Whitesides, *JACS* **1989**, *111*, 627-635.

²¹⁶ http://www.sigmaaldrich.com/content/dam/sigma-aldrich/docs/Sigma/General_Information/2/aldolase.pdf

α -Glycerophosphate dehydrogenase (GDH)/Triosephosphate isomerase enzyme (TPI) solution (α -GDH/TPI); (Immediately before use, a solution containing 50 α -GDH U/mL of α -Glycerophosphate Dehydrogenase/Triosephosphate isomerase was prepared in cold dH₂O.)

Solution E

Aldolase enzyme solution (Immediately before use, prepare a solution containing 0.25- 0.5 U/mL of RAMA in cold reagent A.

The assay was performed at 25°C and 340 nm in 1 mL cuvettes, adding the freshly prepared solutions in the given order (**Table 35**).

Table 35 Procedure for Fructose-1,6-bisphosphate aldolase activity assays

		Final volume [μ L]
A	Buffer	866.6
B	F-1,6-BP	33.3
C	NADH	33.3
D	GDH/TPI	33.3
E	RAMA	33.3

Immediately after the addition of the aldolase solution (**E**) to a solution mixture **A-D** (blank signal), the NADH consumption was recorded at 340 nm *via* absorbance decrease for some minutes (**Figure 92**).

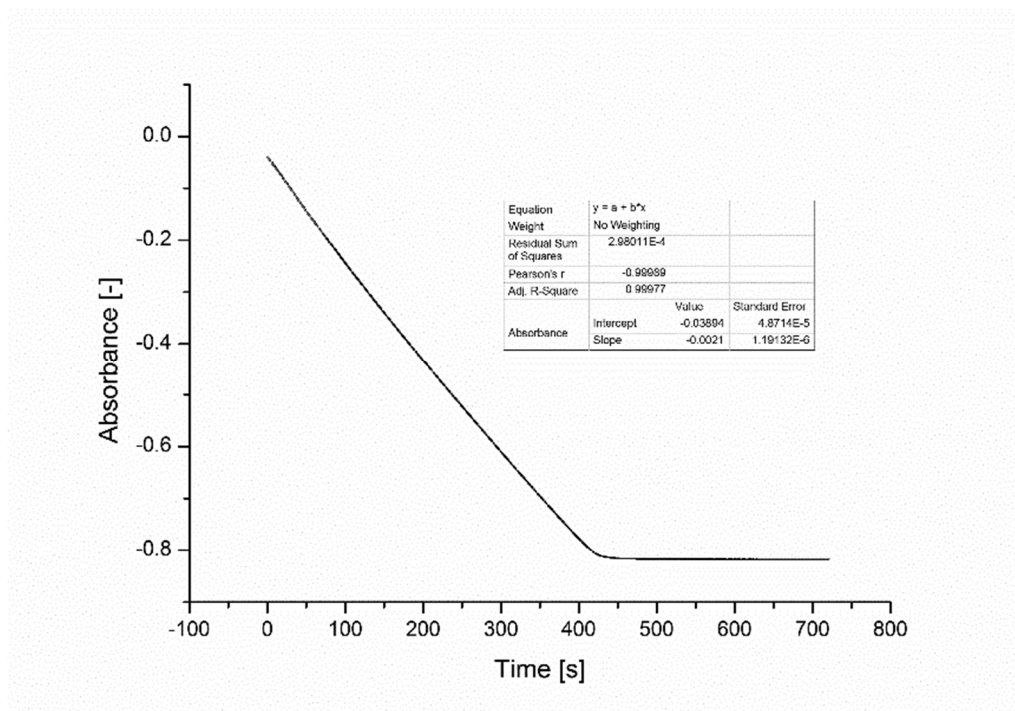


Figure 92 NADH consumption monitored at 340 nm over time for the C-C bond cleavage activity assay of FucA.

For calculation of the aldolase activity (U/mL) the following formula was used:

$$\frac{U}{\text{ml}} \text{ enzyme} = \frac{r(\text{Abs}) * 1 * \text{df}}{2 * 6.22 * 0.033}$$

1 = Total volume (in mL) of assay

df = 30

2 = 2 moles of β -NADH converted to 2 moles of β -NAD⁺ per mole of Fructose 1,6-Diphosphate

6.22 = Millimolar extinction coefficient of β -NADH at 340 nm

0.033 = Volume (in mL) of enzyme used

To exclude rate determining effects and related deviations of RAMA activity, different GDH/TPI concentrations were applied. Activity assay results for purchased RAMA powder gave around 37% activity in comparison to reported supplier data due to lack of cooling during shipping.

The same assay was performed for cell free extract of FruA (0.8 mg/mL or 24 mg/mL), and F-1,6-BP (natural substrate) was converted within seconds to the DHAP and GAP, based on NADH consumption. Additionally, the control experiment using *E. coli* BL21 (DE3) cell free extract did not show any NADH consumption.

A 1.2 Organic Solvent Studies for DHAP Aldolases

In addition to aldolases being classified due to their donor specificity (DHAP, DHA, etc.), they can be subdivided into microbial metal-dependent Class II or mammalian Class I enzymes. In comparison to class I, prokaryotic class II showed significantly higher stability at high temperatures and in the presence of organic solvents as well as activity towards non-natural substrates.²¹⁷ For this organic solvent stability studies, Schoevaart *et al.* have applied four different microbial class II aldolases, which were subcloned into the *E. coli* vector pT7-7 and expressed. The activity of purified aldolases and purchased RAMA was determined by the previously described photometric NADH assay. Therefore, several solvents (e.g. DMF, DMSO, acetone, *t*-butanol, acetonitrile) in various concentrations were assayed and concerning to enzyme stability, the best results for RAMA were obtained with 50% v/v DMSO, 40% DMF or 20% acetonitrile.²¹⁸

Since preliminary experiments with DMSO and DMF have interfered the product purification and isolation during Pathway I, the therefore better suited acetonitrile was tested with our model substrate (**B₃**). Beneficially, acetonitrile was working perfectly for Pathway I or more precisely for AlkJ mediated

²¹⁷ R. Schoevaart, F. van Rantwijk, R. A. Sheldon, *Biotechnol. Bioeng.* **2000**, *70*, 349-352.

²¹⁸ G. Labbe, S. de Groot, T. Rasmussen, G. Milojevic, G. I. Dmitrienko, J. G. Guillemette, *Protein expression and purification* **2011**, *80*, 224-233.

alcohol oxidations, which is also crucial for Pathway II. The introduction of AlkJ will solve the mentioned aldehyde solubility issues and non-cytotoxic primary alcohols will serve as starting materials.

To evaluate the product formation rate using analytical techniques, experiments were carried out in glass vials ($V_r = 625.5 \mu\text{L}$). Besides DMF, the most commonly used organic solvent for RAMA mediated reactions,²¹⁹ DMSO and acetonitrile were tested (**Figure 93, Table 36**). All reactions were performed in biological duplicates in glass vials at 25°C and 250 rpm overnight with 20% v/v organic solvent.

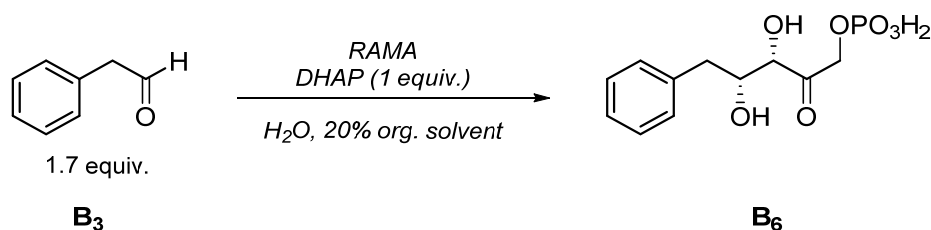


Figure 93 RAMA catalyzed C-C coupling reaction of phenylacetaldehyde (**B₃**) and DHAP.

Table 36 Reaction conditions for RAMA catalyzed C-C coupling reaction applied for solvent suitability studies.

Reaction mixture	Eq.	Final concentration
DHAP (pH 6.9) in dH ₂ O	1.0	0.06 mmol
Phenylacetaldehyde in organic solvent	1.7	0.1 mmol
RAMA (74 U/mL)		7 U/mL

RAMA cell powder was rehydrated in dH₂O and added to an aqueous DHAP solution (pH 6.9). Next, an aldehyde stock solution (in DMF, DMSO, MeCN: 20% final concentration) was added in portions and a cloudy solution was obtained. The reaction was vigorously shaken overnight and the reaction progress was monitored *via* RP-TLC (MeOH: H₂O/ 66:33) after 0.5, 1.5, 6, and 20 h.

After 20 h the product formation was indicated for the reactions in DMF and acetonitrile, which fits to the desired product concerning the $R_f = 0.75$ in comparison to DHAP ($R_f = 0.95$) and the aldehyde ($R_f = 0.2$) on RP material. Additionally, to confirm the product formation, LC/MS measurements were performed and in SIM negative mode, a peak correlating to the desired phosphorylated compound was obtained (m/z 289). Interestingly, DMSO did not give any product formation according to RP-TLC and LC/MS.

To clarify the obtained results on analytical base and to isolate the corresponding phosphorylated aldol adduct, preparative scale experiments yielding the DHAP adduct of **B₃** mediated by RAMA were accomplished.

²¹⁹ P. Clapés, X. Garrabou, *Adv. Synth. Catal.* **2011**, 353, 2263-2283.

A I.2.1 Synthesis of (3*S*,4*R*)-1,3,4-trihydroxy-5-phenylpentan-2-one phosphate Mediated by RAMA Lyophilizates

To demonstrate the applicability of these optimized reaction settings for the isolation of phosphorylated aldol adducts, the aldol reaction was carried out with substrate **B₃** (20% v/v DMF or acetonitrile) and RAMA as catalyst in a preparative scale experiment (**Figure 93**).

RAMA cell powder was rehydrated and the activity was determined prior to use by the described activity assay. The purification of phosphorylated aldol adducts is a major issue for low isolated yields for such type of transformations. One of the most promising methods is the precipitation of the phosphorylated compound as the corresponding barium salt.^{220,221} To verify this method, initial studies were accomplished for the purification of hydroxyacetonephosphate (**HAP**) and described in detail in section **A III.2.3**.

The pH of 4.0 mL DHAP stock solution was adjusted to 6.9 and the DMF- or acetonitrile-aldehyde mixture was added to the aqueous DHAP solution in 100 μ L portion under intensively shaking.

Biotransformations were performed in 15 mL Greiner tubes at 25°C and 250 rpm in an orbital shaker. The reaction progress was followed by LC/MS and RP-TLC (MeOH/H₂O 3:1). After 4 h, the biotransformation was stopped at -80°C and after centrifugation of solid material, a barium precipitation protocol for the isolation of the phosphorylated aldol adduct was applied. Therefore, 2.5 equiv. BaCl₂ 2*H₂O were added to the pH 6.5 adjusted reaction mixture. After addition of BaCl₂, a cloudy solution was immediately obtained and precipitated material was collected by centrifugation. This solid material was dissolved in water with 2% 2 N HCl and confirmed by RP-TLC MeOH:H₂O (3:1). In contrast to the described literature protocol, the precipitation process showed a significant deviation. According to published protocols,²²² the addition of ethanol should initiate the product precipitation by shifting the solubility equilibrium. In our case, the presence of 20% DMF seems to affect the solubility and the product precipitates immediately by the addition of BaCl₂. To ensure full product recovery from the supernatant, additional BaCl₂ (0.5 equiv.) and two reaction volumes of ethanol were added until no product was remaining in the solution according to RP-TLC. After 18 h at 4°C, the solid material was collected by centrifugation (14000 rpm x 15 min), washed with cold ethanol and dried under high *vacuo* for several hours. The obtained colorless powder was dissolved in 700 μ L water with 10 μ L DCl and analyzed by ¹H NMR and ³¹P NMR.

The NMR data were in good agreement with expected shifts, in detail, the CH₂ next to the phosphate group was shifted to the low field. Additionally, the *J*_{H-31} coupling constant of 7.9 Hz was recorded in

²²⁰ I. Sánchez-Moreno, V. Hélaïne, N. Poupard, F. Charmantray, B. Légeret, L. Hecquet, E. García-Junceda, R. Wohlgemuth, C. Guérard-Hélaïne, M. Lemaire, *Adv. Synth. Catal.* **2012**, *354*, 1725-1730.

²²¹ M. D. Bednarski, E. S. Simon, N. Bischofberger, W. D. Fessner, M. J. Kim, W. Lees, T. Saito, H. Waldmann, G. M. Whitesides, *JACS* **1989**, *111*, 627-635.

²²² V. Hélaïne, R. Mahdi, G. V. Sudhir Babu, V. de Bernardinis, R. Wohlgemuth, M. Lemaire, C. Guérard-Hélaïne, *Adv. Synth. Catal.* **2015**, *357*, 1703-1708.

the expected range for such compounds.²²³ Besides some interferences during the BaCl₂ precipitation protocol, around 35% DMF are remaining in the obtained barium aldol product. To reduce this amount, 20 mg of Ba-aldol material was dissolved in 700 μL D₂O and 35 μL DCl (5%). The aqueous solution was extracted three times with 350 μL dichloromethane-d₂ and one time with hexane. The dichloromethane-d₂ and the aqueous layer were directly analyzed *via* ¹H NMR and a reduced amount of DMF of approx. 60% (35 to 10%) was obtained, in comparison to the non-extracted material. Additional extraction attempts slightly reduced the DMF, but DMF was still present.

Consequently, 20% v/v acetonitrile was investigated for preparative biotransformations to synthesize (3*S*,4*R*)-1,3,4-trihydroxy-5-phenylpentan-2-one phosphate by RAMA lyophilizates.

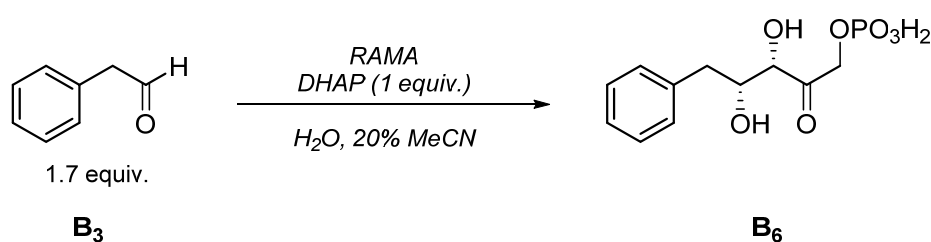


Figure 94 RAMA catalyzed C-C coupling reaction of phenylacetaldehyde (B₃) and DHAP.

All reagents were prepared in defined stock solutions and mixed in an 8 mL reaction vial in the following order ($V_R = 4.0$ mL):

The reaction was stirred vigorously at room temperature until full consumption of DHAP monitored by RP-TLC (MeOH:H₂O/1:1). After apparent completion, the mixture was frozen at -80°C in order to stop the reaction and solid biotransformation residues were separated by centrifugation after thawing (13000 rpm, 5 min, 4°C). The supernatant was transferred into a 50 mL Greiner tube and the desired product was isolated by the described barium purification protocol. For that purpose, the pH of the solution was adjusted to 6.5 and 2.5 equiv. of BaCl₂*2H₂O were added to precipitate the phosphorylated aldol adduct as the corresponding barium salt. After 1 h of cooling at -20°C still no product precipitation was visible thus additional 7.5 equiv. of BaCl₂*2H₂O were added together with 20 mL of ethanol and the mixture was cooled at -20°C overnight. The colorless precipitate formed was isolated by centrifugation and washed with CH₂Cl₂ and the obtained crystalline product was dried under high *vacuo* for several hours. Interestingly, NMR analysis of the desired product indicated the presence of DHAP and the corresponding hydrate.

To improve the product purity, some adaptations of the described protocol were performed: The DHAP solution was added in four portions within 4 hours. After an additional hour, the reaction progress was monitored *via* RP-TLC and since it was not completed, 5 U/mL of RAMA was added. After vigorously

²²³ C. Stanetty, M. Walter, P. Kosma, *J. Org. Chem.* **2014**, *79*, 582-598.

shaking overnight, still DHAP residues were indicated by RP-TLC, additional 5 U/mL RAMA and 7 mg (0.5 equiv.) of phenylacetaldehyde (**B**₃) in 75 μ L MeCN were added and stirred until full DHAP consumption was obtained. Finally, the phosphorylated aldol target compound was isolated as the corresponding barium salt and the colorless powder was dissolved in D₂O and DCl for NMR analysis (**Figure 95**).

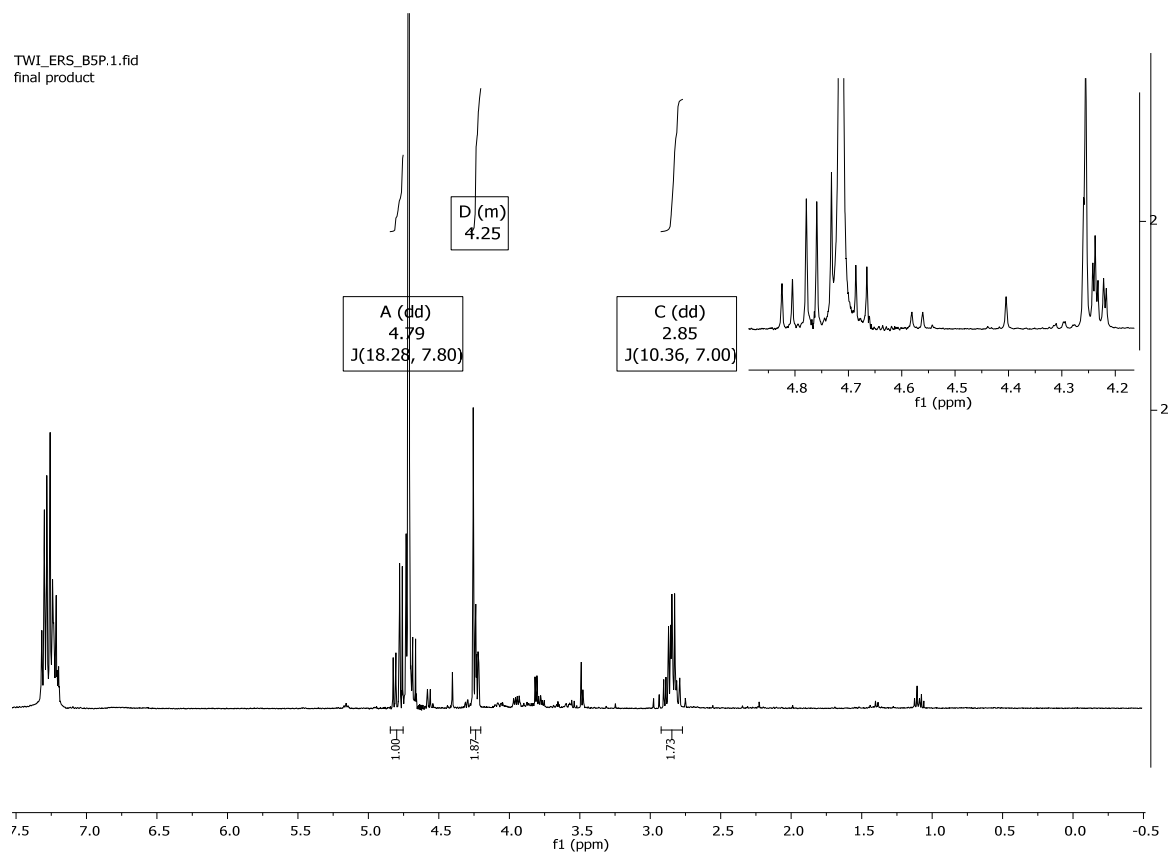


Figure 95 ¹H NMR of pure (*3S*, *4R*)-1,3,4-trihydroxy-5-phenylpentan-2-one phosphate after purification by barium precipitation.

In **Figure 95**, the ¹H NMR of the desired phosphorylated aldol product (**B**₆) is depicted. At 4.74 ppm the characteristic phosphate coupling (m, $J = 7.8$ Hz, 2H) to the attached CH₂ group, also confirmed by ³¹P NMR (**Figure 96**), was obtained. Besides the triplet for the phosphoester, inorganic phosphate at 0 ppm was present in the sample. The formation of the phosphoester -CH₂OPO₃H₂ was also clarified by a ¹H-³¹P HMBC experiment.

TW1_ERS_BSP.2.fid
final product

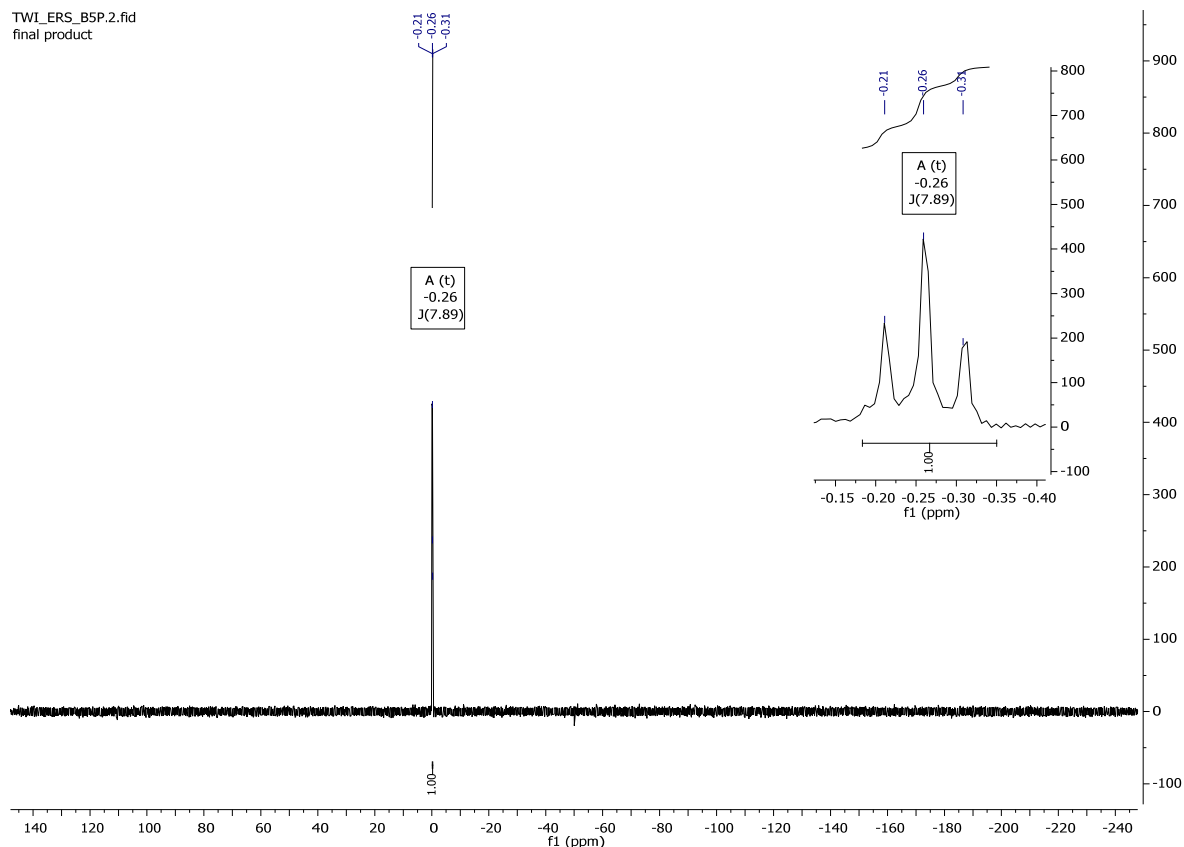


Figure 96 ^{31}P NMR of pure (3*S*, 4*R*)-1,3,4-trihydroxy-5-phenylpentan-2-one phosphate after purification by barium precipitation.

As mentioned above, the low stability of polyhydroxylated compounds (Pathway I) and DHAP depicts a major issue, similar behavior was expected for related phosphorylated aldol compound (**B₆**). To verify the stability under basic and acidic conditions, stability experiments of **B₆** at different pH values were conducted and monitored by ^1H and ^{31}P NMR. Therefore, a NMR sample was split into two parts and the pH of one was adjusted by NaOD until neutral conditions were reached. Both mixtures were dried at high *vacuo* and the received colorless powder was dissolved again in D_2O and DCI without detectable degradation (^1H and ^{31}P NMR) of the phosphorylated aldol product.

A II C-C Bond Forming Reactions mediated by FucA, FruA and RhuA

For the isolation of the related *syn* and *anti* diastereomers catalyzed by FucA, FruA, and RhuA, the optimized reaction conditions, which were established for the RAMA mediated transformations (e.g. 20% acetonitrile, pH 6.9 of the DHAP stock solution), were applied.

For the determination of active DHAP dependent aldolases (FucA, FruA, RhuA), experiments on an analytical scale were conducted and the product formation was monitored by RP-TLC and LC/MS (**Figure 97**). Additionally, these experiments were performed to get information of the stereochemical purity of the aldol adduct (**Figure 97, B₅'**) and about unselective dephosphorylation by *E. coli* BL21(DE3) background activity (**Figure 97, B₅**). Therefore, the same substrates as in Pathway I (**B₃, D₃, E₃, G₃**) and DHAP under the optimized RAMA reaction conditions were investigated. Therefore, cell free extracts of the three in-house available aldolase were prepared and the expression control was verified *via* SDS PAGE (FucA (25 kDa), FruA (36 kDa), and RhuA (30 kDa)) for insoluble and soluble fractions, respectively. Cell lysis was performed by sonication and the soluble fraction was separated *via* centrifugation.

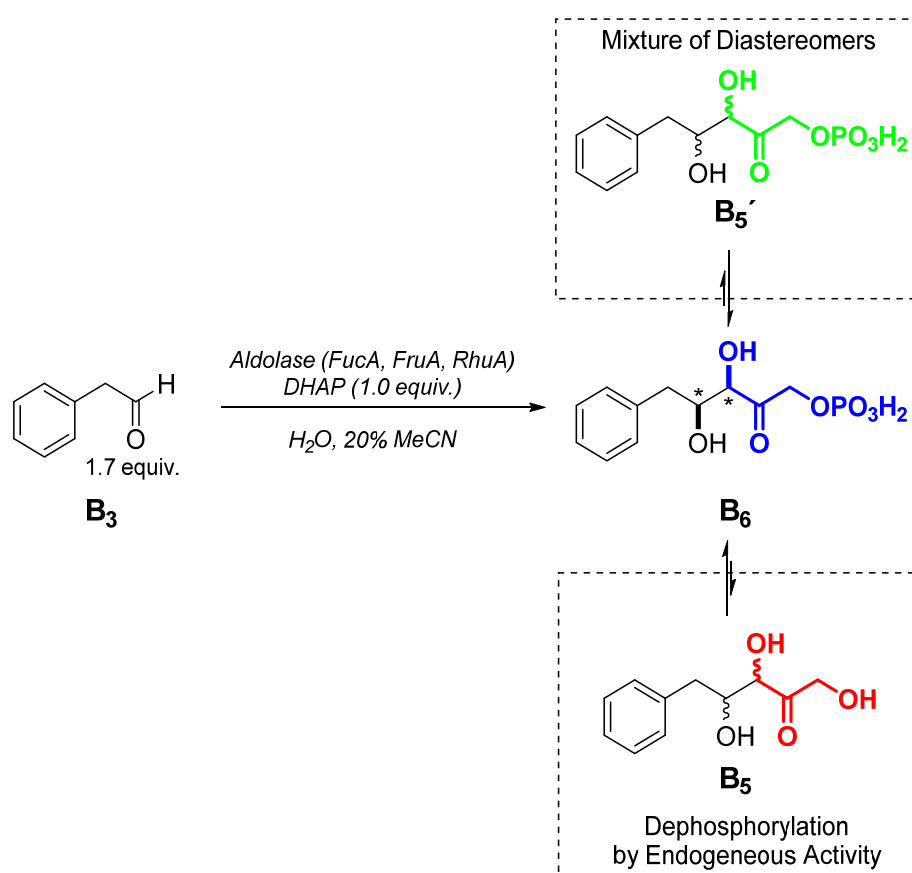


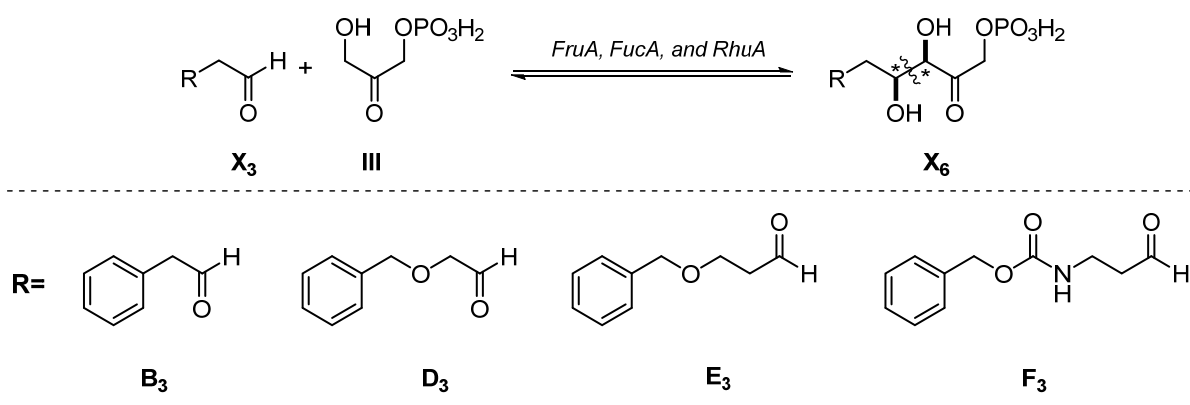
Figure 97 Selective studies of cell free extracts (FucA, FruA, and RhuA) for the formation of phosphorylated aldol adducts to determine dephosphorylation activity.

Previously prepared **B**_{5,II} (see Pathway I) and **B**₆ mediated by RAMA lyophilizates and purified via BaCl₂ precipitation have served as reference material for the FucA, FruA, and RhuA catalyzed transformations. In Table 39, all reagents and amounts are given, the ratio H₂O to CFE correlates to the enzyme concentration, which was determined by Bradford analysis.

Table 37 Reaction conditions for DHAP dependent aldolase for selective C-C coupling between phenylacetaldehyde (B**₃) and DHAP (analytical scale; V_r= 625.5 μL).**

Reaction mixture	Eq.	Final concentration
DHAP (pH 6.9) (110 mg/mL)	1.0	0.03 mmol
Aldehyde in MeCN	1.7	0.05 mmol
FruA, FucA, RhuA or BL21 (DE3)		5 mg/mL
H ₂ O		

To a solution of CFE, H₂O, and DHAP stock solution (pH 6.9), 250 μL of phenylacetaldehyde in acetonitrile was added in 5 portions. The observed, cloudy reaction mixture was shaken at 25°C overnight and the C-C bond formation was monitored *via* RP-TLC and LC/MS towards the formation of phosphorylated ([M- H⁻] *m/z* 289) or dephosphorylated aldol adducts ([M-Na] *m/z* 233) (**Figure 98**).



Aldol Acceptor Molecules				
Aldolases	B ₃	D ₃	E ₃	F ₃
FruA		1		
FucA	1	1	1	2
RhuA	1	1	2	2

No conversion of the aldol acceptor
 Only phosphorylated aldol adduct
 Mixture of phosphorylated/dephosphorylated

Figure 98 Substrate promiscuity and phosphorylation/dephosphorylation activity of DHAP dependent aldolases towards the model substrates **B**₃, **D**₃, **E**₃, and **F**₃.

The established standard conditions were applied to all our model substrates and the obtained results are given in Figure 98. Besides the formation of phosphorylated aldol adducts, LC/MS and RP-TLC measurements were conducted to detect unselective dephosphorylation by background activity of used aldolase CFE's. During these screenings, FucA and RhuA showed exclusively the formation of the phosphorylated compound without dephosphorylation to the undesired **B_{5,II}**. Interestingly, FruA showed no C-C bond forming activity within 24 h as well as no endogenous host activity (BL21 (DE3)) towards our standard substrate was obtained.

As depicted in Figure 98, FucA and RhuA are active enzymes for a C-C coupling between our aldehyde library compounds and DHAP. Interestingly, increased chain lengths in the acceptor molecules (**E₃**, **G₃**) resulted in mixtures of phosphorylated to non-phosphorylated aldol adduct.

A II.1 Preparative Scale Biotransformation Using Cell Free Extract of DHAP Dependent Aldolases

To demonstrate the C-C bond forming activity under the established conditions, preparative scale experiments of phenyl acetataldehyde (**B₃**) with cell free extracts of DHAP dependent aldolases were accomplished in 5.0 mL reaction scale. Since FruA showed no activity during initial substrate screenings at all, FucA and RhuA were used for the synthesis of the corresponding diastereomers. The reaction was performed in 8 mL reaction vials and initiated by the addition of the aldol acceptor aldehyde. After RP-TLC indicated full DHAP consumption ($R_f = 0.95$), the reaction was stopped at -80°C and the previously described barium precipitation protocol was applied. Therefore, the solid material was separated by centrifugation, the supernatant was transferred to another Greiner tube. The pH of the reaction solution was adjusted to 6.5 and immediately after the addition of 250 mg $\text{BaCl}_2 \cdot 2\text{H}_2\text{O}$ (2.5 equiv.) and 15 mL of ethanol, a cloudy solution was obtained. Finally, after storage at -20°C overnight, the solid material was collected by centrifugation and washed with cold H_2O /ethanol (1/3) and two times with cold acetone. After lyophilization for several hours, the obtained colorless powder was dissolved for NMR analysis in D_2O and 5% DCl.

These experiments, using cell free extract of FucA and RhuA demonstrated that the described barium precipitation protocol for phosphorylated material in presence of buffer salts and *E. coli* background is limited. Besides the known ^1H NMR pattern for protons at position C3 and C4, massive impurities that are most likely related to cell free extract residues were observed. When not using purified aldolases, barium precipitation leads to the concomitant precipitation of phosphorylated or charged cellular components, which cannot be separated from the desired aldol products. In the literature, mainly purified FucA and RhuA enzyme preparations are reported, purified for example by immobilized metal ion affinity chromatography (IMAC) followed by ammonium sulfate precipitation for storage reasons.

Since our FucA and RhuA are not tagged (e.g. His tag) and the precipitation protocol of phosphorylated aldol adducts led to mixtures of product and biotransformation residues, an alternative strategy had to be investigated. With regards to Pathway I, an optimized SPE protocol may overcome the described purification issues. In order to identify optimal retention conditions of phosphorylated aldol adducts on RP material, several solvent combinations of water, methanol or acetonitrile, and dichloromethane were applied. Different mixtures of water, methanol, acetonitrile gave no retention for the phosphorylated material on RP material ($R_f = 0.9$) and a controlled elution of the compound was not possible by using different quantities of organic solvent. Only higher amounts of acetonitrile showed some effect but in this case, a massive tailing over the whole RP-plate ($R_f \sim 0.1-0.3$) due to low solubility of phosphorylated material was observed. Based on these results, purification of phosphorylated aldol adducts by the developed SPE protocol was not possible. Due to strong interactions of charged molecules and silica gel, isolation of these compounds is very uncommon and difficult to achieve. The observed R_f values for **B**_{5,11} and **B**₆ with dichloromethane/methanol mixtures underlines that results. In summary, purification of phosphorylated aldol adducts mediated by cell free extracts of DHAP dependent aldolases is limited because of (i) BaCl₂ precipitation is not selective in presence of biotransformation material and (ii) running behavior on RP and silica gel.

Alternatively, an *in vitro* cascade assembly, containing a DHAP dependent aldolase and an acidic phosphatase to furnish the dephosphorylated products in a one-pot fashion would solve these isolation problems (**Figure 99**). Moreover, analytical data are presented for the dephosphorylated analogs.^{224,225}

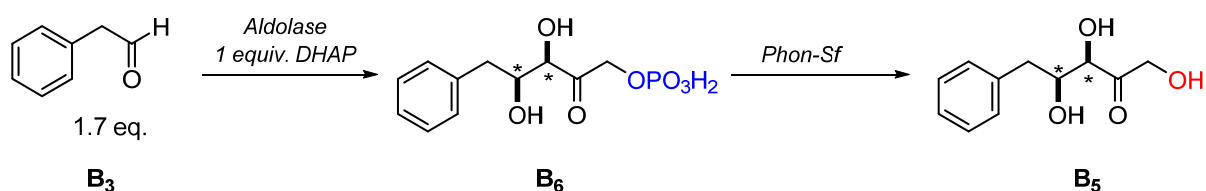


Figure 99 Synthetic strategy for the identification of aldol diastereomers (*syn/anti*) catalyzed by FucA or RhuA.

²²⁴ I. Oroz-Guinea, K. Hernández, F. Camps Bres, C. Guérard-Hélaine, M. Lemaire, P. Clapés, E. García-Junceda, *Adv. Synth. Catal.* **2015**, 357, 1951-1960.

²²⁵ L. Iturrate, I. Sanchez-Moreno, E. G. Doyaguez, E. Garcia-Junceda, *Chem. Commun.* **2009**, 1721-1723.

A III Chemical Route to Phosphorylated Aldol Adducts

Until now, fully characterized phosphorylated aldol compounds are not reported in the literature. To confirm the enzyme mediated aldol reaction to the desired product, a chemical route was established. Therefore, the optimized Pathway I protocol (POP construct, SPE purification) was performed in several fermentation scale experiments to isolate **B_{5,II}** in sufficient amounts for upcoming chemical transformations.

A III.1 Chemical Route I-Phosphorylated Aldol Compound

In order to suppress phosphorylation of the 1,2-diol moiety, a selective acetonide protection was envisioned, first (**Figure 100**). Next, phosphorylation by the established protocol during the DHAP synthesis, followed by global deprotection under acidic conditions (acetonide cleavage) as well as phenyl deprotection under hydrogenation conditions mediated by PtO₂ was planned to afford the phosphorylated target aldol adduct (**B_{6,chem.}**).

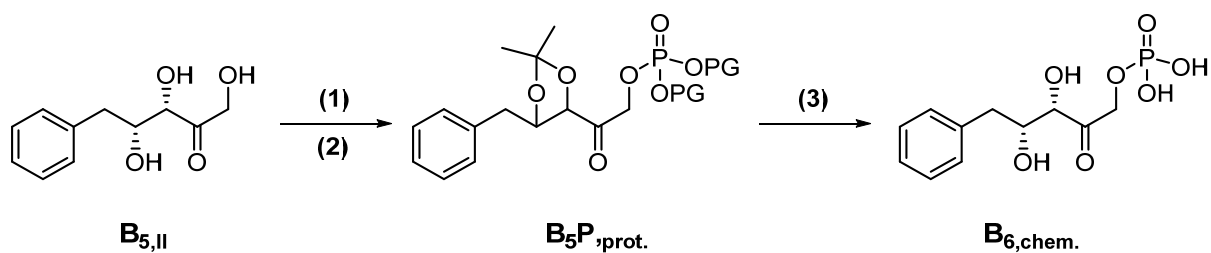


Figure 100 Envisioned chemical route I for the synthesis of (3*S*,4*R*)-1,3,4-trihydroxy-5-phenylpentan-2-one phosphate containing (1) acetonide protection, (2) phosphorylation of the free primary alcohol (3) Deprotection step to the final product.

A III.1.1 Acetonide Protection-Methoxypropane to Protect 1,2-diols

To avoid byproduct formation during the first protecting step of the 1,2-diols, especially in the presence of 1,3-diols, methoxypropane under acidic catalysis (*pTsOH*) was used to synthesize the corresponding acetonide (**Figure 101**). Another approach using acetone in the presence of ZnI did not lead to the acetonide protected compound within several days of stirring and additional amounts of ZnI.

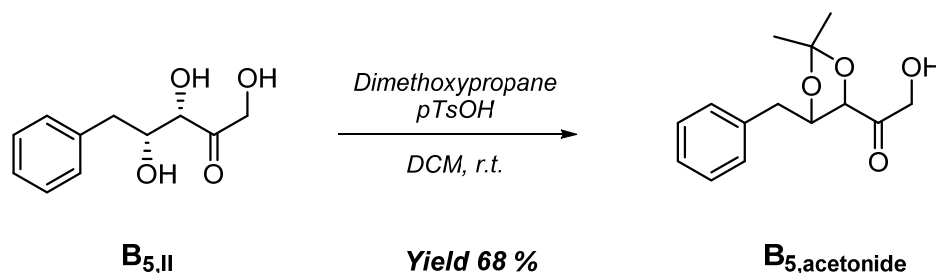


Figure 101 Acetonide protection of **B_{5,II}** by using methoxypropane under acidic conditions.

The aldol compound (**B_{5,II}**) (1 equiv.) was acetonide protected by using methoxypropane with 5 mol% of *p*toluolsulfonic acid and after extractive work-up, the pure product (**B_{5,acetonide}**) was obtained in moderate yields of around 68%.

A III.1.2 Phosphorylation with Diphenyl-phosphorylchloride

As previously described for the synthesis of DHAP, diphenyl phosphoryl chloride (DPPC) in anhydrous pyridine can be used for phosphorylation of free primary alcohols (**Figure 102**).

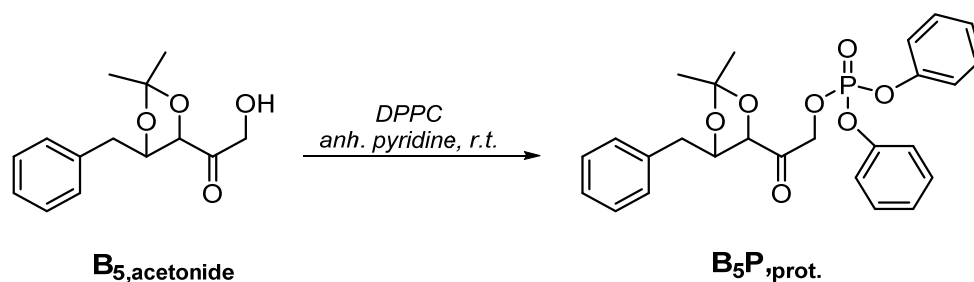


Figure 102 Phosphorylation of acetonide protected **B_{5,II}** with DPPC to the fully protected phosphorylated aldol adduct.

In a 8 mL flame-dried reaction vial, 5 mg of **B_{5,acetonide}** (1 equiv.) were dissolved in 100 μ L $\text{CH}_2\text{Cl}_2\text{-d}_2$ and anhydrous pyridine (3 equiv.), followed by the dropwise addition of DPPC (3 equiv.) at 4°C. After the final addition of DPPC, the ice bath was removed and the reaction progress was monitored by NMR. After 24 hours of stirring at room temperature, the formation of **B_{5P,prot.}** was indicated by an AB coupling pattern with related phosphorous coupling in the ^1H NMR (δ 5.04 ppm). After full starting material consumption, the excess of phosphorylation agent was quenched by addition of methanol- d_4 . But also, careful handling during the workup or storage at -80°C led to partial to complete dephosphorylation, indicated by the missing AB pattern at 5.04 ppm in the proton NMR. To overcome these bottlenecks, another phosphorylation methodology was selected and implemented to the chemical route II.

A III.2 Chemical Route II-Phosphorylated Aldol Compound

The first synthetic strategy was limited due to the low stability of the diphenyl protected phosphorylated aldol intermediate. Even under mild conditions (concentration at 30°C), storage at -80°C, or during work up, partial to complete decomposition occurred. Alternatively, a phosphorylation protocol using dibenzyl *N,N*-diisopropylaminophosphoramidite, which was presented by Stanetty *et al.* for the synthesis of 4-O-phosphorylated heptoside derivatives was investigated (**Figure 103**).²²⁶ All other protection/deprotection steps were planned as described for chemical route I, except the benzyl deprotection (Pd/C and H₂ balloon) would not require high pressure equipment (50 psi H₂) and PtO₂.

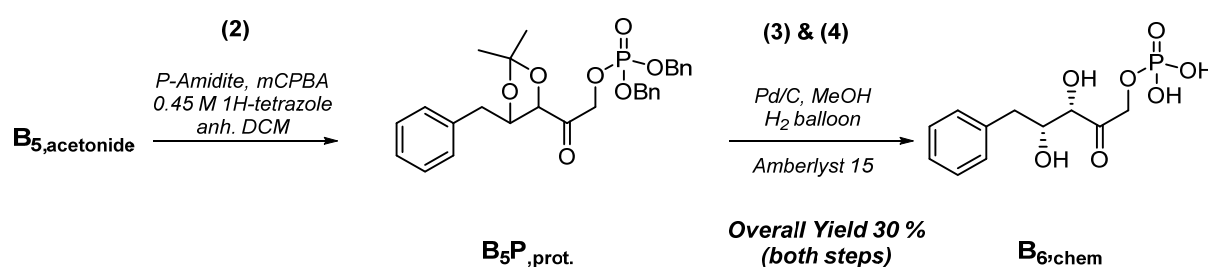


Figure 103 Chemical route II for the synthesis of (3*S*,4*R*)-1,3,4-trihydroxy-5-phenylpentan-2-one phosphate containing (1) acetonide protection (see chemical route I), (2) phosphorylation of the free primary alcohol by DPPC, (3) Phenyl-deprotection under hydrogenation conditions, and (4) acidic acetonide cleavage.

A III.2.1 Phosphorylation of Hydroxyacetone

Based on the results obtained for the synthesis of aldol adducts (e.g. Pathway I, RAMA), we hypothesized that the carbonyl group in β -position is probably responsible for stability issues during work up or storage. Hydroxyacetone was used as a model substrate to identify these bottlenecks and to establish a purification strategy for this class of compounds (**Figure 104**).

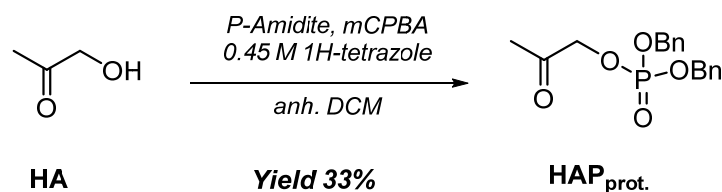


Figure 104 Phosphorylation by dibenzyl *N,N*-diisopropylaminophosphoramidite of the model substrate hydroxyacetone HA to HAP_{prot.}

In a round bottom flask, hydroxyacetone (1 equiv.), P-amidite (1.5 equiv.) were dissolved in dry DCM, followed by a dropwise addition of a 0.45 M 1*H*-tetrazole in acetonitrile solution (1.3 equiv.). The addition *m*CPBA (2 equiv. prediluted in dry CH₂Cl₂) at -78°C gave the the desired product within 45 min

²²⁶ C. Stanetty, M. Walter, P. Kosma, *J. Org. Chem.* **2014**, *79*, 582-598.

and the reaction was quenched by the addition of triethylamine. After extractive work up, the combined organic layers were concentrated at high *vacuo* ($T < 35^{\circ}\text{C}$).

Since ^1H and ^{31}P NMR gave promising results, the crude material was purified by silica gel chromatography (33% yield) and the stability towards acidic extraction was investigated. Therefore, 10 mg of the crude material was dissolved in CH_2Cl_2 and extracted with 1 N AcOH, satd. NaHCO_3 and twice with EtOAc, dried over Na_2SO_4 , and concentrated to afford the pure product ($\geq 95\%$ recovery) without any degradation according to ^1H NMR.

A III.2.2 Dibenzyl-deprotection *via* Pd/C and H_2 Balloon to Hydroxyacetonephosphate

Next, the desired phosphate moiety was approached by a heterogeneous Pd/C catalyzed dibenzyl cleavage in methanol (**Figure 105**).

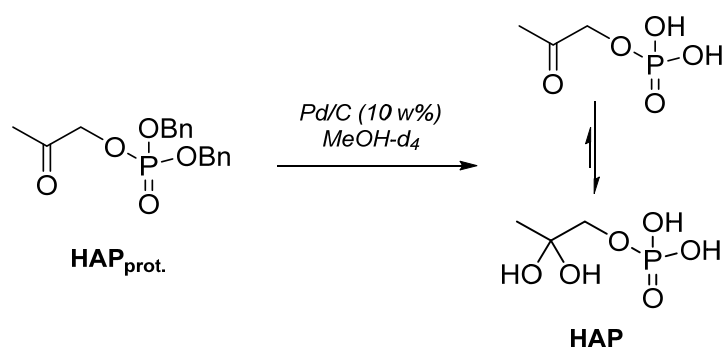


Figure 105 Benzyl-deprotection under hydrogenation conditions (H_2 balloon) catalyzed by Pd/C.

Initial studies were performed in 8 mL reaction vial, equipped with an H_2 balloon using 10 w% Pd/C in methanol- d_4 for direct product monitoring *via* NMR. Therefore, aliquots were taken, Pd/C was separated by centrifugation and filtration through a syringe filter and the deprotection step was completed within 14 h. Interestingly, a duplet at 3.84 ($J = 5.0 \text{ Hz}$, 2H) was detected in the ^1H NMR, which indicates the formation of the corresponding the hydrate. Similar results were also observed during NMR studies of DHAP, which have indicated a mixture of keto and hydrated form in an aqueous environment. The methyl group next to the carbonyl was obtained in a range, which indicates the formation of the hydrated form (δ 1.35). Especially, the formation of the dehydrate or a deuteromethoxy ketal was confirmed by ^{13}C NMR. Instead, of the carbonyl signal at around 200 ppm, the related hydrate signal at 100.74 ppm was obtained. Phosphorylation of the primary alcohol should give a significant shift of CH_2 next to it towards 5 ppm. However, after hydrogenation of the dibenzyl phosphoester to the free phosphate, a signal for the $\text{CH}_2\text{OPO}_3\text{H}_2$ at around 4.0 ppm was observed, which is in the same range like the $\text{CH}_2\text{-OH}$ of HA. To differentiate between the phosphorylated and non-phosphorylated compound, phosphorus coupling and two dimensional ^1H - ^{31}P NMR experiments

were performed and considered exactly. For all phosphorylated compounds, which were synthesized during this thesis, ^1H - ^{31}P NMR HMBC experiments were performed and analyzed carefully.

A III.2.3 Purification of HAP by BaCl_2 Precipitation

The reaction solution after hydrogenation was directly purified by the previously described $\text{BaCl}_2 \cdot 2\text{H}_2\text{O}$ precipitation protocol (**Figure 106**).

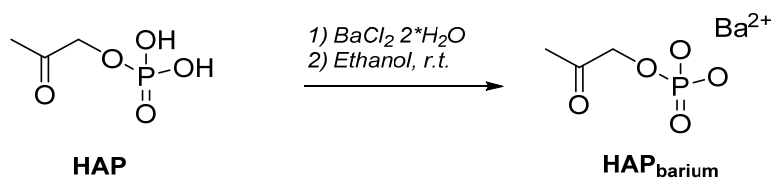


Figure 106 Purification of HAP by barium precipitation in ethanol.

HAP was dissolved in 100 μL H_2O (pH 6.9), $\text{BaCl}_2 \cdot 2\text{H}_2\text{O}$ and ethanol (500 μL) were added and immediately a cloudy solution was obtained, which was cooled to 4°C overnight o/n. The purification efficiency was tested *via* TLC (EtOAc:PE3:1) by checking the supernatant towards remaining starting material. For ^1H and ^{31}P NMR measurements, the obtained barium salt (**HAP_{barium}**) was dissolved in 600 μL D_2O and DCl (20 μL) until a clear solution (pH 1) was obtained. Similar signals and pattern for the CH_3 and CH_2 were observed for the barium purified and the starting material that confirms that procedure.

A III.2.4 HAP Stability

Since DHAP (**III**) is known as a very labile compound towards hydrolysis/dephosphorylation over time or under acidic conditions, **HAP** was used to identify ways to overcome these issues. HAP in methanol- d_4 was analyzed by ^1H NMR over time, without detectable degradation/dephosphorylation of the HAP. Furthermore, control experiments under acidic (pH 1.8) or neutral (pH 7.5) conditions as well as concentration at 42°C for 2 h on the rotavap did not give any significant **HAP** decomposition. We concluded that these results indicated that **HAP** and in consequently DHAP are sufficiently stable for further synthetic applications.

A III.2.5 Phosphorylation of Acetonide Protected Aldol Intermediate

The first approach which utilized unprotected aldol (**B_{5,II}**) did not give phosphorylation using the optimized phosphoramidite-based coupling methodology. Instead, phosphorylation of the acetonide protected aldol compound with dibenzyl *N,N*-diisopropylaminophosphoramidite/*1H*-tetrazole followed by oxidation with *m*CPBA afforded the desired product (**Figure 107**).

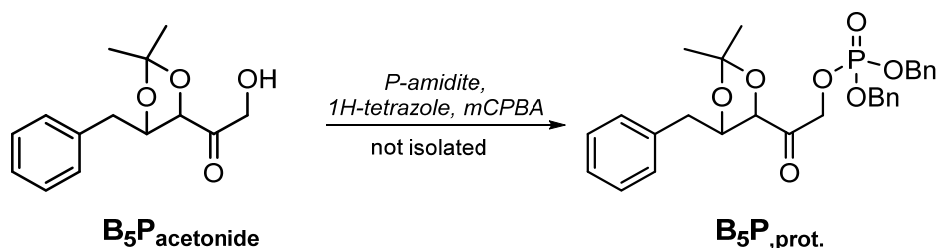


Figure 107 Phosphorylation by dibenzyl *N,N*-diisopropylaminophosphoramidite of **B₅P_{acetonide}**.

The acetonide protected aldol was dissolved in 600 μL CD_2Cl_2 and the phosphorylation of the free primary alcohol was performed according to established protocol for HAP (A III.2.1). To verify the product formation (**B₅P_{prot.}**) by NMR (^1H , ^{31}P and $^1\text{H}/^{31}\text{P}$ HMBC), 300 μL of the reaction solution were dissolved with 300 μL CD_2Cl_2 . The phosphoester formation at C1 was confirmed by $^1\text{H}/^{31}\text{P}$ HMBC and heteronuclear spin-coupling interactions ($^1\text{H}/^{31}\text{P}$). The reaction was stopped with trimethylamine (2.5 equiv.) at -20°C . To evaluate product stability during the work up by NMR, the crude mixture of **B₅P_{prot.}** was concentrated at room temperature under reduced pressure (crude yield 18 mg) and redissolved again in CD_2Cl_2 . First NMR measurements, directly after concentration indicated complete decomposition of phosphorylated aldol. These results underline the low stability under basic conditions, since Et_3N and isopropylamine (LG of *P*-amidite) are mainly present after concentration at high *vacuo*. To avoid degradation under basic conditions, the reaction mixture was extracted with 2 N HCl and according to NMR (^1H & ^{31}P) no significant decomposition was detected. Due to these results, column chromatography on acidic silica gel was investigated on this stage of the synthetic route, to separate especially *m*CPBA and other reaction residues, which can be toxic for the upcoming heterogeneous catalyzed hydrogenation. Additionally, the following benzyl- and acetonide deprotection will only generate toluene and acetone, both can be removed under reduced pressure to afford the final target molecule (**B₆**).

Column chromatography was performed with preconditioned silica gel (pure PE) and the desired product was eluted with EtOAc:PE/1:1 ($R_f = 0.45$). The combined product fractions were concentrated at 35°C and obtained NMR spectra were in good agreement to the *in situ* measurement (^{31}P NMR $\delta = 0.99$) of the crude reaction mixture. Unfortunately, any byproduct was still present after purification, which gave two significant signals in the proton NMR at around 1.5 and 3.4 ppm as well as in the ^{31}P NMR at 8.5 ppm. Also, 2-dimensional NMR experiments ($^1\text{H}/^{31}\text{P}$ HMBC) indicate the presence of a

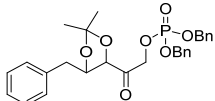
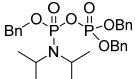
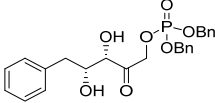
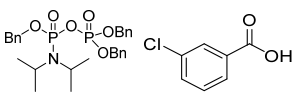
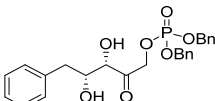
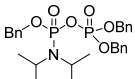
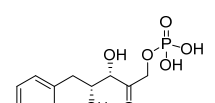
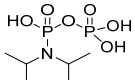
second phosphorylated species, which was identified by Stanetty C. as a dimerization product of the dibenzyl *N,N*-diisopropylaminophosphoramidite (**Table 41**).²²⁷

The byproduct formation was confirmed by matching the obtained NMR data (CH₃ at 1.5 ppm, CH at 3.4, and characteristic phosphorous coupling for CH₂OPO₃H₂) to data of the isolated compound.

For the isolation of the phosphorylated aldol compound (**B**_{6,chem}), several purification attempts on different stages of the synthetic route were performed (**Table 41**). Major problem during that work was the separation of the dimerization byproduct, which was not separable by column purification in the presence of acetonide protected aldol material (**Table 41, A**).

Similar results were obtained for the phosphorylated aldol adduct, after acetonide deprotection and column chromatography, because of massive tailing and co-elution of the described byproduct (**Table 41, B**).

Table 38 Summary of applied purification strategies for the phosphorylated aldol adduct during the chemical route II to afford (3*S*,4*R*)-1,3,4-trihydroxy-5-phenylpentan-2-one phosphate.

#	Target molecule	Purification	Byproduct
A		<ol style="list-style-type: none"> 1. Extraction with water/CH₂Cl₂ 2. Column purification 	
B		<ol style="list-style-type: none"> 1. Extraction with water/CH₂Cl₂ 2. Acetonide deprotection 3. Column purification 	
C		<ol style="list-style-type: none"> 1. Extraction with water/CH₂Cl₂ 2. Extraction with NaHCO₃ 3. Acetonide deprotection 4. Column purification 	
D		<ol style="list-style-type: none"> 1. Extraction with water/NaHCO₃/CH₂Cl₂ 2. Acetonide deprotection 3. Benzyl deprotection 4. BaCl₂ · 2H₂O precipitation 	

For that experiments, several mobile phase compositions (PE:EtOAc) were investigated but without any improvements towards the separation efficiency. After applying purification attempt **B**, 2-chlorobenzoic acid was identified as minor byproducts of *m*CPBA by NMR. To remove that, an additional extraction step using sat. NaHCO₃ was successfully applied (**Table 41, C**). Since the polarity of our final target product is different to the expected byproducts, global deprotection (benzyl and

²²⁷ Stanetty C., private conversation.

acetonide) and isolation by the described BaCl₂·2H₂O purification protocol should afford the pure product (**Table 41, D**).

A III.2.6 Global Deprotection of Acetonide and Benzyl to (3*S*,4*R*)-1,3,4-trihydroxy-5-phenylpentan-2-one phosphate

Due to the low stability of the phosphorylated compounds, initial NMR scale experiments were accomplished to evaluate mild deprotection conditions (**Figure 108**).

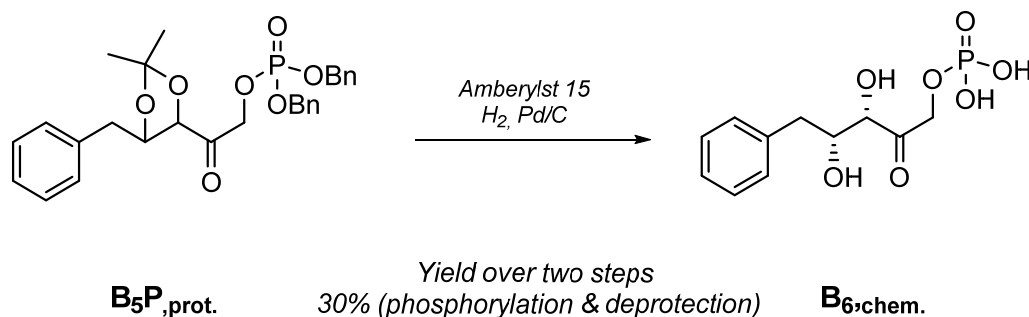


Figure 108 Global deprotection 1) acidic acetonide deprotection, and 2) benzyl deprotection under hydrogenation conditions (H₂ balloon) catalyzed by Pd/C to afford B_{6,chem}.

First, the fully protected but not column purified aldol adduct was dissolved in 600 μ L methanol-d₄ and around 10 w% Amberlyst 15 was added. The reaction was stirred at room temperature and full starting material consumption was indicated by TLC (PE:EtOAc 1:1, R_f= 0.1) after 14 hours. The crude NMR showed complete acetonide deprotection, because of the missing doublet for the CH₃ groups as well as shifted proton signals for at C3 and C4. Additionally, obtained coupling constants differed to those of the cyclized starting material. Next, the reaction mixture was transferred into an 8 mL reaction vial equipped with a H₂ balloon without any further purification steps. For the final benzyl deprotection, 10 w% of Pd/C were added and stirred over night at room temperature. The product formation of the final phosphorylated compound was confirmed *via* RP-TLC (MeOH:H₂O 3:1, R_f= 0.85) and NMR (¹H, ³¹P and ¹H-³¹P HMBC). To prove the synthetic route for the generation of the required phosphorylated aldol compound, 50 mg of fully protected aldol were used. After global deprotection, the previously described BaCl₂ purification protocol afforded the pure product, confirmed by NMR.

A III.2.7 Characterization of (3*S*,4*R*)-1,3,4-trihydroxy-5-phenylpentan-2-one phosphate

In Figure 109, ¹H NMR spectra of the phosphorylated aldol products (**B₆**) are presented (upper: RAMA mediated, bottom: synthetic route).

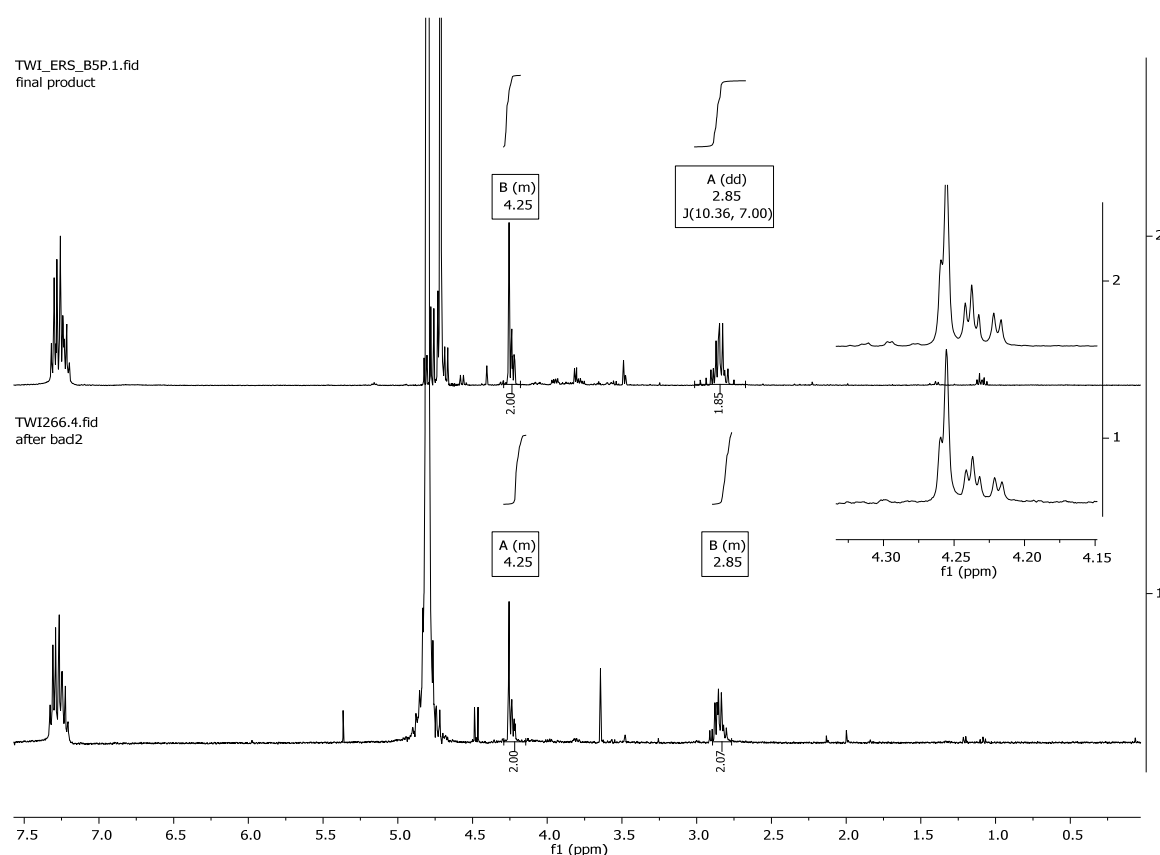
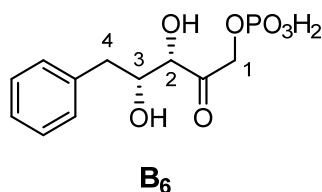


Figure 109 Comparison of the recorded ¹H NMR of (3*S*,4*R*)-1,3,4-trihydroxy-5-phenylpentan-2-one phosphate. Upper spectra: RAMA catalyzed, bottom spectra: chemical route II.

Both spectra showed identical shifts for protons attached to C2, C3 (4.25 ppm), and C4 (2.85 ppm). In particular, similar splitting patterns for the protons located at carbons of the diols (**Figure 109**, shortcut) and the CH₂ next to the phosphoester at 4.8 ppm clearly indicates the formation of the target compound **B₆** by both synthetic protocols. For the bottom spectra, the phosphorus coupling is covered by the water peak, which is present due to the water content in methanol-d₄ or residual water from the reaction itself. Additional ³¹P and ¹H-³¹P HMBC (4.8 ppm to 0.25 ppm) experiments underline the phosphoester formation and isolation by the applied BaCl₂ precipitation protocol (**Figure 110**).

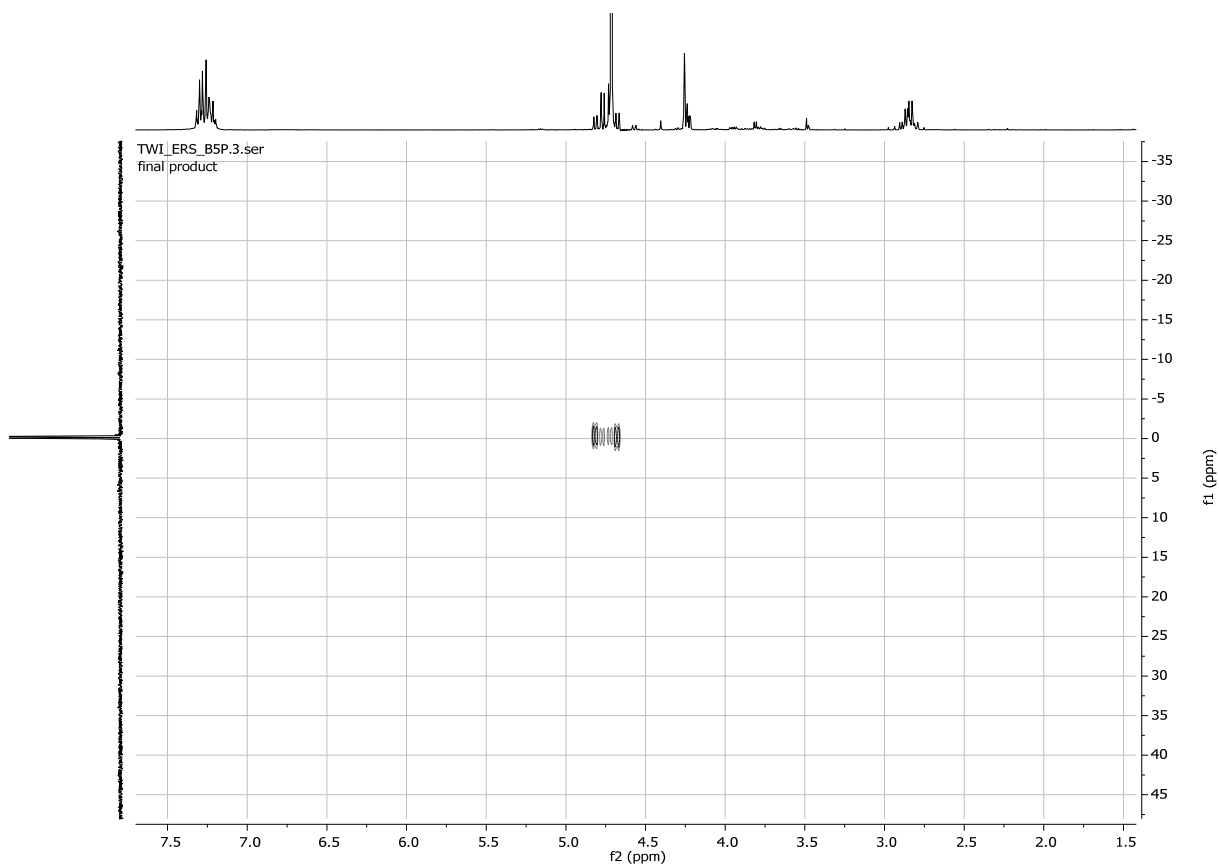


Figure 110 ^1H - ^{31}P HMBC of (3*S*,4*R*)-1,3,4-trihydroxy-5-phenylpentan-2-one phosphate.

A IV Phosphatases Mediated-Dephosphorylation

By definition, phosphatases are enzymes that are applied for the selective cleavage of phosphate esters to the corresponding alcohol (**Figure 111**). In general, several chemical and enzymatic methods for cleaving the phosphate group are known (1),(2) acid-catalyzed hydrolysis (3) cation-exchange resins, and hydrolysis catalyzed by (1) acid phosphatase (EC 3.1.3.2) or (4) alkaline phosphatase (EC 3.1.3.1)

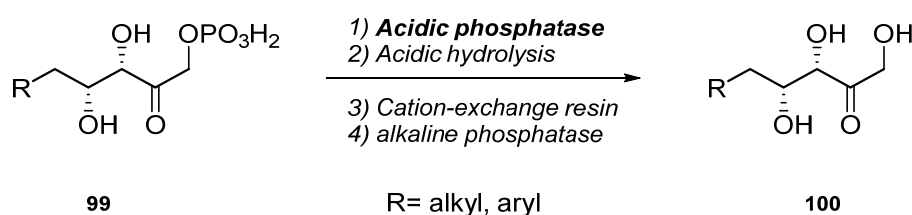


Figure 111 Dephosphorylation strategies for phosphorylated aldol adducts (**B₆**).

Both, non-enzymatic routes (strongly acidic conditions) as well as alkaline phosphatase (pH optima 8-9) led to decomposition of the aldol adduct due to the required reaction conditions. The most selective procedure for dephosphorylation is the use of acidic phosphatases (EC 3.1.3.2), which operate in a pH range of (pH 5-7) and tolerate a broad range of substrates.^{228,229}

In order to implement Pathway II into *E. coli*, selective dephosphorylation to the target molecule is required to transport the aldol adduct through the lipophilic cell membrane, which forms a barrier for the charged phosphate. Additionally, the cleavage of the phosphate group simplifies the product isolation.

A IV.1 Phosphatase Phon-Sf: Dephosphorylation Activity

According to the described esterase assay, an activity assay for dephosphorylation activity of Phon-Sf from *Shigella flexneri* to afford the UV active *p*-nitrophenol (**92**), was applied.²²⁹ In this case, the enzyme mediated phosphate cleavage of *p*-NO₂-phenylphosphate (pNPP, **91**) was monitored at 405 nm (**Figure 112 & Figure 113**).

²²⁸ M. D. Bednarski, E. S. Simon, N. Bischofberger, W. D. Fessner, M. J. Kim, W. Lees, T. Saito, H. Waldmann, G. M. Whitesides, *JACS* **1989**, *111*, 627-635.

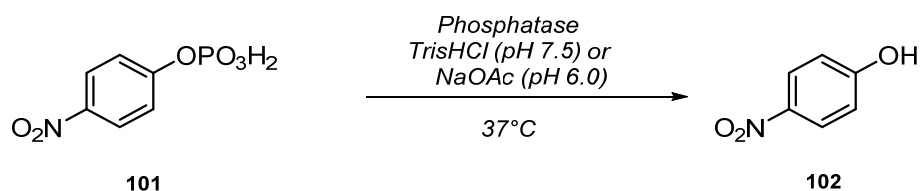


Figure 112 Photometric activity assay for phosphatases by determine the formation of $p\text{NO}_2$ -phenol.

Table 39 Reaction conditions for the photometric phosphatase activity assay.

Reaction mixture	Final concentration
50 mM pNPP in TrisHCl (pH 7.5)	5 mMl
Phon-Sf (0.3 mg/mL)	0.03 mg/mL
TrisHCl (pH 7.5) or 20 mM NaOAc (pH 6.0)	

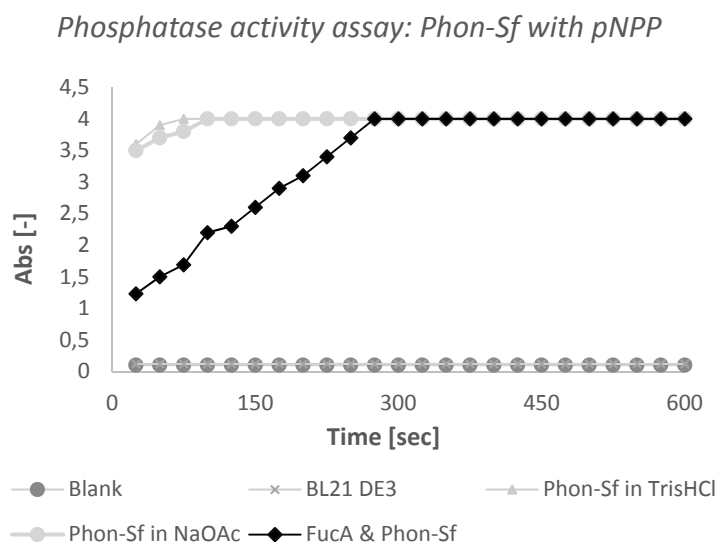


Figure 113 Photometric activity assay of acidic phosphatase at 405 nm.

In general, Phon-Sf activity in 100 mM TrisHCl (pH 7.5) was compared with standard conditions in 20 mM NaOAc (pH 6.0).²²⁹ Figure 113 displays the dephosphorylation activity of Phon-Sf by increasing absorption over 10 min at 405 nm (37°C). In comparison to the blank (w/o enzyme) and the negative control (BL 21 (DE3)), both attempts of Phon-Sf in different buffer solution showed dephosphorylation to the UV active product on a quantitative level. Additionally, a FucA/Phon-Sf cell free extract mixture was added to *p*-nitrophenol phosphate that confirmed the dephosphorylation activity of Phon-sf, in presence of another Pathway II enzyme.

²²⁹ T. van Herk, A. F. Hartog, L. Babich, H. E. Schoemaker, R. Wever, *Chembiochem* **2009**, *10*, 2230-2235.

A IV.1.1 Dephosphorylation of Phon-Sf Towards the Model Substrate

For initial studies, 5 mg of barium precipitated **B**₆ was dissolved in 100 μ L H₂O and 5% 2 N HCl and the dephosphorylation activity of Phon-Sf was determined by LC/MS and RP-TLC (MeCN:H₂O 1:1, R_f= 0.7). Additionally, the BL21(DE3) control experiment was performed with the same reaction settings.

Table 40 Reaction conditions for the dephosphorylation of **B**₆ using CFE of Phon-Sf.

Reaction mixture	Final concentration
5 mg of B ₆	
Phon-Sf (3.2 mg/mL)	1.6 mg/mL
20 mM NaOAc (pH 6.0)	

For RP-TLC analysis, 10 μ L of the reaction sample was diluted with 50 μ L of acetonitrile, centrifuged and the supernatant was compared to Fsa1 A129S (DHA dependent, Pathway I) synthesized **B**₅. According to qualitative RP-TLC and LC/MS experiments, dephosphorylation was completed within 6 h after addition of Phon-Sf. The control experiments by BL21(DE3) gave a mixture of **B**₆ (phosphorylated aldol) and **B**_{5,II} (dephosphorylated aldol) due to *E. coli* related phosphatases.

A V Pathway II Assembly

Besides the described strategies to generate DHAP, Wever *et al.* described an easy method in which commercially available DHA or glycerol are phosphorylated by the acidic phosphatase (Phon-Sf).²³⁰ The generated DHAP is coupled to an aldehyde in a concurrent aldolase mediated condensation (RAMA) reaction to the corresponding aldol adduct, which is finally dephosphorylated by the Phon-Sf to afford the diastereomerically pure product (**Figure 114**).²³¹

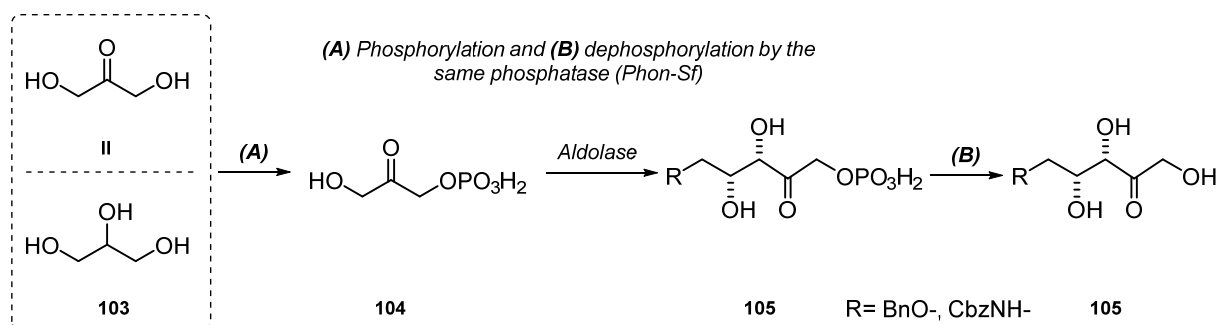


Figure 114 Phosphorylation and dephosphorylation by using Phon-Sf. (A) phosphorylation of glycerol or DHA and (B) dephosphorylation to afford the target product.

To enhance the DHAP formation rate, further studies were accomplished. For example, different variants of the bacterial phosphatase from *Salmonella enterica ser. Typhimurium* (Phon-Se) were applied to an aldolase cascade set up. Furthermore, the whole cascade was immobilized and implemented into a continuous flow reactor to demonstrate the usefulness of this DHAP generating and aldol dephosphorylating system under *in vitro* conditions.²³²

Another strategy to circumvent elaborate DHAP generation protocols was to hijack the phosphorylated aldol donor molecule (DHAP) from the glycolytic pathway (**Figure 115**). For that methodology, an engineered organism of co-expressed aldolase and phosphatase (YqaB from *E. coli*) genes was required.²³³ The established *in vivo* pathway is directly connected to the central carbon metabolism of the host organism, which is managing the DHAP supply for the aldol reaction by consuming glucose from the growth media. During their studies, three aldolases (FucA, FruA, RhuA) were introduced to control the stereochemistry of the corresponding products. Additionally, solubility issues of aldol acceptor aldehydes were mentioned and to overcome this bottleneck, synthesized 3-trifluoroacetamido-propanal (**107**) was used for all optimization studies, due to the excellent water solubility.

²³⁰ L. Babich, L. J. C. van Hemert, A. Bury, A. F. Hartog, P. Falcicchio, J. van der Oost, T. van Herk, R. Wever, F. P. J. T. Rutjes, *Green Chem.* **2011**, *13*, 2895-2900.

²³¹ T. van Herk, A. F. Hartog, L. Babich, H. E. Schoemaker, R. Wever, *ChemBioChem* **2009**, *10*, 2230-2235.

²³² L. Babich, A. F. Hartog, L. J. van Hemert, F. P. Rutjes, R. Wever, *ChemSusChem* **2012**, *5*, 2348-2353.

²³³ M. Wei, Z. Li, T. Li, B. Wu, Y. Liu, J. Qu, X. Li, L. Li, L. Cai, P. G. Wang, *ACS Catal.* **2015**, *5*, 4060-4065.

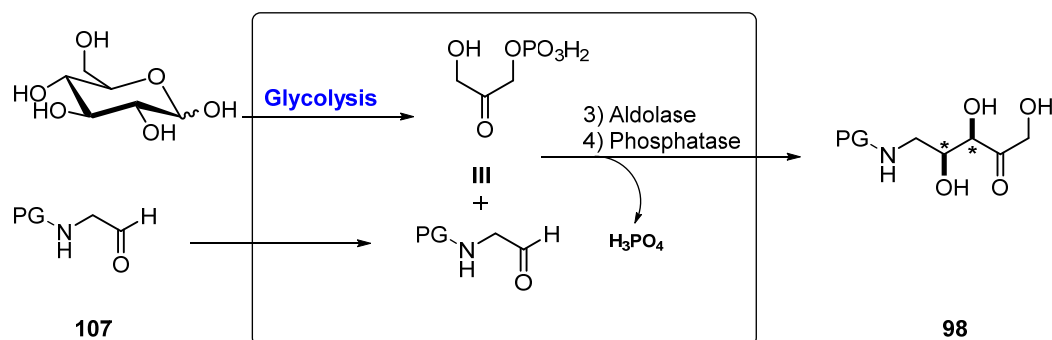


Figure 115 Illustration of the first *in vivo* pathway, which is connected to the glycolysis for efficient DHAP supply by the host organism.²³⁴

In order to avoid retro aldol or product decomposition, a high substrate loading of around 100 mM aldehyde was required and was added 12 hours after induction with IPTG to the fermentation solution. To enhance the overall performance, studies towards different growth media, glucose concentrations as well as the induction with IPTG at different levels of cell density were investigated to identify the optimal fermentation conditions. The improved reaction settings were applied for the synthesis of several clinically relevant imino-sugars such as *D*-Fagomine, 1-deoxymannojirimycin (DMJ), and 1-deoxynojirimycin (DNJ) in moderate yields (35%) and good diastereoselectivity (d.r. 90:10), and illustrates the utility of this artificial pathway.

First, initial studies to confirm the compatibility of our model substrate (**B₃**) with *in vitro* combined aldolase (FucA or RhuA) and Phon-Sf under previously evaluated conditions were conducted (**Figure 116**, **Table 44**). The reaction was performed in two different ways (i) in a one pot fashion (cell free extracts of both enzymes were added simultaneously) or (ii) in a sequential mode. Both reactions were carried out, using 5 mg/mL of each enzyme in the presence of 20% acetonitrile at 25°C overnight.

Table 41 Reaction conditions for the synthesis of (*3R*, *4R*) diastereomer by FucA or the (*3R*, *4S*) diastereomer by RhuA followed by selective dephosphorylation catalyzed by Phon-Sf.

Reaction mixture	Eq.	Final concentration
DHAP (pH 6.9) (110 mg/mL)	1.0	0.03 mmol
Aldehyde in MeCN	1.7	0.05 mmol
FucA/Phon-Sf		

The reaction progress was monitored as usual by LC/MS and RP-TLC and in the case of the sequential setup, crude cell extract of Phon-Sf was added after full consumption of DHAP was indicated (around 14 h).

²³⁴ M. Wei, Z. Li, T. Li, B. Wu, Y. Liu, J. Qu, X. Li, L. Li, L. Cai, P. G. Wang, *ACS Catal.* **2015**, *5*, 4060-4065.

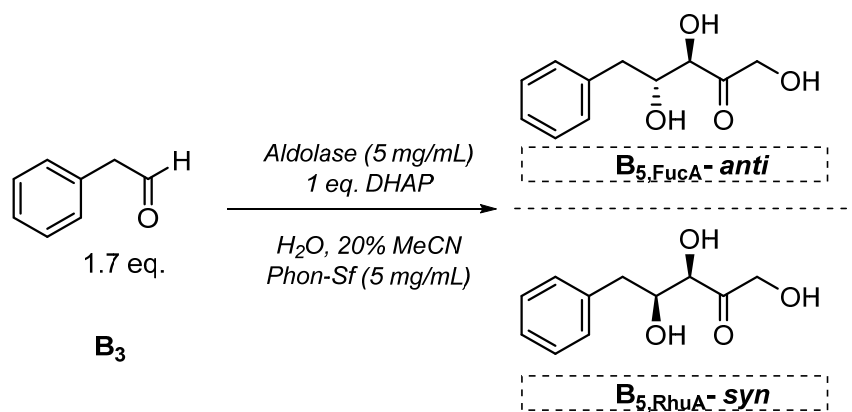


Figure 116 *In vitro* cascade approach containing a DHAP dependent aldolase (FucA or RhuA) and Phon-Sf for the synthesis of the corresponding aldol adducts.

For both settings, the formation of the dephosphorylated aldol adduct was exclusively detected on a qualitative level (no calibrated LC/MS). These promising results were the starting point for further improvements on process parameters (solvent, DHAP concentration, spiking of aldol donor or acceptor over time). Finally, the optimized reaction parameters were used for the synthesis and identification of the phosphorylated diastereomers (*syn/anti*) by NMR. In particular, detailed analytical data of these compounds would be interesting, since these are still not presented in literature.

A V.1 Solvent Studies for Two-Step *In Vitro* Transformation (FucA and Phon-Sf)

To identify the optimal reaction conditions for the formation of (3*R*,4*R*)-1,3,4-trihydroxy-5-phenylpentan-2-one (**B_{5,FucA}**), experiments using FucA and Phon-Sf (expression control *via* SDS page, activity by photometric assay) were conducted in biological duplicates (**Figure 117**). Time dependent optimum was identified by GC/FID and HPLC analysis, analyzing samples after 0, 1, 6, and 24 h.

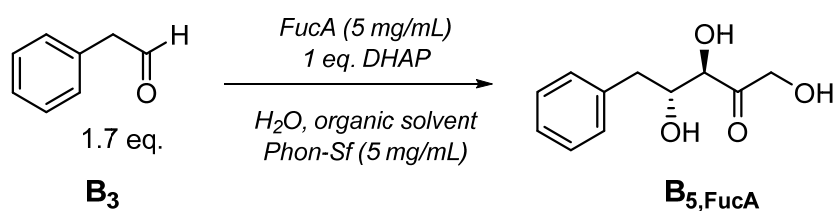


Figure 117 *In vitro* cascade approach containing FucA and Phon-Sf, which were applied in a one-pot fashion for the identification of a suitable cascade solvent.

Since aldol acceptor molecules are poorly soluble in water they require high amounts of organic solvents (e.g. 20% DMF or DMSO), which led to the formation of an emulsion with sufficient activity for an aldol reaction. Acetonitrile turned out to be the most beneficial co-solvent for Pathway I and performing the alcohol oxidation with ALKJ as a catalyst. Furthermore, DMF a well-known co-solvent for DHAP reactions was compared in solvent studies. (**Figure 118** & **Figure 119**).

Table 42 Reaction conditions for *in vitro* cascade solvent studies.

Reaction mixture	Eq.	Final concentration
DHAP (pH 6.9) (110 mg/mL)	1.0	0.03 mmol
Aldehyde in DMF/ MeCN	1.7	0.05 mmol
FucA/Phon-Sf (3 mg/mL)		

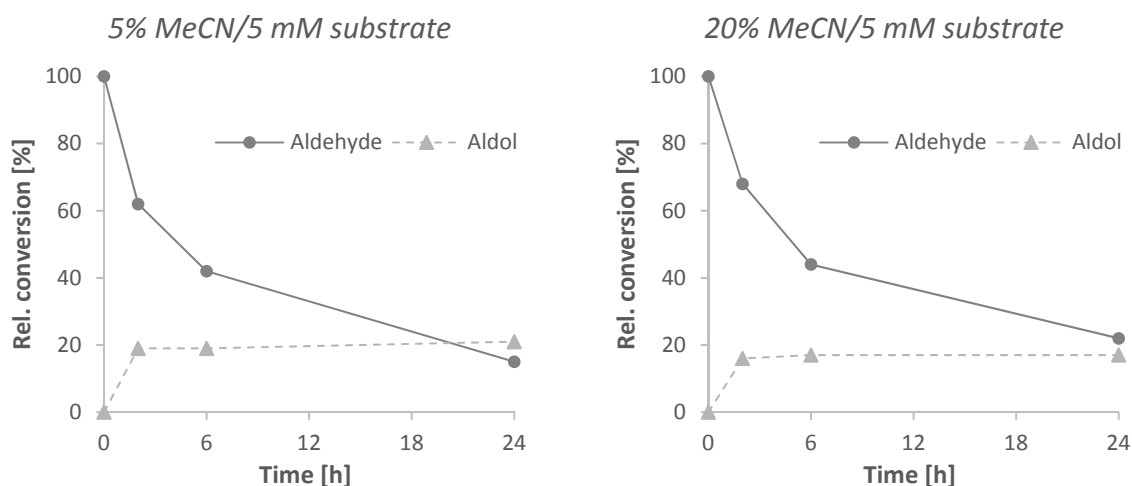


Figure 118 Aldehyde consumption vs. aldol adduct formation by FucA and Phon-Sf using 5 or 20% of acetonitrile.

In Figure 118 & 119 good aldehyde consumption is shown within 24 h and interestingly no significant byproduct formation (alcohol or carboxylic acid) was detected. Interestingly, around 50% of the starting material was not recovered most likely because of evaporation of the aldehyde or degradation/formation of unknown compounds. But in principle, no significant byproduct was detected and thus no detailed information about the inaccurate mass balance was possible.

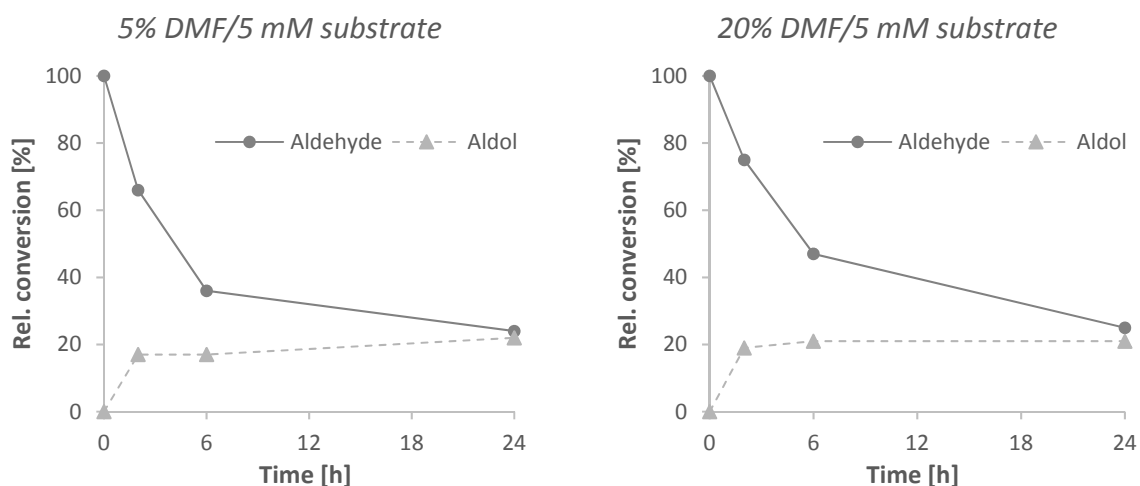


Figure 119 Aldehyde consumption vs. aldol adduct formation by FucA and Phon-Sf using 5 or 20% of DMF.

Varying the solvent concentration between 5% and 20% acetonitrile yielded in slightly higher amounts of aldol adduct using only 5% of organic solvent. Considering reaction time, product formation reached

a plateau of around 20% within the first hour. This fact may indicate some bottlenecks concerning biocatalyst inhibition or degradation of DHAP over time. In comparison to acetonitrile, different DMF amounts also yielded in approx. 20% product formation. Since DMF gave intense peak tailing on HPLC, especially at retention times of the desire product, acetonitrile was selected as better suited solvent for Pathway II. Mainly, because AlkJ and Pathway I are also performed in 5% acetonitrile and with respect to implement AlkJ into Pathway II, acetonitrile is our solvent of choice.

A V.2 Optimization of *In Vitro* Assembled Pathway II

During the previously described solvent studies, limited product formation of approx. 25% was observed over 24 h. These experiments pointed out that several reaction parameters can influence the reaction progress: (i) substrate or product inhibition, (ii) biocatalyst instability in the presence of organic solvents (DMF, MeCN), and (iii) low DHAP concentration.

To identify these bottlenecks, further experiments were accomplished and depicted in Figure 120 and Figure 121. The reactions were performed under the same conditions as the described solvent experiments (**Table 45**).

In a first attempt, we wanted to elucidate how ratios between aldol donor and acceptor molecules influence the product formation.

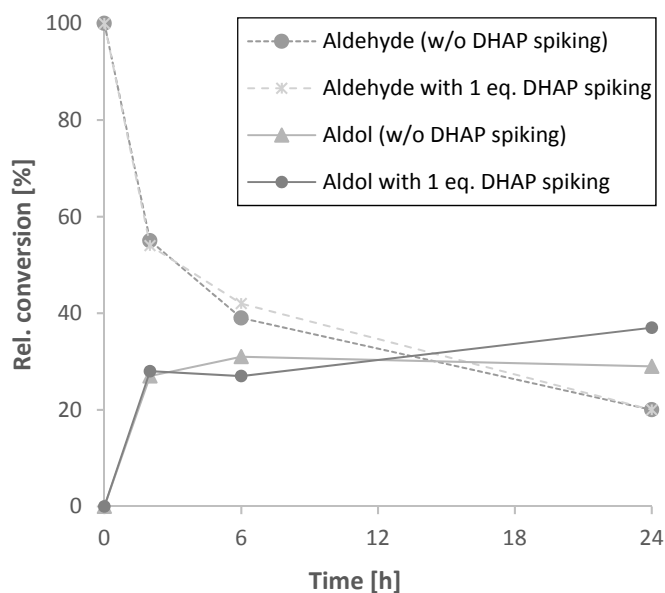


Figure 120 Aldehyde consumption vs. aldol adduct formation by FucA and Phon-Sf using 5% acetonitrile with spiking of an additional 1 equiv. DHAP after 4 h.

After 4 h, an additional equivalent of DHAP was added to the reaction mixture and increased product formation was obtained up to 40%, as compared to the control experiment without DHAP spiking (30%). Increasing the DHAP concentration improved the product formation of around 10%, but a product formation plateau was reached after 6 h. These results may be related to decomposition of

DHAP to methylglyoxalate or inorganic phosphates, both strong aldolases inhibitors.²³⁵ Moreover, product inhibition cannot be excluded and to identify substrate inhibition, control experiments using only 1 mM phenyl acetaldehyde were accomplished without significant effects to the product formation rate.

Increasing the aldehyde concentration by the addition of 1.7 equivalents after 4 h causes nearly no increase in product formation compared to the simultaneously performed control experiment (**Figure 121**).

These results are in agreement with the donor concentration studies of Pathway I, where best conversions were observed by the addition of high aldol donor quantities (20 equiv. DHA or HA) to drive the reaction to completion. As depicted in Figure 121, the higher quantities of the aldol acceptor did not facilitate the aldol adduct formation.

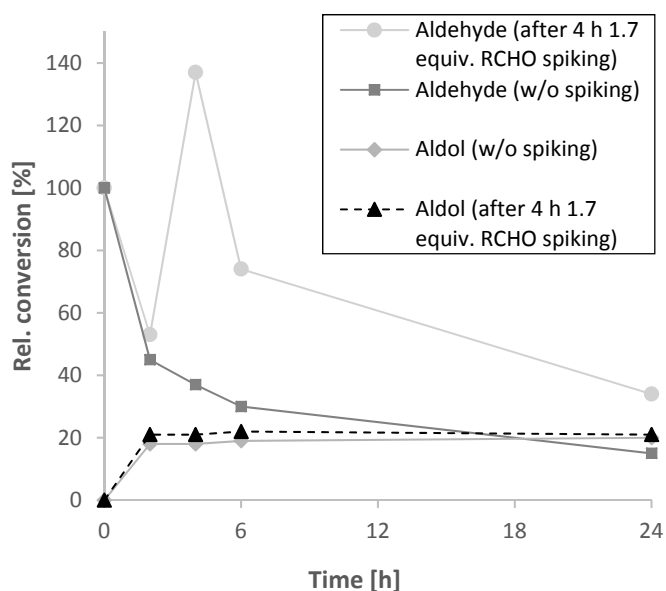


Figure 121 Aldehyde consumption vs. aldol adduct formation by FucA and Phon-Sf using 5% acetonitrile with spiking of additional 1.7 equiv. aldehyde (B_3) after 4 h.

To identify inhibition of DHAP degradation compounds (e.g. methylglyoxalate or inorganic phosphate), DHAP was added in 0.25 equivalent portions over 4 h to the reaction mixture.

²³⁵ T. Suau, G. Álvaro, M. D. Benaiges, J. López-Santín, *Biotechnol. Bioeng.* **2006**, *93*, 48-55.

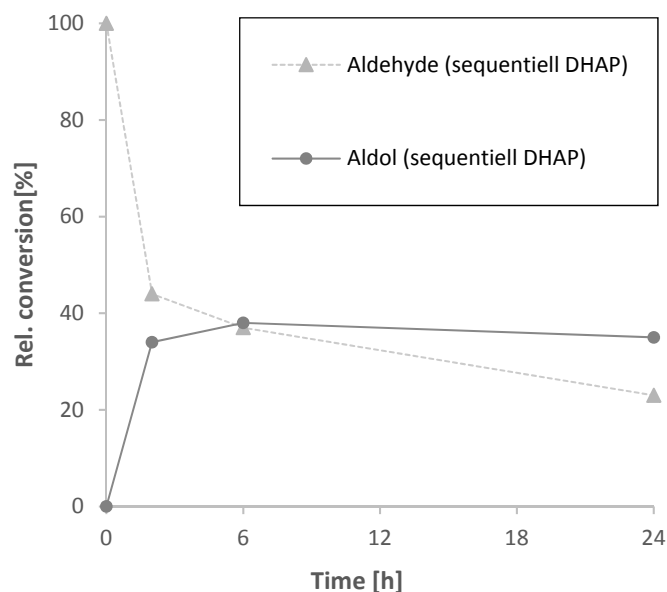


Figure 122 Aldehyde consumption vs. aldol adduct formation by FucA and Phon-Sf using 5% acetonitrile with sequential addition of aldehyde (B₃) over 4 h.

As shown in Figure 122, the product concentration (approx. 35%) was not increased by the stepwise addition of the donor molecule DHAP. Additionally, experiments were with higher amounts of enzyme or spiking of more enzyme was performed on analytical and preparative scale (**A VI.1**) without any improved product formation rates. Of course, this kind of statements has to be carefully discussed and gave only a hint, how the reaction was affected by the donor and acceptor concentrations.

In brief, the highest aldol concentration was reached by spiking of additional 1.7 equiv. DHAP (in total 3.4 equiv.) after 4 h. In order to shift the reaction equilibrium to the aldol adduct and avoid side product formation an increased quantity of aldol donor (DHAP) will be beneficial.

With regards to the performed *in vitro* Pathway II experiments some yield determining factors were noticed: (i) a high DHAP concentration may be beneficial to drive the reaction to completion and increase the product formation (>35%), (ii) enzyme inhibition by known aldolases inhibitors (e.g. methylglyoxalate or inorganic phosphates, which are DHAP degradation products) can not be excluded as a limiting parameter. A whole cell biocatalysts should manage (i) the DHAP supply under optimized fermentation conditions (e.g. medium composition) (ii) the product secretion after dephosphorylation to exclude product inhibition by the phosphorylated target compound (X₆), and (iii) DHAP degradation should be avoided²³⁵For validation of robust cell growing conditions, which are mandatory for DHAP hijacking due to the increased DHAP production at the beginning of the exponential phase, several experiments were performed and summarized in **A VII**.

A VI Isolation of Aldol Diastereomers

A VI.1 Pathway II-*In Vitro* Preparative Scale Experiments using FucA & Phon-Sf or RhuA & Phon-Sf

After optimized *in vitro* conditions (FucA and Phon-sf) were identified, a preparative scale transformation was performed to gather information about the stereochemical properties of related *anti* aldol conformer (**Figure 123**).

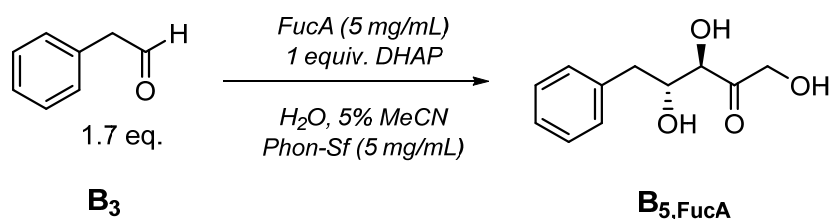


Figure 123 Synthesis of (3*S*,4*S*)-1,3,4-trihydroxy-5-phenylpentan-2-one by FucA and Phon-Sf in a one-pot fashion (preparative scale).

For the synthesis (3*R*,4*R*)-1,3,4-trihydroxy-5-phenylpentan-2-one (**B_{5,FucA}**), FucA and Phon-Sf (expression & activity confirmed) were used in a one-pot fashion. The reaction was performed in a 8 mL reaction flask, using 5 mg/mL of each enzyme, 5% v/v acetonitrile, and an excess of DHAP (1.7 equiv.) prediluted and pH adjusted in water (pH 6.9)

The flask was shaken vigorously overnight at room temperature until full DHAP consumption was monitored *via* RP-TLC (MeOH:H₂O 50:50 $R_{f(DHAP)} = 0.95$; $R_{f(product)} = 0.8$). The reaction was stopped by freezing -80°C, precipitated biotransformation residues were separated by centrifugation after thawing. The supernatant was purified by our SPE purification protocol. In contrast to Pathway I under *in vivo* conditions, several unknown biotransformation residues were present and a slightly adapted solvent gradient was required to afford the pure product in 17% yield after concentration at <30°C and high *vacuo* (**Figure 124**).

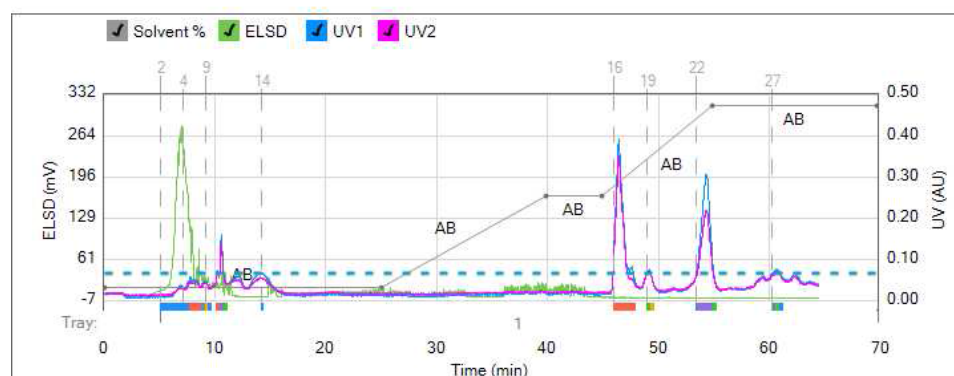


Figure 124 Illustration of the optimized SPE protocol for a preparative FucA/Phon-Sf cascade approach (Substrate **B₃** at 48 min; not known/assignable compound at 49 min according to NMR, Product **B_{5,FucA}** at 53 min).

As indicated in Figure 124, highly water-soluble residues from the biotransformation were transferred through the C18 material within the first 40 min and the product was eluted after around 48 min. Due to the lipophilic aromatic scaffold, the product was eluting after 48 min as well as perfect separation from the aldehyde (54 min) was observed, which was added in an excess to shift the reaction equilibrium.

In comparison to the literature (average value 90:10), we observed a mixture of *anti/syn* isomers in a 70/30 ratio.

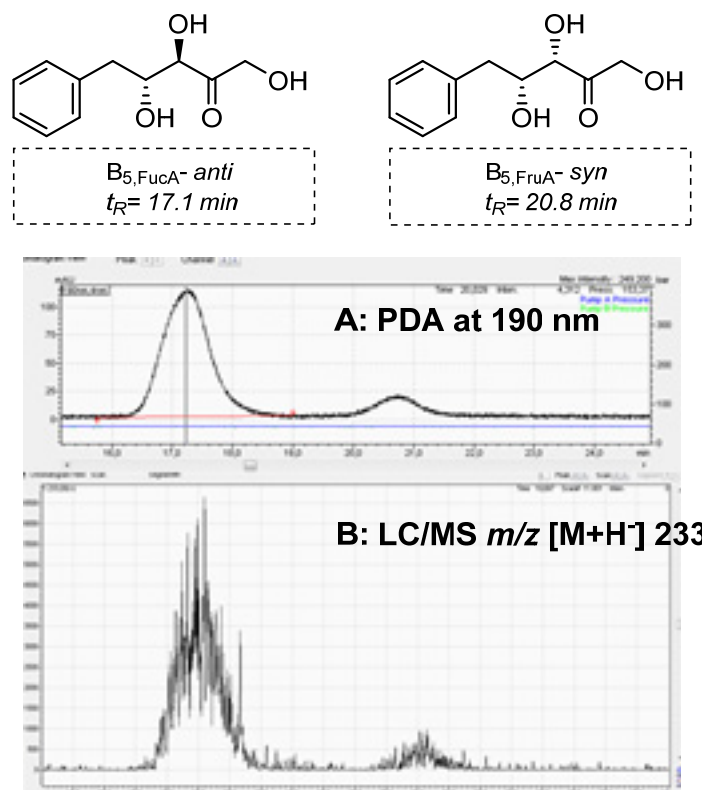


Figure 125 Separation of FucA (*anti*) and FruA (*syn*) diastereomers on a ROA 8% organic acid column.

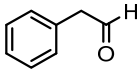
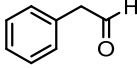
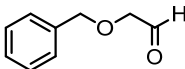
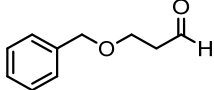
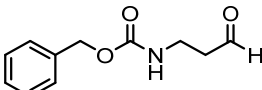
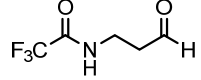
These values were determined by NMR (**Figure 125**) and confirmed by HPLC (ROA column, Pathway I method; **A**: PDA at 190 nm; **B**: LC/MS: m/z $[M+H]^+$ 233) and displays the distribution of the aldol product into the *syn* conformer ($3S, 4R$) at 20.8 min (FruA/Fsa1 A129S) and the *anti*-orientation ($3S, 4S$) of the diol moiety for the FucA mediated C-C coupling at 17.1 min (**Figure 125**).

Similar conditions were used to synthesize ($3R,4S$)-1,3,4-trihydroxy-5-phenylpentan-2-one, the corresponding RhuA diastereomer. The desired *syn* product was obtained in 15% yield, but again in a 80:20 mixture with the *anti* isomer (**Table 46**).

Furthermore, all model substrates (**Table 46, B₃, D₃, F₃**) as well as the water soluble CF₃-protected amino aldehyde (**L₃**) were used with FucA/Phon-Sf cell free extracts to synthesize the corresponding product.

All compounds were isolated by the SPE protocol and fully characterized by NMR and LC/MS.

Table 43 Yield and stereoselectivity of RhuA or FucA with Phen-Sf under optimized *in vitro* conditions for the isolation of the corresponding aldol adduct by SPE purification.

#	Substrate	Aldolase	Yield [%]	Stereoselectivity (<i>syn/anti</i>)
B _{5,FucA}		RhuA	15%	80/20
B _{5,RhuA}		RhuA	29%	60/40
D _{5,FucA}		FucA	10 %	[A]
E _{5,FucA}		FucA	n.a. [B]	-
G _{5,FucA}		FucA	10 %	[A]
L _{5,FucA}		FucA	n.a. [B]	-

[A]: *syn/anti* mixtures, mainly biotransformation impurities (4-2 ppm); **[B]:** according to LC/MS no product in the collected fractions after SPE.

In general, the purification was working as depicted in Figure 124 for the corresponding phenylacetaldehyde products, but interestingly, for the attempts (**C** & **E**), in all collected fractions no product was detected, neither by NMR or LC/MS. For **B** and **D**, product formation was confirmed by LC/MS and also indicated by NMR (¹H, ³¹P). Besides, the significant product signals, also byproducts, most likely biotransformation residues (e.g. buffer, carbohydrates) were detected.

To improve the overall yields as well as the product purity, the easiest way will be by the use of Pathway II under *in vivo* conditions. Besides the cheap DHAP generation by the host organism, also the SPE purification will be more efficient (see Pathway I), because of less crude cell and biotransformation residues in the supernatant.

A VI.2 Identification of Aldol Diastereomers *via* ^1H NMR

In the literature, a conclusive interpretation and detailed analytical data of *syn/anti* aldol diastereomers were until now under represented. In general, the identification of stereochemical properties of such compounds were reported for the cyclic product, which were observed by *in situ* hydrogenation. Access to *3R,4S* (RhuA) and *3R,4R* (FucA) configuration products requires DHAP dependent aldolases and, after selective dephosphorylation, the target molecule was isolated by the SPE purification protocol. When phenyl acetaldehyde was used as aldol acceptor for Pathway I or for Pathway II, the depicted spectra were observed (**Figure 126**).

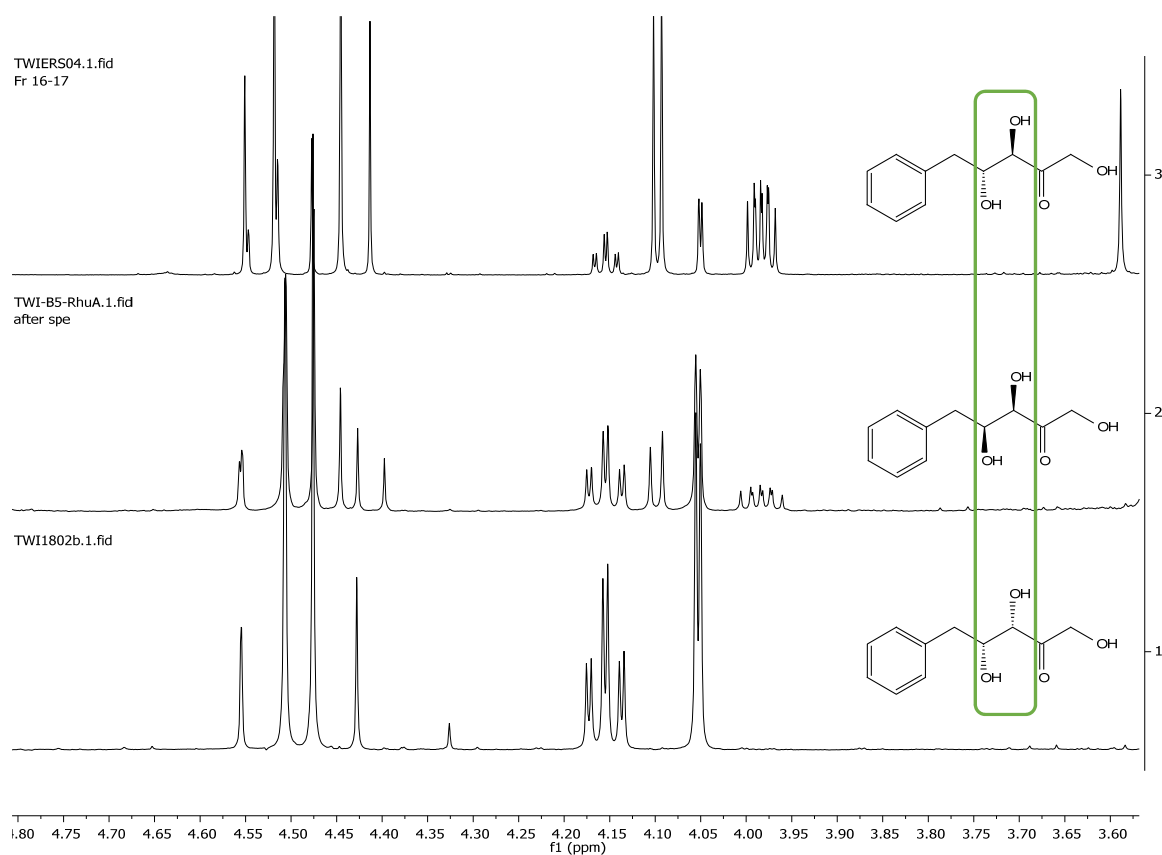


Figure 126 ^1H NMR of aldol all isolated aldol diastereomers observed by Pathway I or by *in vitro* biotransformations using FucA/RhuA with Phon-Sf.

The given spectra (TWI180b) represents the *3S,4R* isomer (*syn* configuration), which is exclusively formed by the Fructose-6-phosphate variant Fsa1 A129S. According to textbooks, the opposite *syn* isomer can be synthesized by simply selecting RhuA as a catalyst for the C-C bond formation between aldehyde and DHAP. As shown in Figure 125, a mixture of *syn* (4.05 ppm, d & 4.16 ppm, dt) and *anti* (4.00 ppm, m & 4.10 ppm, d) isomers in a 70/30 ratio was obtained for the two step transformation (Pathway II) of phenyl acetaldehyde. Additionally, the asymmetric synthesis of the related *anti* isomer catalyzed by FucA was not observed diastereomerically pure (*syn/anti* 20/80).

These results fit to reported data where the effect of reaction temperature, solvent, acceptor/donor concentration etc. for the stereochemical properties was discussed.²³⁶ Additionally, an issue for these experiments the used cell free extract, since *E. coli* contains both stereocomplementary aldolases (FucA & RhuA) which is mainly responsible for the observed *syn/anti* mixtures.

A VII Pathway II-*In Vivo* Setting Evaluation

In vitro studies confirmed the compatibility and activity of FucA and Phon-Sf under nearly physiological conditions (pH 6.9). The capability of an aldolase to utilize the donor molecule provided by the organism's central carbon metabolism (glycolysis) to afford phosphorylated aldol adducts is investigated. To overcome intercellular accumulation of phosphorylated material, which can lead to an increased metabolic burden, dephosphorylation by a co-expressed phosphatase is mandatory for product secretion. Hijacking DHAP from glycolysis of the host organism can charge the energy balance and may reduce growth of bacterial cells and therefore of course also the DHAP supply is limited (**Figure 127**). To identify such bottlenecks, studies with different aldol acceptors (**B₃**, **L₃**) in various solvents were conducted (**Figure 130, 132 & 133**).

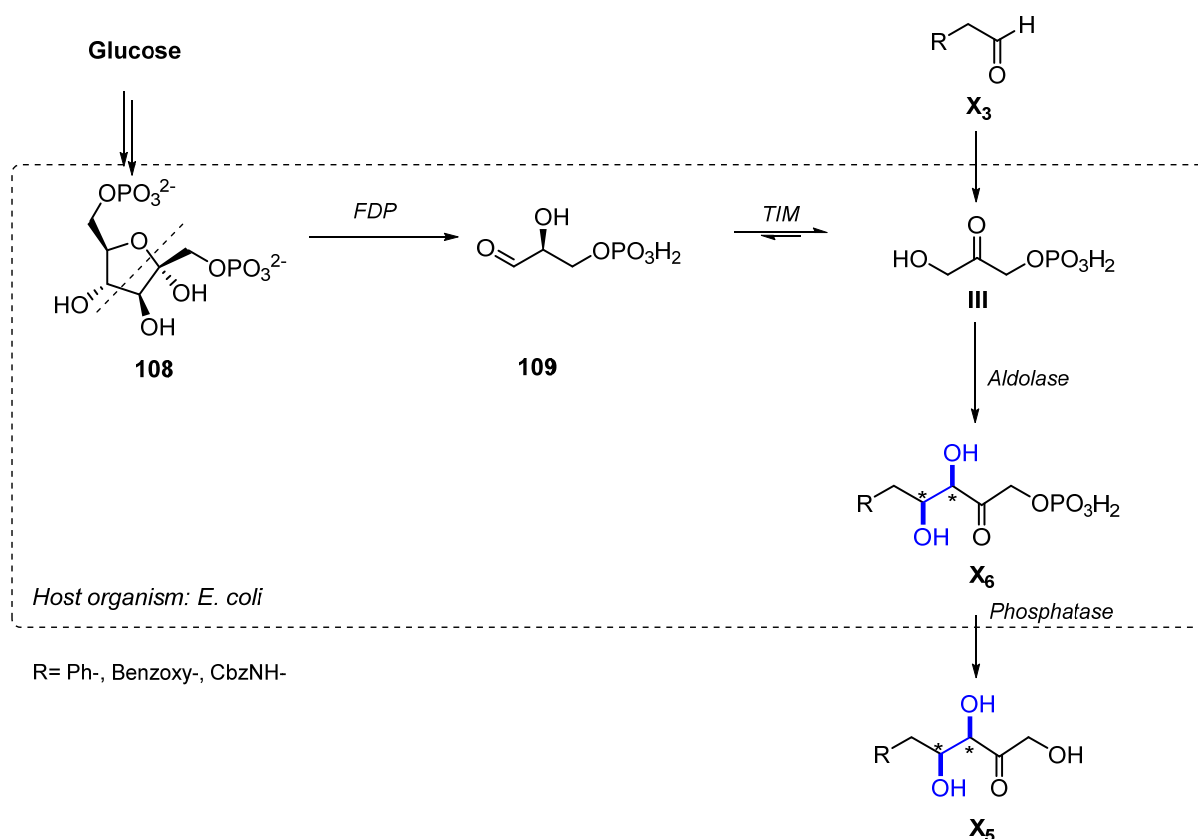


Figure 127 Illustration of the general Pathway II assembly containing a DHAP dependent aldolase, an acidic phosphatase and the aldol donor DHAP is hijacked form the central carbon metabolism of the host organism.

²³⁶ R. Schoevaart, F. van Rantwijk, R. A. Sheldon, *Biotechnol. Bioeng.* **2000**, *70*, 349-352.

Since the *in vitro* biotransformations using 5 mM substrate gave promising aldehyde consumption over 24 h, growing cells of co-expressed FucA and Phon-Sf were prepared and growth rates as well as substrate conversion and product formation were evaluated by GC/FID and HPLC.

A recombinant *E. coli* strain consisting of co-expressed *fucA* and *phon-sf* genes (two plasmids) was grown overnight at 37°C, 275 rpm in the pre-culture medium LB-0.8G (LB medium with 0.8 g/L glucose) (Table 50). Growing cells were prepared in 250 mL shaking flasks containing 15 mL of the auto induction medium LB 5052 (Table 50) and were inoculated with 30 µL overnight culture (ONC) for 4 h at 37°C and 275 rpm. Prior to induction, the temperature was reduced to 20°C, 1 mM ZnCl₂ was added and after additional 2 h, 5 mM phenyl acetaldehyde (**B₃**) were fed to the growing cells.

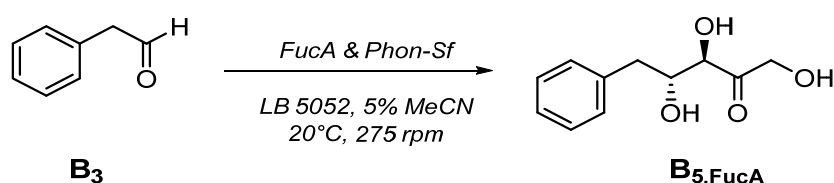


Figure 128 *In vivo* cascade for the synthesis of (3R,4R)-1,3,4-trihydroxy-5-phenylpentan-2-one.

To determine the growth behavior in presence of substrate (cytotoxic aldehyde) and organic solvent (acetonitrile or DMF), OD₅₉₀ values of the main culture with or without substrate addition were compared. To evaluate the product formation as well as starting material consumption samples after 0, 2, 6 and 24 h of aldehyde addition were analyzed by HPLC and GC/FID.

As shown in Figure 128 for the control experiment (without addition of substrate/organic solvent), the exponential growth starts shortly after induction (4 h). With focus to a sufficient DHAP production, which should occur during that growth period, the substrate was added after 6 h.

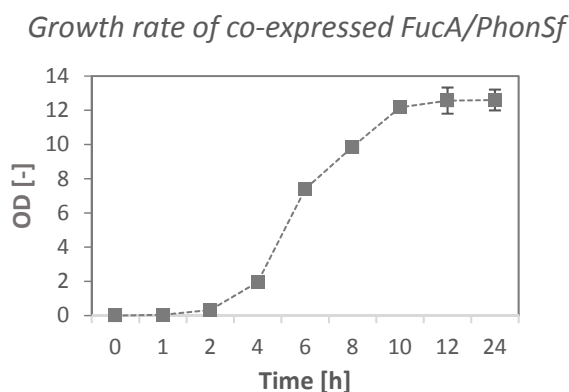


Figure 129 Growth rate of co-expressed FucA/Phon-Sf in LB 5052.

Addition of 5 mM phenyl acetaldehyde in 5% v/v acetonitrile after 6 h, has affected the growth behavior of cells dramatically or more precisely, cell growth was immediately interrupted at OD₅₉₀=7.0 (Figure 129, left).

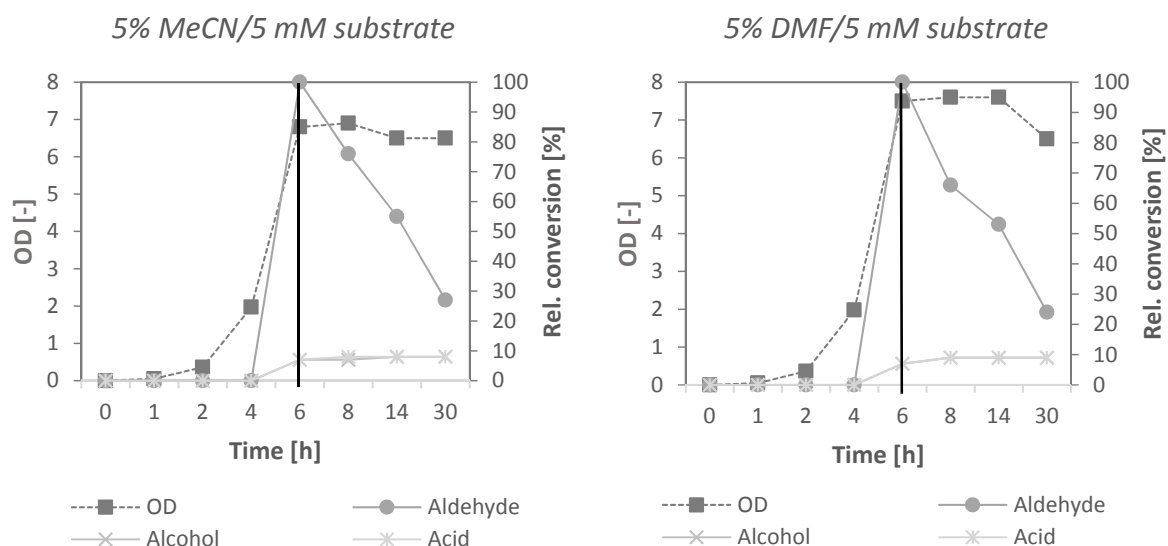


Figure 130 Aldehyde consumption and aldol adduct formation vs. cell growth after the addition of B_3 in 5% acetonitrile or DMF over time.

A similar drop in growth for co-expressed FucA/Phon-Sf growing cells was observed after the addition of 5 mM starting material and 5% v/v DMF (**Figure 129, right**). The reactions progress was again monitored *via* GC/FID and LC/MS but no product formation was indicated by HPLC, but the aldehyde consumption by GC/FID was detected. The decreasing concentration may be occurring due to evaporation, since the reaction was performed in shaking flasks at 275 rpm and 25°C. Another reason can be that the cytotoxic aldehyde was metabolized to any unknown or detectable side product (GC/FID or LC/MS).

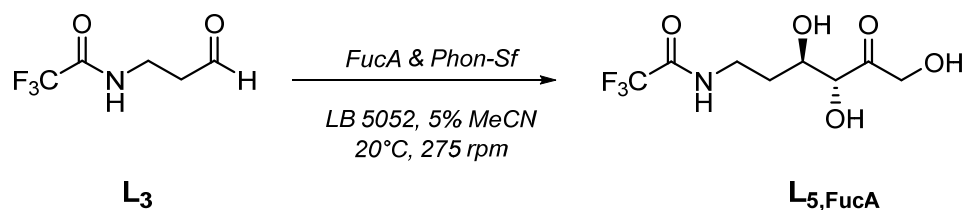


Figure 131 *In vivo* cascade for the synthesis of the 2,2,2-trifluoro-*N*-((3*R*,4*R*)-3,4,6-trihydroxy-5-oxohexyl)acetamide using the water soluble aldehyde 3-trifluoroacetoamindo-propanal.

The water solubility of aldehydes can be yield determining and to overcome this bottleneck, 3-trifluoroacetoamindo-propanal was introduced as perfectly suitable due to the excellent solubility in water and also high activities of DHAP aldolases towards this compound were observed.²³⁷

As demonstrated in Figure 131, CF_3CO -protected amino-propanal as well as the corresponding alcohol, which should be in general less cytotoxic, turned out to be also growth detrimental in presence of

²³⁷ M. Wei, Z. Li, T. Li, B. Wu, Y. Liu, J. Qu, X. Li, L. Li, L. Cai, P. G. Wang, *ACS Catal.* **2015**, *5*, 4060-4065.

acetonitrile (5% v/v). Interestingly, the neat addition of the water-soluble aldehyde after 6 h led to similar growth behavior, compared with the control experiment (without substrate/organic solvent).

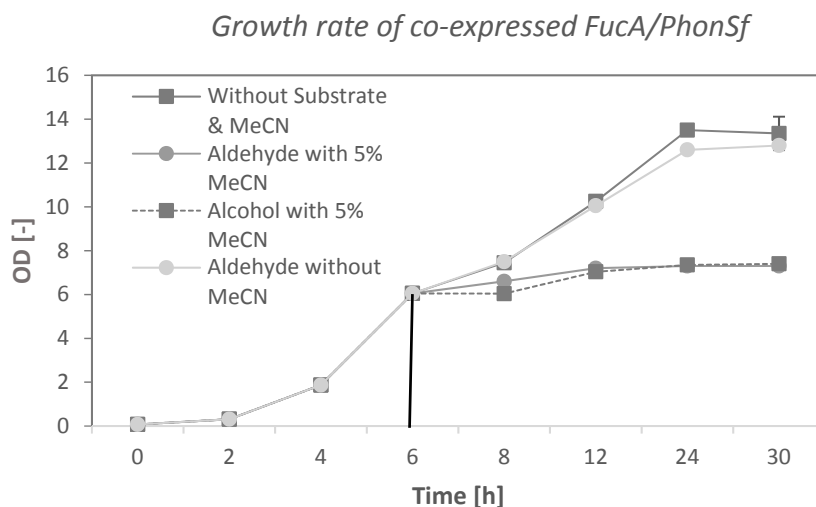


Figure 132 Consumption of 3-trifluoroacetoamindo-propanal or 3-trifluoroacetoamindo-propanal and aldol adduct formation vs. cell growth in 5% acetonitrile over time.

Unfortunately, analytical scale as well as preparative *in vitro* experiments using 3-trifluoroacetoamindo-propanal as substrate did not lead to the desired product (**Figure 132**). These preliminary results indicate that the amount of organic solvent is the major problem for growing cells. Therefore, solvent studies with our model substrate **B₃** in different concentrations of acetonitrile, DMF, and dioxane were accomplished (**Figure 133**).

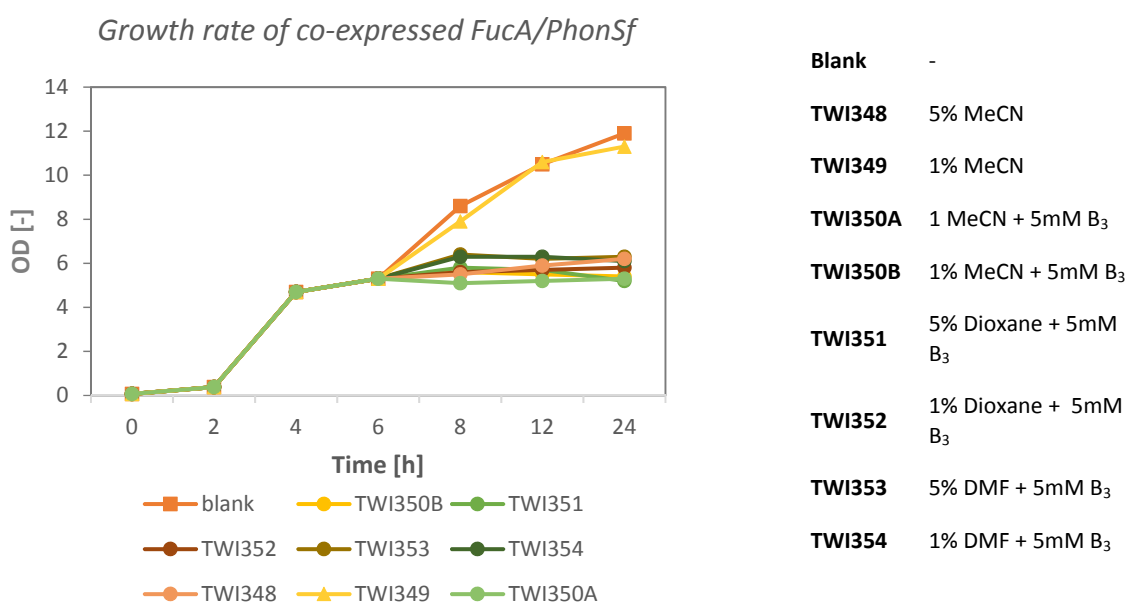


Figure 133 Growth rate of co-expressed FucA/Phon-Sf in LB 5052 using 5mM phenylacetaldehyde with different solvents and concentrations.

The observed cell growth results demonstrate that the combination of aldehyde and with organic solvent (>1%) is the limiting factor. To overcome this, a possibility would be to implement ALKJ to Pathway II and primary alcohols can serve as starting material as seen in Pathway I. But as shown by the growth curve in Figure 133, the combination of acetonitrile and a primary alcohol also turned out to be not suitable and a careful monitoring/evaluation of optimal fermentation conditions have to be performed.

A VIII Conclusion and Outlook of Pathway II

To summarize the results of Pathway II:

- (1) Isolation and characterization of phosphorylated aldol compounds (**B₆**) synthesized by a four-step sequence or *via* the DHAP dependent aldolase RAMA.
- (2) *In vitro* Pathway II assembly led to the isolation of related FucA, FruA (RAMA), and RhuA diastereomers in moderate yields by the established SPE purification.
- 3) Finally, *in vivo* test experiments using co-expressed FucA/ Phon-Sf were performed and the limited product formation due to different parameters (e.g. DHAP concentration, solvent, aldehyde toxicity) depicts a major bottleneck of Pathway II. Despite the fact that the cell growth is interrupted by the addition of substrate and consequently the host organism cannot manage the DHAP (**III**) supply, higher quantities of DHAP would be beneficial to improve the overall performance of Pathway II.

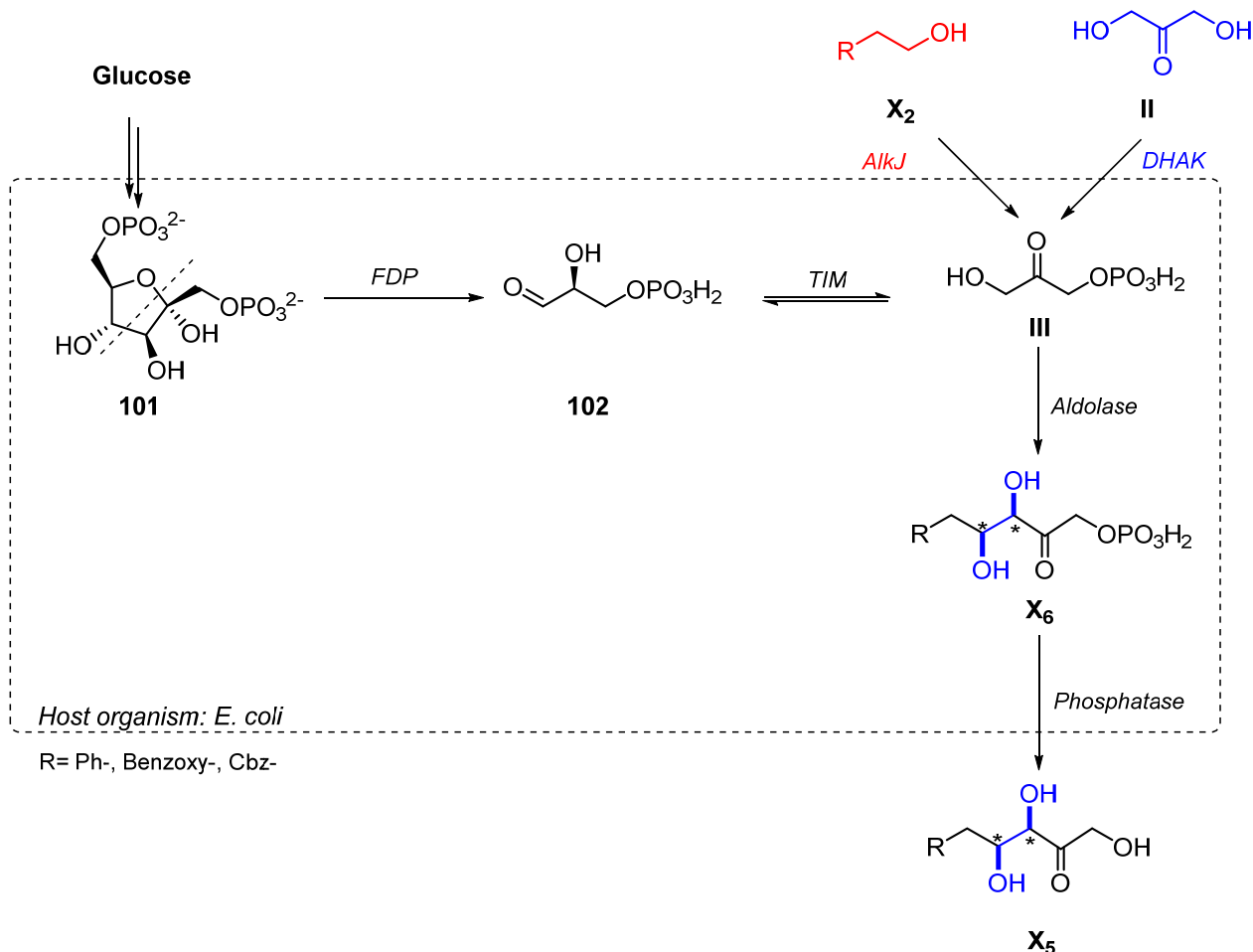


Figure 134 Illustration of an artificial pathway, containing a DHAP dependent aldolases and phosphatase to afford dephosphorylated aldol adducts. Additionally, DHAK to enhance the DHAP concentration in cell and AlkJ are implemented.

To enhance the DHAP concentration in the cell, the heterologous introduction of the ATP-dependent DHAK dihydroxyacetone kinase (DHAK) will be a future solution (**Figure 134**).^{238,239,240} Until now, in several *in vitro* cascade approaches, DHAK was used for phosphorylation of DHA and was successfully combined with DHAP dependent aldolases to afford the corresponding polyhydroxylated target molecule. Since the uptake of DHA by *E. coli* was studied in detail for Pathway I, DHAK combined with Pathway II can boost the overall performance. With regards to the observed *E. coli* background activity (CFE of Phon-Sf), the use of an *E. coli* related phosphatase (e.g YqaB from *E. coli*) can reduce the metabolic burden and can increase the substrate flux through Pathway II.

²³⁸ L. Iturrate, I. Sanchez-Moreno, E. G. Doyaguez, E. Garcia-Junceda, *Chem. Commun.* **2009**, 1721-1723.

²³⁹ L. Iturrate, I. Sánchez-Moreno, I. Oroz-Guinea, J. Pérez-Gil, E. García-Junceda, *Chem. Eur. J.* **2010**, *16*, 4018-4030.

²⁴⁰ I. Sánchez-Moreno, L. Iturrate, E. G. Doyagüez, J. A. Martínez, A. Fernández-Mayoralas, E. García-Junceda, *Adv. Synth. Catal.* **2009**, *351*, 2967-2975.

Experimental part

A IX Materials and Methods—General & Chemical Synthesis

Unless noted otherwise, all reagents were purchased from commercial suppliers and used without further purification. DCM, Et₂O, dioxane, MeOH, THF and toluene intended for water-free reactions were pre-distilled and then desiccated on Al₂O₃ columns (PURESOLV, Innovative Technology). Chromatography solvents were distilled prior to use. For all other solvents quality grade is given in the reaction procedures.

NMR spectra were recorded from CDCl₃, D₂O, DCl or methanol-d₄ solutions on a Bruker AC 200 (200 MHz), Bruker Advance UltraShield 400 (400 MHz) or Bruker Advance UltraShield 600 (600 MHz) spectrometer and chemical shifts are reported in ppm using tetramethylsilane as an internal standard. Whenever possible calibration *via* residual solvent peaks was performed. Peak assignment is based on correlation experiments or software prediction.

GC/MS analysis was carried out on a Thermo Finnigan Focus GC/DSQ II equipped with a standard capillary column BGB5 (30m x 0.32 mm ID).

GC/FID analysis was carried out on a Thermo Finnigan Focus GC/DSQ II using an RXi-5Sil MS (15 m x 0.25 mm ID, 0.1 μm film) column with Thermo Focus GC/FID detector.

LC/MS analysis of aldolase mediated reactions was performed on UPLC (Nexera Shimadzu) using an ROA-Organic Acid H⁺ (8%) column and isocratic elution (HPLC grade H₂O with 0.1 % FA). Peak detection was enabled by a photodiode array detector (PDA) for quantification of analytes at λ = 190 nm; the refractive index (RI) detector and the electrospray ionization (ESI) ion source with a quadrupole mass analyzer (LC/MS 2020 Shimadzu).

HPLC analysis for reaction monitoring of esterase mediated hydrolysis was conducted on the same UPLC machine using an Kinetex[®] (5μm C18 100 Å, 150 x 4.6 mm, Phenomenex, USA) column and water/acetonitrile gradient elution.

HPLC analysis for reaction monitoring of phosphorylated aldol adducts was performed on a 1200 series system (Agilent Technologies, USA) using a Kinetex[®] (5μm C18 100 Å, 50 x 4.6 mm, Phenomenex, USA) column and water/acetonitrile gradient elution. Peak detection was enabled *via* DAD (Agilent Technologies) as well as a Bruker HCT Esquire Ion Trap MS.

HR-MS analysis was carried out from methanol solutions (concentration: 10 ppm) by using an HTC PAL system autosampler (CTC Analytics AG, Zwingen, Switzerland), an Agilent 1100/1200 HPLC with binary pumps, degasser and column thermostat (Agilent Technologies, Waldbronn, Germany) and Agilent 6230 AJE-ESI-TOF mass spectrometer (Agilent Technologies, Palo Alto, United States).

Preparative reversed phase column chromatography was performed on a Waters auto-purification system [2545 (Binary gradient module); SFO (System fluidics organizer); 2767 (Sample manager)] using an xSelect® CSHTM C18 5 µm (4.6 mm x 150 mm) column on an Acquity QDa detector.

Medium pressure liquid chromatography was performed on a Büchi Sepacore Flash System (2 x Büchi Pump Module C-605, Büchi Pump Manager C-615, Büchi UV Photometer C-635, Büchi Fraction Collector C-660) or standard manual glass columns using silica gel from Merck (40-63 µm) using LP, EtOAc or CH₂Cl₂ mixtures. In general, a ratio of 30:1 silica gel to compound mixture was used.

SPE purification was performed on a Grace REVELERIS X Flash Chromatography System with integrated ELS/UV/UV-Vis detection using a BUCHI Sepacore Flash Cartridge (C18; 25 g) and HPLC grade water or methanol. Preparative column chromatography was performed on a Waters auto-purification system [2545 (Binary gradient module); SFO (System fluidics organizer); 2767 (Sample manager)] using an xSelect® CSHTM C18 5 µm (4.6 mm x 150 mm) column on an Acquity QDa detector.

Specific rotation was measured on an Anton Paar MCP500 polarimeter at the specified conditions.

Melting points were recorded on a Büchi B-545 melting point apparatus and are uncorrected.

Microwave reactions were carried out in a BIOTAGE Initiator sixty.

A Zenyth 3100 plate reader was used to determine protein concentration (Bradford; 590 nm) as well as for the esterase (405 nm) and phosphatase activity (405 nm).

For thin layer chromatography (TLC), alumina backed silica gel 60 F254 (Merck) and for reversed phase (RP)-TLC, aluminum TLC plates, RP-18 modified silica gel F254s (Merck) with different staining solutions were used (**Table 47**).

Table 44 Recipes for TLC staining solutions used in this thesis.

KMnO ₄		Cerium molybdate		Anisaldehyde	
6 g	KMnO ₄	10 g	phosphomolybdic acid hydrate	3.5 mL	p-Anisaldehyde
0.5 g	KOH	1 g	cerium ammonium nitrate	350 mL	EtOH
40 g	K ₂ CO ₃	20 g	H ₂ SO ₄ conc.	15 mL	AcOH
600 mL	dH ₂ O	300 mL	EtOH	50 mL	H ₂ SO ₄ conc.

A X Materials and Methods– Enzyme Production, SDS-PAGE Analysis, Biocatalyst Preparation and Characterization

Unless noted otherwise, all reagents were purchased from commercial suppliers and used without further purification. All (plastic) consumables and standard glass equipment were either sterile upon purchase or sterilized prior to use by autoclaving (121°C, 15 min, elevated pressure; Tuttnauer 2540EL autoclave). All reagent and media solutions were sterilized prior use by autoclaving (121°C, 20 min, elevated pressure; Tuttnauer 2540EL autoclave).

A X.1 General Stock Solutions

All of the following aqueous stock solutions were sterilized by filtration (sterile syringe filter, 0.2 µm cellulose acetate). Stock solutions were stored at -20°C. The Cam stock was not sterilized by filtration.

Table 45 Commonly used stock solutions.

Reagent	Concentration in dH₂O	Standard working concentration
Amp	50 mg/mL	100 µg/mL
Cam	34 mg/mL (in abs. EtOH)	34 µg/mL
Kan	50 mg/mL	50 µg/mL
IPTG	0.1 M	Varying
PMSF	0.1 mM (in abs. ⁱ PrOH)	0.1 µM

All of the following aqueous stock solutions were sterilized by filtration (sterile syringe filter, 0.2 µm cellulose acetate). Stock solutions were stored at -20°C. The Cam stock was not sterilized by filtration.

A X.2 Standard Media Preparations

Unless noted otherwise, amounts of reagents refer to the preparation of 1000 mL medium. All media were stored in the dark at room temperature after sterilization and, once opened, at 4 C. Visual control was done prior to use.

Table 46 Constituents of all bacterial growth media used in this thesis.

LB Medium		TB Medium	
10 g	bacto-peptone	12 g	bacto-tryptone
5 g	yeast extract	24 g	yeast extract
10 g	NaCl	16.4 g	K ₂ HPO ₄ 3*H ₂ O
		2.3 g	KH ₂ PO ₄

For LB-0.8G and LB-5052 (auto induction medium (AIM)), bacto-peptone, yeast extract and NaCl were dissolved, filled up to 929 mL with dH₂O and was sterilized by autoclavation. The 1 M MgSO₄, 20x NPS, 50x 5052, and 40% (w/v) glucose were prepared and autoclaved separately and added under sterile conditions. LB-0.8G was used for pre-culture preparation and LB-5052 for bacterial growth and enzyme production.

Table 47 Constituents of bacterial autoinduction medium (AIM).

LB-0.8G		LB-5052 (AIM)		20x NPS		50x 5052	
10.0 g	Bacto-peptone	10.0 g	Bacto-peptone	66.0 g	(NH ₄) ₂ SO ₄	250 g	Glycerol
5.0 g	Yeast extract	5.0 g	Yeast extract	136 g	KH ₂ PO ₄	25.0 g	Glucose
10.0 g	NaCl	10.0 g	NaCl	142 g	Na ₂ HPO ₄	100 g	α-lactose
1.0 mL	1 M MgSO ₄	1.0 mL	1 M MgSO ₄				
20.0 mL	40%(w/v) glucose	20.0 mL	50x 5052				
50.0 mL	20x NPS	50.0 mL	20x NPS				

All stock solutions were prepared and sterilized separately (**Table 50**). Trace element solution, 1 mM thiamine-HCl, 0.1 FeCl₃ and 20% (w/v) glucose were sterilized by filtration (sterile syringe filter, 0.2 μm cellulose acetate). For M9-N*medium preparation, all solutions were mixed under sterile conditions and filled up to the final volume with sterile dH₂O.

Table 48 Constituents of bacterial minimal media used in this thesis.

M9-N* Medium		100x Trace Elements Solution		10x M9 salts	
100 mL	10x M9 salts	0.18 g	ZnSO ₄ ·7*H ₂ O	5.0 g	NaCl
1.0 mL	1.0 M MgSO ₄	0.12 g	CuCl ₂ ·2*H ₂ O	75.0 g	Na ₂ HPO ₄ 2*H ₂ O
1.0 mL	0.1 M CaCl ₂	0.12 g	MnSO ₄ ·H ₂ O	30.0 g	KH ₂ PO ₄
0.6 mL	0.1 M FeCl ₃ ·6*H ₂ O	0.18 g	CoCl ₂ ·6*H ₂ O	24.0 g	(NH ₄) ₂ SO ₄
2.0 mL	1 mM thiamine·HCl	0.03 g	H ₃ BO ₃		
10.0 mL	Trace elements sol.	0.025 g	Na ₂ MoO ₄ 2*H ₂ O		
100 mL	20% (w/v) glucose	0.084 g	Na ₂ EDTA 2*H ₂ O		

All stock solutions, which were used for the preparation of resting cell medium or 10x M9 salts (N free) were sterilized separately (Table 49). For resting cell medium preparation, components were mixed under sterile conditions and filled up to the final volume with sterile dH₂O.

Table 49 Constituents of resting cell medium.

Resting cell medium		10x M9 salts (N free)	
100 mL	10x M9 salts (N free)	5 g	NaCl
3 mL	1 M MgSO ₄	75 g	Na ₂ HPO ₄ 2*H ₂ O
1 mL	1 M CaCl ₂	30 g	KH ₂ PO ₄
50 mL	20% (w/v) glucose ^[a]		

^[a] Sterile filtration with a sterile syringe filter, 0.2 µm cellulose, acetate membrane (VWR) and was added prior to use.

A X.2.1 Buffer Solutions

All used buffer solutions were prepared according to Table 50, pH was adjusted with the related acid or base and filled up to the final volume with dH₂O.

Table 50 Constituents of aqueous buffer solutions used in this thesis, diluted with 1000 mL dH₂O.

50 mM Tris HCl (pH 7.5)		50 mM Borate (pH 7.1)		50 mM Gly Gly (pH 8.0)	
6.05 g	Tris hydrochloride	10.06 g	Na ₂ B ₄ O ₇	6.61 g	GlycylGlycine

A X.2.2 SDS Sample Buffer

For 10% APS stock solution, 50 mg APS were dissolved in 500 µL dH₂O and stored at 4°C. For a 30% acrylamide/bis-acrylamide, acrylamide and bis-acrylamide were weighed carefully by the use of protective equipment and dissolved in 100 mL, filtrated (0.4 µm acetate filter), and store at 4°C in the dark. For a SDS stock solution, SDS was weighed carefully by the use of protective equipment and dissolved in 100 mL, and stored at room temperature.

Table 51 Constituents of 10% APS, 30% Acrylamide/bis-acrylamide, and 10% SDS.

10% APS		30% Acrylamide/bis- acrylamide		10% SDS	
50.0 mg /500 µL	APS	29.2 g	Acrylamide	10.0 g	SDS
		0.8 g	bis-acrylamide		

To 950 µL SDS sample buffer, 50 µL β-mercaptoethanol are added prior to use.

Table 52 Constituents of SDS sample buffer and 10x running buffer.

SDS sample buffer		10x Running buffer	
3.55 mL	dH ₂ O	30.3 g	Tris hydrochloride
1.25 mL	0.5 M Tris-HCl (pH 6.8)	144 g	glycerin
2.5 mL	Glycerol	10 g/L	SDS
2.0 mL	10% (w/v) SDS		
0.2 mL	0.5% (w/v) bromophenol blue		

A XI Bacterial Growth and Enzyme Production

For bacterial growth and protein production, either LB medium, LB-0.8G, LB-5052, TB medium or M9-N* medium were prepared according to Table 46 and Table 47.

Bacterial cultures were incubated in baffled Erlenmeyer flasks in orbital shakers (InforsHT Multitron 2 Standard) at 200 rpm. Bacteria on Agar plates were incubated in an Heraeus Instruments FunctionLine incubator under air. All materials and biotransformation media were sterilized by autoclaving at 121°C for 20 min. Various aqueous stock solutions were sterilized by filtration through 0.20 µm syringe filters. Agar plates were prepared with LB_{amp} medium supplemented by 1.5% w/v Agar Agar. Cells lysis for the preparation of CCEs was affected using a Bandelin KE76 sonotrode connected to a Bandelin Sonopuls HD 3200 wave generator.

Table 53 Expression conditions of used esterases Pfe I and BS2

Enzyme(s)	Pfe I	BS 2
Vector	pET21b(+)	pRR
Marker (µg · mL ⁻¹)	Amp (100)	Cam (34)
Medium	TB	TB
OD ₅₉₀ (rpm/°C)	0.5 (120/37)	0.3 (120/37)
Supplement (rpm/°C/h)	-	-
IPTG [mM]	1	0.025
Expression (rpm/°C/h)	120/30/20	120/25/20
SDS-PAGE [kDa]	26.7	24

Table 54 Expression conditions of all enzymes used for Pathway I.

Enzyme(s)	LK-ADH	RR-ADH	ADH-ht	ADH-a	AlkJ	Fsa1 A129S	AlkJ + Fsa1 A129S	AlkJ + Fsa1 A129S
Vector	pET21b(+)	pRR	pET26b(+)	pET22b(+)	pKA1	pET16b	pKA1 + pET16b	pKA1
Marker (µg/mL)	Amp (100)	Cam (34)	Kan (50)	Amp (100)	Cam (34)	Amp (100)	Amp (100) Cam (34)	Cam (34)
Medium	TB	TB	TB	TB	TB	TB	M9-N*	[a]
OD₅₉₀	0.5	0.3	0.5	+	++	0.6	0.5	0.5
(rpm/°C)	(120/37)	(120/37)	(120/37)	(120/30)	(120/30)	(200/37)	(275/37)	(275/37)
Supplement (rpm/°C/h)	-	1 mM ZnCl ₂	1 mM ZnCl ₂	1 mM ZnCl ₂	-	1 mM ZnCl ₂	1 mM ZnCl ₂	1 mM ZnCl ₂
		(120/25/0.5)	(120/20/0.5)			(120/20/0.5)	(120/20/0.5)	
IPTG [mM]	1	0.025	1	2	0.5	0.5	0.5	[a]
Expression (rpm/°C/h)	120/30/20	120/25/20	120/20/22	120/20/24	120/25/20	200/30/18	150/25/20	150/20/20
SDS-PAGE [kDa]	26.7	24	36.3	37.5	55	20	55 + 20	55 + 20

+ Growth at given conditions overnight prior to induction; ++ growth for 6 h prior to induction, [a] LB-0.8G: Auto induction media (AIM) (2.0% (ω/v) α-lactose)

Table 55 Expression conditions of all enzymes used for Pathway II.

Enzyme(s)	FucA	FruA	RhuA	Phon-Sf	FucA + Phon-Sf
Vector	pKA1	pKK	pKK	pET26b(+)	pKA1+ pET26b(+)
Marker (µg/mL)	Cam (34)	Amp (100)	Amp (100)	Kan (50)	Cam (34) + Kan (50)
Medium	[a]	TB	TB	[a]	[a]
OD₅₉₀	2.0	0.5	0.5	2.0	2.0
(rpm/°C)	(275/37)	(150/37)	(150/37)	(275/37)	(275/37)
Supplement (rpm/°C/h)	1 mM ZnCl ₂	1 mM ZnCl ₂	1 mM ZnCl ₂		1 mM ZnCl ₂
IPTG [mM]	[a]	0.1	0.1	[a]	[a]
Expression (rpm/°C/h)	150/20/20	150/25/20	150/20/22	150/20/6	150/20/20
SDS-PAGE [kDa]	22	36	27	27	22+ 27

[a] LB-0.8G: Auto induction media (AIM) (2.0% (w/v) α-lactose)

All expression studies and optimizations were conducted by T. Bayer.²⁴²

²⁴¹ 1 mM ZnCl₂ was added 30 min prior to induction

²⁴² T.Bayer, PhD 2017.

A XII General Protocol for Protein Expression & Cell Free Extract Preparation

A XII.1 Preparation of Permanent Cultures

The respective *E. coli* strain were incubated at 37°C on LB plates with the appropriated antibiotic for 12-24 h. A single colony was selected and 10 mL pre-culture was inoculated and incubated (10 mL LB-amp, 50 mL shaking flask, 37°C, 12–24 h). After addition glycerol in a ratio of 1:2, the mixture was transferred in 1 mL aliquots into Eppendorf vials and stored at -80°C until further use.

A XII.2 Preparation of LB Agar Plates

Permanent culture was used to prepare an LB plate containing the right antibiotic and the plate was incubated in the cabinet (37°C) o/n. The plate was closed by a parafilm foil and stored at 4°C for maximum 2 months.

A XII.3 Preparation of pre-cultures– LB medium

A single colony of desired *E. coli* strain was picked and transferred to a 10 mL Greiner tube to prepare an o/n culture in LB medium containing the right antibiotic (4 mL) at 37°C, 200 rpm.

A XII.4 Preparation of Pre-cultures-LB-0.8G

A single colony of desired *E. coli* strain was picked and transferred to a 25 mL baffled Erlenmeyer flask to prepare an o/n culture in LB-0.8G medium containing the right antibiotic (10 mL) at 37°C, 275 rpm.

A XII.5 Preparation of Growing Cells of Pfel or BS2

A 15 mL Greiner tube was charged with LB medium with appropriate antibiotics supplement (4 mL), inoculated with a bacterial single colony from an Agar plate and incubated at 37°C in an orbital shaker o/n. The biotransformation medium, supplemented with appropriate antibiotics, was then inoculated with 1% v/v of the preculture and incubated for approx. 2-3 h under the same conditions until an optical density of 0.2-0.6 was reached. Protein production was induced with IPTG final (**Table 54**) and the main culture was shaken at 30°C, 120 rpm for additional 30 min and splitted into 24-well plates.

A XII.6 Preparation of Whole Cell Lyophilizates of *E. coli* BL21(DE3)/pET21b(+)_*lk-adh*

The pET21b(+) containing the *lk-adh* gene from *Lactobacillus kefir* was provided by Uwe T. Bornscheuer, Ernst-Moritz-Arndt University Greifswald, Germany. For the preparation of whole cell lyophilizates, 4 mL of LB medium supplemented with Amp (100 µg·mL⁻¹) were inoculated with a single colony of *E. coli* BL21(DE3)/pET21b(+)_*lk-adh* and incubated at 37°C, 200 rpm overnight. TB medium supplemented with Amp (100 µg·mL⁻¹) was inoculated with 1/100 culture volume of the pre-culture. Cells were grown at 37°C, 120 rpm until an OD₅₉₀= 0.5 was reached. Protein production was induced with 1 mM IPTG final concentration from a 0.1 M IPTG stock and expression performed at 30°C, 120 rpm. Cells were harvested by centrifugation (6 000 x g, 15 min, 4°C) after 20 h. The medium was discarded, cells re-suspended in sterile dH₂O, snap frozen in liquid nitrogen and lyophilized.

A XII.7 Preparation of Resting Cells of *E. coli* BL21(DE3)/pRR_*rr-adh*

The pRR vector containing the *rr-adh* gene from *Rhodococcus ruber* was provided by Uwe T. Bornscheuer, Ernst-Moritz-Arndt University Greifswald, Germany. For protein production, 4 mL of LB medium supplemented with Cam (37 µg·mL⁻¹) were inoculated with a single colony of *E. coli* BL21(DE3)/pRR_*rr-adh* and incubated at 37°C, 200 rpm overnight. TB medium supplemented with Cam was inoculated with 1/100 culture volume of the pre-culture. Cells were grown at 37°C, 120 rpm until an OD₅₉₀= 0.3 was reached, before 1 mM ZnCl₂ was added, cells were incubated with shaking at 25°C for 30 min. Protein production was induced with 25 µM IPTG and expression was performed at 25°C, 120 rpm. Cells were harvested by centrifugation (6 000 x g, 15 min, 4°C) after 22 h. Resting cells were prepared by resuspension in resting cell medium containing (1% (w/v) glucose, 8.6 mM NaCl, 42 mM Na₂HPO₄, 22 mM KH₂PO₄, 3 mM MgSO₄, 0.1 mM CaCl₂, 0.06 mM FeCl₃, 0.002 mM thiamine-HCl).

A XII.8 Preparation of Whole Cell Lyophilizates of *E. coli* BL21(DE3)/pET22b(+)_*adh-a*

The *adh-a* gene from *Rhodococcus ruber* was synthesized and subcloned by GenScript into pET22b(+) utilizing the 5' *NdeI* and the 3' *BamHI* restriction sites. For enzyme production, an adapted protocol from *Rhodococcus ruber* was used as briefly described in the following. TB medium (200 mL) supplemented with Amp (100 µg·mL⁻¹) was inoculated with a single colony of *E. coli* BL21(DE3)/pET22b(+)_*adh-a* in a 1 L baffled shaking flask. ZnCl₂ was added from a 100 mM stock to a

final concentration of 1 mM and cells were grown at 30°C with shaking (120 rpm) for about 20 h. The OD₅₉₀ was checked (OD₅₉₀≈ 6.0) and 200 µL of Amp stock solution (50 mg·mL⁻¹) were added. Protein production was performed in the presence of 2 mM IPTG and cells were cultivated at 20°C with shaking (120 rpm) for 24 h. Cells were harvested by centrifugation (6 000 x g, 15 min, 4°C). The medium was discarded, cells re-suspended in sterile dH₂O, snap frozen in liquid nitrogen and lyophilized.

A XII.9 Preparation of Cell Free Extract of *E. coli* BL21(DE3)/pET26b(+)_*adh-ht*

The *adh-ht* gene from *Geobacillus stearothermophilus* was synthesized by GenScript with flanking 5' *NdeI* and 3' *XhoI* restriction sites and delivered in a standard delivery vector. Expression conditions were adapted from *Bacillus stearothermophilus*. Briefly, 10 mL of LB supplemented with Kan (50 µg·mL⁻¹) were inoculated with a single colony of *E. coli* BL21(DE3)/pET26b(+)_*adh-ht* and incubated at 30°C, 120 rpm for 16 h. LB medium supplemented with Kan and 1 mM ZnCl₂ were inoculated with 1/335 culture volume of the preculture and incubated at 37°C, 120 rpm for 2 h. Protein expression was performed in the presence of 1 mM IPTG at 20°C, 120 rpm for 22 h. Cells were harvested by centrifugation (6 000 x g, 15 min, 4°C). *ADH-ht* was purified by heat shock (HS) as follows: The cell free extracts (CFEs) were incubated at 60°C in a water bath for 20 min and rested on ice for 2 h. The heat shock was repeated and insolubles separated by centrifugation at 14 000 x g, 4°C for 45 min.

A XII.10 Preparation of Resting Cells of *E. coli* BL21(DE3)/pKA1_*alkJ*

The expression protocol was used as published before. Briefly, 4 mL of LB supplemented with cam (34 µg·mL⁻¹) were inoculated with a single colony of *E. coli* BL21(DE3)/pKA1_*alkJ* and incubated at 37°C, 120 rpm overnight. TB medium supplemented with Cam was inoculated with 1/100 volume of the preculture and cells were grown at 37°C, 120 rpm for 6 h prior to induction of protein production by adding IPTG to a final concentration 0.5 mM. Expression was performed at 25°C, 120 rpm for 20–24 h. Cells were harvested by centrifugation (6 000 x g, 4°C, 15 min), the supernatant discarded and cells re-suspended in resting cell medium.

A XII.11 Preparation of Heat Shock-purified Fsa1 A129S Lyophilisates

Fsa1 A129S lyophilisates were prepared as follows: LB medium supplemented with Amp (100 µg·mL⁻¹) was inoculated with 1% (v/v) of a fresh *E. coli* BL21(DE3)/pET16b_*fsa1 A129S* overnight culture. Cells were grown with shaking (200 rpm) at 37°C until an OD₅₉₀= 0.5 was reached. Enzyme production was

induced with 0.5 mM IPTG and cells were cultivated at 30°C for 20 h. Cells were harvested by centrifugation (6 000 x g, 4°C for 20 min), re-suspended in 50 mM GlyGly buffer (pH 8.0), frozen at -20°C and thawed on ice. For cell lysis, 72 µL lysozyme (10 mg·mL⁻¹ dissolved in 10 mM GlyGly buffer), 4 µL 0.25 M EDTA (pH 8.0), 1 µL benzonase (1 kU·mL⁻¹) and 1 µL PMSF (0.1 M in *i*PrOH) per mL cell suspension were added. Lysis was performed with shaking (350 rpm) at 37°C for 1 h. Lysed cells were incubated at 70°C for 30 min and centrifuged (16 000 x g, 4°C for 20 min). The supernatant containing the soluble Fsa1 A129S was transferred into a round bottom flask, snap frozen in liquid nitrogen and lyophilized.

A XII.12 Preparation of Resting Cells of *E. coli* BL21(DE3)

For enzyme expression, a single colony of the desired *E. coli* (BL21 (DE3)) was incubated in 10 mL LB medium at 37°C with shaking (275 rpm) for 12–24 h. The main culture medium M9-N* was inoculated with 0.2% (v/v) of the pre-culture and incubated at 37°C with shaking (150 rpm) for 4 h. After the addition of IPTG, the temperature was lowered to 20°C and the main culture shaken for 20 h. For resting cell (RC) preparation, cells were harvested by centrifugation (6000 x g at 4°C, 15 min). The pellet was re-suspended in 1/10 volume of the main culture in resting cell medium and centrifuged. The washed cell pellet was re-suspended in a sufficient volume of resting cell medium until an OD₅₉₀ = 20.0 was reached.

A XII.13 Preparation of Resting Cells of Fsa1 A129

Resting cells of Fsa1 A129S were prepared as follows: LB medium supplemented with Amp (100 µg·mL⁻¹) was inoculated with 1% (v/v) of a fresh *E. coli* BL21(DE3)/pET16b_ *fsa1* A129S overnight culture. Cells were grown with shaking (200 rpm) at 37°C until an OD₅₉₀ = 0.5 was reached. Enzyme production was induced with 0.5 mM IPTG and cells were cultivated at 30°C for 20 h. For resting cell (RC) preparation, cells were harvested by centrifugation (6000 x g at 4°C, 15 min). The pellet was re-suspended in 1/10 volume of the main culture in resting cell medium and centrifuged. The washed cell pellet was re-suspended in a sufficient volume of resting cell medium until an OD₅₉₀ = 14 was reached.

A XII.14 Preparation of Pretreated Resting Cells of Fsa1 A129

Resting cells of Fsa1 A129S were prepared according to C IV.13. For pretreated resting cell (RC) preparation, cells were harvested by centrifugation (6000 x g at 4°C, 15 min). The pellet was re-suspended in 100 mM TrisHCl (pH 7.5) and 1% v/v toluene as well as 5 mM EDTA were added and the mixture was shaken (100 rpm) at 30°C for 10 min. Pretreated cells were collected by centrifugation

(3000 g x 10 min, 4°C) and the pellet was re-suspended in a sufficient volume of resting cell medium until an OD₅₉₀=14 was reached.

A XII.15 Preparation of Resting Cells Co-expressing AlkJ and Fsa1 A129S from Two Plasmids

Competent *E. coli* BL21(DE3) cells were co-transformed as described above with pKA1_alkJ and pET16b_fsa1 A129S. For enzyme expression, a single colony of the *E. coli* BL21(DE3) co-transformant was incubated in 4 mL LB medium containing the two antibiotics Cam (34 µg·mL⁻¹) and Amp (100 µg·mL⁻¹) with shaking (275 rpm) overnight at 37°C. The main culture medium M9-N* was inoculated with 1/75 of the culture volume in the presence of 1 mM ZnCl₂ at 37°C, 200 rpm until an OD₅₉₀ = 0.5 was reached. After the addition of IPTG to a final concentration of 0.5 mM, the temperature was lowered to 25°C and the main culture shaken at 150 rpm for 20 h. For resting cell preparation, cells were harvested by centrifugation (6000 x g at 4°C, 15 min). The pellet was re-suspended in 1/10 volume of the main culture in resting cell medium containing (1% (w/v) glucose, 8.6 mM NaCl, 42 mM Na₂HPO₄, 22 mM KH₂PO₄, 3 mM MgSO₄, 0.1 mM CaCl₂, 0.06 mM FeCl₃, 0.002 mM thiamine-HCl) and centrifuged. The washed cell pellet was re-suspended in a sufficient volume of resting cell medium until an OD₅₉₀ = 20.0 was reached. Resting cells were stored at 4°C up to one day. The preparation of resting cell medium was adapted from Cold Spring Harbor Protocols.²⁴³

A XII.16 Preparation of Resting Cells of the POP construct: AlkJ and Fsa1 A129S

For enzyme expression, a single colony of the desired *E. coli* transformant was incubated in 10 mL LB-0.8G medium supplemented with Cam (34 µg mL⁻¹) at 37°C with shaking (275 rpm; InforsHT Multitron 2 Standard) overnight. Auto-induction medium LB-5052 supplemented with Cam was inoculated with 0.2% (v/v) of the pre-culture and incubated at 37°C with shaking (150 rpm) for 4 h. The temperature was lowered to 20°C and the main culture shaken for 20 h. The preparation of AIM was in accordance to Studier *et al.*²⁴⁴ For resting cell (RC) preparation, cells were harvested by centrifugation (6000 x g at 4°C, 15 min). The pellet was washed with resting cell medium. The washed cell pellet was re-suspended in a sufficient volume of resting cell medium until an OD₅₉₀= 20.0 was reached. RCs were stored at 4°C up to one day.

²⁴³ Cold Spring Harbor Protocols **2010**, pdb.rec12295

²⁴⁴ F. W. Studier, *Protein expression and purification* **2005**, *41*, 207-234.

A XII.17 Preparation of Cell Free Extract of DHAP Dependent Aldolases (FruA, FucA, RhuA)

A XII.17.1 Fuculose-1,6-bisphosphate (FucA) Aldolase

For enzyme expression, a single colony of the desired *E. coli* transformant was incubated in 10 mL LB-0.8G medium supplemented with Cam ($34 \mu\text{g mL}^{-1}$) at 37°C with shaking overnight. Auto-induction medium LB-5052 supplemented with Cam was inoculated with 0.2% (v/v) of the pre-culture and incubated at 37°C with shaking (150 rpm) for 3.5 h. 1 mM ZnCl_2 was added prior to auto-induction after 4 h temperature to 20°C and the main culture was shaken for 20 h. For cell free extract preparation, cells were harvested by centrifugation ($6000 \times g$ at 4°C , 15 min) The pellet was washed with 50 mM Tris HCl buffer (pH 7.25) and centrifuged ($6000 \times g$ at 4°C , 15 min). The washed cell pellet was re-suspended with 50 mM Tris HCl buffer (pH 7.25) and cell lysis was performed by sonification in an ice bath with a 5 s pulse/55 s break interval for 9 min. The soluble and insoluble fractions were separated by centrifugation ($14000 \times g$ at 4°C , 20 min) and the protein concentration of the soluble fraction was determined by Bradford analysis. Cell free extracts were stored at -20°C up to 3 months.

A XII.17.2 Fructose-1,6-bisphosphate (FruA) & Rhamnulose-1,6-bisphosphate (RhuA) Aldolase

For enzyme expression, a single colony of the desired *E. coli* transformant was incubated in 4 mL LB medium supplemented with Amp ($100 \mu\text{g mL}^{-1}$) at 37°C with shaking overnight. TB medium supplemented with Amp was inoculated with 1% (v/v) of the pre-culture and incubated at 37°C with shaking (150 rpm) for 3.5 h. 1 mM ZnCl_2 was added prior to induction by IPTG and after 4 h temperature was decreased 20°C and the main culture was shaken at 120 rpm for 20 h. For cell free extract preparation, cells were harvested by centrifugation ($6000 \times g$ at 4°C , 15 min) The pellet was washed with 50 mM Tris HCl buffer (pH 7.25) and centrifuged ($6000 \times g$ at 4°C , 15 min). The washed cell pellet was re-suspended with 50 mM Tris HCl buffer (pH 7.25) and cell lysis was performed by sonification in an ice bath with a 5 s pulse/55 s break interval for 9 min. The soluble and insoluble fraction were separated by centrifugation ($14000 \times g$ at 4°C , 20 min) and the protein concentration of the soluble fraction was determined by Bradford analysis. Cell free extracts were stored at -20°C up to 3 months.

A XII.18 Preparation of Cell Free Extract of Phon-Sf

For enzyme expression, a single colony of the desired *E. coli* transformant was incubated in 4 mL LB medium supplemented with Kan ($50 \mu\text{g mL}^{-1}$) at 37°C with shaking overnight. TB medium supplemented with Amp was inoculated with 1% (v/v) of the pre-culture and incubated at 37°C with shaking (150 rpm) for 4 h. The temperature was lowered to 20°C and the main culture shaken for 20 h. For cell free extract preparation, cells were harvested by centrifugation ($6000 \times g$ at 4°C , 15 min) The pellet was washed with 50 mM Tris HCl buffer (pH 7.25) and centrifuged ($6000 \times g$ at 4°C , 15 min). The washed cell pellet was re-suspended with 50 mM Tris HCl buffer (pH 7.25) and cell lysis was performed by sonification in an ice bath with a 5 s pulse/55 s break interval for 9 min. The soluble and insoluble fraction were separated by centrifugation ($14000 \times g$ at 4°C , 20 min) and the protein concentration of the soluble fraction was determined by Bradford analysis. Cell free extracts were stored at -20°C up to 3 months.

A XII.19 Determination of Protein Concentration *via* Bradford

The final protein concentration of the soluble and insoluble fraction was measured by following the standard protocol using a platereader (Abs 595nm) in 96 well plates and was determined in duplicates. Therefore, pre-dilute protein samples 1:50 with dH_2O (insoluble and soluble fraction). Bradford reagent was prepared 1:5 with dH_2O and 200 μL were added to a 96 well plate. 5 μL of pre-diluted protein were added, shake to mix the sample and then incubate the sample 15 min at room temperature. Blanks were prepared with 200 μL Bradford reagent and 5 μL of dH_2O . In the well plate reader, the $\text{Abs}_{595\text{nm}}$ of the sample was determined. The protein concentrations were calculated by BSA standard calibration.

A XII.20 General Procedure for Expression Control-SDS PAGE

For SDS-PAGE analysis, a resolving gel as well as a stacking gel (volume for 2 gels or adjusted volume) were prepared as follows:

Table 56 Constituents of the resolving gel.

12% Resolving Gel	
2.72 mL	dH ₂ O
3.2 mL	30% Acrylamide/bis-acrylamide
2.0 mL	1.5 M Tris-HCl (pH 8.8)
80 µL	10% SDS
40 µL	10% APS
4 µL	TEMED

Mix the buffer solution, dH₂O, SDS, and acrylamide together and degas with N₂ for 15 min. Immediately prior to pouring the gel, add freshly prepared 10% APS and TEMED (inducer for radical polymerization) and swirl gently to initiate polymerisation. Allow the gel to polymerize for at least 30 min. Cover the resolving gel with a layer of isopropyl alcohol.

Table 57 Constituents of the stacking gel.

4% Stacking Gel	
3.66 mL	dH ₂ O
0.78 mL	30% Acrylamide/bis-acrylamide
1.5 mL	0.5 M Tris-HCl (pH 6.8)
60 µL	10% SDS
30 µL	10% APS

Mix the buffer solution, dH₂O, SDS, and acrylamide together and degas with N₂ for 15 min. Remove the isopropyl alcohol completely. Immediately prior to pouring the gel, add freshly prepared 10% APS and TEMED and swirl gently to initiate polymerization. Insert the combs and allow the gel to polymerize for at least 20 min. Expression control was done by SDS-PAGE analysis under reducing conditions. Whole cell samples (10 µL) were denatured in 30 µL SDS sample buffer (125 mM Tris-HCl, 50% (w/v) glycerol, 4% (w/v) SDS, 0.02% (w/v) bromophenol blue, 5% (v/v) β-mercapto-ethanol) and cell lysates (15 µL) with 25 µL SDS sample buffer for 10 min at 95°C, respectively. Routinely, 15 µL sample solution were loaded onto 12% (w/v) polyacrylamide gels and run at 13 mA/gel for sample stacking, then 25 mA/gel using the Mini-PROTEAN® system with a PowerPac Basic power supply (BioRad). Staining was performed in the microwave and adapted from user manual provided by the manufacturer. Briefly,

the resolving gel was covered with dH₂O and heated at 750 W for 1 min. It was incubated with shaking (120 rpm; PSU-10i, Grant-Bio) at RT for 2 min. The dH₂O was exchanged, heated at 500 W for 1 min and shaken at RT for 2 min. The water was discarded, the gel covered in SimplyBlue™ SafeStain solution (Novex®), incubated at 350 W for 45 s and shaken at RT for 5 min. The dyeing solution was discarded and the gel washed in dH₂O for 10 min. The gel was preserved in 20% (w/v) NaCl overnight.

A XIII General Biotransformation Conditions

A XIII.1 Pfe I & BS2 Biotransformation Conditions

Cultivation was performed according to **(Table 54)** and after induction by IPTG, the main culture was applied after one hour to the described esterase activity assay. Active growing cells of esterase PfeI or BS2 were shaken for additional 30 min and for each biotransformation 950 µL were transferred into 24-well plates. The reaction was started by the addition of 5 mM acetate and the hydrolysis process was monitored *via* LC/MS.

A XIII.1.1 LK-ADH Biotransformation Conditions

Whole cell powder containing LK-ADH (2 mg) were added to a solution of 5 mM alcohol (1 equiv.) in 160 µL acetone, 1 mM NAD⁺ and dissolved in a 50 mM Tris HCl buffer (pH 7.5) to a final volume ($V_R = 1000 \mu\text{L}$) and shaken at 250 rpm at 30°C in an orbital shaker. Positive control experiment was performed by using *rac*-phenylethanol.

A XIII.1.2 RR-ADH Biotransformation Conditions

E. coli BL21(DE3) RCs expressing RR-ADH ($OD_{590} = 10.0$) were mixed with 4 mM alcohol (1 equiv.) in 100 µL acetonitrile (HPLC grade) and filled up to a final volume of $V_R = 1000 \mu\text{L}$ with resting cell medium. The mixture was shaken at 30°C, 200 rpm in an orbital shaker. Positive control experiments were performed with cyclohexanol accordingly.

A XIII.1.3 ADH-a Biotransformation Conditions

Whole cell powder containing ADH-a (2 mg) were added to a solution of 5 mM alcohol (1 equiv.), 100 µL acetone (1 equiv.), 1 mM NAD⁺ in a 50 mM Tris HCl buffer (pH 7.5) to a final volume ($V_R = 1000 \mu\text{L}$) and shaken at 250 rpm at 30°C in an orbital shaker. Positive control experiment was performed by using *rac*-phenylethanol.

A XIII.1.4 ADH-ht Biotransformation Conditions

Purified cell free extract of ADH-ht (2 mg/mL) was added to a solution of 25 mM alcohol, 250 mM co-substrate 250 mM acetaldehyde (10 equiv.), 1 mM NAD⁺ dissolved in a 100 mM phosphate buffer (pH 7.0) to a final volume ($V_R = 1000 \mu\text{L}$) and shaken at 250 rpm at 30°C in an orbital shaker. Positive control experiments were performed by using benzylalcohol.

A XIII.1.5 AlkJ Biotransformation Conditions

Resting cells of AlkJ (typically $OD_{590} = 10$) were added to a solution of 5 mM substrate dissolved in 10% v/v MeCN and M9 minimal medium (N free) to a final volume ($V_R = 1000 \mu\text{L}$) and shaken at 200 rpm at 25°C in an orbital shaker.

A XIII.2 Alcohol Dehydrogenases-Sample Preparation for GC/FID

All enzyme mediated oxidations were monitored *via* GC/FID and for the analysis, 100 μL of the reaction mixture were added to 1.5 mL Eppendorf tube containing 10 μL 2 M HCl and 200 μL EtOAc supplemented with 1 mM methyl benzoate as internal standard (IS). It was vortexed at maximum speed for 30–35 s and spun down for 1 min (VWR Silverstar bench top centrifuge). The organic layer was transferred into a new 1.5 mL tube. The sample was extracted a second time with 190 μL EtOAc supplemented with 1 mM IS. The combined organic layers were dried over Na_2SO_4 and transferred into a 1.5 mL glass vial equipped with a 0.1 mL micro-insert.

A XIII.3 Screening Conditions using a Two-Plasmid System of AlkJ and Fsa1 A129S

Resting cells of the two-plasmid system were prepared as described above. 100 mM stock solution of 1,3-Dihydroxyacetone (DHA) dimer was dissolved in resting cell medium and for monomerization, the resulting solution was shaken at 250 rpm, 37°C for 3 h. The reaction mixture was prepared in 8 mL vials with screw cap as follows:

Table 58 Resting cell screening using two plasmid system.

Reaction mixture	Final concentration
2.600 mL RCs ($OD_{590} = 12.5$)	$OD_{590} = 10.0$
0.060 mL DHA monomer (1 M)	20 mM (4 equiv.)
0.333 mL Substrate (50 mM in MeCN)	5 mM (10% (v/v) MeCN)

A XIII.4 Parameter Optimization by the pseudo-operon (POP) Construct with Different DHA Concentrations

1,3-Dihydroxyacetone (DHA) dimer (0.9 g, 5 mmol) was dissolved in 9 mL resting cell medium and filled up to 10 mL. For monomerization, the resulting solution was shaken (250 rpm; InforsHT Multitron 2 Standard) at 37°C for 3 h. The final concentration was 1 M of the DHA monomer.

Resting cells of the desired *E. coli* BL21-Gold(DE3) containing the pKA1_alkJ:fsa1 A129S plasmid with the two genes in pseudo-operon configuration (referred to as POP), were prepared as described above. The reaction mixture was prepared in 8 mL vials with screw cap as follows:

Table 59 General screening conditions for POP resting cell experiments (analytical scale).

Reaction mixture		Final concentration
2.0 mL	RCs (OD ₅₉₀ = 20.0)	OD ₅₉₀ = 10.0
1.4–1.8 mL	resting cell medium	-
0–0.4 mL	DHA monomer (1 M)	0–20 mM
0.2 mL	substrate (100 mM in MeCN)	5 mM (5% (v/v) MeCN)

Sampling was performed for both GC and HPLC analysis as before at t = 0* (immediately after mixing) and after 1 h, 3 h, 6 h, 15 h and 24 h reaction time.

A XIII.5 Procedure for Co-expressed Resting Cells (AlkJ + Fsa1 A129S)

Resting cells of the *E. coli* transformant (POP) were prepared as described above. The reaction mixture was prepared in 8 mL vials with screw cap as follows: The substrate was added last from 100 mM stock solutions in pure organic solvent (HPLC grade MeCN), the vial closed and mixed by inverting six times. Reaction mixtures were incubated at 25°C with shaking (250 rpm). Screening samples for GC/FID and HPLC were taken at t = 0* (immediately after mixing) and after 1 h, 2 h, 3 h, 6 h, 15 h and 24 h incubation.

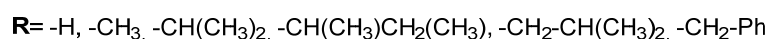
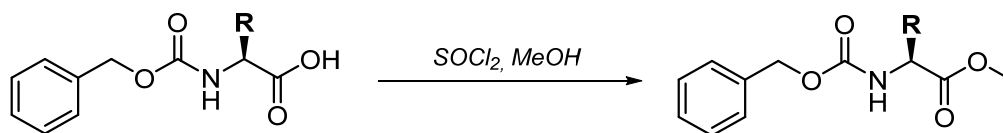
A XIII.6 General Procedure of Preparative Biotransformation Using the POP Construct and DHA or HA

Resting cells of *E. coli* BL21-Gold(DE3) co-expressing AlkJ and Fsa1 A129S were prepared as described before. In the case of DHA, 1.8 g of dimer (10 mmol) were monomerized in resting cell medium for 2 h

at 37°C in an orbital shaker (200 rpm). In a 1 L baffled Erlenmeyer flask, the aldol acceptor molecule (1.0 equiv, 1.0 mmol) was dissolved in MeCN (10 mL) and the DHA or HA monomer solution (20 equiv, 20 mmol) were added to freshly prepared resting cells ($OD_{590} = 10.0$) and shaken at 25°C, 250 rpm ($V_{total} = 200$ mL). The reaction progress was monitored by GC/FID until full consumption of the starting material was observed. The crude reaction mixture was centrifuged and directly transferred for purification on a BUCHI Sepacore flash cartridge (C18, 25 g). Resting cell media ingredients (e.g. salts) and excess DHA were eluted with 5% (v/v) MeOH/95% (v/v) H₂O followed by product elution using 100% (v/v) methanol. The product fraction was concentrated at 25-30°C at high vacuum to obtain the pure product.

A XIV Substrate Profile and Related Synthesis of Reference Material

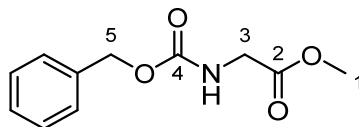
A XIV.1 Esterification of Cbz-protected Amino Acids



General Procedure

A round bottom flask was pre-dried and purged with argon three times. 6 mL dry methanol were added and cooled in an ice bath and thionyl-chloride (3 equiv.) was added dropwise. After 20 minutes of stirring **F₄-L₄** (1 equiv.) was added in one portion and the flask was removed from the ice bath. After 25 minutes, 20 mL dry methanol was added and the reaction was stirred overnight (o/n) until full conversion was monitored *via* TLC (LP: EtOAc 1:5, drops of AcOH). The solvent was removed under reduced pressure and the residue was dissolved in 30 mL toluene and concentrated two times and one time in 60 mL ethyl acetate. Eliminating the last traces of solvent at high vacuum provides the pure product (**A XIII1.1-1.6**) according to NMR.²⁴⁵

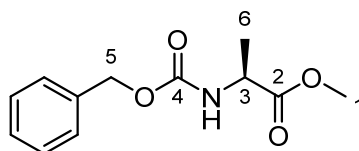
A XIV.1.1 Glycine, *N*-[(phenylmethoxy)carbonyl]-, methyl ester (**F_A**)



General procedure	A XIII.1
Reaction scale	<i>N</i> -Cbz- <i>L</i> -glycine: 1.0 g (4.7 mmol)
Reaction time	24 h
Yield	1.1 g (99%) yellow liquid
Sum formula, m.w.	C ₁₁ H ₁₃ NO ₄ , 223.08
¹H-NMR (200 MHz, CDCl₃)	δ 3.75 (s, 3H, H1), 3.98 (d, 2H, <i>J</i> = 5.47 Hz, H3), 5.13 (s, 2H, H5), 5.27 (bs, 1H, -NH), 7.25-7.48 (m, 5H, H _{aromatic}).
¹³C-NMR (50 MHz, CDCl₃)	δ 42.6 (t, C3), 52.3 (C1), 67.1 (t, C5), 128.1/128.2/128.5 (d, 5 C, C _{arom.}), 136.2 (s, C _{ipso.}), 156.3 (s, C4), 170.5 (s, C2).
LC/MS <i>m/z</i> (ESI⁺)	found [M+H ⁺] 224.18; calculated [M+H ⁺] 224.08

Analytical data was in accordance with literature.²⁴⁶

A XIV.1.2 *L*-Alanine, *N*-[(phenylmethoxy)carbonyl]-, methyl ester (**G_A**)



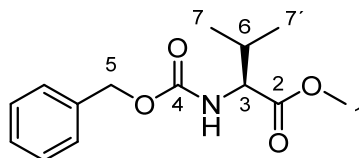
General procedure	A XIII.1
Reaction scale	<i>N</i> -Cbz- <i>L</i> -alanine: 1.0 g (4.5 mmol)
Reaction time	24 h
Yield	1.04 g (97%) yellow liquid
Sum formula, m.w.	C ₁₂ H ₁₅ NO ₄ , 237.35
¹H-NMR (200 MHz, CDCl₃)	δ 1.41 (d, 3H, <i>J</i> = 7.24 Hz, H6), 3.74 (s, 3H, H1), 4.39 (m, 1H, H3), 5.11 (s, 2H, H5), 5.29 (bs, 1H, NH), 7.25-7.42 (m, 5H, H _{arom.}).
¹³C-NMR (50 MHz, CDCl₃)	δ 18.8 (q, C6), 49.6 (q, C1), 52.5 (C3), 67.0 (t, C5), 128.1/128.2/128.5 (d, 5 C, C _{arom.}), 136.3 (s, C _{ipso.}), 155.9 (s, C4), 173.7 (s, C2).
LC/MS <i>m/z</i> (ESI⁺)	found [M+H ⁺] 238.15; calculated [M+H ⁺] 238.35

²⁴⁶ S. T. Heller, R. Sarpong, *Org. Lett.* **2010**, *12*, 4572-4575.

Specific rotation $[\alpha]_{\text{D}}^{25} = -33.3$ (c 1.0, CH₃OH) (Lit.²⁴⁷ $[\alpha]_{\text{D}}^{25} = -33.8$ (c 1.0, CH₃OH))

Analytical data was in accordance with the literature.²⁴⁷

A XIV.1.1 *L*-Valine, *N*-[(phenylmethoxy)carbonyl]-, methyl ester (**H_A**)



General procedure

A XIII.1

Reaction scale

N-Cbz-*L*-valine: 1.5 g (6 mmol)

Reaction time

24 h

Yield

1.64 g (99%) yellow liquid

Sum formula, m.w.

C₁₄H₁₉NO₂, 265.30

¹H-NMR (200 MHz, CDCl₃)

δ 0.93 (d, 6H, *J* = 6.85 Hz, H7, H7'), 1.94-2.21 (m, 1H, H6), 3.73 (s, 3H, H1), 4.11-4.30 (m, 1H, H3), 5.11 (s, 2H, H5), 5.29 (bs, 1H, NH), 7.25-7.43 (m, 5H, H_{arom.}).

¹³C-NMR (50 MHz, CDCl₃)

δ 17.5 (q, C7), 18.9 (q, C7'), 31.4 (d, C6), 52.2 (q, C1), 59.1 (d, C3), 67.1 (t, C5), 128.1/128.2/128.5 (d, 5 C, C_{arom.}), 136.5 (s, C_{ipso}), 156.2 (s, C4), 172.5 (s, C2).

LC/MS *m/z* (ESI⁺)

found [M+H⁺] 266.24; calculated [M+H⁺] 266.30

Specific rotation

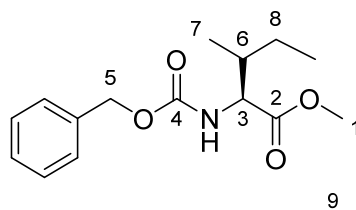
$[\alpha]_{\text{D}}^{20} = -20.4$ (c 1.0, CH₃OH) (Lit.²⁴⁸ $[\alpha]_{\text{D}}^{20} = -21.9$ (c 1.0, CH₃OH))

Analytical data was in accordance with the literature.²⁴⁸

²⁴⁷ K. Orito, M. Miyazawa, T. Nakamura, A. Horibata, H. Ushito, H. Nagasaki, M. Yuguchi, S. Yamashita, T. Yamazaki, M. Tokuda, *J. Org. Chem.* **2006**, *71*, 5951-5958.

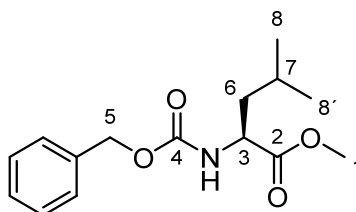
²⁴⁸ H. Zhu, D. M. Coleman, C. J. Dehen, I. M. Geisler, D. Zemlyanov, J. Chmielewski, G. J. Simpson, A. Wei, *Langmuir* **2008**, *24*, 8660-8666.

A XIV.1.2 L-Isoleucine, *N*-[(phenylmethoxy)carbonyl]-, methyl ester (I_A)



General procedure	A XIII.1
Reaction scale	<i>N</i> -Cbz- <i>L</i> -Isoleucine: 1.5 g (5.6 mmol)
Reaction time	24 h
Yield	1.432 g (91%) yellow liquid
Sum formula, m.w.	C ₁₅ H ₂₂ NO ₄ , 279.33
¹H-NMR (200 MHz, CDCl₃)	δ 0.91 (m, 6H, H7, H9), 1.26 (m, 3H, H7), 1.88 (m, 1H, H8), 3.73 (s, 3H, H1), 4.35 (m, 1H, H3), 5.11 (s, 2H, H5), 5.29 (d, 1H, <i>J</i> = 8.4 Hz, -NH), 7.35 (m, 5H, H _{arom.}).
¹³C-NMR (50 MHz, CDCl₃)	δ 11.6 (q, C9), 15.5 (q, C7), 25.0 (t, C8), 38.1 (d, C6), 52.1 (q, C1), 58.4 (d, C3), 67.0 (t, C5), 128.1/128.2/128.5 (d, 5C, C _{arom.}), 136.4 (s, C _{ipso}), 156.3 (s, C4), 172.7 (s, C2).
LC/MS <i>m/z</i> (ESI⁺)	found [M+H ⁺] 280.25; calculated [M+H ⁺] 280.33
Specific rotation	[α] _D ²⁰ = -12.2 (c 1.1, CH ₃ OH) (Lit. ²⁴⁹ [α] _D ²⁰ = -11.5 (c 1.1, CH ₃ OH))
Analytical data was in accordance with the literature. ²⁴⁹	

A XIV.1.1 L-Leucine, *N*-[(phenylmethoxy)carbonyl]-, methyl ester (J_A)



General procedure	A XIII.1
Reaction scale	<i>N</i> -Cbz- <i>L</i> -leucine: 1.5 g (5.6 mmol)
Reaction time	24 h
Yield	1.5 g (93%) yellow liquid
Sum formula, m.w.	C ₁₅ H ₂₂ NO ₄ , 279.33

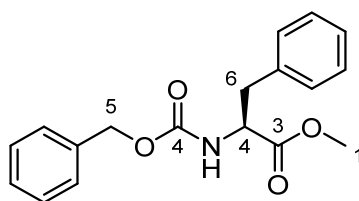
²⁴⁹ Ito, A.; Takahashi, R.; Baba, Y. *Chem. Pharm. Bull.* **1975**, *23*, 3081.

¹H-NMR (200 MHz, CDCl₃)	δ 0.90-1.05 (m, 6H, H8, H8'), 1.45-1.78 (m, 3H, H6, H7), 3.73 (s, 3H, H1), 4.23-4.38 (m, 1H, H3), 5.11 (s, 2H, H5), 5.20 (bs, NH), 7.24-7.49 (m, 5H, H _{arom.}).
¹³C-NMR (50 MHz, CDCl₃)	δ 21.8 (q, C8), 22.8 (q, C8'), 24.7 (d, C7), 42.8 (C6), 52.4 (q, C1), 53.5 (d, C3), 67.0 (t, C5), 128.1/128.2/128.5 (d, 5 C, C _{arom.}), 136.3 (s, C _{ipso}), 156.0 (s, C4), 173.6 (s, C2).
LC/MS <i>m/z</i> (ESI⁺)	found [M+H ⁺] 280.21; calculated [M+H ⁺] 280.33
Specific rotation	$[\alpha]_{\text{D}}^{20} = -25.2$ (c 1.0, CH ₃ OH) (Lit. ²⁵⁰ $[\alpha]_{\text{D}}^{20} = -29.5$ (c 1.0, CH ₃ OH)).

Analytical data was in accordance with the literature.²⁵⁰

²⁵⁰ T. Miyazawa, K. Tanaka, E. Ensatsu, R. Yanagihara, T. Yamada, *J. Chem. Soc., Perkin Trans. 1* **2001**, 87-94.

A XIV.1.1 L-Phenylalanine, *N*-[(phenylmethoxy)carbonyl]-, methyl ester (K_A)



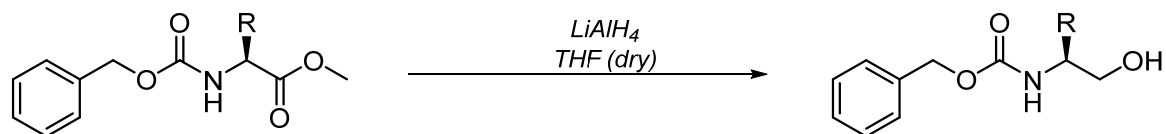
General procedure	A XIII.1
Reaction scale	<i>N</i> -Cbz- <i>L</i> -phenyl alanine: 1.5 g (5 mmol)
Reaction time	24 h
Yield	1.6 g (99%) yellow liquid
Sum formula, m.w.	$C_{18}H_{19}NO_4$, 313.35
1H-NMR (200 MHz, $CDCl_3$)	δ 3.01-3.23 (m, 2H, H6), 3.71 (s, 3H, H1), 4.51-4.76 (m, 1H, H3), 5.09 (s, 2H, H5), 5.22 (bs, 1H, NH), 7.11-7.43 (m, 10H, $H_{arom.}$).
^{13}C-NMR (50 MHz, $CDCl_3$)	δ 38.2 (t, C6), 52.3 (q, C1), 54.8 (d, C3), 67.0 (t, C5), 127.1/128.1/128.2/128.5/128.6/129.3 (d, 10C, $C_{arom.}$), 135.8/136.5 (s, 2C, C_{ipso}), 155.9 (s, C4), 172.0 (s, C2).
LC/MS m/z (ESI$^+$)	found $[M+H]^+$ 314.21; calculated $[M+H]^+$ 314.35
Specific rotation	$[\alpha]_D^{20} = -16.0$ (c 1.0, CH_3OH) (lit. ²⁵¹ $[\alpha]_D^{20} = -17.1$ (c 1.0, CH_3OH))

Analytical data was in accordance with the literature.²⁵²

²⁵¹A. G. M. Barrett, D. Pilipauskas, J. Org. Chem. 1990, 55, 5170-5173.

²⁵²R. Löser, M. Frizler, K. Schilling, M. Gütschow, Angew. Chem. Int. Ed. 2008, 47, 4331-4334.

A XIV.2 Reduction of the Aminoacid-methylesters to the Corresponding Alcohols

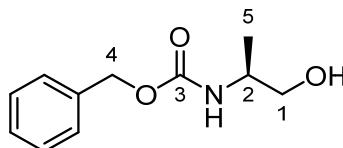


R = CH₃, CH(CH₃)₂, -CH(CH₃)-CH₂(CH₃)

A XIV.2.1 Reduction *via* LiAlH₄

General Procedure Lithium aluminium hydride (1.3 equiv.) was suspended in 16 mL dry THF, cooled in an ice bath and purged with argon. The Cbz-protected amino acid methyl ester (**A XIII.1**) was dissolved in 16 mL dry THF and was added dropwise to the suspension. The reaction vessel was removed from the ice bath and stirred at room temperature until full conversion was obtained, monitored *via* TLC (LP:EtOAc 3:1). The reaction was quenched by adding 2 N HCl until the precipitation was completely dissolved (about the same volume as reaction volume). The aqueous layer was extracted with ethyl acetate five times and the combined organic layers were washed with brine, dried over Na₂SO₄ and concentrated under reduced pressure. Column chromatography (PE:EtOAc 1:1) provided the pure products (**A XIII.2.2-2.4**) according to NMR.

A XIV.2.2 Carbamic acid, *N*-[(*S*)-hydroxy-methylethyl]-, phenylmethyl ester (**H₂**)



General procedure

A XIII.2.1

Reaction scale
mmol)

L-Alanine, *N*-[(phenylmethoxy)carbonyl]-, methyl ester: 1.3 g (4.2

Reaction time

24 h

Purification

MPLC, LP/EtOAc

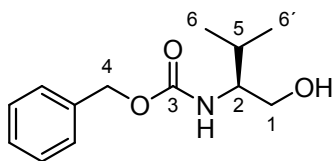
Yield

0.73 g (84%) colorless solid

Sum formula, m.w.	C ₁₁ H ₁₅ NO ₃ , 209.24
m.p.	82-83°C (Lit ²⁵³ 80-82°C)
¹H-NMR (200 MHz, CDCl₃)	δ 1.17 (d, 3H, <i>J</i> = 6.85 Hz, H5), 2.17 (s, 1H, -OH) 3.48-3.63 (m, 2H, H1), 3.68-3.89 (m, 1H, H2), 4.89 (bs, 1H, -NH), 5.10 (s, 2H, H4), 7.23-7.43 (m, 5H, H _{arom.}).
¹³C-NMR (50 MHz, CDCl₃)	δ 17.2 (q, C5), 49.0 (d, C2), 64.8 (t, C1) 66.9 (t, C4), 128.1/128.2/128.5 (d, 5C, C _{arom.}), 136.4 (s, C _{ipso}), 156.7 (s, C3).
LC/MS <i>m/z</i> (ESI⁺)	found [M+Na ⁺] 232.14.; calculated [M+Na ⁺] 232.24
Specific rotation	[α] _D ²⁰ = -11.2 (c 0.55, CH ₂ Cl ₂) (Lit ²⁵³ [α] _D ²³ = -10.7 (c 0.55, CH ₂ Cl ₂))

Analytical data was in accordance with the literature.²⁵³

A XIV.2.1 Carbamic acid, *N*-[(*S*)-hydroxy-isopropylethyl]-, phenylmethyl ester (I₂)



General procedure	A XIII.2.1
Reaction scale	<i>L</i> -Valine, <i>N</i> -[(phenylmethoxy)carbonyl]-, methyl ester: 1.0 g (3.8 mmol)
Reaction time	24 h
Purification	MPLC, LP/EtOAc
Yield	0.64 g (70%) colorless solid
Sum formula, m.w.	C ₁₃ H ₁₉ NO ₃ , 237.29
m.p.:	58-59°C (Lit ²⁵⁴ 58.5-59°C)
¹H-NMR (200 MHz, CDCl₃)	δ 0.76-0.98 (m, 3H, H6, H6'), 1.76-1.95 (m, 1H, H5), 2.01 (s, 1H, -OH), 3.66-3.3.81 (m, 1H, H2), 3.86-3.96 (m, 2H, H1), 4.85 (bs, 1H, -NH), 5.11 (s, 2H, H4), 7.23-7.42 (m, 5H, H _{arom.}).
¹³C-NMR (50 MHz, CDCl₃)	δ 18.5/19.5 (q, 2 C, C6), 29.2 (d, C5), 58.5 (t, C1), 63.8 (C2), 66.9 (t, C4), 128.1/128.2/128.6 (d, 5 C, C _{arom.}), 136.4 (s, C _{arom.}), 157.3 (s, -C3).

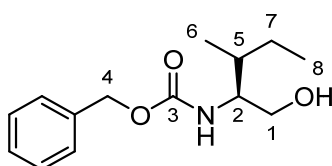
²⁵³ J. Ivkovic, C. Lembacher-Fadum, R. Breinbauer, *Org. Biomol. Chem.* **2015**, *13*, 10456-10460.

²⁵⁴ G. D. Kishore Kumar, S. Baskaran, *J. Org. Chem.* **2005**, *70*, 4520-4523.

LC/MS <i>m/z</i> (ESI⁺)	found [M+Na ⁺] 260.15; calculated [M+Na ⁺] 260.29
Specific rotation	$[\alpha]_{\text{D}}^{20} = -14.3$ (c 1.0, CH ₃ OH) (Lit. ²⁵⁵ $[\alpha]_{\text{D}}^{23} = -15.9$ (c 1.0, CH ₃ OH))

Analytical data was in accordance with the literature.²⁵⁵

A XIV.2.2 Carbamic acid, *N*-[(*S*)-(hydroxymethyl)-methylbutyl]-, phenylmethyl ester (J₂)

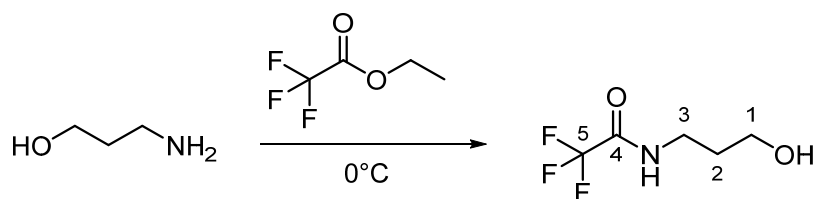


General procedure	A XIII.2.1
Reaction scale	<i>L</i> -Isoleucine, <i>N</i> -[(phenylmethoxy)carbonyl]-, methyl ester: 1.0 g (3.6 mmol)
Reaction time	24 h
Purification	MPLC, LP/EtOAc
Yield	0.644 g (71%) colorless solid
Sum formula, m.w.	C ₁₄ H ₂₁ NO ₃ , 251.32
m.p.	60-62°C (Lit ²⁵⁵ 61-62°C)
¹H-NMR (200 MHz, CDCl₃)	δ 0.78-0.960 (m, 6H, H6, H8), 1.07-1.31 (m, 1H, H5), 1.43-1.68 (m, 2H, H7), 2.25 (s, 1H, -OH), 3.43-3.78 (m, 3H, H1, H2), 4.97 (bs, 1H, -NH), 5.10 (s, 2H, H4), 7.25-7.46 (m, 5H, H _{arom.}).
¹³C-NMR (50 MHz, CDCl₃)	δ 11.4 (q, C8), 15.5 (q, C6), 25.4 (t, C7), 35.9 (d, C5), 57.4 (d, C2), 63.6 (t, C1), 67.0 (t, C4), 128.1/128.2/128.5 (d, 5C, C _{arom.}), 136.4 (s, C _{ipso}), 157.1 (s, C3).
LC/MS <i>m/z</i> (ESI⁺)	found [M+H ⁺] 252.20; calculated [M+H ⁺] 252.32
Specific rotation	$[\alpha]_{\text{D}}^{20} = -13.5$ (c 1.0, CH ₃ OH) (Lit. ²⁵⁶ $[\alpha]_{\text{D}}^{20} = -14$ (c 1.0, CH ₃ OH))
Analytical data was in accordance with the literature. ²⁵⁶	

²⁵⁵ G. D. Kishore Kumar, S. Baskaran, *J. Org. Chem.* **2005**, *70*, 4520-4523.

²⁵⁶ J.-A. Fehrentz, J.-C. Califano, M. Amblard, A. Loffet, J. Martinez, *Tetrahedron Lett.* **1994**, *35*, 569-571.

A XIV.2.3 3-Trifluoroacetamido-propanol (L₂)



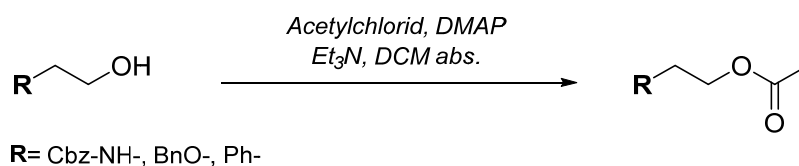
To a stirred solution of 3-aminopropan-1-ol (2 g, 26.7 mmol, 1 equiv), ethyl trifluoroacetate (4.7 g, 1.25 equiv., 39.7 mmol) was added dropwise at 0°C. After TLC (LP:EtOAc 1:1, $R_f = 0.25$) indicated full starting material consumption, the reaction mixture was warmed to room temperature and stirred overnight until full conversion was monitored. The crude product was concentrated at the rotavap and purified by column chromatography to afford the protected alcohol in 85% yield after concentration at high vacuum.

Reaction scale	3-aminopropan-1-ol: 2.00 g (26.7 mmol)
Reaction time	24 h
Purification	Column chromatography (LP:EtOAc)
Yield	4.2 g (85%) yellow liquid
Sum formula, m.w.	C ₅ H ₈ F ₃ NO ₂ , 171.12 g/mol
¹H-NMR (200 MHz, CDCl₃)	δ 1.43-1.56 (m, 2H, H2), 3.11-3.28 (m, 2H, H3), 3.39-3.48 (m, 2H, H1) 4.36 (s, 1H, -OH), 6.76 (bs, 1H, -NH).
¹³C-NMR (50 MHz, CDCl₃)	δ 37.8 (s, C2), 39.1 (s, C3), 58.4 (s, C1), 115.7 (s, ¹ J _{C,F} = 285.6 Hz, C5), 157.9 (s, ² J _{C,F} = 38.5 Hz, C4).
LC/MS m/z (ESI⁺)	found [M+H ⁺] 172.05; calculated [M+H ⁺] 172.08

Analytical data was in accordance with the literature.²⁵⁷

²⁵⁷ Tang, R.; Ji, W.; Wang, C. *Polymer* **2011**, *52*, 921-932.

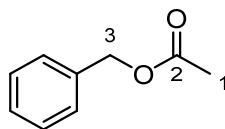
A XIV.3 Acetylation of Primary Alcohols



A XIV.3.1 Acetylation *via* Acetylchloride

General Procedure To a solution of DMAP (10 mol%), Et₃N (1.5 equiv.), 1 equiv. of the corresponding alcohol (**A₂-F₂**) (in 20 mL abs. CH₂Cl₂), freshly distilled acetyl chloride (1.5 equiv.) was added dropwise at 0°C. The reaction progress was monitored *via* TLC (LP:EtOAc 3:1), after full consumption of the starting material, the reaction mixture was extracted with 2 N HCl (2 times), sat. NaHCO₃ and the organic layers were combined and dried over Na₂SO₄. The pure products, according to NMR (**A XIII.3.2-3.8**) were obtained after concentration at high vacuum overnight without any further purification.

A XIV.3.2 Benzyl-acetate (**A₁**)

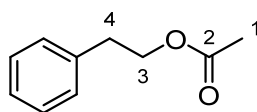


General procedure	A XIII.3.1
Reaction scale	Benzylalcohol: 0.065 g (5.6 mmol)
Reaction time	24 h
Yield	0.66 g (79%) yellow liquid
Sum formula, m.w.	C ₉ H ₁₀ O ₂ , 150.08
¹H-NMR (200 MHz, CDCl₃)	δ = 2.10 (s, 3H, H1), 5.11 (s, 2H, H3), 7.23-7.48 (m, 5H, H _{arom.}).
¹³C-NMR (50 MHz, CDCl₃)	δ 21.0 (q, C1), 64.9 (t, C3), 126.6/128.3/128.6 (d, 5C, C _{arom.}), 135.9 (s, C _{ipso}), 170.9 (s, C2).
GC/MS	<i>m/z</i> 150 (40), 108 (100), 107 (25), 91 (56), 90 (39)

Analytical data was in accordance with the literature.²⁵⁸

²⁵⁸ B. Janza, A. Studer, *J. Org. Chem.* **2005**, *70*, 6991-6994.

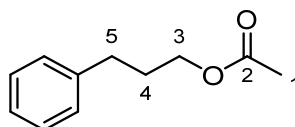
A XIV.3.3 Phenylethyl-acetate (**B**₁)



General procedure	A XIII.3.1
Reaction scale	Phenylethanol: 1 g (8.2 mmol)
Reaction time	24 h
Yield	0.4 g (30%) yellow liquid
Sum formula, m.w.	C ₁₀ H ₁₂ O ₂ , 164.08
¹H-NMR (200 MHz, CDCl₃)	δ 2.03 (s, 3H, H1), 2.93 (t, 2H, <i>J</i> = 7.1 Hz, H4), 4.28 (t, 2H, <i>J</i> = 7.1 Hz, H3), 7.19-7.34 (m, 5H, H _{arom.}).
¹³C-NMR (50 MHz, CDCl₃)	δ 20.9 (q, C1), 35.1 (t, C4), 64.9 (t, C3), 126.6/128.5/128.7 (d, 5C, C _{arom.}), 137.8 (s, C _{ipso}), 171.0 (s, C2).
GC/MS	<i>m/z</i> 104 (11), 104 (100), 91 (18), 78 (7)

Analytical data was in accordance with the literature.²⁵⁹

A XIV.3.4 Phenylpropyl-acetate (**C**₁)



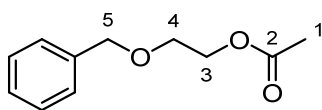
General procedure	A XIII.3.1
Reaction scale	Phenylpropanol: 1 g (7.3 mmol)
Reaction time	24 h
Yield	0.47 g (36%) yellow liquid
Sum formula, m.w.	C ₁₁ H ₁₄ O ₂ , 178.10
¹H-NMR (200 MHz, CDCl₃)	δ 1.93-1.96 (m, 2H, H4) 1.96 (s, 3H, H1), 2.69 (t, <i>J</i> = 6.4 Hz, 2H, H5), 4.08 (t, <i>J</i> = 7.4 Hz, 2H, H3), 7.16-7.29 (m, 5H, H _{arom.}).
¹³C-NMR (50 MHz, CDCl₃)	δ 20.9 (q, C1), 40.2 (t, C4), 63.5 (t, C5), 66.9 (t, C3), 128.2/128.3/128.7 (d, 5C, C _{arom.}), 136.5 (s, C _{ipso}), 171.0 (s, C2).
GC/MS	<i>m/z</i> 118 (83), 117 (100), 91 (37), 70 (15), 61 (14)

Analytical data was in accordance with the literature.²⁶⁰

²⁵⁹ S. Magens, B. Plietker, *J. Org. Chem.* **2010**, *75*, 3715-3721.

²⁶⁰ A. Sakakura, K. Kawajiri, T. Ohkubo, Y. Kosugi, K. Ishihara, *JACS* **2007**, *129*, 14775-14779.

A XIV.3.5 2-(Benzyloxy)ethyl-acetate (D₁)

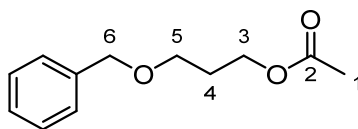


General procedure	A XIII.3.1
Reaction scale	2-(benzyloxy)ethanol: 1.5 g (9.8 mmol)
Reaction time	24 h
Yield	1.43 g (75%) yellow liquid
Sum formula, m.w.	C ₁₁ H ₁₄ O ₃ , 194.03
¹H-NMR (200 MHz, CDCl₃)	δ 2.09 (s, 3H, H1), 3.67 (t, <i>J</i> = 4.9 Hz, 2H, H4), 4.24 (t, <i>J</i> = 4.7 Hz, 2H, H3), 4.57 (s, 2H, H5), 7.27-7.38 (m, 5H, H _{arom.}).
¹³C-NMR (50 MHz, CDCl₃)	δ 21.0 (q, C1), 63.6 (t, C3), 67.8 (t, C4), 73.2 (t, C5), 127.8/128.4 (d, 5C, C _{arom.}), 137.8 (s, C _{ipso}), 171.4 (s, C2).
GC/MS	<i>m/z</i> 105 (17), 104 (100), 91 (26), 78 (12), 77 (10), 65 (11)

Analytical data was in accordance with the literature.²⁶¹

²⁶¹ N. Asao, H. Aikawa, S. Tago, K. Umetsu, *Org. Lett.* **2007**, 9, 4299-4302.

A XIV.3.6 3-(Benzyloxy)propyl-acetate (**E**₁)

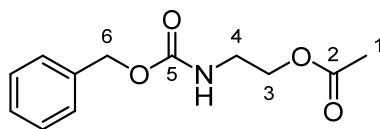


General procedure	A XIII.3.1
Reaction scale	2-(benzyloxy)propanol: 1.5 g (9.0 mmol)
Reaction time	24 h
Yield	1.3 g (70%) yellow liquid
Sum formula, m.w.	C ₁₂ H ₁₆ O ₃ , 208.11
¹H-NMR (200 MHz, CDCl₃)	δ 1.90-1.97 (m, 2H, H ₄), 2.03 (s, 3H, H ₁), 3.55 (t, <i>J</i> = 6.3 Hz, 2H, H ₅), 4.19 (t, <i>J</i> = 6.5 Hz, 2H, H ₃), 4.51 (s, 2H, H ₆), 7.29-7.37 (m, 5H, H _{arom.}).
¹³C-NMR (50 MHz, CDCl₃)	δ 21.0 (q, C ₁), 29.0 (t, C ₄) 61.7 (t, C ₃), 66.6 (t, C ₅), 73.0 (t, C ₆), 127.6/128.4 (d, 5C, C _{arom.}), 138.3 (s, C _{ipso}), 171.1 (s, C ₂).
GC/MS	<i>m/z</i> 148 (30), 147 (53), 106 (45), 101 (31), 90 (100), 64 (13)

Analytical data was in accordance with the literature.²⁶²

²⁶² A. Kawata, K. Takata, Y. Kuninobu, K. Takai, *Angew. Chem. Int. Ed.* **2007**, *46*, 7793-7795.

A XIV.3.7 2-(((Benzyloxy)carbonyl)amino)ethyl-acetate (F₁)



General procedure

A XIII.3.1

Reaction scale

Benzyl-(2-hydroxyethyl)carbamate: 1.5 g (7.7 mmol)

Reaction time

24 h

Yield

1.33 g (73%) yellow liquid

Sum formula, m.w.

C₁₂H₁₅NO₂, 237.10

¹H-NMR (200 MHz, CDCl₃)

δ 2.04 (s, 3H, H1), 3.41-3.49 (m, 2H, H4), 4.13 (t, *J* = 5.1 Hz, 2H, H3), 5.10 (s, 1H, H6) 7.25-7.37 (m, 5H, H_{arom.}).

¹³C-NMR (50 MHz, CDCl₃)

δ 21.0 (q, C1), 40.2 (t, C4), 63.5 (t, C3), 67.0 (t, C6), 126.0/128.4/128.4 (d, 5C, C_{arom.}), 136.4 (s, C_{ipso}), 156.4 (2, C5) 171.2 (s, C2).

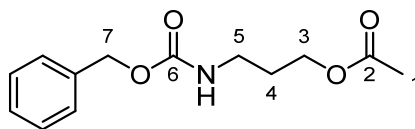
GC/MS

m/z 108 (78), 107 (33), 91 (100), 79 (12), 65 (15)

Analytical data was in accordance with the literature.²⁶³

²⁶³ R. V. Ohri, A. T. Radosevich, K. J. Hrovat, C. Musich, D. Huang, T. R. Holman, F. D. Toste, *Org. Lett.* **2005**, *7*, 2501-2504.

A XIV.3.8 3-(((Benzyloxy)carbonyl)amino)propyl-acetate (**G**₁)



General procedure

A XIII.3.1

Reaction scale

Benzyl (3-hydroxypropyl)carbamate: 1.5 g (7.2 mmol)

Reaction time

24 h

Yield

1.44 g (80%) yellow liquid

Sum formula, m.w.

C₁₃H₁₇NO₄, 251.12

¹H-NMR (200 MHz, CDCl₃)

δ 1.81-1.87 (m, 2H, H₄), 2.05 (s, 3H, H₁), 3.23-3.33 (m, 2H, H₅), 4.13 (t, *J* = 6.1 Hz, 2H, H₃), 4.96 (bs, 1H, -NH), 5.10 (s, 2H, H₇), 7.28-7.41 (m, 5H, H_{arom.}).

¹³C-NMR (50 MHz, CDCl₃)

δ 20.9 (q, C₁), 29.0 (t, C₄), 37.9 (t, C₅), 61.8 (t, C₃), 66.7 (t, C₇), 128.1/128.5 (d, 5C, C_{arom.}), 132.5 (s, C_{ipso}), 156.4 (s, C₆), 171.2 (s, C₂).

GC/MS

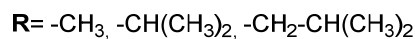
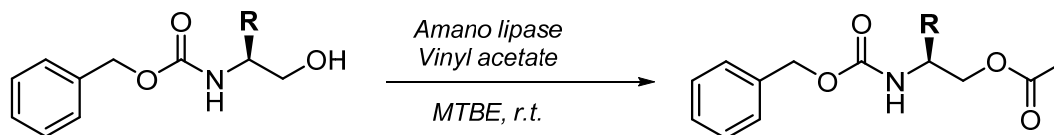
m/z 108 (75), 107 (30), 91 (100), 79 (16), 65 (12)

Analytical data was in accordance with the literature.²⁶⁴

²⁶⁴ A. Golebiowski, J. Raczko, J. Jurczak, *Bull. Pol. Acad. Sci., Chem.* **1989**, 36, 209-214.

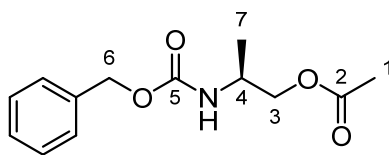
A XIV.3.9 Synthesis of *N*-Cbz-*L*-aminoacid-acetates using Lipase

For side chain substituted amino acids, acetylation was performed *via* Amano lipase, vinylacetate in MTBE to avoid racemization at the α -position.



General Procedure *N*-Cbz-*L*-amino alcohol (**H₂-J₂**) (1 equiv.) and vinyl acetate (1.5 equiv.) were dissolved in 5.5 mL MTBE. 100 mg Amano lipase PS (immobilized on diatomite) was added and the suspension was stirred at room temperature. After three hours full conversion of the starting material was indicated *via* TLC (LP:EtOAc 1:1). The lipase was removed by flash filtration through Celite and the solvent was removed at reduced pressure and 40°C. The pure products (**A XIII.3.10-12**) were obtained by concentration under high vacuum overnight without any further purification.

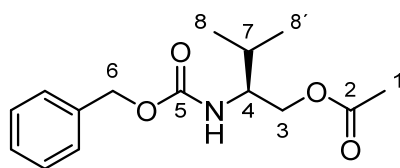
A XIV.3.10 (S)-2-(((Benzyloxy)carbonyl)amino)propyl-acetate (H₁)



General procedure	A XIII.3.9
Reaction scale	<i>N</i> -Cbz- <i>L</i> -alaninol: 0.27 g (1.3 mmol)
Reaction time	4 h
Yield	0.28 g (86%) colorless solid
Sum formula, m.w.	C ₁₃ H ₁₇ NO ₄ , 251.28
m.p.	70-71°C (not given in lit.)
¹H-NMR (200 MHz, CDCl₃)	δ 1.18 (d, 3H, <i>J</i> = 6.26 Hz, H7), 2.04 (s, 3H, C1), 3.96-4.12 (m, 3H, H3, H4), 4.87 (bs, 1H, -NH), 5.10 (s, 2H, C6), 7.26-7.43. (m, 5H, H _{arom.}).
¹³C-NMR (50 MHz, CDCl₃)	δ 17.7 (q, C7), 20.8 (q, C1), 46.1 (d, C4), 66.8 (t, C6), 67.1 (t, C3), 128.1/128.2/128.5 (d, 5C, C _{arom.}), 136.5 (s, C _{ipso}), 155.7 (s, C5), 170.9 (s, C2).
LC/MS <i>m/z</i> (ESI⁺)	found [M+H ⁺] 252.16; calculated [M+H ⁺] 252.28
Specific rotation	[α] _D ²⁰ = -13.9 (c 1.0, CH ₃ OH) (Lit ²⁶⁵ [α] _D ²⁰ = -15.4 (c 1.8, CHCl ₃))
Analytical data was in accordance with the literature. ²⁶⁵	

²⁶⁵ A. Golebiowski, J. Raczko, J. Jurczak, *Bull. Pol. Acad. Sci., Chem.* **1989**, 36, 209-214.

A XIV.3.11 (S)-2-(((Benzyloxy)carbonyl)amino)-3-methylbutyl-acetate (**I₁**)



General procedure

A XIII.3.9

Reaction scale

N-Cbz-*L*-valinol: 0.27 g (1.1 mmol)

Reaction time

4 h

Yield

0.32 g (99%) colorless liquid

Sum formula, m.w.

C₁₅H₂₁NO₄, 279.33

¹H-NMR (200 MHz, CDCl₃)

δ 0.92 (d, 3H, *J* = 2.93 Hz, H₈), 0.96 (d, 3H, *J* = 2.93 Hz, H_{8'}), 1.71-1.84 (m, 1H, H₇), 2.01 (s, 3H, C₁), 3.68-3.79 (m, 1H, H₄), 4.02-4.16 (m, 2H, H₃), 4.80 (bs, 1H, -NH), 5.11 (s, 2H, H₆), 7.27-7.43 (m, 5H, H_{arom.}).

¹³C-NMR (50 MHz, CDCl₃)

δ 18.3 (q, C₈), 19.3 (q, C_{8'}), 20.8 (q, C₁), 29.7 (d, C₇), 55.3 (d, C₄), 66.8 (t, C₆), 64.7 (t, C₃), 128.1/128.2/128.5 (d, 5C, C_{arom.}), 136.5 (s, C_{ipso}), 156.3 (s, C₅), 171.0 (s, C₂).

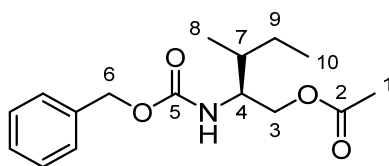
HR/MS *m/z* (ESI⁺)

found [M+H⁺] 280.1563; calculated [M+H⁺] 280.1563

Specific rotation

[α]_D²⁰ = -5.8 (c 1.0, CH₃OH)

A XIV.3.12 (2*S*,3*R*)-2-(((Benzyloxy)carbonyl)amino)-3-methylpentyl-acetate (**J₁**)

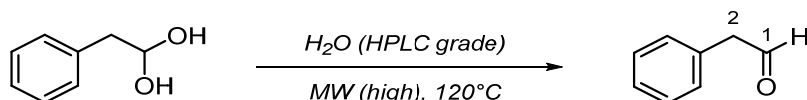


General procedure	A XIII.3.9
Reaction scale	<i>N</i> -Cbz- <i>L</i> -isoleucinol C VI.2.4: 0.27 g (1.1 mmol)
Reaction time	4 h
Yield	0.31 g (99%) colorless solid
Sum formula, m.w.	C ₁₆ H ₂₃ NO ₄ , 293.36
m.p.	54-55°C
¹H-NMR (200 MHz, CDCl₃)	δ 0.79-0.93 (m, 6H, H8, H10), 1.06-1.21 (m, 1H, H7), 1.37-1.59 (m, 2H, H9), 2.01 (s, 3H, H1), 3.68-3.82 (m, 1H, H4), 4.13 (d, 2H, H3), 4.80 (bs, 1H, -NH), 5.11 (s, 2H, H6), 7.2-7.45 (m, 5H, H _{arom.}).
¹³C-NMR (50 MHz, CDCl₃)	δ 11.3 (q, C10), 15.3 (q, C8), 20.8 (q, C1), 25.3 (t, C9), 36.4 (d, C7), 54.2 (d, C4), 64.4 (t, C3), 66.8 (t, C6), 128.1/128.5 (d, 5C, C _{arom.}), 136.5 (s, C _{ipso}), 156.2 (s, C5), 171.0 (s, C2).
HR/MS (ESI⁺)	found [M+Na ⁺] 294.1706; calculated [M+Na ⁺] 294.1700
Specific rotation	[α] _D ²⁰ = -4.9 (c 1.0, CH ₃ OH)

A XIV.4 Aldehyde Synthesis

To synthesize the corresponding aldehyde compounds different strategies were followed, like classical oxidations using Dess Martin, PCC etc.

A XIV.4.1 Acetate Deprotection to 2-Phenylacetaldehyde (**B**₃)



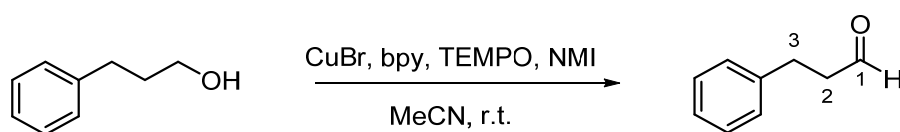
Procedure Phenylacetaldehyde-dimethyl acetale (0.66 g, 4 mmol) was suspended in 12 mL H₂O (HPLC grade) and heated in a biotage microwave oven (120°C) for 60 minutes and the reaction progress was monitored *via* TLC (LP:EtOAc 10:1). The reaction mixture was extracted three times with CH₂Cl₂ and the combined organic layers were washed with brine and dried over Na₂SO₄. Evaporation of the solvent provided the pure product according to NMR.

Reaction scale	Phenyl acetaldehyde dimethyl acetale: 0.66g (4 mmol)
Reaction time	24 h
Yield	0.37 g (77%) colorless liquid
Sum formula, m.w.	C ₈ H ₈ O, 120.15
¹H-NMR (200 MHz, CDCl₃)	δ 3.68 (d, 2H, <i>J</i> = 2.34 Hz, H ₂), 7.23-7.42 (m, 5H, H _{arom.}), 9.75 (t, 1H, <i>J</i> = 2.34 Hz, H ₁).
¹³C-NMR (50 MHz, CDCl₃)	δ 50.6 (t, C ₂), 127.5/129.0/129.6 (d, 5C, C _{arom.}), 131.8 (s, C _{ipso}), 199.6 (d, C ₁).
GC/MS	<i>m/z</i> 120 (24), 91 (100), 65 (23), 63 (7)

Analytical data was in accordance with the literature.²⁶⁶

²⁶⁶ M. W. C. Robinson, K. S. Pillinger, I. Mabbett, D. A. Timms, A. E. Graham, *Tetrahedron* **2010**, *66*, 8377-8382.

A XIV.4.2 Synthesis of 3-Phenylpropanal (C₃) using CuBr/BYP/TEMPO/NMI



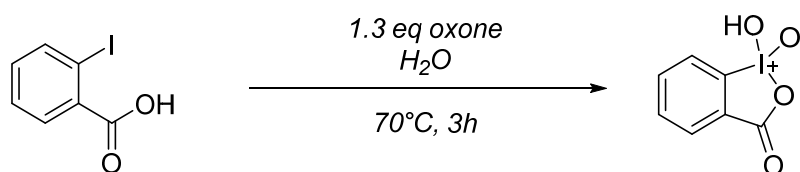
Procedure In a round bottom flask, 3-phenylpropanol (0.6 g, 4.4 mmol, 1 equiv.), CuBr (32 mg, 0.22 mmol, 0.05 equiv.), 2,2-bipyridine (34 mg, 0.22 mmol, 0.05 equiv.), TEMPO (34 mg, 0.22 mmol, 0.05 equiv.) and of NMI (36 mg, 0.44 mmol, 0.1 equiv.) were dissolved in 4.5 mL acetonitrile each. The reagents were added to the dissolved alcohol in the order given above, resulting in a brown reaction solution. After 5.5 hours the color changed to green, but according to TLC (LP:EtOAc 2:1) still starting material was remaining. After o/n a color change to blue-green was obtained and TLC showed full conversion of the starting material. The reaction mixture was diluted with 45 mL H₂O (HPLC grade) and extracted three times with 90 mL CH₂Cl₂. The combined organic layers were washed with brine until a colorless solution was obtained. The reaction mixture was dried Na₂SO₄, concentrated under reduced pressure and after column chromatography (LP:EtOAc 2:1) the pure product was obtained.

Reaction scale	Phenylpropanol: 0.6 g (4.4 mmol)
Reaction time	24 h
Purification	MPLC, LP:EtOAc (2:1)
Yield	0.4 g (66%) colorless liquid
Sum formula, m.w.	C ₁₁ H ₁₀ O, 279.33
¹H-NMR (200 MHz, CDCl₃)	2.63-2.84 (m, 2H, H ₂), 2.91-3.04 (m, 2H, H ₃), 7.21-7.42 (m, 5H, H _{arom.}), 9.81 (t, 1H, <i>J</i> = 1.37 Hz, H ₁).
¹³C-NMR (50 MHz, CDCl₃)	δ 28.3 (t, C ₃), 45.5 (t, C ₂), 126.3/128.3/128.6 (d, 5C, C _{arom.}), 140.5 (s, C _{ipso}), 201.7 (d, C ₁).
GC/MS	<i>m/z</i> 134 (57), 91 (100), 78 (64), 77 (45), 65 (35)

Analytical data was in accordance with the literature.²⁶⁷

²⁶⁷ R. J. McGorry, S. K. Allen, M. D. Pitzen, T. C. Coombs, *Tetrahedron Lett.* **2017**, *58*, 4623-4627.

A XIV.4.3 IBX Synthesis



Procedure In a 500 mL round bottom flask, 5.0 g of 2-iodobenzoic acid (5.0 g, 0.020 mol) were added to a 200 mL oxone solution in dH₂O (37.2 g, 3 equiv., 0.061 mol). The suspension was stirred with a KPG stirrer at 70°C for 1 h until a clear solution was obtained. After cooling the reaction mixture to room temperature, the suspension was stored at -20°C o/n. The solid material was filtered through a sintered-glass funnel (porosity 4) and washed repeatedly with pre-cooled water (6x 10 mL) and acetone (2x 10 mL). The obtained colorless powder was dried at high vacuum o/n at room temperature.

Reaction scale 2-iodobenzoic acid: 5.0 g (0.020 mol)

Reaction time 2 h

Yield 3.29 g (59%) colorless solid

Purification -

Sum formula, m.w. C₇H₅IO₅, 280.02

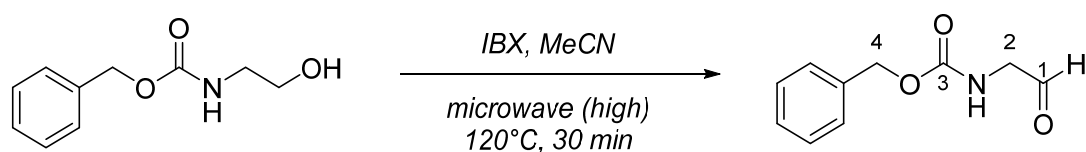
m.p. 231.2-232.5 (Lit²⁶⁸ 233)

¹H-NMR (200 MHz, d₆-DMSO) δ 7.83-8.40 (m, 4H) ppm.

Analytical data was in accordance with the literature.²⁶⁸

²⁶⁸ M. Frigerio, M. Santagostino, S. Sputore, *J. Org. Chem.* **1999**, *64*, 4537-4538.

A XIV.4.4 Benzyl (2-oxoethyl)carbamate (F₃)

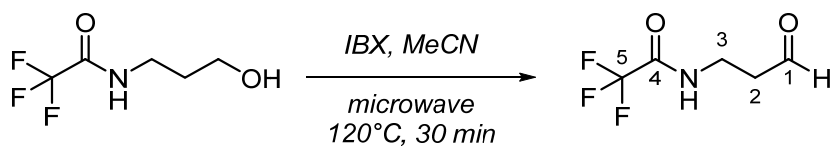


Procedure	In a microwave vial, <i>N</i> -Cbz-ethanolamine (0.555 g, 2.8 mmol, 1 equiv.) was dissolved in 20 mL degassed acetonitrile and IBX (1.6 g, 5.6 mmol, 2 equiv.) was added. The suspension was heated in a Biotage microwave oven (120°C) for around 30 minutes until full conversion, monitored <i>via</i> TLC (LP:EtOAc 1:3). After flash chromatography with diethyl ether, the final product was obtained after concentration at high vacuum.
Reaction scale	Benzyl (2-hydroxyethyl)carbamate: 0.555 g (2.8 mmol)
Reaction time	1 h
Purification	Flash filtration with Et ₂ O
Yield	0.376 g (70%) colorless liquid
Sum formula, m.w.	C ₁₀ H ₁₈ O ₂ , 193.20
¹H NMR (200 MHz, CDCl₃)	δ 4.13 (d, 2H, <i>J</i> = 5.17 Hz, H ₂), 5.13 (s, 2H, H ₄), 5.46 (bs, 1H, -NH), 7.26-7.42 (m, 5H, H _{arom.}), 9.64 (s, 1H, H ₁).
¹³C NMR (50 MHz, CDCl₃)	δ 51.7 (t, C ₂), 67.2 (t, C ₄), 128.1/128.3/128.6 (d, 5C, C _{arom.}), 136.1 (s, C _{ipso}), 156.3 (s, C ₃), 196.4 (d, C ₁).
GC/MS	<i>m/z</i> 164 (1), 108 (13), 107 (10), 91 (100), 65 (12)

Analytical data was in accordance with the literature.²⁶⁹

²⁶⁹ J. F. Hooper, S. Seo, F. R. Truscott, J. D. Neuhaus, M. C. Willis, *JACS* **2016**, *138*, 1630-1634.

A XIV.4.5 Oxidation to 3-Trifluoroacetamido-propanal (**L₃**)



Procedure

3-Trifluoroacetamido-propanol (0,6 g, 3 mmol, 1 equiv.) was dissolved in 20 mL degassed acetonitrile and IBX (1.6 g, 5.6 mmol, 2 equiv.) was added. The suspension was heated to reflux for 3 hours until full conversion was indicated by TLC (LP:EtOAc 1:1). The crude material was purified by column chromatography to afford the pure product in 78% yield.

Reaction scale

3-Trifluoroacetamido-propano: 602 mg (3 mmol)

Reaction time

4 h

Purification

MPLC, PE: EtOAc (1:1)

Yield

470 mg (78%) yellow liquid

Sum formula, m.w.

C₅H₆F₃NO₂, 169.12 g/mol

¹H NMR (400 MHz, CDCl₃)

δ 2.81 (dt, 2H, *J* = 5.9 Hz, H2), 3.61 (t, 2H, H3), 7.28 (bs, 1H, -NH), 9.7 (s, 1H, H1).

¹³C NMR (50 MHz, CDCl₃)

δ 33.3 (t, C3), 42.2 (t, C2), 115.8 (q, ¹*J*_{C,F} = 284.7 Hz, C5), 157.2 (q, ²*J*_{C,F} = 36.5 Hz, C4), 200.7 (d, C1).

LC/MS *m/z* (ESI⁺)

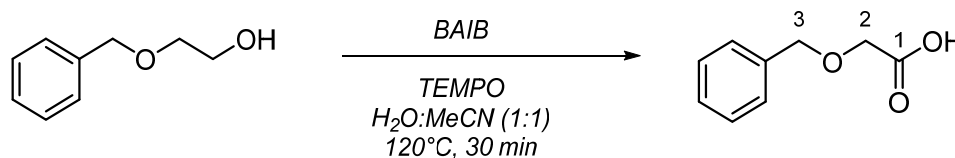
found [M+H⁺] 168.04; calculated [M+H⁺] 168.08.

Analytical data was in accordance with the literature.²⁷⁰

²⁷⁰ M. Wei, Z. Li, T. Li, B. Wu, Y. Liu, J. Qu, X. Li, L. Li, L. Cai, P. G. Wang, *ACS Catal.* **2015**, *5*, 4060-4065.

A XIV.5 Synthesis of Carboxylic Acids

A XIV.5.1 2-(Benzyloxy)acetic acid (**D**₄)



Procedure In a 8 mL reaction vial, Diacetoxyiodo-benzene (BAIB) (1.0 g, 2.5 mmol, 2.3 equiv.), TEMPO (55 mg, 0.23 mmol, 0.2 equiv.) were dissolved in 2mL (H₂O:MeCN 1:1) and 2-(benzyloxy)ethan-1-ol (**D**₂) (150 mg, 1.1 mmol, 1 equiv.) was added. Reaction progress monitored *via* TLC (LP:EtOAc 1:1 and drops of AcOH). Reaction mixture was concentrated and triturated two times with Et₂O and acetone and concentrated under reduced pressure. The crude product was dissolved in Et₂O and extracted with 1 N HCl. The organic layer was dried over Na₂SO₄ and concentrated under reduced pressure and the pure product was obtained after concentration at high vacuum overnight.

Reaction scale 2-(benzyloxy)ethan-1-ol: 150 mg (1.1 mmol)

Reaction time 24 h

Yield 0.16 g (88%) yellow liquid

Sum formula, m.w. C₉H₁₀O₃, 166.08

¹H-NMR (200 MHz, CDCl₃) δ 4.14 (s, 2H, C2), 4.65 (s, 2H, C3), 7.27-7.40 (m, 5H, H_{arom.}) 9.48 (bs, 1H, C1).

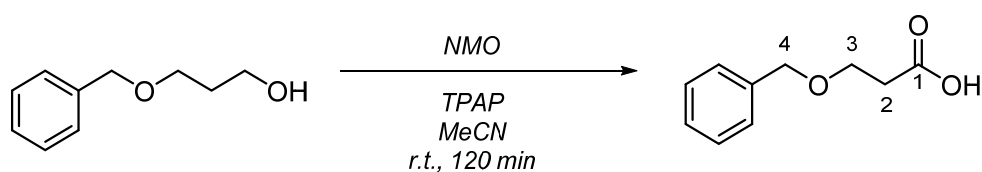
¹³C-NMR (50 MHz, CDCl₃) δ 66.7 (t, C2), 73.5 (t, C3), 128.3/128.4/128.7 (d, 5C, C_{arom.}), 136.7 (s, C_{ipso}), 175.2 (s, C1).

GC/MS *m/z* 166 (1), 107 (72), 91 (100), 79 (47), 65 (12).

Analytical data was in accordance with the literature.²⁷¹

²⁷¹ C. W. Wullschleger, J. Gertsch, K.-H. Altmann, *Org. Lett.* **2010**, *12*, 1120-1123.

A XIV.5.2 3-(Benzyloxy)propanoic acid (E₄)

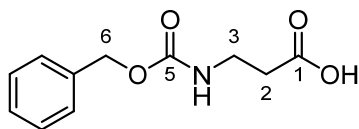


Procedure	To a stirred solution of 3-(benzyloxy)propan-1-ol (83 mg, 0.5 mmol, 1 equiv.) and of NMO (676 mg, 5.00 mmol, 10 equiv.) in acetonitrile (2 mL), TPAP (18 mg, 10 mol%) was added. The reaction mixture was stirred at room temperature for 2 h until full conversion was obtained, monitored <i>via</i> TLC (LP:EtOAc 1:1 and drops of AcOH). The reaction was stopped by a dropwise addition of 5 mL isopropanol. The reaction mixture was filtered through Celite and concentrated under reduced pressure and after column chromatography (DCM:EtOAc 1:1 with 1% AcOH) the pure product was obtained.
Reaction scale	3-(benzyloxy)propan-1-ol: 83 mg (0.5 mmol)
Reaction time	24 h
Purification	MPLC, DCM:EtOAc
Yield	75 mg (83%) colorless liquid
Sum formula, m.w.	C ₁₀ H ₁₂ O ₃ , 180.20
¹H-NMR (200 MHz, CDCl₃)	δ 2.68 (d, <i>J</i> = 6.3 Hz, 2H, H ₂), 3.79 (d, <i>J</i> = 6.3 Hz, 2H, H ₃), 4.56 (s, 2H, H ₄), 7.26-7.39 (m, 5H, H _{arom}) 10.69 (bs, 1H, C1).
¹³C-NMR (50 MHz, CDCl₃)	δ 34.8 (t, C ₂), 65.2 (t, C ₃), 73.2 (t, C ₄), 127.7/127.8/128.4 (d, 5C, C _{arom.}), 137.7 (s, C _{ipso}), 176.8 (s, C1).
GC/MS	<i>m/z</i> 180 (3), 107 (100), 91 (81), 79 (52), 77 (26)

Analytical data was in accordance with the literature.²⁷²

²⁷² N. Kinarivala, J. H. Suh, M. Botros, P. Webb, P. C. Trippier, *Bioorg. Med. Chem. Lett.* **2016**, 26, 1889-1893.

A XIV.5.3 3-(((Benzyloxy)carbonyl)amino)propanoic acid (**G**₄)



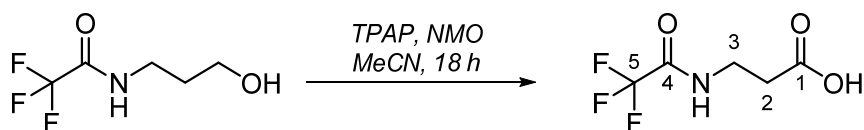
Procedure In a 8 mL reaction vial, β -alanine (0.8 g, 9 mmol, 1 equiv.) was dissolved in 4 mL 2 N NaOH, cooled with an ice bath and under vigorous stirring benzylchloroformate (1.7 mL, 11.7 mmol, 1.3 equiv.) was added dropwise and stirred at room temperature and the reaction progress was monitored *via* TLC (70% EtOH with drops of CH₃COOH). The reaction mixture was extracted three times with Et₂O and the aqueous layer was acidified with 2 N HCl to pH 1-2. The aqueous solution was extracted three times with EtOAc and the combined organic layers were washed with brine, dried over Na₂SO₄ and concentrated under reduced pressure. The pure product was obtained after recrystallized in H₂O (HPLC grade) with drops of ethanol and 2 N HCl, filtration and finally the colorless powder was dried overnight in the 65°C.

Reaction scale	β -alanine: 0.8 g (9 mmol)
Reaction time	24 h
Purification	Recrystallization
Yield	0.56 g (27%) colorless solid
Sum formula, m.w.	C ₁₁ H ₁₃ NO ₄ , 223.08
m.p.	102-104°C (Lit. 104-106°C) ²⁷³
¹H-NMR (200 MHz, CDCl₃)	δ 2.61 (t, <i>J</i> = 5.7 Hz, 2H, H ₂), 3.42-3.56 (m, 2H, H ₃), 5.10 (s, 2H, H ₆), 5.30 (bs, 1H, -NH) 7.27-7.40 (m, 5H, H _{arom.}), 10.57 (bs, 1H, C ₁).
¹³C-NMR (50 MHz, CDCl₃)	δ 34.3 (t, C ₂), 36.5 (t, C ₃), 67.0 (t, C ₆), 128.3/128.3/128.7 (d, 5C, C _{arom.}), 136.4 (s, C _{ipso}), 156.5 (s, C ₅), 177.6 (s, C ₁).
LC/MS <i>m/z</i> (ESI⁺)	found [M+Na ⁺] 246.18; calculated [M+Na ⁺] 246.07

Analytical data was in accordance with the literature.²⁷³

²⁷³ A. K. Mallik, H. Qiu, T. Sawada, M. Takafuji, H. Ihara, *Chem. Commun.* **2011**, 47, 10341-10343.

A XIV.5.4 3-Trifluoroacetamido-propionic acid (L₄)



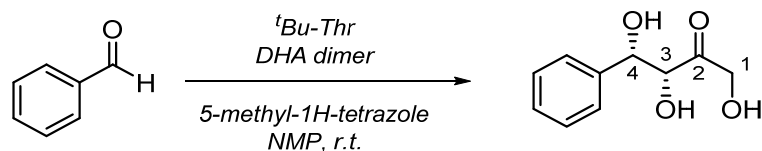
Procedure 3-Trifluoroacetamido-propanol (0.5 g, 2.9 mmol, 1 equiv.) and NMO (3.72 g, 29.7 mmol, 10 equiv.) were dissolved in 25 mL HPLC grade acetonitrile. Under stirring at room temperature TPAP (105 mg, 0.3 mmol, 0.1 equiv.) was added and the reaction mixture was stirred until full conversion was obtained, monitored *via* TLC (LP:EtOAc 1:1 and drops of CH₃COOH). After filtration of TPAP and solid residues through Celite, the solvent was removed under reduced pressure. The brown crude liquid was dissolved in 20 mL hexane and washed two times with 10 ml of 1 N HCl, three times with 10 mL brine, and dried over Na₂SO₄. The solvent was removed under reduced pressure yielding in colorless crystalline material. Since the ¹H NMR indicates some impurities, the crude product was resuspended in 7 mL heptane and cooled overnight at -20°C. The pure product was obtained by centrifugation (14000g x 10 min) and lyophilization in 37% yield.

Reaction scale	3-Trifluoroacetamido-propanol: 0.5 g (2.9 mmol)
Reaction time	18 h
Purification	Recrystallization
Yield	198 mg (37%) colorless solide
Sum formula, m.w.	C ₅ H ₆ F ₃ NO ₃ , 185.10
m.p.	114-116°C (Lit. 113-115°C) ²⁷⁴
¹H NMR (400 MHz, D₂O)	δ 2.70 (t, <i>J</i> = 6.5 Hz, 2H, H ₂), 3.60 (t, <i>J</i> = 6.5 Hz, 2H, H ₃).
¹³C NMR (101 MHz, D₂O)	δ 32.7 (t, C ₂), 35.5 (t, C ₃), 115.8 (q, ¹ <i>J</i> _{C,F} = 285.7 Hz, C ₅), 158.9 (d, ² <i>J</i> _{C,F} = 37.4 Hz, C ₄), 175.6 (s, C ₁).
LC/MS m/z (ESI⁺)	found [M+Na ⁺] 186.43; calculated [M+Na ⁺] 186.10
Analytical data was in accordance with the literature. ²⁷⁴	

²⁷⁴ M. S. Cherevin, Z. P. Zubreichuk, L. A. Popova, T. G. Gulevich, V. A. Knizhnikov, *Russian Journal of General Chemistry* **2007**, 77, 1576-1579.

A XIV.6 Synthesis of Aldol Adducts

A XIV.6.1 ^tBu-Thr Catalyzed Aldol reaction with DHA (A_{5,I})



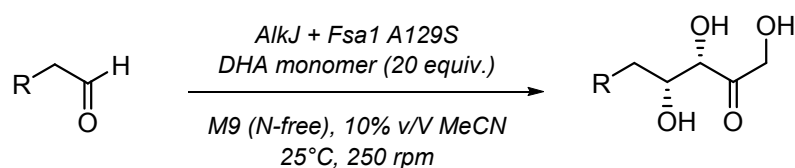
Procedure In a 8 mL reaction vial, 287 mg freshly distilled benzaldehyde (1.5 equiv., 3 mmol), 329 mg DHA dimer (1 equiv., 2 mmol), 141 mg ^tBu-*D*-Thr (0.1 equiv 0.8 mmol) and 16 mg 5-methyl-1H-tetrazole (0.1 equiv., 0.2 mmol) were dissolved in 2.5 mL NMP and stirred at room temperature overnight. The reaction progress was monitored *via* TLC (CH₂Cl₂:Isopropanol 10:1) and after full conversion of the starting material, the reaction mixture was filtered through Celite and concentrated at reduced pressure. The pure product was obtained *via* preparative HPLC (MeOH:H₂O 2:1) and concentration at high vacuum for overnight.

Reaction scale	Benzaldehyde: 287 mg (3 mmol)
Reaction time	12 h
Purification	preparative HPLC (C18), MeOH/H ₂ O gradient
Yield	70 mg (12%) yellow liquid
Sum formula, m.w.	C ₁₀ H ₁₂ O ₄ , 196.02
¹H NMR (400 MHz, Methanol-<i>d</i>₄)	δ 4.28-4.34 (m, 1H, H1), 4.47 (d, <i>J</i> = 2.9 Hz, 1H, H3), 5.04 (d, <i>J</i> = 3.0 Hz, 1H, H4), 7.21-7.46 (m, 5H, H _{arom.}),
¹³C NMR (101 MHz, Methanol-<i>d</i>₄)	δ 68.12 (d, C1), 75.51 (d, C4), 80.99 (d, C3), 127.59/128.43/129.11 (d, 5C, C _{arom.}), 142.72 (d, C _{ipso}), 213.00 (s, C2).
LC/MS m/z (ESI⁺)	found [M+Na ⁺] 219.05; calculated [M+Na ⁺] 219.02
Specific rotation	[α] _D ²² = -38.7 (c=0.5 in MeOH) (lit. ²⁷⁵ [α] _D ²² = -45.6 (c=0.5 in MeOH)).

Analytical data was in accordance with the literature.²⁷⁵

²⁷⁵ S. Luo, H. Xu, L. Zhang, J. Li, J.-P. Cheng, *Org. Lett.* **2008**, *10*, 653-656.

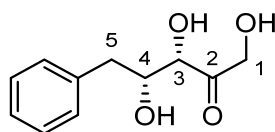
A XIV.7 Synthesis of Acyclic Aldol Compounds with DHA and Co-expressed AlkJ and Fsa1 A129S



General procedure

Resting cells of *E. coli* BL21-Gold(DE3) co-expressing AlkJ and Fsa1 A129S were prepared as described (A XII.16). 1.8 g of the DHA dimer (10 mmol) were monomerized in resting cell medium for 2 h at 37°C in an orbital shaker (200 rpm). In a 1 L baffled Erlenmeyer flask, the aldol acceptor molecule (1.0 equiv, 1.0 mmol) was dissolved in MeCN (10 mL) and the DHA monomer solution (20 equiv, 20 mmol) was added to freshly prepared resting cells (OD₅₉₀ = 10.0) and shaken at 25°C, 250 rpm (V_{total} = 200 mL). The reaction progress was monitored by GC/FID until full consumption of the starting material was observed. The crude reaction mixture was centrifuged and directly transferred for purification on a BUCHI Sepacore flash cartridge (C18, 25 g). Resting cell media ingredients (e.g. salts) and excess DHA were eluted with 5% (v/v) MeOH/95% (v/v) H₂O followed by product elution using 100% (v/v) methanol. The product fraction was concentrated at 25-30°C at high vacuum to obtain the pure product (A XIV.2.1-2.4).

A XIV.7.1 (3*S*,4*R*)-1,3,4-Trihydroxy-5-phenylpentan-2-one (B_{5,II})



General procedure

Reaction scale

Reaction time

Purification

Yield

Sum formula, m.w.

¹H NMR (400 MHz, Methanol-d₄)

¹³C NMR (101 MHz, Methanol-d₄)

LC/MS *m/z* (ESI⁺)

Specific rotation

Analytical data was in accordance with the literature.²⁷⁷

A XIV.2

Phenylacetaldehyde: 122 mg (1 mmol)

2 h

SPE purification

163 mg (78%) yellow liquid

C₁₁H₁₄O₄, 210.23

δ 2.84 (dd, $J = 13.4$ Hz, 7.4, 1H, H5), 2.94 (dd, $J = 13.4$ Hz, 7.1 Hz, 1H, H5), 4.04 (d, $J = 2.2$ Hz, 1H, H3), 4.14 (td, $J = 7.2$ Hz, 2.1 Hz, 1H, H4), 4.41-4.54 (m, 2H, H1), 7.17-7.31 (m, 5H, H_{arom.}).

δ 40.73 (t, C5), 67.88 (q, C1), 74.99 (d, C4), 78.25 (d, C3), 127.4/129.4/130.5 (d, 5C, C_{arom.}), 139.80 (d, C_{ipso}), 214.02 (s, C2).

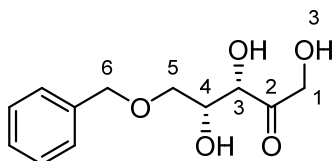
found [M+Na⁺] 223.05; calculated [M+Na⁺] 233.07

$[\alpha]_{\text{D}}^{22} = +21.8$ ($c = 1.07$ in CHCl₃) (Lit²⁷⁶ $[\alpha]_{\text{D}}^{22} = +26.7$ ($c = 1.07$ in CHCl₃); (Lit²⁷⁷ $[\alpha]_{\text{D}}^{22} = +35$ ($c = 1.0$ in CHCl₃))

²⁷⁶ A. J. Humphrey, N. J. Turner, R. McCague, S. J. C. Taylor, *Chem. Commun.* **1995**, 2475-2476.

²⁷⁷ A. L. Concia, C. Lozano, J. A. Castillo, T. Parella, J. Joglar, P. Clapes, *Chem. Eur. J.* **2009**, *15*, 3808-3816.

A XIV.7.2 5-*O*-Benzyl-*D*-xylulose ($D_{5,II}$)



General procedure

A XIV.2

Reaction scale

2-(benzyloxy)acetaldehyde: 152 mg (1 mmol)

Reaction time

2 h

Purification

SPE purification

Yield

142 mg (60%) yellow liquid

Sum formula, m.w.

$C_{12}H_{16}O_5$, 240.10

1H NMR (200 MHz, Methanol- d_4)

δ 3.53 (dd, $J = 9.6$ Hz, 6.1 Hz, 1H, H5), 3.63 (dd, $J = 9.6$ Hz, 6.6 Hz, 1H, H5), 4.12 (td, $J = 6.5$ Hz, 1.8 Hz, 1H, H4), 4.31 (d, $J = 2.0$ Hz, 1H, H3), 4.43-4.57 (m, 2H, H1), 4.55 (s, 2H, H6), 7.24-7.37 (5H, $H_{aromatic}$).

^{13}C NMR (50 MHz, Methanol- d_4)

δ 67.9 (t, C1), 71.6 (d, C4), 72.1 (t, C5), 74.3 (t, C6), 77.2 (d, C3), 128.8/129.5/130.6 (d, 5C, $C_{arom.}$), 139.6 (d, C_{ipso}), 213.5 (s, C2)

LC/MS m/z (ESI $^+$)

found $[M+Na^+]$ 263.05; calculated $[M+Na^+]$ 263.08

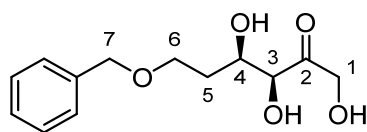
Specific rotation

$[\alpha]_D^{22} = +5.3$ ($c=1.0$ in $CHCl_3$) (lit.²⁷⁸ $[\alpha]_D^{22} = +2.8$ ($c=1.0$ in $CHCl_3$))

Analytical data was in accordance with the literature.²⁷⁸

²⁷⁸ A. L. Concia, C. Lozano, J. A. Castillo, T. Parella, J. Joglar, P. Clapes, *Chem. Eur. J.* **2009**, *15*, 3808-3816.

A XIV.7.3 5-*O*-Benzyl-6-*D*-fructose (**E**_{5,II})



General procedure

Reaction scale

Reaction time

Purification

Yield

Sum formula, m.w.

¹H NMR (600 MHz, Methanol-*d*₄)

¹³C NMR (151 MHz, Methanol-*d*₄)

HR/MS *m/z* (ESI⁺)

Specific rotation

A XIV.2

3-(benzyloxy)propanal: 166 mg (1 mmol)

2 h

SPE purification

162 mg (64%) yellow liquid

C₁₃H₁₈O₅, 254.12

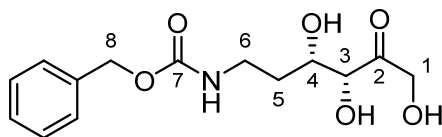
δ 1.84-1.91 (m, 2H, H5), 3.58-3.66 (m, 2H, H6), 4.13-4.15 (m, 2H, H3, H4), 4.43-4.55 (m, 4H, H7, H1), 7.25–7.35 (5H, H_{arom.}).

δ 34.3 (t, C5), 67.8 (t, C6), 68.1 (t, C1), 70.8 (d, C4), 74.0 (t, C7), 79.4 (d, C3), 128.6/128.8/129.4 (d, 5C, C_{arom.}), 139.67 (d, C_{ipso}), 213.48 (s, C2).

found [M+Na⁺] 277.1044; calculated [M+Na⁺]277.1046

[α]_D²² = 5.8 (c=1.0 in MeOH)

A XIV.7.4 5,6-dideoxy-6-[[[(phenylmethoxy)carbonyl]amino]-L-threo-2-Hexulose (**G_{5,II}**)



General procedure

Reaction scale

Reaction time

Purification

Yield

Sum formula, m.w.

¹H NMR (400 MHz, Methanol-d₄)

¹³C NMR (101 MHz, Methanol-d₄)

LC/MS *m/z* (ESI⁺)

Specific rotation

A XIV.2

Benzyl (3-oxopropyl)carbamate :209 mg (1 mmol)

2 h

SPE purification

270 mg (91%) yellow liquid

C₁₄H₁₉NO₆, 279.12

δ 1.73-1.79 (m, 2H, H5), 3.19-3.27 (m, 2H, H6), 3.98 (td, *J*= 8.1 Hz, 2.4 Hz, 1H, H4), 4.13 (d, *J*= 2.3 Hz, 1H, H3), 4.43-4.52 (m, *J*= 19.2 Hz, 2H, H1), 5.07 (s, 2H, H8), 7.26-7.37 (5H, H_{arom.})

δ 34.4 (t, C5), 38.7 (t, C6), 67.4 (t, C1), 67.8 (t, C8), 71.1 (d, C4), 79.4 (d, C3), 128.8/129.0/129.5 (d, 5C, C_{arom.}), 138.4 (d, C_{ipso}), 159.0 (s, C7), 213.4 (s, C2).

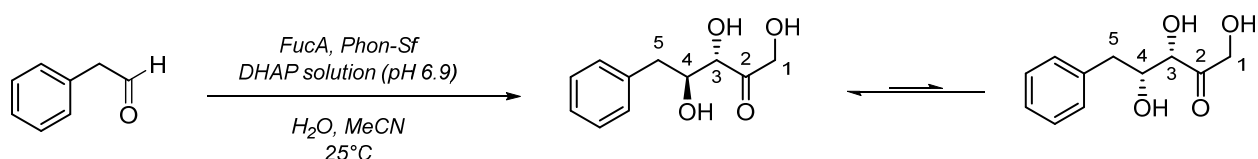
found [M+Na⁺] 320.11; calculated [M+Na⁺] 320.10

[α]_D²² = +5.8 (c=1.0 in MeOH) (lit.²⁷⁹ [α]_D²² = +9 (c=1.0 in MeOH))

Analytical data was in accordance with the literature.²⁷⁹

²⁷⁹ J. A. Castillo, J. Calveras, J. Casas, M. Mitjans, M. P. Vinardell, T. Parella, T. Inoue, G. A. Sprenger, J. Joglar, P. Clapes, *Org. Lett.* **2006**, *8*, 6067-6070.

A XIV.8 Synthesis of (3*S*,4*S*)-1,3,4-Trihydroxy-5-phenylpentan-2-one (B_{5,FucA}) by FucA and Phon-Sf



Cell free extracts of FucA and Phon-Sf were prepared as described in the sections A XII.17.1 and A XII.18. For the synthesis (3*S*, 4*S*)-1,3,4-trihydroxy-5-phenylpentan-2-one, the reagent solutions were prepared according to the optimized reaction settings (A II.1) and were added in a 8 mL reaction flask in the following order:

Table 60 Reagents for preparative *in vitro* cascade approach using FucA and Phon-Sf.

	Reaction mixture	Equiv.	Final concentration	
1	215 μ L DHAP (pH 6.9)	1.0	0.12 mmol	21.5 mg
2	250 μ L Aldehyde in MeCN	1.7	0.2 mmol	24 mg
3	785 μ L dH ₂ O			
4	1250 μ L FucA (25 mg/mL)		5 mg/mL	
5	2500 μ L Phon-Sf (10 mg/mL)		5 mg/mL	

The flask was shaken vigorously overnight at room temperature and the DHAP consumption was monitored *via* RP-TLC (MeOH:H₂O 1:1 $R_{f(DHAP)} = 0.95$; $R_{f(product)} = 0.8$). The reaction was stopped at -80°C in order to precipitate biotransformation residues, which were separated by centrifugation after thawing (13000 rpm, 5 min, 4°C). The supernatant was transferred for SPE purification on a BUCHI Sepacore flash cartridge (C18, 25 g). All biotransformation residues (e.g. salts) were eluted with 5% (v/v) MeOH/95% (v/v) H₂O followed by product elution applying a MeOH:H₂O gradient. The product fractions were concentrated at 25-30°C at high vacuum to afford the pure product in 17% yield.

Reaction scale	Phenylacetaldehyde: 24 mg (0.2 mmol)
Reaction time	18 h
Purification	SPE purification
Yield	7 mg (17%) colorless liquid (<i>syn/anti</i> 30/70)
Sum formula, m.w.	C ₁₁ H ₁₄ O ₄ , 210.23
¹H NMR (400 MHz, Methanol-d₄)	<i>anti</i> diastereomer

δ 2.74 (dd, $J = 13.8$ Hz, 8.6 Hz, 1H, H5), 2.93 (dd, $J = 13.8$ Hz, 4.4 Hz, 1H, H5), 3.98 (m, 1H, H4), 4.10 (d, $J = 5.3$ Hz, 1H, H3), 4.43-4.56 (m, 2H, H1), 7.24-7.37 (m, 5H, H_{arom.}).

syn diastereomer

δ 2.86 (dd, $J = 13.4$ Hz, 7.4 Hz, 1H, H5), 2.93 (dd, $J = 13.8$ Hz, 4.4 Hz, 1H, H5), 4.05 (d, $J = 2.0$ Hz, 1H, H3), 4.15 (td, $J = 7.3, 2.1$, 1H, H4), 4.45-4.54 (m, 2H, H1), 7.15-7.25 (m, 5H, H_{arom.}).

¹³C NMR (101 MHz, Methanol-d₄)

anti diastereomer

δ 38.7 (t, C5), 66.8 (q, C1), 74.3 (d, C4), 77.6 (d, C3), 125.8/127.8/129.3 (d, 5C, C_{arom.}), 138.5 (d, C_{ipso}), 211.8 (s, C2).

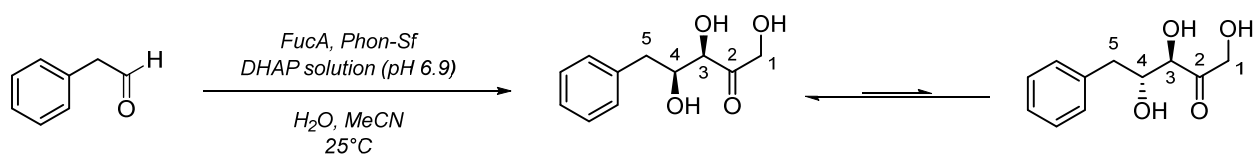
syn diastereomer

δ 39.3 (t, C5), 66.5 (q, C1), 73.6 (d, C4), 76.8 (d, C3), 125.9/128.0/129.1 (d, 5C, C_{arom.}), 138.4 (d, C_{ipso}), 212.7 (s, C2).

LC/MS m/z (ESI⁺)

found [M+Na⁺] 223.15; calculated [M+Na⁺] 233.07

A XIV.9 Synthesis of (3*R*,4*S*)-1,3,4-Trihydroxy-5-phenylpentan-2-one (B_{5,RhuA}) by RhuA and Phon-Sf



Cell free extracts of FucA and Phon-Sf were prepared as described in the sections A XII.17.1 and A XII.18. For the synthesis (3*R*, 4*S*)-1,3,4-trihydroxy-5-phenylpentan-2-one, the reagent solutions were prepared according to the optimized reaction settings (A II.1) and were in a 8 mL reaction flask in the following order:

Table 61 Reagents for preparative *in vitro* cascade approach using RhuA and Phon-Sf

	Reaction mixture		Equiv.	Final concentration	
1	215 μL	DHAP (pH 6.9)	1.0	0.12 mmol	21.5 mg
2	250 μL	Aldehyde in MeCN	1.7	0.2 mmol	24 mg
3	785 μL	dH ₂ O			
4	1250 μL	FucA (25 mg/mL)		5 mg/mL	
5	2500 μL	Phon-Sf (10 mg/mL)		5 mg/mL	

The flask was shaken vigorously overnight at room temperature and the DHAP consumption was monitored *via* RP-TLC (MeOH:H₂O 50:50 R_{f(DHAP)}= 0.95; R_{f(product)}= 0.8). The reaction was stopped at - 80°C in order to precipitate biotransformation residues, which were separated by centrifugation after thawing (13000 rpm, 5 min, 4°C). The supernatant was transferred for SPE purification on a BUCHI Sepacore flash cartridge (C18, 25 g). All biotransformation residues (e.g. salts) were eluted with 5% (v/v) MeOH/95% (v/v) H₂O followed by product elution applying a MeOH:H₂O gradient. The product fractions were concentrated at 25-30°C at high vacuum to afford the pure product in 29% yield.

Reaction scale	Phenylacetaldehyde: 24 mg (0.2 mmol)
Reaction time	18 h
Purification	SPE purification
Yield	12 mg (29%) yellowish liquid; (<i>syn/anti</i> 60/40)
Sum formula, m.w.	C ₁₁ H ₁₄ O ₄ , 210.23

¹H NMR (400 MHz, Methanol-d₄) *syn diastereomer*

δ 2.86 (dd, J = 13.4 Hz, 7.4 Hz, 1H, H5), 2.96 (dd, J = 13.4 Hz, 7.1 Hz, 1H, H5), 4.06 (d, J = 2.0 Hz, 1H, H3), 4.10 (td, J = 7.2 Hz, 2.0 Hz, 1H, H4), 4.42-4.48 (m, 2H, H1), 7.25-7.32(m, 5H, H_{arom.}).

anti diastereomer

δ 2.74 (dd, J = 13.8 Hz, 8.5 Hz, 1H, H5), 2.92 (dd, J = 13.8 Hz, 4.3 Hz, 1H, H5), 3.99 (m, 1H, H4), 4.10 (d, J = 5.3 Hz, 1H, H3), 4.40-4.56 (m, 2H, H1), 7.13-7.24 (m, 5H, H_{arom.}).

¹³C NMR (101 MHz, Methanol-d₄)

syn diastereomer

δ 39.3 (t, C5), 66.5 (q, C1), 73.6 (d, C4), 76.8 (d, C3), 126.0/128.0/129.1 (d, 5C, C_{arom.}), 138.4 (d, C_{ipso}), 212.7 (s, C2).

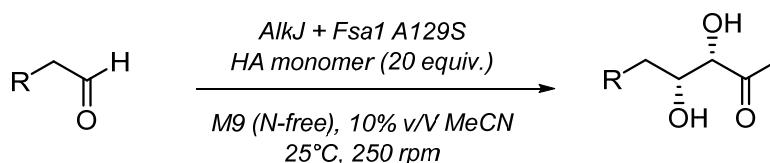
anti diastereomer

δ 38.7 (t, C5), 66.5 (q, C1), 74.3 (d, C4), 77.6 (d, C3), 125.8/127.8/129.3 (d, 5C, C_{arom.}), 138.5 (d, C_{ipso}), 211.8 (s, C2).

LC/MS m/z (ESI⁺)

found [M+Na⁺] 223.13; calculated [M+Na⁺] 233.07

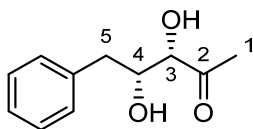
A XIV.10 Synthesis of acyclic Aldol compounds with HA and co-expressed AlkJ and Fsa1 A129S



General procedure

Resting cells of *E. coli* BL21-Gold(DE3) co-expressing AlkJ and Fsa1 A129S were prepared as described (**A XII.16**). In a 1 L baffled Erlenmeyer flask, the aldol acceptor molecule (1.0 equiv, 1.0 mmol) was dissolved in acetonitrile (10 mL) and 1.5 mL HA (20 equiv, 20 mmol) were added to freshly prepared resting cells ($OD_{590} = 10.0$) and shaken at 25°C, 250 rpm ($V_{\text{total}} = 200$ mL). The reaction progress was monitored by GC/FID until full consumption of the starting material was observed. The crude reaction mixture was centrifuged and directly transferred for purification on a BUCHI Sepacore flash cartridge (C18, 25 g). Resting cell media ingredients (e.g. salts) and excess DHA were eluted with 5% (v/v) MeOH/95% (v/v) H₂O followed by product elution using 100% (v/v) methanol. The product fraction was concentrated at 25-30°C at high vacuum to afford the pure product (**A XIV.5.1-5.4**).

A XIV.10.1 (3*S*,4*R*)-3,4-Dihydroxy-5-phenylpentan-2-one (B_{5,I})



General procedure

A XIV.5

Reaction scale

Phenylacetaldehyde: 122 mg (1 mmol)

Reaction time

2 h

Purification

SPE purification

Yield

135 mg (70%) yellow liquid

Sum formula, m.w.

C₁₁H₁₄O₃, 194.09

¹H NMR (400 MHz, Methanol-d₄)

δ 2.18 (s, 3H, H1), 2.77–3.04 (m, 2H; H5), 3.94 (d, *J* = 2.0 Hz, 1H, H3), 4.16 (td, *J* = 7.2 Hz, 2.0 Hz, 1H, H4), 7.10–7.38 (m, 5H, H_{arom.}).

¹³C NMR (101 MHz, Methanol-d₄)

26.5 (q, C1), 41.0 (t, C5), 74.7 (d, C4), 79.7 (d, C3), 127.3/129.4/130.5 (d, 5C, C_{arom.}), 139.8 (d, C_{ipso}), 212.4 (s, C2).

LC/MS *m/z* (ESI⁺)

found [M+Na⁺] 217.07; calculated [M+Na⁺] 217.08

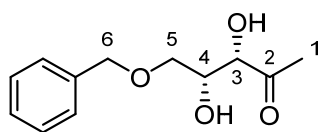
Specific rotation

[α]_D²² = +31.7 (c=1.0 in MeOH) (lit.²⁸⁰ [α]_D²² = +29.8 (c=1.0 in MeOH))

Analytical data was in accordance with the literature.²⁸⁰

²⁸⁰ A. L. Concia, C. Lozano, J. A. Castillo, T. Parella, J. Joglar, P. Clapes, *Chem. Eur. J.* **2009**, *15*, 3808-3816.

A XIV.10.2 5-*O*-Benzyl-1-deoxy-*D*-xylulose (**D**_{5,1})



General procedure

Reaction scale

Reaction time

Purification

Yield

Sum formula, m.w.

¹H NMR (400 MHz, Methanol-*d*₄)

¹³C NMR (101 MHz, Methanol-*d*₄)

LC/MS *m/z* (ESI⁺)

Specific rotation

Analytical data was in accordance with the literature.²⁸¹

A XIV.5

2-(benzyloxy)acetaldehyde: 152 mg (1 mmol)

24 h

SPE purification

199 mg (89%) yellow liquid

C₁₂H₁₆O₄, 224.10

δ 2.24 (s, 3H, H1), 3.56 (dd, *J* = 9.5 Hz, 6.2 Hz, 1H, H5), 3.66 (dd, *J* = 9.5 Hz, 6.5 Hz, 1H, H5), 4.17 (td, *J* = 6.3 Hz, 2.3 Hz, 1H, H4), 4.22 (d, *J* = 2.4 Hz, 1H, H3), 4.55-4.59 (m, 2H, H6), 7.28-7.39 (5H, H_{arom.}).

δ 26.6 (q, C1), 71.8 (d, C4), 71.9 (t, C5), 74.3 (t, C6), 78.7 (d, C3), 128.7/128.9/129.4 (d, 5C, C_{arom.}) 139.6 (d, C_{ipso}), 212.0 (s, C2).

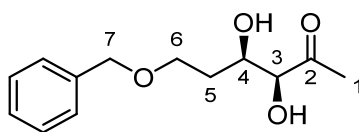
found [M+Na⁺]247.06; calculated [M+Na⁺] 247.09

[α]_D²² = +51.9 (c=1.0 in CH₂Cl₂) (lit.²⁸¹ [α]_D²² = +58.2 (c=1.0 in CH₂Cl₂); lit.²⁸² [α]_D²² = +27.8 (c=0.89 in CH₂Cl₂))

²⁸¹ A. L. Concia, C. Lozano, J. A. Castillo, T. Parella, J. Joglar, P. Clapes, *Chem. Eur. J.* **2009**, *15*, 3808-3816.

²⁸² C. A. Citron, N. L. Brock, P. Rabe, J. S. Dickschat, *Angew. Chem. Int. Ed.* **2012**, *51*, 4053-4057.

A XIV.10.3 5-*O*-Benzyl-6-deoxy-*D*-fructose (E_{5,I})



General procedure

A XIV.5

Reaction scale

3-(benzyloxy)propanal: 166 mg (1 mmol)

Reaction time

2 h

Purification

SPE purification

Yield

144 mg (61%) yellow liquid

Sum formula, m.w.

C₁₃H₁₈O₄, 238.12

¹H NMR (600 MHz, Methanol-d₄)

δ 1.87-1.90 (m, 2H, H5), 2.21 (s, 3H, H1), 3.57-3.68 (m, 2H, H6), 4.02 (d, *J* = 2.3 Hz, 1H, H3), 4.17 (td, *J* = 6.2 Hz, 2.3 Hz, 1H, H4), 4.53-4.56 (m, 2H, H7), 7.26-7.36 (5H, H_{aromatic}).

¹³C NMR (151 MHz, Methanol-d₄)

δ 26.6 (q, C1), 34.6 (t, C5), 68.1 (t, C6), 70.4 (d, C4), 74.0 (t, C7), 81.0 (d, C3), 128.6/128.9/129.4 (d, 5C, C_{arom.}), 139.7 (d, C_{ipso}), 212.0 (s, C2).

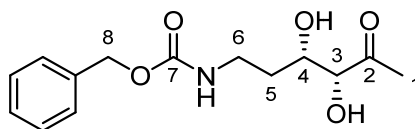
HR/MS *m/z* (ESI⁺)

found [M+Na⁺] 261.1108; calculated [M+Na⁺] 261.1097

Specific rotation

[α]_D²² = +45.1 (c=1.0 in MeOH)

A XIV.10.4 *L*-threo-2-Hexulose-1,5,6-trideoxy-6-[(phenylmethoxy)-carbonyl]amino] (**G_{5,l}**)



General procedure

Reaction scale

Reaction time

Purification

Yield

Sum formula, m.w.

¹H NMR (400 MHz, Methanol-d₄)

¹³C NMR (101 MHz, Methanol-d₄)

LC/MS *m/z* (ESI⁺)

Specific rotation

Analytical data was in accordance with the literature²⁸³

A XIV.5

Benzyl-(3-hydroxypropyl)carbamate: 209 mg (1 mmol)

2 h

SPE purification

233 mg (83%) yellow liquid

C₁₄H₁₉NO₅, 281.13

δ 1.75-1.80 (m, 2H, H6), 3.20 (s, 3H, H1), 3.20-3.29 (m, 2H, H5), 4.01 (td, *J* = 6.8 Hz, 2.3 Hz, 1H, H4), 4.05 (d, *J* = 2.3 Hz, 1H, H3), 5.07 (s, 2H, H8), 7.27-7.37 (5H, H_{aromatic}).

δ 26.5 (q, C1) 34.7 (t, C5), 38.7 (t, C6), 67.4 (t, C8), 70.7 (d, C4), 80.9 (d, C3), 128.8/128.9/129.4 (d, 5C, C_{arom.}), 138.4 (d, C_{ipso}), 159.0 (s, C7), 211.9 (s, C2).

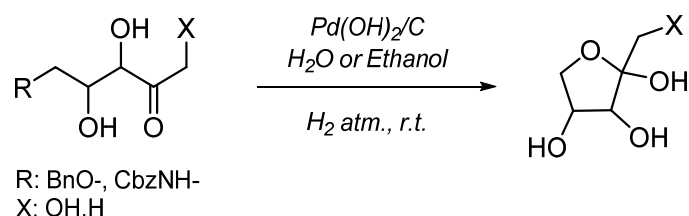
found [M+Na⁺] 304.12; calculated [M+Na⁺] 304.11.

[α]_D²² = +50.5 (c=1.0 in CH₂Cl₂).

²⁸³ M. Sugiyama, Z. Hong, P.-H. Liang, S. M. Dean, L. J. Whalen, W. A. Greenberg, C.-H. Wong, *JACS* **2007**, *129*, 14811-14817.

A XV Hydrogenation of acyclic Aldol Compounds

A XV.1 Deprotection to the Cyclic Aldol Product



A XV.1.1 Hydrogenation in the Parr Apparatus

General procedure

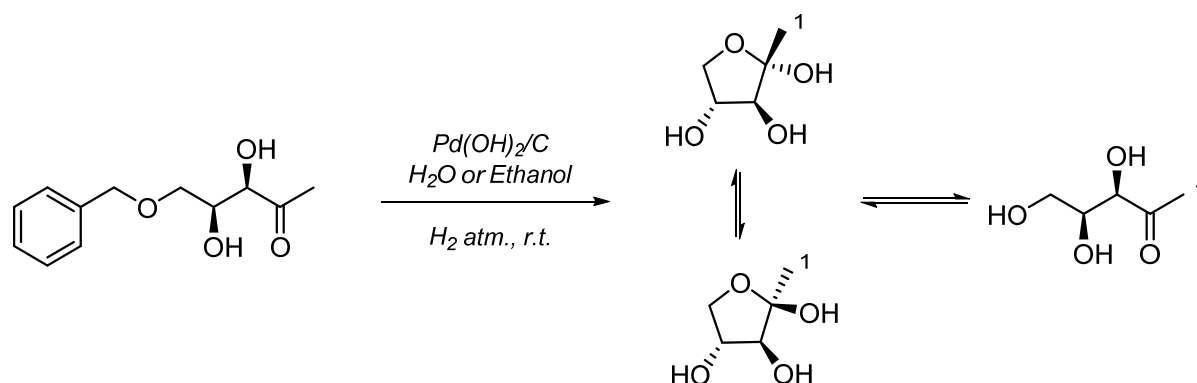
In a high-pressure PARR glas vial, crude lyophilized acyclic aldol product was dissolved in ethanol and Pd(OH)₂ (0.024 g, 10 w%) was added. Hydrogenation was performed at room temperature, o/n in a PARR apparatus at 50 psi H₂ until full conversion was monitored via RP-TLC and LC/MS.

A XV.1.2 Hydrogenation using an H₂ Balloon

General procedure

In a 8 mL reaction vial equipped with a hydrogen balloon, acyclic aldol material (25 mg, 1 equiv.) was dissolved in 1.5-2 mL ethanol and Pd(OH)₂/C (2.5 mg, 10 w%) was added to the degassed (with argon and hydrogen) reaction mixture and the reaction progress was monitored *via* TLC (LP:EtOAc 1:5) or RP-TLC (MeOH:H₂O 2:1). After full conversion, the solvent was removed by lyophilization overnight and the pure product was obtained by flash filtration (RP18, MeOH:H₂O 2:1) and concentration at high vacuum.

A XV.2 1-Deoxy-D-xylulose



General procedure

Reaction scale

A XV.1.2

36 mg (0.16 mmol)

Reaction time

72 h

Purification

flash filtration, MeOH:H₂O 2:1, RP silica 60.

Yield

21 mg (quant.) colorless oil

Sum formula, m.w.

C₅H₁₀O₄, 134.13

¹H-NMR (400 MHz, D₂O)

mixture of α/β and the acyclic adduct:

δ 1.38/1.43/2.24 (s, 9H, H1), 3.10-5.11 ppm (all other H, no assignment possible due to low resolution).

¹³C-NMR (400 MHz, D₂O)

δ 25.9, 62.2, 62.3, 63.2, 71.2, 71.3, 72.4, 73.3, 74.3, 75.5, 77.6, 77.9, 93.4, 97.7, 213.1 (s, C2) ppm (no assignment possible due to low resolution).

LC/MS *m/z* (ESI⁺)

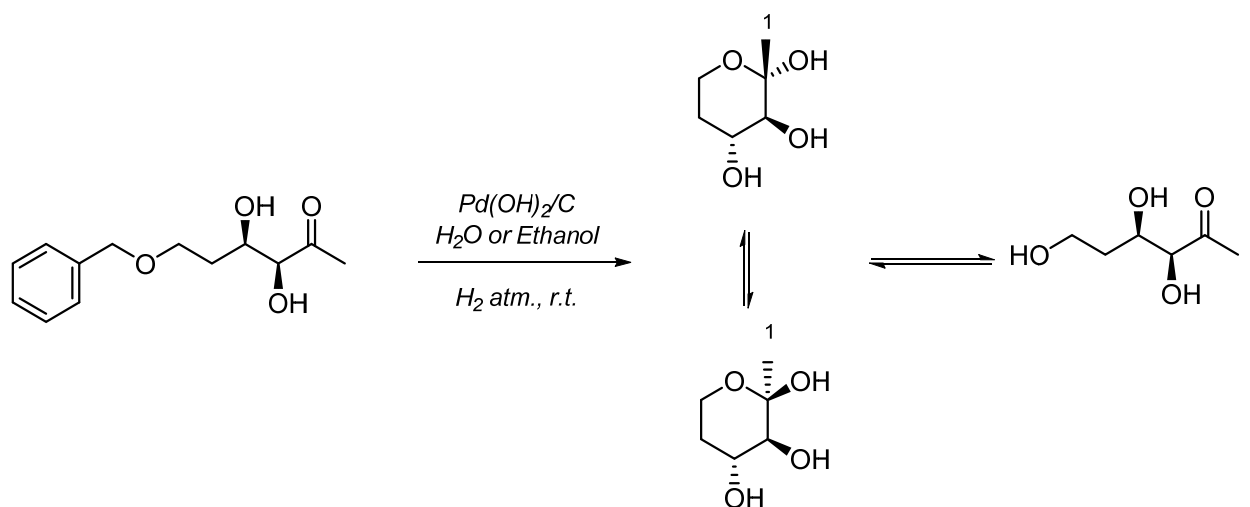
found [M+Na⁺] 157.17; calculated [M+Na⁺] 157.13

Analytical data was in accordance with the literature.^{284,285}

²⁸⁴ A. L. Concia, C. Lozano, J. A. Castillo, T. Parella, J. Joglar, P. Clapes, *Chem. Eur. J.* **2009**, *15*, 3808-3816.

²⁸⁵ L. Espelt, T. Parella, J. Bujons, C. Solans, J. Joglar, A. Delgado, P. Clapes, *Chem. Eur. J.* **2003**, *9*, 4887-4899.

A XV.3 (3*S*,4*R*)-2-Methyltetrahydro-2*H*-pyran-2,3,4-triol



General procedure

Reaction scale

Reaction time

Purification

Yield

Sum formula, m.w.

¹H-NMR (400 MHz, D₂O)

¹³C-NMR (400 MHz, D₂O)

LC/MS *m/z* (ESI⁺)

Analytical data was in accordance with literature.^{286,287}

A XV.1.2

32 mg (0.13 mmol)

72 h

flash filtration, MeOH/H₂O 2:1, RP silica 60

20 mg (quant.) colorless oil

C₆H₁₂O₄, 148.16

mixture of α/β and the acyclic adduct:

δ 1.40/1.58/1.85 (s, 9H, H1), 2.24-5.11 ppm (all other H, no assignment possible due to low resolution).

δ 23.6, 26.5, 35.6, 40.3, 43.8, 46.3, 59.7, 60.2, 63.3, 70.3-79.8 (3C), 94.4, 98.6, 99.3, 118.1, 124.9, 202.00 (s,C2) ppm (no assignment possible due to low resolution).

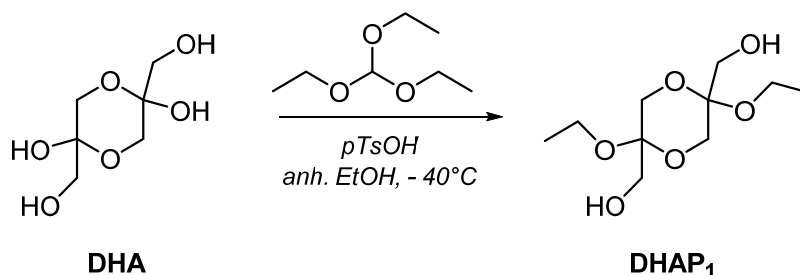
found [M+Na⁺] 171.23; calculated [M+Na⁺] 171.16

²⁸⁶ A. L. Concia, C. Lozano, J. A. Castillo, T. Parella, J. Joglar, P. Clapes, *Chemistry* **2009**, *15*, 3808-3816.

²⁸⁷ L. Espelt, T. Parella, J. Bujons, C. Solans, J. Joglar, A. Delgado, P. Clapes, *Chemistry* **2003**, *9*, 4887-4899.

A XVI DHAP Synthesis

A XVI.1.1 Protection of the Acetale Position of the Dimer



Procedure

In a round bottom flask (three times evaporated and flushed with argon), *p*-toluolsulfonic acid (42 mg, 0.24 mmol, 0.005 equiv.) and triethyl-orthoformate (19.1 mL, 116 mmol, 2.2 equiv.) were dissolved in 90 mL anhydrous ethanol. The solution was then cooled *via* ice bath and DHA (9.55 g, 53 mmol, 1 equiv.) was added in portions over 5 h. After completion of the addition, the ice bath was removed and the reaction mixture was stirred at room temperature until full conversion, monitored *via* TLC (EtOAc:LP; 10:1). The solution was again cooled *via* ice bath and anhydrous NaHCO₃ (40 mg, 0.5 mmol, 0.01 equiv.) was added and stirred for additional 30 minutes at 0°C. Afterwards the reaction mixture was warmed to room temperature, insoluble compounds were removed by filtration through Celite and the organic solvent was removed under reduced pressure at 40°C. The solid crude product was triturated with 50 mL EtOAc and 50 mL heptane and purified *via* recrystallization in EtOAc. The colorless precipitate was collected, washed with cold EtOAc and dried at high vacuum to afford **DHAP₁** (1,4-Dioxane-2,5-dimethanol, 2,5-diethoxy-).

Reaction scale

Dihydroxyacetone dimer: 9.55 g (53 mmol)

Reaction time

48 h

Purification

Recrystallization in EtOAc

Yield

5.0 g (40%) colorless solid

Sum formula, m.w.

C₁₀H₂₀O₆, 236.13

m.p.

121.5-122.5°C (Lit. not given)

¹H-NMR (200 MHz, D₂O)

δ 1.03-1.231 (m, 6H, H2), 3.33-3.85 (m, 12H, H1).

¹³C-NMR (50 MHz, D₂O)

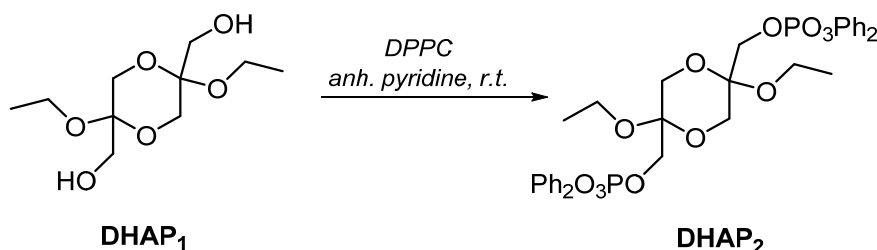
syn/anti mixture: δ 14.3 & 14.5 (q, 6C), 56.9 (t, 1C), 57.4 (t, 1C), 59.2 (t, 1C), 60.5 (t, 1C), 61.1 (t, 1C), 63.2 (t, 1C), 95.3 (s, 1C) 98.1 (s, 1C).

LC/MS *m/z* (ESI⁺)

found [M+Na⁺] 259.20; calculated [M+Na⁺] 259.13

Analytical data was in accordance with the literature.²⁸⁸

A XVI.1.2 Phosphorylation of the Primary Alcohol with Diphenylphosphorochloride



Procedure

In a round bottom flask compound **DHAP₁** (5 g, 21 mmol, 1 equiv.) was dissolved in 23 mL anhydrous pyridine under argon atmosphere and diphenyl phosphoryl chloride (DPPC) (8.7 mL, 42 mmol, 2 equiv.) was added slowly at 4°C and the formed suspension was stirred o/n at room temperature until full conversion monitored *via* TLC (EtOAc:LP; 5:1). Subsequently the reaction mixture was poured onto 150 mL EtOAc and 2 N HCl (approx. 30 mL) was added until a clear two-phase solution was obtained. The reaction mixture was washed two times with 30 mL brine and 30 mL NaHCO₃ (aq) and an additional time with 30 mL brine. The combined organic phases were dried over Na₂SO₄ and the organic solvent was removed under reduced pressure at 40°C, dried at high vacuum and **DHAP₂** was obtained as a colorless solid.

Reaction scale

DHAP-A: 9 g (42.4 mmol)

Reaction time

1 h

Yield

14.6 g (99%) colorless solid

Sum formula, m.w.

C₃₆H₃₈O₁₂P₂, 700.18

m.p.

76-78°C (Lit. not given)

¹H-NMR (200 MHz, CDCl₃)

δ 1.14 (dt, *J* = 10.0 Hz, 7.0 Hz, 6H, H₂), 3.34-3.83 (m, 8H, H₁), 3.96-4.40 (m, 4H, H₃), 7.10-7.43 (m, 20H, H_{aromatic}).

¹³C NMR (101 MHz, CDCl₃)

syn/anti mixture: δ 15.3 (d, 6C), 56.8 (d, 4C), 60.9 (d, 2C), 63.6 (d, 2C), 64.7 (d, 2C), 66.3 (d, 2C), 93.7 (s, 1C) 97.0 (s, 1C), 120.1/125.6/129.9 (d, 5C, C_{arom.}), 150.4 (s, 4C, C_{ipso}).

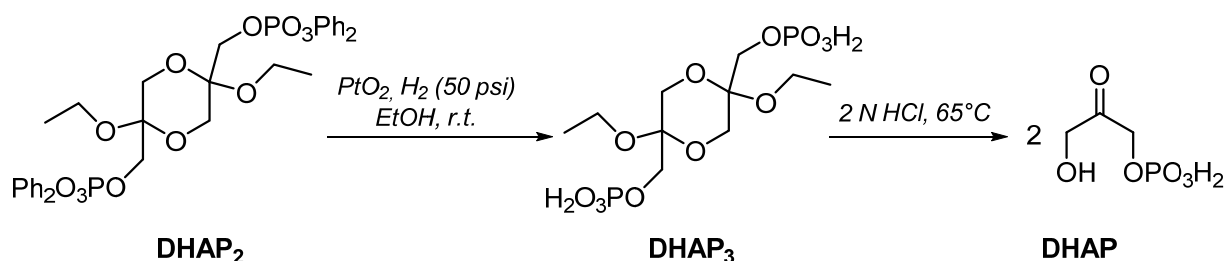
²⁸⁸ S.-H. Jung, J.-H. Jeong, P. Miller, C.-H. Wong, *J. Org. Chem.* **1994**, *59*, 7182-7184.

LC/MS m/z (ESI⁺)

found $[M+H]^+$ not detectable; calculated $[M+H]^+$ 701.18.

Analytical data was in accordance with the literature.²⁸⁹

A XVI.1.3 Hydrogenation for the Phenyl Deprotection *via* PtO₂



Procedure

DHAP₂ (0.6 g, 0.8 mmol, 1 equiv.) was dissolved in 40 mL EtOH and PtO₂ (60 mg, 10 w%) was added. The reaction mixture was shaken at a PAAR apparatus under 50 psi H₂ pressure at room temperature. The reaction progress was monitored *via* TLC and ¹H NMR and after full conversion of DHAP₂, the crude reaction mixture was used without further purification for the final acidic hydrolysis to the DHAP monomer.

Reaction scale

DHAP₂: 0.6 g (0.8 mmol)

Reaction time

o/n

Yield

not isolated, crude yield 90%

Sum formula, m.w.

C₁₂H₂₂O₁₂P₂, 396.06

¹H NMR (200 MHz, D₂O)

δ 0.93-1.25 (m, 6H, -H₂), 3.31-4.51 (m, 12H, -H₁).

Analytical data was in accordance with the literature.²⁷⁴

²⁸⁹ S.-H. Jung, J.-H. Jeong, P. Miller, C.-H. Wong, *J. Org. Chem.* **1994**, 59, 7182-7184.

A XVI.1.4 Acidic Hydrolysis (DHAP Monomer)

Procedure The crude mixture of **DHAP₃** was diluted with H₂O (HPLC grade), acidified to pH 1 with 2 N HCl, and stirred for 5 h at 65°C. After full conversion of the starting material, monitored *via* RP-TLC (MeOH:H₂O 3:1) the mixture was cooled to room temperature and the pH was adjusted to 3.7 with 3 N NaOH to obtain the final stock solution of DHAP. To determine the end concentration of the obtained aqueous DHAP solution, LC-MS/MS measurements were performed. Therefore, the synthesized DHAP stock solution was diluted with H₂O (HPLC grade) to an end concentration of 20 μM and was compared with a standard calibration of purchased DHAP.

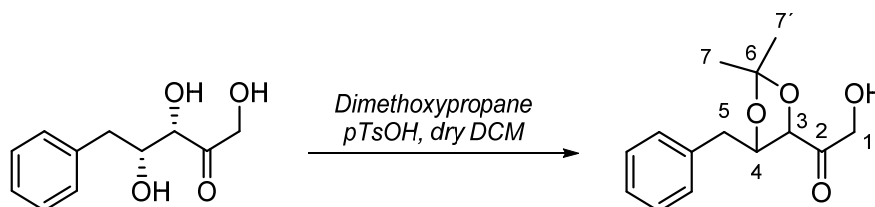
Final concentration 0.42 M

LC-MS/MS compared with standard calibration of purchased DHAP with the q1/q3 *m/z* [M-H] 169/97

Analytical data was in accordance with the literature.²⁸⁷

A XVII Chemical Route to Phosphorylated Aldol Adduct

A XVII.1 Acetonide Protection to (**B**_{5,II})



Procedure:

In a 8 mL reaction vial, **B**_{5,II} (100 mg, 0.22 mmol, 1. equiv.) was dissolved in 4000 μ L $\text{CH}_2\text{Cl}_2\text{-d}_2$ and dimethoxypropane (41 μ L, 0.24 mmol, 1.3 equiv.) as well as *p*-toluenesulfonic acid (2.8 mg, 5 mol%) were added and stirred at r.t. The reaction progress was monitored *via* TLC (LP:EtOAc 3:1) and after approx. 2 h the reaction mixture was poured into satd. NaHCO_3 and the aqueous solution was extracted three times with CH_2Cl_2 and brine. The combined organic layers were dried over Na_2SO_4 and concentrated under reduced pressure at 35°C. The pure product was obtained after column chromatography (EtOAc:LP 3:1) and concentration at high vacuum overnight.

Reaction scale

B_{5,II}: 100 mg (0.5 mmol)

Reaction time

3 h

Purification

Column chromatography (EtOAc:LP 3:1)

Yield

81 mg, 65%, colorless oil

Sum formula, m.w.

$\text{C}_{14}\text{H}_{18}\text{O}_4$, 250.12

¹H NMR (400 MHz, CD_2Cl_2)

δ 1.30 (d, $J = 4.0$ Hz, 6H, H7, H7'), 2.80-2.88 (m, 1H, H5), 3.03-3.05 (m, 1H, H5), 4.07-4.18 (m, 3H, H3, H4, H6), 4.29-4.50 (m, 2H, H1), 7.00-7.30 (m, 5H, H_{arom.}).

¹³C NMR (101 MHz, CD_2Cl_2)

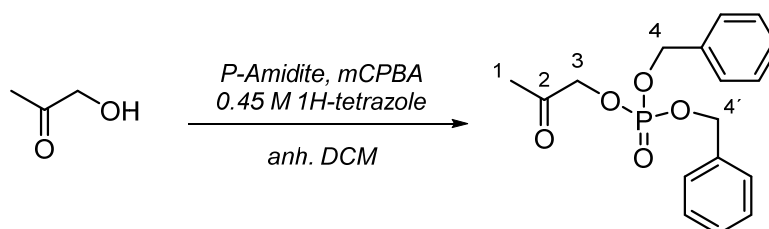
δ 26.3 (q, C7), 27.2 (q, C7'), 39.3 (t, C5), 66.6 (t, C1), 79.0 (d, C3), 83.1 (d, C4), 111.3 (s, C6), 127.0-130.0 (d, 5C, C_{arom.}), 137.5 (d, C_{ipso}), 209.8 (s, C2).

GC/MS

m/z 191 (45), 133 (100), 105 (59), 91 (69), 59 (55)

A XVII.2 Phosphorylation using Dibenzyl-*N,N*-diisopropylphosphoramidite

A XVII.2.1 Dibenzyl-*N,N*-diisopropylphosphoramidite with HA



Procedure

In a Schlenk tube, hydroxyacetone (92.6 μL , 1.3 mmol, 1 equiv.) was dissolved in 6.6 mL dry CH_2Cl_2 (1:19 dilution), P-amidite (0.680 mL, 2.0 mmol, 1.5 equiv.) was added followed by the dropwise addition of 3.9 mL of a 0.45 M 1-H-tetrazole in MeCN solution. The reaction mixture was stirred until full conversion to the phosphite intermediate was obtained, monitored *via* TLC (EtOAc:LP 5:1) and then cooled to -78°C . A solution of *m*CPBA (242 mg, 2.7 mmol, 2 equiv.) in 2.2 mL CH_2Cl_2 was added slowly and reaction was stirred at -78°C until full conversion to the phosphate product, monitored *via* TLC (EtOAc:LP; 5:1, $R_f = 0.45$) is obtained. The reaction was stopped by the addition of trimethylamine (0.464 mL, 3.4 mmol, 2.5 equiv.) and the cold reaction mixture was then warmed to room temperature. The reaction mixture was extracted with NaHCO_3 and the aqueous layer was extracted three times with CH_2Cl_2 . The combined organic layers were washed with brine, dried over Na_2SO_4 and concentrated at high vacuum. The pure product was obtained by column chromatography (EtOAc:LP 5:1).

Reaction scale

Hydroxyacetone: 100 mg (1.3 mmol)

Reaction time

3 h

Purification

Column chromatography (EtOAc:LP 5:1)

Yield

285 mg, 65%, colorless oil

Sum formula, m.w.

$\text{C}_{12}\text{H}_{22}\text{O}_{12}\text{P}_2$, 334.10

^1H NMR (400 MHz, CDCl_3)

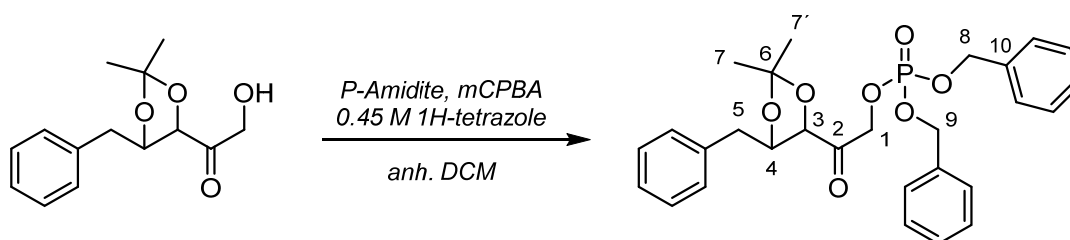
δ 2.13 (s, 3H, H1), 4.46 (d, $J = 9.4$ Hz, 2H, H3), 4.90-5.28 (m, 2H, H4, H4'), 7.31-7.47 (m, 5H, H_{arom}).

¹³C NMR (101 MHz, CDCl₃) δ 26.0 (q, C1), 69.8 (d, *J*_{C,P}= 5.7 Hz, 2C, C4, C4'), 70.7 (d, *J*_{C,P}= 5.9, C3), 128.1 /128.7/128.7 (d, 5C, C_{arom.}) 135.54 (d, C_{ipso}), 202.46 (s, C2).

³¹P NMR (162 MHz, CDCl₃) δ -1.19 (p, *J*= 8.8 Hz).

GC/MS *m/z* 136(100), 107 (15), 104 (31), 91 (90), 65 (18)

A XVII.2.2 Phosphorylation of Acetonide Protected Aldol using Dibenzyl-*N,N*-diisopropylphosphoramidite (B₅P_{prot})



Procedure

In a 8 mL reaction vial, acetonide protected aldol (40 mg, 0.16 mmol, 1 equiv.) was dissolved in 2.6 mL CH₂Cl₂, P-amidite (0.081 mL, 0.24 mmol, 1.5 equiv.) was added followed by the dropwise addition of 0.446 mL of a 0.45 M 1*H*-tetrazole in MeCN solution. The reaction mixture was stirred at r.t. for 45 min, the reaction progress was monitored *via* TLC (EtOAc:LP 3:1, R_f=0.95) and additional P-amidite (0.008 mL, 0.15 equiv.) was added, until full conversion to the phosphite intermediate is obtained. The reaction mixture was then cooled to -78°C and a solution of *m*CPBA (55 mg, 0.3 mmol, 2 equiv.) in 0.6 mL dry CH₂Cl₂ was added slowly and the reaction mixture was stirred at -78°C until full conversion to the phosphate product was obtained, monitored *via* TLC (EtOAc:LP 5:1, R_f= 0.5). After extraction with water and three times with CH₂Cl₂, the organic layers were combined, dried over Na₂SO₄, and concentrated under reduced pressure at 35°C. The product was obtained *via* column chromatography (EtOAc:LP 5:1).

Reaction scale B₅,_{acetonide}: 10 mg (0.04 mmol)

Reaction time 3 h

Yield 13 mg, 65%, yellow oil

Sum formula, m.w.

C₁₂H₂₂O₁₂P, 510.18

¹H NMR (400 MHz, CD₂Cl₂)

δ 1.14 (d, *J* = 6.8 Hz, 1H, H7'), 1.27 (d, *J* = 6.8 Hz, 1H, H7), 2.78 (dd, *J* = 14.4 Hz, 7.8 Hz, 1H, H5), 3.03 (dd, *J* = 14.4 Hz, 3.3 Hz, 1H, H5), 4.01 (d, *J* = 8.1 Hz, 1H, H3), 4.13 (td, *J* = 8.0, 3.2 Hz, 1H, H4), 4.90-5.04 (m, 2H, H1), 7.07-7.45 (m, 5H, H_{arom.}).

¹³C NMR (101 MHz, CD₂Cl₂)

δ 22.3 (q, C7'), 25.9 (q, C7), 38.9 (t, C5), 69.2 (t, C1), 69.6 (t, 2C, C8, C9), 78.5 (d, C3), 82.7 (d, C4), 126.6-129.7 (d, 16C, C_{arom.}), 202.7 (s, C2).

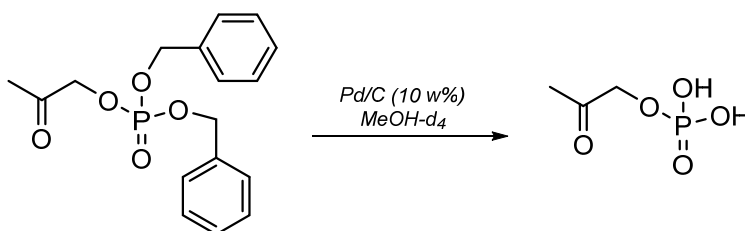
³¹P NMR (162 MHz, CD₂Cl₂)

δ -0.99 (h, *J* = 9.0 Hz).

LC/MS or GC/MS

not found

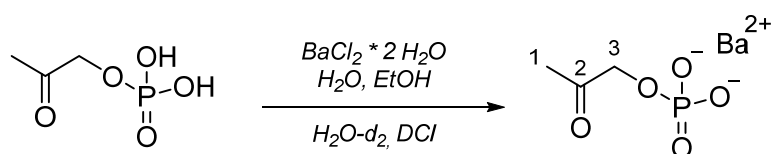
A XVII.3 Dibenzyl-deprotection of HAP *via* Pd/C and H₂ Balloon



Procedure

In a 8 mL reaction vial, equipped with an H₂ balloon, 30 mg of starting material was dissolved in 0.7 mL methanol-d₄ and Pd/C (3 mg, 10 w%) was added and stirred at room temperature overnight. The reaction progress was monitored *via* TLC and NMR. The reaction was stopped by centrifugation (14000g x 15 min) and filtration (Celite) of Pd/C and the methanol layer was concentrated at reduced pressure. The obtained crude, colorless oil product was confirmed by ¹H NMR and was further purified by applying a BaCl₂ precipitation protocol (A XVIII.3.1).

A XVII.3.1 BaCl₂ Precipitation of HAP



Procedure

In a 1.5 mL eppi, HAP (4 mg, 0.027 mmol, 1 equiv.) was dissolved in 100 μ L H₂O and the pH was adjusted to 6.9. To the solution, BaCl₂*2H₂O (26 mg, 0.11 mmol, 4.0 equiv.) was added and the residual precipitates were collected *via* centrifugation (14000g x 15 min), separated, and 500 μ L ethanol were added to the supernatant. Immediately a cloudy solution was obtained, which was cooled to 4°C o/n. The precipitation efficiency was determined *via* TLC (EtOAc:LP 10:1) by checking the supernatant towards remaining starting material. Finally, the obtained colorless powder was lyophilized and the HAP-barium salt was dissolved in 600 μ L D₂O and 20 μ L DCl for NMR measurements until a clear solution (pH 1) was obtained.

Reaction scale

Hydroxyacetonephosphate: 4 mg (0.9 mmol)

Reaction time

o/n

Yield

quant.

Sum formula, m.w.

C₃H₇O₅P, 154.00

¹H NMR (400 MHz, D₂O/DCl)

δ 2.07 (s, 3H, C1), 4.52 (d, *J* = 8.3 Hz, 2H, H3)

¹³C NMR (101 MHz, D₂O/DCl)

δ 20.4 (q, C1), 69.9 (t, C3), 176.6 (s, C2).

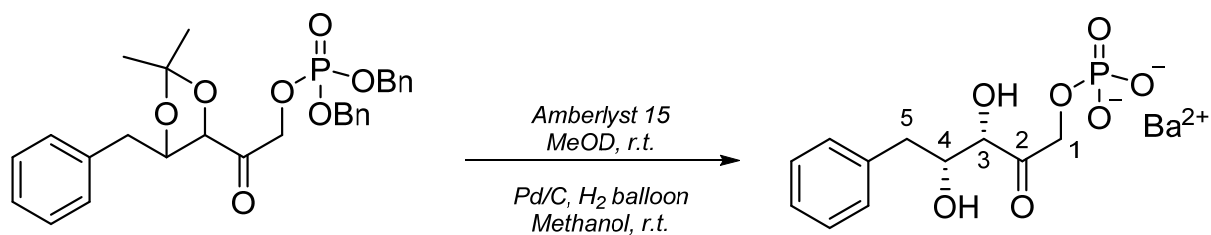
³¹P NMR (162 MHz, D₂O/DCl)

δ -0.46 (t, *J* = 8.3 Hz).

HR/MS *m/z* (ESI⁺)

found [M+H⁺] 155.0107; calculated [M+H⁺] 155.0104.

A XVII.4 Deprotection to (3*S*,4*R*)-1,3,4-Trihydroxy-5-phenylpentan-2-one (**B_{6,chem}**)



Procedure

The fully protected, crude aldol adduct (**B_{5P,prot}**) (13 mg, 0.025 mmol, 1 equiv.) was dissolved in 0.6 mL methanol-*d*₄ and 2 mg (approx. 10 w%) Amberlyst 15 was added. The reaction was stirred at room temperature for 14 h and the progress was monitored *via* TLC (EtOAc:LP 1:1). The crude mixture was transferred with additional 0.4 mL methanol-*d*₄ into a 8 mL reaction vial, which was then equipped with a H₂ balloon for the hydrogenation mediated by Pd/C (2 mg, > 15w%). The reaction was stirred at room temperature and full starting material consumption was indicated *via* TLC (EtOAc:LP 10:1; RP-TLC MeCN:H₂O 3:1) after 14 h. Additionally, the formation of the phosphorylated target product was confirmed by ¹H, ³¹P and H-P HSQC. The crude product was purified by the previously established BaCl₂·2 H₂O precipitation protocol. Therefore, the solvent was evaporated at high vacuum for 1 h. The residue (10 mg) was dissolved in 0.5 mL D₂O and the pH was adjusted to 6.5. This aqueous solution was treated with (21 mg, 0.84 mmol, 4.0 equiv.) BaCl₂·2 H₂O and 2.0 mL ethanol. The obtained cloudy solution was stored overnight at -20°C and the formed, colorless precipitants were collected by centrifugation at 13000 rpm for 5 min at 4°C and washed two times with 3 mL CH₂Cl₂. The solid product was concentrated at high vacuum to afford the target molecule as colorless powder in 81% yield. For NMR measurements, the product-barium salt was dissolved in 600 μL D₂O and 20 μL DCl until a clear solution (pH 1) was obtained.

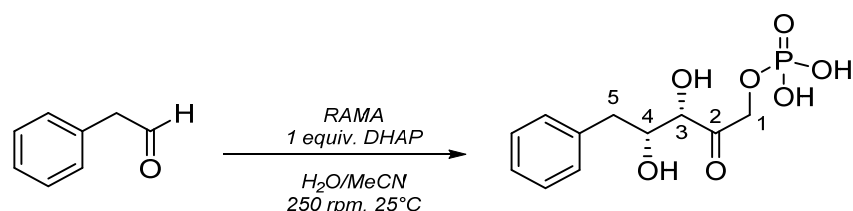
Reaction scale

B_{5P,prot}: 13 mg (0.025 mmol)

Reaction time	o/n
Sum formula, m.w.	C ₁₁ H ₁₅ O ₇ P, 290.06
Yield	≤5 mg (81%) colorless solid
¹H NMR (400 MHz, D₂O)	δ = 2.79-2.90 (m, 2H, H5), 4.22-4.26 (m, <i>J</i> = 6.5 Hz, 2.0 Hz, 2H, H3, H4), 4.74 (m, 2H, H1), 7.07-7.36 (m, 5H, H _{arom.}).
¹³C NMR (101 MHz, D₂O)	δ 38.6 (t, C5), 68.9 (t, C1), 72.8 (d, C4), 76.8 (d, C3), 126.6/128.7/129.5 (d, 5C, C _{arom.}), 137.9 (s, C _{ipso}), 209.4 (s, C2).
³¹P NMR (162 MHz, D₂O)	δ -0.49 (t, <i>J</i> = 8.3 Hz).
LC/MS <i>m/z</i> (ESI⁺)	found [M-H] 289.24; calculated [M-H] 289.21
Specific rotation	see A XVIII.5

A XVII.5 Biocatalytic route by RAMA to (3*S*,4*R*)-1,3,4-Trihydroxy-5-phenylpentan-2-one (B₆)

RAMA was purchased from Sigma Aldrich and the determine activity was only 37% in comparison to the reported activity on the data sheet. This value was used for the preparation of a 100 U/mL RAMA stock solution.



For the synthesis (3*S*,4*R*)-1,3,4-trihydroxy-5-phenylpentan-2-one phosphate catalyzed by RAMA, the reagent solutions were prepared and added in a 8 mL reaction flask in the following order:

Table 62 Reagents for the synthesis of (3*S*,4*R*)-1,3,4-trihydroxy-5-phenylpentan-2-one phosphate catalyzed by RAMA.

Reaction mixture		Equiv.	Final concentration
1	215 μ L DHAP (pH 6.9)	1.0	0.12 mmol 21.5 mg
2	250 μ L Phenylacetaldehyde in MeCN	1.7	0.2 mmol 24 mg
3	3335 μ L dH ₂ O		
4	200 μ L RAMA (100 U/mL)		5 U/mL

The flask was shaken vigorously overnight at room temperature and the DHAP consumption was monitored *via* RP-TLC (MeOH/H₂O 50/50 $R_{f(\text{DHAP})} = 0.95$; $R_{f(\text{product})} = 0.8$). RP-TLC do not indicate full DHAP consumption after five hours as well as on the next day, additional 5 U/mL of RAMA were added at both time points. After 14 h of reaction time, additional phenyl acetaldehyde (7 mg, 0.5 equiv.) in 75 μ L acetonitrile was added and stirred until full DHAP consumption was observed. The reaction was stopped at -80°C in order to precipitate the biotransformation residues and centrifuged after thawing (13000 rpm, 5 min, 4°C). The supernatant was transferred 50 mL Greiner tube and desired product was isolated by the BaCl₂*2 H₂O precipitation protocol. For that purpose, the pH of the biotransformation solution (6.25% MeCN) was set to 6.5 and 120 mg of BaCl₂*2 H₂O was added together with 20 ml of ethanol and the mixture was stored at -20°C overnight. The formed, colorless precipitate was centrifuged (13000 rpm, 5 min, 4°C) and resuspended two times in 3 mL of CH₂Cl₂. The solvent was removed and the crystalline product was dried under high vacuum for 1 h to afford the target

compound. For NMR measurements, the product-barium salt was dissolved in 600 μL D_2O and 20 μL DCl until a clear solution (pH 1) was obtained.

Reaction scale	Phenylacetaldehyde 24 mg (0.2 mmol)
Reaction time	18 h
Purification	$\text{BaCl}_2 \cdot 2 \text{H}_2\text{O}$ precipitation
Yield	17 mg (20% calculated for the Ba-salt form), colorless solid
Sum formula, m.w.	$\text{C}_{11}\text{H}_{15}\text{O}_7\text{P}$, 290.06
^1H NMR (400 MHz, D_2O)	δ 2.83-2.96 (m, 2H, H5), 4.21-4.39 (m, 2H, H3, H4), 4.74 (m, , 2H, H1), 7.19-7.32 (m, 5H, $\text{H}_{\text{arom.}}$).
^{13}C NMR (101 MHz, D_2O)	δ 38.6 (t, C5), 68.9 (t, $J=4.4$ Hz, C1), 72.8 (d, C4), 76.8 (d, C3), 126.6/128.7/129.5 (d, 5C, $\text{C}_{\text{arom.}}$), 137.92 (s, C_{ipso}), 209.4 (C2).
^{31}P NMR (162 MHz, D_2O)	δ -0.26 (t, $J=7.9$ Hz).
LC/MS m/z (ESI$^+$)	found [M-H] 289.27; calculated [M-H] 289.21
Specific rotation	$[\alpha]_{\text{D}}^{22} = +4.1$ (c=1.0 in H_2O).

Abbreviation List

ADH	Alcohol dehydrogenase	MeOH	Methanol
AIM	Auto induction media	MS	Mass spectrometry
Amp	Ampicillin	MW	Microwave
APS	Ammonium persulfate	n.a.	Not applicable
Cam	Chloramphenicol	n.r.	Not recovered
Cbz	Carboxybenzyl	NAD ⁺	Nicotinamide adenine dinucleotide
CFE	Cell free extract	NADH	Nicotinamide adenine dinucleotide (reduced)
DCM	Dichloromethane	NADP ⁺	Nicotinamide adenine dinucleotide phosphate
DHA	Dihydroxyacetone	NADPH	Nicotinamide adenine dinucleotide phosphate (reduced)
DHAP	Dihydroxyacetone phosphate	NMR	Nuclear magnetic resonance
DMF	Dimethylformamide	NP	Normal phase
DMSO	Dimethyl sulfoxide	o/n	Overnight
dr	Diastereomeric excess	OD	Optical density
<i>E. coli</i>	Escherichia coli	PG	Protecting group
ee	Enantiomeric excess	PMSF	Phenylmethylsulfonyl fluoride
ELS	Evaporative Light Scattering Detector	ppm	Parts per million
equiv.	Equivalents	r.t.	Room temperature
EtOAc	Ethyl acetate	RAMA	Fructose-1,6-bisphosphate aldolase form rabbit muscle
EtOH	Ethanol	RCs	Resting cells
FAD ⁺	Flavin adenine dinucleotide	RhuA	Rhamnulose-1,6-bisphosphate aldolase
FGI	Functional group interconversion	RP	Reversed phase
FID	Flame ionization detector	rpm	Rounds per minute
FruA or FDA	Fructose-1,6-bisphosphate aldolase	SDS	
FSA	Fructose-6-phosphate aldolase	PAGE	Sodium dodecyl sulfate polyacrylamide gel electrophoresis
FucA	Fuculose-1,6-bisphosphate aldolase	SEC	Size exclusion chromatography
G6P	Glucose-6-phosphate	SPE	Solid phase extraction
GC	Gas chromatography	TagA	Tagatose-1,6-bisphosphate aldolase
GDH	α -Glycerophosphate dehydrogenase	TB	Terrific broth
HA	Hydroxyacetone	TEMED	N, N, N', N'-tetramethylethylenediamine
HPLC	High-performance liquid chromatography	THF	tetrahydrofuran
HR	High resolution	TIM	Triosephosphate isomerase
IBX	2-Iodoxybenzoic acid	TLC	Thin layer chromatography
IPTG	Isopropyl- β -D-thiogalactopyranoside	TPI	Triosephosphate isomerase
Kan	Kanamycin	Tris	tris(hydroxymethyl)aminomethane
LB	Lysogeny broth	UV	Ultraviolet
LC	Liquid chromatography	v/v	volume per volume
m.p.	Melting point	w.t.	Wild type
MeCN	Acetonitrile		

References

- [1] M. T. Reetz, *JACS* **2013**, *135*, 12480-12496.
- [2] T. Hudlicky, *Chem. Rev.* **2011**, *111*, 3995-3997.
- [3] T. Hudlicky, J. W. Reed, *Chem. Soc. Rev.* **2009**, *38*, 3117-3132.
- [4] C. M. Clouthier, J. N. Pelletier, *Chem. Soc. Rev.* **2012**, *41*, 1585-1605.
- [5] Y. Ni, D. Holtmann, F. Hollmann, *ChemCatChem* **2014**, *6*, 930-943.
- [6] M. T. Reetz, *Chem. Rec.* **2016**, 2449-2459.
- [7] U. T. Bornscheuer, G. W. Huisman, R. J. Kazlauskas, S. Lutz, J. C. Moore, K. Robins, *Nature* **2012**, *485*, 185-194.
- [8] U. T. Bornscheuer, *Angew. Chem., Int. Ed.* **2016**, *55*, 4372-4373.
- [9] B. M. Nestl, S. C. Hammer, B. A. Nebel, B. Hauer, *Angew. Chem., Int. Ed.* **2014**, *53*, 3070-3095.
- [10] G. A. Strohmeier, H. Pichler, O. May, M. Gruber-Khadjawi, *Chem. Rev.* **2011**, *111*, 4141-4164.
- [11] R. O. M. A. de Souza, L. S. M. Miranda, U. T. Bornscheuer, *Chem. Eur. J.* **2017**, 12040-12063.
- [12] M. T. Reetz, *Angew. Chem., Int. Ed.* **2011**, *50*, 138-174.
- [13] K. A. Powell, S. W. Ramer, S. B. del Cardayré, W. P. C. Stemmer, M. B. Tobin, P. F. Longchamp, G. W. Huisman, *Angew. Chem., Int. Ed.* **2001**, *40*, 3948-3959.
- [14] M. T. Reetz, J. D. Carballeira, *Nat. Protocols* **2007**, *2*, 891-903.
- [15] S. B. J. Kan, R. D. Lewis, K. Chen, F. H. Arnold, *Science* **2016**, *354*, 1048-1051.
- [16] R. C. Simon, E. Busto, N. Richter, V. Resch, K. N. Houk, W. Kroutil, *Nature Commun.* **2016**, *7*, 13323.
- [17] R. C. Simon, N. Richter, E. Busto, W. Kroutil, *ACS Catal.* **2013**, *4*, 129-143.
- [18] A. Bruggink, R. Schoevaart, T. Kieboom, *Org. Process Res. Dev.* **2003**, *7*, 622-640.
- [19] J. H. Schrittwieser, S. Velikogne, M. Hall, W. Kroutil, *Chem. Rev.* **2017**.
- [20] J. H. Schrittwieser, J. Sattler, V. Resch, F. G. Mutti, W. Kroutil, *Curr. Opin. Biotechnol.* **2011**, *15*.
- [21] W.-D. Fessner, *N. Biotechnol.* **2015**, *32*, 658-664.
- [22] M. Schrewe, N. Ladkau, B. Bühler, A. Schmid, *Adv. Synth. Catal.* **2013**, *355*, 1693-1697.
- [23] B. Lin, Y. Tao, *Microb. Cell. Fact.* **2017**, *16*, 106.
- [24] J. Wachtmeister, D. Rother, *Curr. Opin. Biotechnol.* **2016**, *42*, 169-177.
- [25] S. Boyarskiy, D. Tullman-Ercek, *Curr. Opin. Chem. Biol.* **2015**, *28*, 15-19.
- [26] T. Bayer, S. Milker, T. Wiesinger, M. Winkler, M. D. Mihovilovic, F. Rudroff, *ChemCatChem* **2017**, 2919-2923.
- [27] A. M. Weeks, M. C. Chang, *Biochem.* **2011**, *50*, 5404-5418.
- [28] T. Bayer, S. Milker, T. Wiesinger, F. Rudroff, M. D. Mihovilovic, *Adv. Synth. Catal.* **2015**, *357*, 1587-1618.
- [29] Q. M. Dudley, A. S. Karim, M. C. Jewett, *Biotechnol. J.* **2015**, *10*, 69-82.
- [30] M. Brovetto, D. Gamenara, P. Saenz Méndez, G. A. Seoane, *Chem. Rev.* **2011**, *111*, 4346-4403.
- [31] N. G. Schmidt, E. Eger, W. Kroutil, *ACS Catal.* **2016**, *6*, 4286-4311.
- [32] M. Hönig, P. Sondermann, N. J. Turner, E. M. Carreira, *Angew. Chem., Int. Ed.* **2017**, *56*, 8942-8973.
- [33] C. C. Johansson-Seechurn, M. O. Kitching, T. J. Colacot, V. Snieckus, *Angew. Chem., Int. Ed.* **2012**, *51*, 5062-5085.
- [34] A. H. Hoveyda, A. R. Zhugralin, *Nature* **2007**, *450*, 243-251.
- [35] T. Gensch, M. N. Hopkinson, F. Glorius, J. Wencel-Delord, *Chem. Soc. Rev.* **2016**, *45*, 2900-2936.
- [36] H. M. L. Davies, D. Morton, *J. Org. Chem.* **2016**, *81*, 343-350.
- [37] N. J. Turner, E. O'Reilly, *Nat. Chem. Biol.* **2013**, *9*, 285-288.
- [38] E. J. Corey, *Chem. Soc. Rev.* **1988**, *17*, 111-133.
- [39] P. Both, H. Busch, P. P. Kelly, F. G. Mutti, N. J. Turner, S. L. Flitsch, *Angew. Chem., Int. Ed.* **2016**, *55*, 1511-1513.
- [40] J. Muschiol, C. Peters, N. Oberleitner, M. D. Mihovilovic, U. T. Bornscheuer, F. Rudroff, *Chem. Commun.* **2015**, *51*, 5798-5811.
- [41] N. Ladkau, A. Schmid, B. Bühler, *Curr. Opin. Biotechnol.* **2014**, *30*, 178-189.
- [42] M. Schrewe, M. K. Julsing, B. Bühler, A. Schmid, *Chem. Soc. Rev.* **2013**, *42*, 6346-6377.
- [43] E.-M. Fischereder, D. Pressnitz, W. Kroutil, *ACS Catal.* **2016**, *6*, 23-30.
- [44] M. Mifsud, S. Gargiulo, S. Iborra, I. W. Arends, F. Hollmann, A. Corma, *Nat. Commun.* **2014**, *5*, 3145.
- [45] H. Gröger, W. Hummel, *Curr. Opin. Chem. Biol.* **2014**, *19*, 171-179.
- [46] E. García-Junceda, I. Lavandera, D. Rother, J. H. Schrittwieser, *J. Mol. Catal. B: Enzym.* **2015**, *114*, 1-6.
- [47] H. Sato, W. Hummel, H. Gröger, *Angew. Chem., Int. Ed.* **2015**, *54*, 4488-4492.
- [48] J. Latham, J.-M. Henry, H. H. Sharif, B. R. K. Menon, S. A. Shepherd, M. F. Greaney, J. Micklefield, *Nature Commun.* **2016**, *7*.
- [49] Á. Gómez Baraibar, D. Reichert, C. Mügge, S. Seger, H. Gröger, R. Kourist, *Angew. Chem., Int. Ed.* **2016**, *55*, 14823-14827.
- [50] N. Ríos-Lombardía, C. Vidal, E. Liardo, F. Morís, J. García-Álvarez, J. González-Sabín, *Angew. Chem., Int. Ed.* **2016**, *55*, 8691-8695.
- [51] E. Liardo, N. Ríos-Lombardía, F. Morís, F. Rebolledo, J. González-Sabín, *ACS Catal.* **2017**, 4768-4774.
- [52] M. Heidlindemann, G. Rulli, A. Berkessel, W. Hummel, H. Gröger, *ACS Catal.* **2014**, *4*, 1099-1103.
- [53] R. C. Simon, E. Busto, J. H. Schrittwieser, J. H. Sattler, J. Pietruszka, K. Faber, W. Kroutil, *Chem. Commun.* **2014**, *50*, 15669-15672.
- [54] M. Müller, G. A. Sprenger, M. Pohl, *Curr. Opin. Chem. Biol.* **2013**, *17*, 261-270.

- [55] T. Sehl, H. C. Hailes, J. M. Ward, U. Menyes, M. Pohl, D. Rother, *Green Chem.* **2014**, *16*, 3341-3348.
- [56] T. Sehl, H. C. Hailes, J. M. Ward, R. Wardenga, E. von Lieres, H. Offermann, R. Westphal, M. Pohl, D. Rother, *Angew. Chem., Int. Ed.* **2013**, *52*, 6772-6775.
- [57] B. R. Lichman, E. D. Lamming, T. Pesnot, J. M. Smith, H. C. Hailes, J. M. Ward, *Green Chem.* **2015**, *17*, 852-855.
- [58] S. T. Ahmed, F. Parmeggiani, N. J. Weise, S. L. Flitsch, N. J. Turner, *Org. Lett.* **2016**, *18*, 5468-5471.
- [59] A. Dennig, E. Busto, W. Kroutil, K. Faber, *ACS Catal.* **2015**, *5*, 7503-7506.
- [60] E. Busto, M. Gerstmann, F. Tobola, E. Dittmann, B. Wilttschi, W. Kroutil, *Catal. Sci. Technol.* **2016**.
- [61] E. Busto, R. C. Simon, W. Kroutil, *Angew. Chem., Int. Ed.* **2015**, *54*, 10899-10902.
- [62] Y. Zhou, S. Wu, Z. Li, *Angew. Chem., Int. Ed.* **2016**, *55*, 11647-11650.
- [63] S. Wu, Y. Zhou, T. Wang, H.-P. Too, D. I. C. Wang, Z. Li, *Nat. Commun.* **2016**, *7*.
- [64] M. Schrewe, M. K. Julsing, K. Lange, E. Czarnotta, A. Schmid, B. Bühler, *Biotechnology and Bioengineering* **2014**, *111*, 1820-1830.
- [65] A. M. Kunjapur, K. L. J. Prather, *Environ. Microbiol. Rep* **2015**, *81*, 1892-1901.
- [66] F. Morís-Varas, X.-H. Qian, C.-H. Wong, *JACS* **1996**, *118*, 7647-7652.
- [67] D. Güclü, A. Szekrenyi, X. Garrabou, M. Kickstein, S. Junker, P. Clapés, W.-D. Fessner, *ACS Catal.* **2016**, *6*, 1848-1852.
- [68] A. L. Concia, L. Gomez, J. Bujons, T. Parella, C. Vilaplana, P. J. Cardona, J. Joglar, P. Clapes, *Org. Biomol. Chem.* **2013**, *11*, 2005-2021.
- [69] S. M. Dean, W. A. Greenberg, C.-H. Wong, *Adv. Synth. Catal.* **2007**, *349*, 1308-1320.
- [70] A. L. Concia, C. Lozano, J. A. Castillo, T. Parella, J. Joglar, P. Clapes, *Chemistry* **2009**, *15*, 3808-3816.
- [71] R. S. B. Gonçalves, A. C. Pinheiro, E. T. da Silva, J. C. S. da Costa, C. R. Kaiser, M. V. N. de Souza, *Synth. Commun.* **2011**, *41*, 1276-1281.
- [72] K. Schwetlick, *Organikum*, Wiley, **2009**.
- [73] A. Procopio, M. Gaspari, M. Nardi, M. Oliverio, A. Tagarelli, G. Sindona, *Tetrahedron Lett.* **2007**, *48*, 8623-8627.
- [74] J. D. More, N. S. Finney, *Org. Lett.* **2002**, *4*, 3001-3003.
- [75] M. Frigerio, M. Santagostino, S. Sputore, *J. Org. Chem.* **1999**, *64*, 4537-4538.
- [76] M. Sudar, Z. Findrik, D. Vasic-Racki, P. Clapes, C. Lozano, *Enzyme Microb. Technol.* **2013**, *53*, 38-45.
- [77] U. T. Bornscheuer, R. J. Kazlauskas, in *Hydrolases in Organic Synthesis*, Wiley-VCH Verlag GmbH & Co. KGaA, **2006**, pp. 61-140.
- [78] M. Breuer, K. Ditrich, T. Habicher, B. Hauer, M. Keßeler, R. Stürmer, T. Zelinski, *Angew. Chem., Int. Ed.* **2004**, *43*, 788-824.
- [79] K. Faber, *Biotransformations in organic chemistry*, Springer-Verlag, **2011**.
- [80] M. Schmidt, E. Henke, B. Heinze, R. Kourist, A. Hidalgo, U. T. Bornscheuer, *Biotechnol. J.* **2007**, *2*, 249-253.
- [81] M. Schmidt, E. Barbayianni, I. Fotakopoulou, M. Höhne, V. Constantinou-Kokotou, U. T. Bornscheuer, G. Kokotos, *J. Org. Chem.* **2005**, *70*, 3737-3740.
- [82] D. B. Dess, J. C. Martin, *J. Org. Chem.* **1983**, *48*, 4155-4156.
- [83] A.-K. C. Schmidt, C. B. W. Stark, *Org. Lett.* **2011**, *13*, 4164-4167.
- [84] S. Wertz, A. Studer, *Green Chem.* **2013**, *15*, 3116-3134.
- [85] F. Hollmann, I. W. C. E. Arends, K. Buehler, A. Schallmeyer, B. Bühler, *Green Chem.* **2011**, *13*, 226.
- [86] W. Kroutil, H. Mang, K. Edegger, K. Faber, *Curr. Opin. Biotechnol.* **2004**, *8*, 120-126.
- [87] J. H. Sattler, M. Fuchs, K. Tauber, F. G. Mutti, K. Faber, J. Pfeffer, T. Haas, W. Kroutil, *Angew. Chem., Int. Ed.* **2012**, *51*, 9156-9159.
- [88] N. Oberleitner, C. Peters, J. Muschiol, M. Kadow, S. Saß, T. Bayer, P. Schaaf, N. Iqbal, F. Rudroff, M. D. Mihovilovic, U. T. Bornscheuer, *ChemCatChem* **2013**, *5*, 3524-3528.
- [89] M. Pickl, M. Fuchs, S. M. Glueck, K. Faber, *Appl. Microbiol. Biotechnol.* **2015**, *99*, 6617-6642.
- [90] A. Weckbecker, W. Hummel, *Biocatalysis and Biotransformation* **2006**, *24*, 380-389.
- [91] W. Stampfer, B. Kosjek, C. Moitzi, W. Kroutil, K. Faber, *Angewandte Chemie* **2002**, *41*, 1014-1017.
- [92] R. Cannio, M. Rossi, S. Bartolucci, *Eur. J. Biochem.* **1994**, *222*, 345-352.
- [93] C. Wuensch, H. Lechner, S. M. Glueck, K. Zangger, M. Hall, K. Faber, *ChemCatChem* **2013**, *5*, 1744-1748.
- [94] K. Napora-Wijata, K. Robins, A. Osorio-Lozada, M. Winkler, *ChemCatChem* **2014**, *6*, 1089-1095.
- [95] J. E. Dueber, G. C. Wu, G. R. Malmirchegini, T. S. Moon, C. J. Petzold, A. V. Ullal, K. L. Prather, J. D. Keasling, *Nat. Biotechnol.* **2009**, *27*, 753-759.
- [96] J. Kofoed, T. Darbre, J. L. Reymond, *Chem. Commun.* **2006**, 1482-1484.
- [97] N. Mase, C. F. Barbas, 3rd, *Org. Biomol. Chem.* **2010**, *8*, 4043-4050.
- [98] D. Enders, C. Grondal, *Angew. Chem., Int. Ed.* **2005**, *44*, 1210-1212.
- [99] B. List, R. A. Lerner, C. F. Barbas, *JACS* **2000**, *122*, 2395-2396.
- [100] S. S. V. Ramasastry, K. Albertshofer, N. Utsumi, C. F. Barbas, *Org. Lett.* **2008**, *10*, 1621-1624.
- [101] N. Utsumi, M. Imai, F. Tanaka, S. S. V. Ramasastry, C. F. Barbas, *Org. Lett.* **2007**, *9*, 3445-3448.
- [102] J. T. Suri, D. B. Ramachary, C. F. Barbas, *Org. Lett.* **2005**, *7*, 1383-1385.
- [103] M. Markert, R. Mahrwald, *Chem. Eur. J.* **2008**, *14*, 40-48.
- [104] J. Huang, X. Zhang, D. W. Armstrong, *Angew. Chem., Int. Ed.* **2007**, *46*, 9073-9077.
- [105] S. S. V. Ramasastry, K. Albertshofer, N. Utsumi, F. Tanaka, C. F. Barbas, *Angew. Chem., Int. Ed.* **2007**, *46*, 5572-5575.

- [106] C. Wu, X. Fu, X. Ma, S. Li, *Tetrahedron: Asymmetry* **2010**, *21*, 2465-2470.
- [107] P. Clapés, X. Garrabou, *Adv. Synth. Catal.* **2011**, *353*, 2263-2283.
- [108] T. Saravanan, M.-L. Reif, D. Yi, M. Lorilliere, F. Charmantray, L. Hecquet, W.-D. Fessner, *Green Chem.* **2017**.
- [109] C. H. Wong, G. M. Whitesides, *J. Org. Chem.* **1983**, *48*, 3199-3205.
- [110] M. D. Bednarski, E. S. Simon, N. Bischofberger, W. D. Fessner, M. J. Kim, W. Lees, T. Saito, H. Waldmann, G. M. Whitesides, *JACS* **1989**, *111*, 627-635.
- [111] W.-D. Fessner, C. Walter, *Angew. Chem., Int. Ed.* **1992**, *31*, 614-616.
- [112] D. Franke, T. Machajewski, C. C. Hsu, C. H. Wong, *J. Org. Chem.* **2003**, *68*, 6828-6831.
- [113] B. Bechi, S. Herter, S. McKenna, C. Riley, S. Leimkuhler, N. J. Turner, A. J. Carnell, *Green Chem.* **2014**, *16*, 4524-4529.
- [114] S. Herter, S. M. McKenna, A. R. Frazer, S. Leimkuhler, A. J. Carnell, N. J. Turner, *ChemCatChem* **2015**, *7*, 2313-2317.
- [115] A. L. Concia, L. Gómez, T. Parella, J. Joglar, P. Clapés, *J. Org. Chem.* **2014**, *79*, 5386-5389.
- [116] I. Oroz-Guinea, K. Hernández, F. Camps Bres, C. Guérard-Hélaine, M. Lemaire, P. Clapés, E. García-Junceda, *Adv. Synth. Catal.* **2015**, *357*, 1951-1960.
- [117] W.-D. Fessner, D. Heyl, M. Rale, *Catal. Sci. Technol.* **2012**, *2*, 1596-1601.
- [118] M. Rale, S. Schneider, G. A. Sprenger, A. K. Samland, W. D. Fessner, *Chem. Eur. J.* **2011**, *17*, 2623-2632.
- [119] C. L. Windle, M. Muller, A. Nelson, A. Berry, *Curr. Opin. Chem. Biol.* **2014**, *19*, 25-33.
- [120] A. Szekrenyi, X. Garrabou, T. Parella, J. Joglar, J. Bujons, P. Clapés, *Nat. Chem.* **2015**, *7*, 724-729.
- [121] R. Roldán, I. Sanchez-Moreno, T. Scheidt, V. Hélaine, M. Lemaire, T. Parella, P. Clapés, W.-D. Fessner, C. Guérard-Hélaine, *Chem. Eur. J.* **2017**, *5005*-5009.
- [122] R. Obexer, A. Godina, X. Garrabou, P. R. E. Mittl, D. Baker, A. D. Griffiths, D. Hilvert, *Nat. Chem.* **2016**.
- [123] A. Soler, M. L. Gutiérrez, J. Bujons, T. Parella, C. Minguillon, J. Joglar, P. Clapés, *Adv. Synth. Catal.* **2015**, *357*, 1787-1807.
- [124] J. A. Castillo, C. Guérard-Hélaine, M. Gutiérrez, X. Garrabou, M. Sancelme, M. Schürmann, T. Inoue, V. Hélaine, F. Charmantray, T. Gefflaut, L. Hecquet, J. Joglar, P. Clapés, G. A. Sprenger, M. Lemaire, *Adv. Synth. Catal.* **2010**, *352*, 1039-1046.
- [125] M. Sugiyama, Z. Hong, P. H. Liang, S. M. Dean, L. J. Whalen, W. A. Greenberg, C. H. Wong, *JACS* **2007**, *129*, 14811-14817.
- [126] M. Schurmann, G. A. Sprenger, *J Biol Chem* **2001**, *276*, 11055-11061.
- [127] R. Z. Jin, E. C. C. Lin, *Microbiology* **1984**, *130*, 83-88.
- [128] Y. J. Zhou, W. Yang, L. Wang, Z. Zhu, S. Zhang, Z. K. Zhao, *Microb. Cell. Fact.* **2013**, *12*, 103-103.
- [129] Z.-C. Hu, Y.-G. Zheng, Y.-C. Shen, *Bioresour. Technol.* **2011**, *102*, 7177-7182.
- [130] H. J. Park, J. Jung, H. Choi, K. N. Uhm, H. K. Kim, *J. Microbiol. Biotechnol.* **2010**, *20*, 1300-1306.
- [131] M. Mifsud, A. Szekrényi, J. Joglar, P. Clapés, *J. Mol. Catal. B: Enzym.* **2012**, *84*, 102-107.
- [132] M. Sudar, Z. Findrik, D. Vasic-Racki, A. Soler, P. Clapes, *RSC Adv.* **2015**, *5*, 69819-69828.
- [133] T. Wiesinger, T. Bayer, S. Milker, M. D. Mihovilovic, F. Rudroff, *ChemBiochem* **2017**.
- [134] C. Li, A. Wen, B. Shen, J. Lu, Y. Huang, Y. Chang, *BMC Biotechnol.* **2011**, *11*, 92.
- [135] Y. Zhang, U. Werling, W. Edlmann, *Nucleic Acids Res.* **2012**, *40*, e55.
- [136] J. A. Castillo, J. Calveras, J. Casas, M. Mitjans, M. P. Vinardell, T. Parella, T. Inoue, G. A. Sprenger, J. Joglar, P. Clapes, *Org. Lett.* **2006**, *8*, 6067-6070.
- [137] M. Gutierrez, T. Parella, J. Joglar, J. Bujons, P. Clapes, *Chem. Commun.* **2011**, *47*, 5762-5764.
- [138] M. Wei, Z. Li, T. Li, B. Wu, Y. Liu, J. Qu, X. Li, L. Li, L. Cai, P. G. Wang, *ACS Catal.* **2015**, *5*, 4060-4065.
- [139] M. J. Fink, M. Schön, F. Rudroff, M. Schnürch, M. D. Mihovilovic, *ChemCatChem* **2013**, *5*, 724-727.
- [140] G. Sirasani, L. Tong, E. P. Balskus, *Angew. Chem., Int. Ed.* **2014**, *53*, 7785-7788.
- [141] A. M. Kunjapur, Y. Tarasova, K. L. J. Prather, *JACS* **2014**, *136*, 11644-11654.
- [142] M. H. Wei, Z. J. Li, T. H. Li, B. L. Wu, Y. P. Liu, J. Y. Qu, X. Li, L. Li, L. Cai, P. G. Wang, *ACS Catal.* **2015**, *5*, 4060-4065.
- [143] K. Fesko, M. Gruber-Khadjawi, *ChemCatChem* **2013**, *5*, 1248-1272.
- [144] S.-H. Jung, J.-H. Jeong, P. Miller, C.-H. Wong, *J. Org. Chem.* **1994**, *59*, 7182-7184.
- [145] L. Babich, L. J. C. van Hemert, A. Bury, A. F. Hartog, P. Falcicchio, J. van der Oost, T. van Herk, R. Wever, F. P. J. T. Rutjes, *Green Chem.* **2011**, *13*, 2895-2900.
- [146] T. Suau, G. Álvaro, M. D. Benaiges, J. López-Santín, *Biotechnol. Bioeng.* **2006**, *93*, 48-55.
- [147] R. Schoevaart, F. van Rantwijk, R. A. Sheldon, *Biotechnol. Bioeng.* **2000**, *70*, 349-352.
- [148] G. Labbe, S. de Groot, T. Rasmusson, G. Milojevic, G. I. Dmitrienko, J. G. Guillemette, *Protein expression and purification* **2011**, *80*, 224-233.
- [149] I. Sánchez-Moreno, V. Hélaine, N. Poupard, F. Charmantray, B. Légeret, L. Hecquet, E. García-Junceda, R. Wohlgemuth, C. Guérard-Hélaine, M. Lemaire, *Adv. Synth. Catal.* **2012**, *354*, 1725-1730.
- [150] V. Hélaine, R. Mahdi, G. V. Sudhir Babu, V. de Berardinis, R. Wohlgemuth, M. Lemaire, C. Guérard-Hélaine, *Adv. Synth. Catal.* **2015**, *357*, 1703-1708.
- [151] C. Stanetty, M. Walter, P. Kosma, *J. Org. Chem.* **2014**, *79*, 582-598.
- [152] L. Iturrate, I. Sanchez-Moreno, E. G. Doyaguez, E. Garcia-Junceda, *Chem. Commun.* **2009**, 1721-1723.

- [153] T. van Herk, A. F. Hartog, A. M. van der Burg, R. Wever, *Adv. Synth. Catal.* **2005**, *347*, 1155-1162.
- [154] T. van Herk, A. F. Hartog, L. Babich, H. E. Schoemaker, R. Wever, *Chembiochem* **2009**, *10*, 2230-2235.
- [155] L. Babich, A. F. Hartog, L. J. van Hemert, F. P. Rutjes, R. Wever, *ChemSusChem* **2012**, *5*, 2348-2353.
- [156] L. Iturrate, I. Sánchez-Moreno, I. Oroz-Guinea, J. Pérez-Gil, E. García-Junceda, *Chem. Eur. J.* **2010**, *16*, 4018-4030.
- [157] I. Sánchez-Moreno, L. Iturrate, E. G. Doyagüez, J. A. Martínez, A. Fernández-Mayoralas, E. García-Junceda, *Adv. Synth. Catal.* **2009**, *351*, 2967-2975.
- [158] F. W. Studier, *Protein expression and purification* **2005**, *41*, 207-234.
- [159] K. Orito, M. Miyazawa, T. Nakamura, A. Horibata, H. Ushito, H. Nagasaki, M. Yuguchi, S. Yamashita, T. Yamazaki, M. Tokuda, *J. Org. Chem.* **2006**, *71*, 5951-5958.
- [160] H. Zhu, D. M. Coleman, C. J. Dehen, I. M. Geisler, D. Zemlyanov, J. Chmielewski, G. J. Simpson, A. Wei, *Langmuir* **2008**, *24*, 8660-8666.
- [161] T. Miyazawa, K. Tanaka, E. Ensatsu, R. Yanagihara, T. Yamada, *J. Chem. Soc., Perkin Trans. 1* **2001**, 87-94.
- [162] J. Ivkovic, C. Lembacher-Fadum, R. Breinbauer, *Org. Biomol. Chem.* **2015**, *13*, 10456-10460.
- [163] G. D. Kishore Kumar, S. Baskaran, *J. Org. Chem.* **2005**, *70*, 4520-4523.
- [164] K. Higashiura, K. Ienaga, *J. Org. Chem.* **1992**, *57*, 764-766.
- [165] J.-A. Fehrentz, J.-C. Califano, M. Amblard, A. Loffet, J. Martinez, *Tetrahedron Lett.* **1994**, *35*, 569-571.
- [166] A. Golebiowski, J. Raczko, J. Jurczak, *Bull. Pol. Acad. Sci., Chem.* **1989**, *36*, 209-214.
- [167] S. Luo, H. Xu, L. Zhang, J. Li, J.-P. Cheng, *Org. Lett.* **2008**, *10*, 653-656.
- [168] A. J. Humphrey, N. J. Turner, R. McCague, S. J. C. Taylor, *Chem. Commun.* **1995**, 2475-2476.
- [169] A. L. Concia, C. Lozano, J. A. Castillo, T. Parella, J. Joglar, P. Clapes, *Chem. Eur. J.* **2009**, *15*, 3808-3816.
- [170] L. Espelt, T. Parella, J. Bujons, C. Solans, J. Joglar, A. Delgado, P. Clapes, *Chem. Eur. J.* **2003**, *9*, 4887-4899.

Curriculum Vitae

Thomas Wiesinger

April 16, 1986

Haspingergasse 1-3/5

1080 Wien



Education

- 01/2013-
01/2018 **PhD Thesis, TU Wien**
Focus: Organic chemistry, Biocatalysis
Degree: Dr. techn.
- 02/2007-
01/2013 **Bachelor & Master, TU Graz**
Focus: Macromolecular chemistry
Degree: Dipl. Ing.
- 2000-
2005 **General Qualification for University Entrance, HTBLA
Vöcklabruck**
Focus: Environmental Technology

Work Experience

- 04/2017-
Clinical Research Scientist at ARCHIMEDLife Science GmbH.
1110 Vienna.
- 01/2013-
03/2017 **Scientific Assistant** at the Institute of Applied Synthetic Chemistry,
Vienna University of Technology. 1060 Vienna.
- Summer 2010 & 2011 **Paramedic**, *Österreichisches Rotes Kreuz*, Landesverband OÖ,
4863 Seewalchen am Attersee.
- 06/2009-
08/2009 **Laboratory Chemist**, *Sandoz (former EBEWE, Neuro Pharma)*,
4866 Unterach.
Analytical Laboratories (Quality control)
- Summer 2007 & 2008 **Paramedic**, *Österreichisches Rotes Kreuz*, Landesverband OÖ,
4863 Seewalchen am Attersee.
- 09/2005-
01/2006 **Laboratory Chemist**, *Lenzing AG*, 4860 Lenzing.
Analytical Laboratories (Quality control)

Administration Experience (TU Wien)

01/2013-present
Lab course: *Basic chemistry (4 times)*
Lab course: *Basic synthetic chemistry (4 times)*
Lab course: *Advanced synthetic chemistry (4 times)*
Bachelor work (2 times), several bioorganic lab courses

Personal Data

Personal Characteristics	Team-minded, flexible, reliable
Language skills	German (native), English (fluent)
IT skills	Microsoft Office, Mac OS ChemDraw, Reaxys, Scifinder, Topspin, MestReNova, Chromelone, Excalibur, LabSolutions
Qualification	Paramedic
Organisation	Rotes Kreuz Oberösterreich, Marktmusikkapelle Seewalchen
Hobby	Cycling, Football and Cooking

Publications and Poster Presentations

2017 Cell Factory Design and Optimization for the Stereoselective Synthesis of Polyhydroxylated Compounds; T. Wiesinger, T. Bayer, S. Milker, M. Mihovilovic, F. Rudroff, **2017**, *ChemBioChem*.

2017 *In Vivo* Synthesis of Polyhydroxylated Compounds from a "Hidden Reservoir" of Toxic Aldehyde Species; T. Bayer, S. Milker, T. Wiesinger, M. Mihovilovic, F. Rudroff, **2017**, *ChemCatChem*.

2016 **5th International Conference on Novel Enzymes**, Groningen, Netherlands, Poster presentation. Fine-tuning of an Artificial "Mini"- Pathway for the Synthesis of Polyhydroxylated Compounds.

2015 **12th Biotrans**, Vienna, Austria, Poster presentation. Assembly of an Artificial "Mini"- Pathway with an *in situ* Hydrogenation to Synthesize Polyhydroxylated Compounds.

2015 **16th Tetrahedron Symposium**, Berlin, Germany, Poster presentation. Design of a Non-native Pathway for the Synthesis of Polyhydroxylated Heterocycles.

2015 Designer Microorganisms for Optimized Redox Cascade Reactions- Challenges and Future Perspectives; T. Bayer, S. Milker, T. Wiesinger, F. Rudroff, M. Mihovilovic, **2015**, *Adv. Synth. Catal.*

2014 **Dechema Summer School- Biotransformations**, Bad Herrenalb, Germany, Poster presentation and poster pitch talk. Design of a Non-native Pathway for the Synthesis of Polyhydroxylated Heterocycles.